

# ELEKTOR ELECTRONICS

THE INTERNATIONAL ELECTRONICS MAGAZINE  
JUNE 1993



## DIGITAL READ-OUT FOR VHF/UHF RECEIVER

Real-time Clock for 80C32 Computer

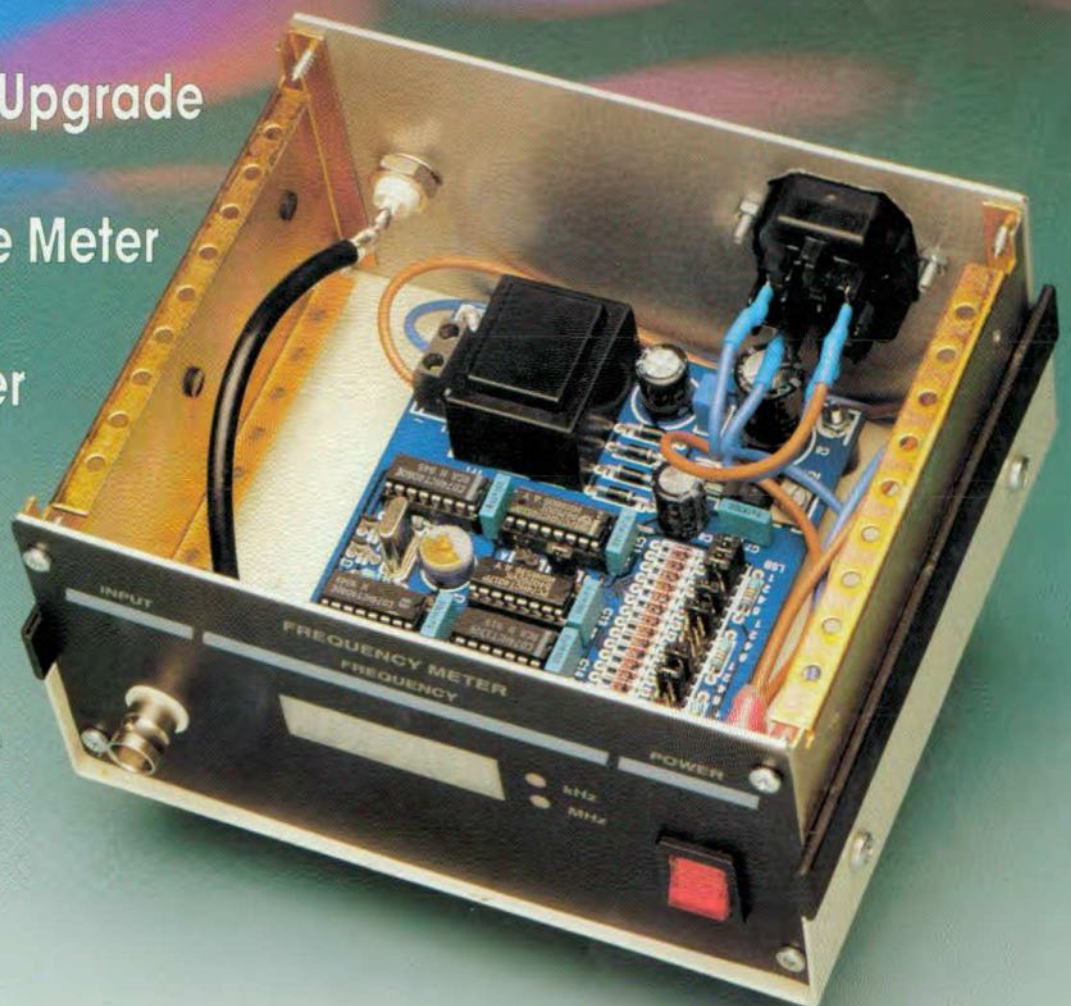
GAL Programmer Upgrade

Inexpensive Phase Meter

Spectrum VU Meter

Electricity from  
the Wind

A CW Compatible  
T/R Switch



# SPECTRUM VU METER

Design by T. Giesberts

Making an audio signal visible on a display is something that appeals to many audio & hi-fi enthusiasts. Most commercial audio equipment is now provided with a display in the form of one or more light bars that move in rhythm with the music. The proposed VU meter offers seven or eight bars that each serve a certain part of the audio spectrum.

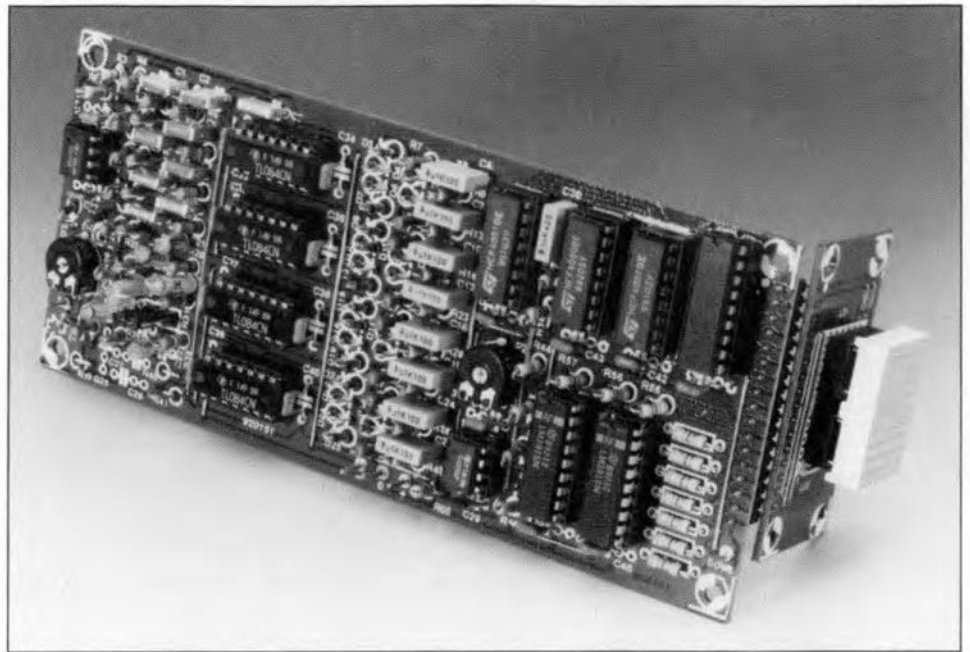
A VU meter used to be a moving-coil meter that indicated the drive power of, for instance, a tape recorder in 'Volume Units'. Modern equipment is normally provided with a VU meter consisting of a bar of small LEDs per channel.

The VU meter described is intended primarily for use with an amplifier and does not only show the strength of the incoming or outgoing signal, but also its spectral distribution. The sound spectrum is divided into seven or eight bands, each of whose strengths is shown on a 10-LED bar. All these LEDs do not present a construction problem, because use is made of two 5x7 or 5x8 matrix displays that are mounted one above the other. These displays are available in various sizes, from 18x26 mm to 61x72 mm.

## Design considerations

The audio input signal is fed to a variable amplifier and then to seven filters (Fig. 1). The eighth filter shown is for use only with large displays that have eight LED bars. The lowest filter is a low-pass section, the five (or six in case of a large display) following ones are band-pass sections, and the highest is a high-pass section. To obtain a good split of the audio spectrum and yet keep the number of components in the filters to a minimum, the cut-off frequencies and Q factors have been chosen to give -10 dB transfer points of adjacent frequencies. That may seem a lot, but it should be borne in mind that the resolution of the display is 3 dB per step at the top and as much as 9 dB per step at the bottom.

To get an even distribution of the audio range of 20 Hz to 20 kHz, the central frequencies of the band-pass filters have been set to 130 Hz, 340 Hz, 880 Hz, 2.3 kHz, and 6 kHz. With a Q factor of 3, the filters interconnect just about at



their -10 dB points.

The cut-off frequency of the low-pass filter is set to 50 Hz and that of the high-pass section to 15 kHz. For small displays, these filters are third-order Butterworth types that fit in well with the band-pass sections, but for large displays their behaviour becomes more of a Chebishev nature.

The filter responses are shown in Fig. 2.

The filter outputs are passed to peak detectors. These are rather more complex than in Fig. 1, but that will be reverted to in the circuit description.

The seven (eight) direct voltages are fed to a multiplexer that passes one of them via buffer-amplifiers to a double comparator-buffer formed by two LED driver ICs. These quasi-series connected ICs enable a range of some 50 dB to be displayed.

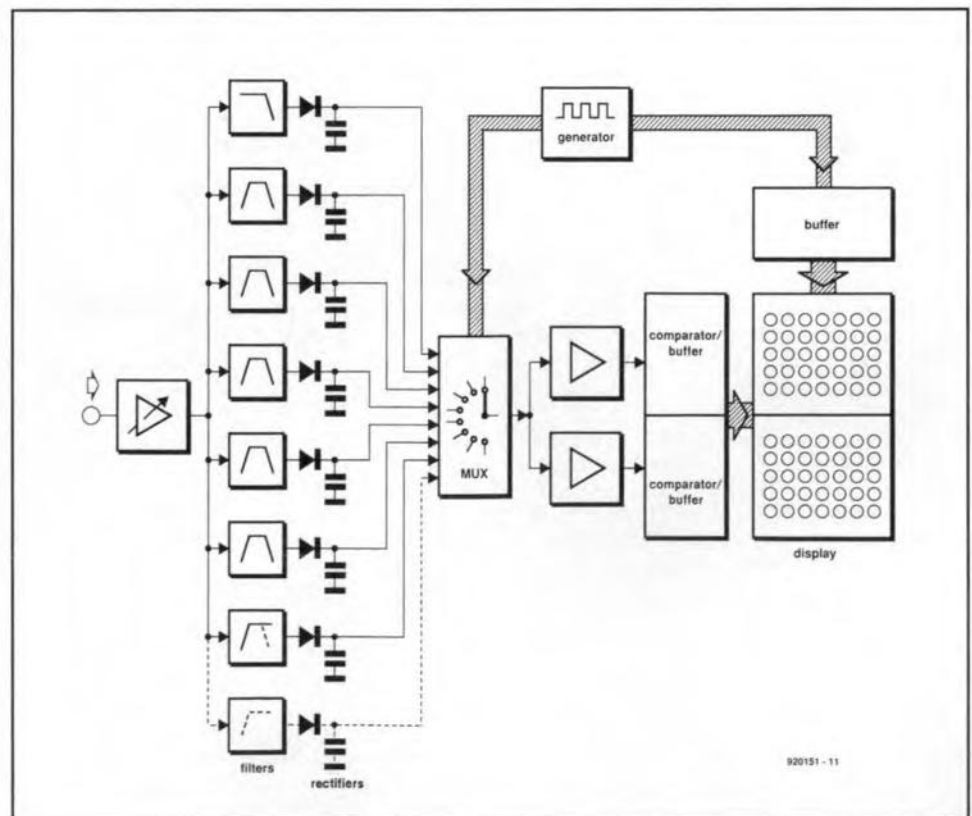


Fig. 1. Block schematic of the VU meter.

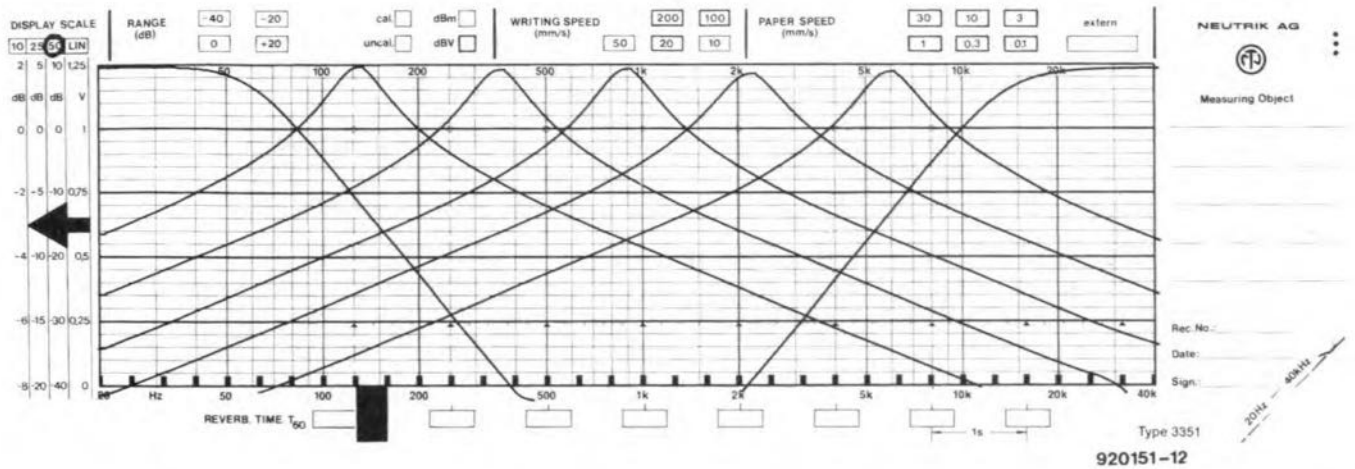


Fig. 2. Response curves of the low-pass, high-pass and band-pass filters when a seven-bar display is used.

A frequency generator provides the clock that switches the multiplexer to each successive direct voltage. At the same time, this signal actuates the LED bar associated with that direct voltage via a number of buffer stages, so that this bar displays only the level monitored at that instant.

### The circuit

The audio input is applied to  $K_1$  (see Fig. 4) and from there to  $IC_1$  via  $P_1$ , which enables it to be attenuated as required. The amplifier has a gain of about 16 dB. The output of  $IC_1$  is fed to the seven or eight filter sections. The multiple feedback band-pass filters are formed by  $IC_{2a}$ ,  $IC_{3d}$ ,  $IC_{3a}$ ,  $IC_{4d}$ , and  $IC_{4a}$ . As already mentioned, their  $Q$  factor is 3.

The third-order low-pass filter, which has a cut-off frequency of 50 Hz, is based on  $IC_{2d}$ .

The third-order high-pass filter, which has a cut-off frequency of 15 kHz, is based on  $IC_{5d}$ .

If a  $10 \times 8$  LED matrix is used, the eighth filter needed is based on  $IC_{5a}$ . In that case, the high-pass filter based on  $IC_{5d}$  is converted to a band-pass section (whence the duplicated component indications; in the  $C_{20}$  position a resistor is then used). Table 1 lists all the component values in case eight filters are used.

The rectifiers are pseudo-active types to ensure proper coverage of the display range of 50 dB. In the prototype, standard passive rectifiers, even Schottky types, gave serious deviations (in some case, a 30 dB signal was attenuated to no less than 12 dB by the rectifier). The design finally chosen consists of a passive rectifier, consisting of a diode ( $D_5$ ,  $D_8$ ,  $D_{11}$ ,  $D_{14}$ ,  $D_{17}$ ,  $D_{20}$ ,  $D_{23}$ ), a capacitor ( $C_4$ ,  $C_7$ ,  $C_{10}$ ,  $C_{13}$ ,  $C_{16}$ ,  $C_{19}$ ,  $C_{24}$ ) and a discharge resistor ( $R_6$ ,  $R_{13}$ ,  $R_{18}$ ,  $R_{23}$ ,  $R_{28}$ ,  $R_{33}$ , and  $R_{38}$ ), coupled with an active compensating

device ( $IC_{2c}$ ,  $IC_{2b}$ ,  $IC_{3c}$ ,  $IC_{3b}$ ,  $IC_{4c}$ ,  $IC_{4b}$ , and  $IC_{5c}$ ).

The active devices compensate the forward bias of the associated diodes as well as the discharge of the capacitors through the diodes when these conduct.

Since each of the ICs, connected in a voltage follower configuration, has negative feedback through two anti-parallel diodes, its output will always be larger by the forward bias of one of the diodes ( $D_3$ ,  $D_6$ ,  $D_9$ ,  $D_{12}$ ,  $D_{15}$ ,  $D_{18}$ ,  $D_{21}$ ) than the input. That bias depends to some extent on the current, which here is determined by the load resistor ( $R_7$ ,  $R_{12}$ ,  $R_{17}$ ,  $R_{22}$ ,  $R_{27}$ ,  $R_{32}$ ,  $R_{37}$ ). The diodes mentioned above are of a type that is identical to the rectifier. The type of the other diode in the feedback loop is not so important.

When the input is small, the drop across  $D_3$ ,  $D_6$ , and so on, may be increased by reducing the value of  $R_7$ ,  $R_{12}$ ,

and so on.

Outputs  $Q_3$ ,  $Q_4$  and  $Q_5$  of oscillator-divider  $IC_8$  switch multiplexer  $IC_6$  at a frequency of about 400 Hz, so that at all times one of the output voltages of the rectifiers is connected to the comparator and drive section,  $IC_9$ ,  $IC_{11}$ ,  $IC_{12}$ .

The same three  $Q$  outputs of  $IC_8$  are also linked to binary-to-decimal converter (BDC)  $IC_7$ . This converter ensures (via a number of buffers contained in  $IC_{10}$ ) that the LED bar associated with the direct voltage output of the multiplexer at that instant is powered.

When all LEDs of a small display with seven bars light, the average current drawn is 263 mA.

The multiplexer is linked to  $IC_{11}$  and  $IC_{12}$  via two opamps,  $IC_{9a}$  and  $IC_{9b}$ . The first serves as a buffer for  $IC_{11}$ , while the second not only buffers the signal to  $IC_{12}$ , but also amplifies it  $\times 32$ .

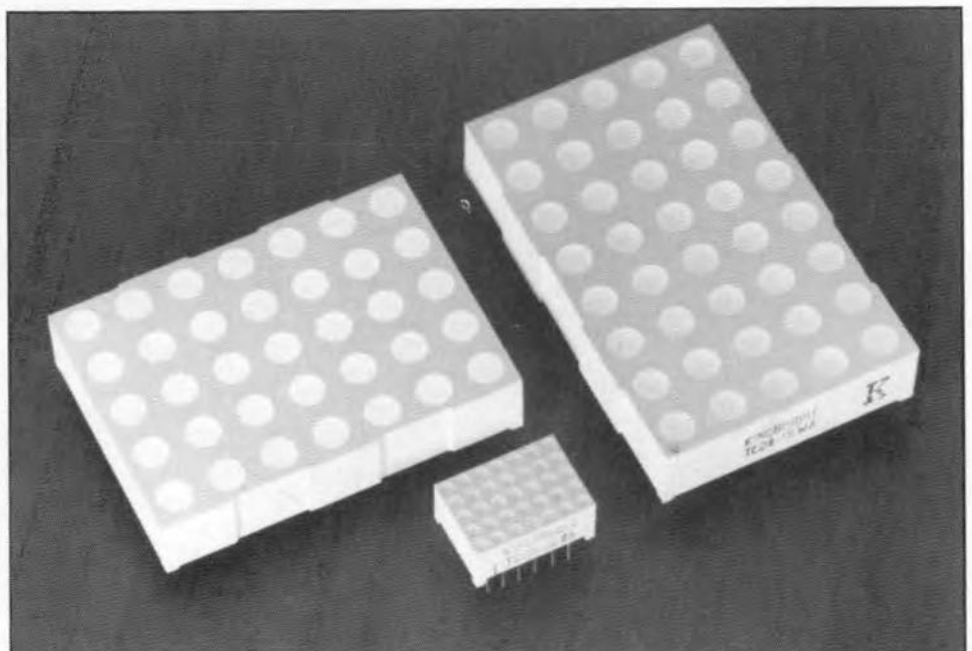


Fig. 3. The displays are available in a variety of sizes.

Circuits IC<sub>11</sub> and IC<sub>12</sub> drive the rows of the display. Each of them contains a 10-step comparator, a variable reference source and a drive circuit for the ten LEDs. Since at the underside of the display larger steps are required than at the top, most outputs of IC<sub>12</sub> are not

used. In that way, the steps on the display are (in dB): 0, -3, -6, -9, -15, -21, -27, -33, -41, and -50.

Resistors R<sub>48</sub>-R<sub>57</sub> serve not so much as current limiters (the outputs of the LM3915s are current sources), but rather as dissipation limiters for the drive transistors contained in IC<sub>11</sub> and IC<sub>12</sub>.

sistors contained in IC<sub>11</sub> and IC<sub>12</sub>.

The power supply needs to provide a stabilized, symmetrical voltage; the positive supply line must be able to deliver a current of at least 330 mA, and the negative line one of about 35 mA.

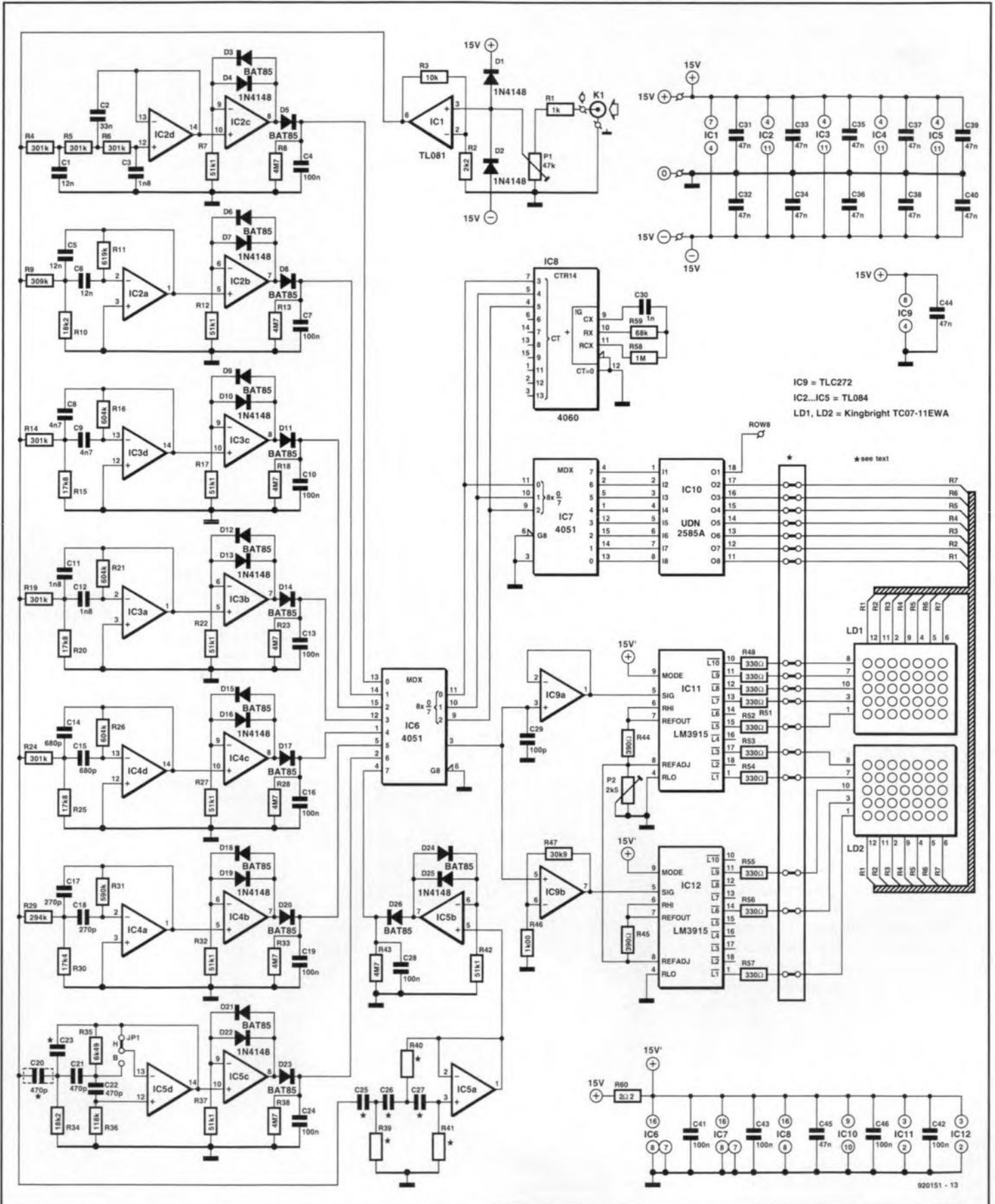


Fig. 4. Circuit diagram of the VU meter.

## Construction

The VU meter is most conveniently built on the printed-circuit board shown in Fig. 5. Start with cutting off the display section if that is to be located elsewhere. Then, all components can be fitted. Note that most resistors and all diodes should be mounted upright. The 270 pF, 470 pF and 680 pF capacitors must be polystyrene types to prevent too high damping of the filters. These capacitors must also be mounted upright.

Once the boards have been completed, they must be interlinked by an angled header (see photograph on p. 8) or 17

discrete, short wires.

The power for the meter may be drawn from the equipment into which it is built, but, owing to the current requirement on the positive line, it is best to build a small, separate supply.

If a larger display is used than shown on the PCB, it must be connected to the board via suitable connectors or half IC sockets. The display section of the board is then useless.

When a small display is used, jumper JP<sub>1</sub> on the board must be placed in position 'H'. Resistors R<sub>41</sub> and R<sub>43</sub> must be replaced by a wire bridge.

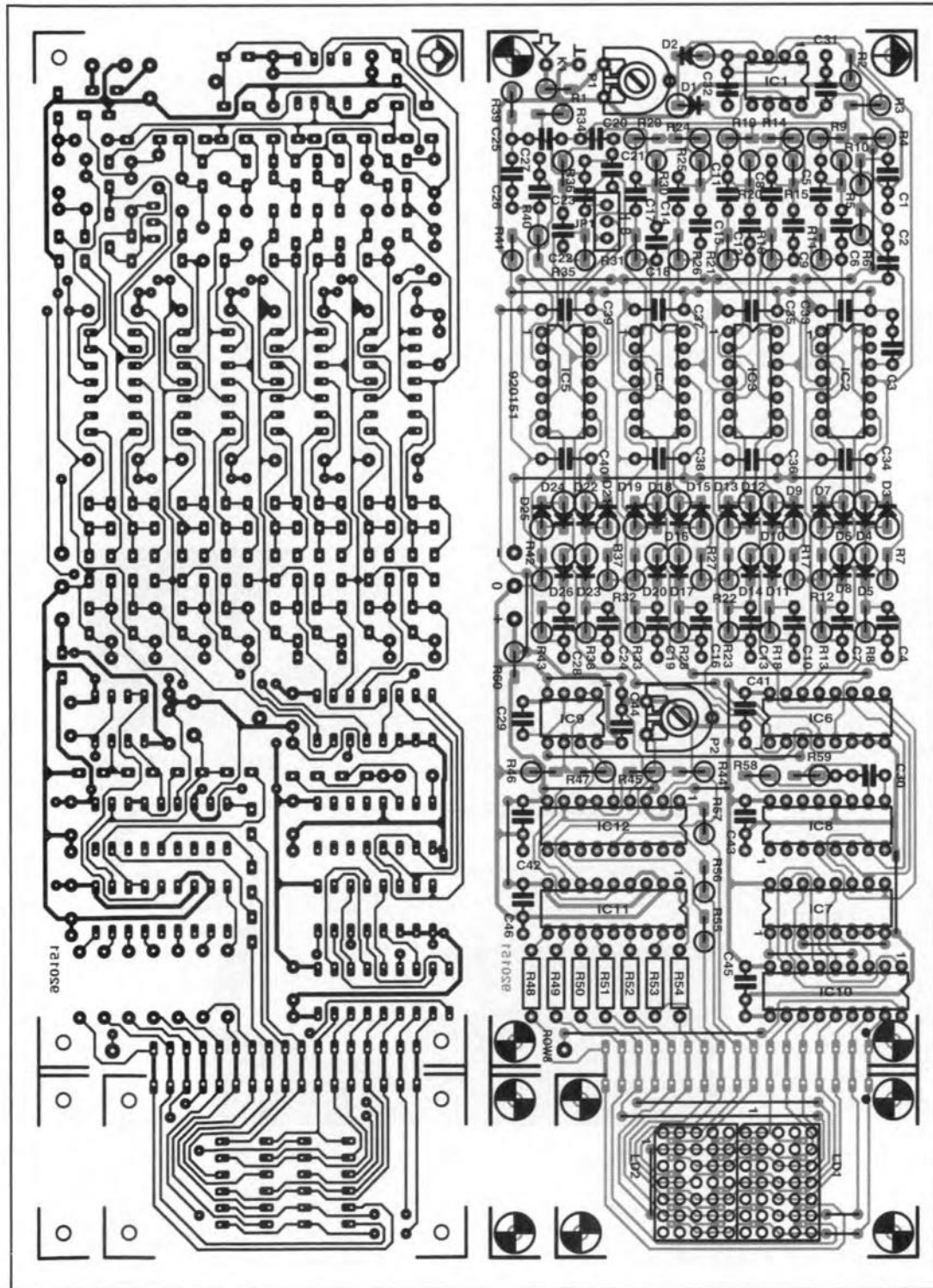


Fig. 4. The printed-circuit board for the VU meter.

## PARTS LIST

### Resistors:

R1=1 kΩ  
 R2=2.2 kΩ  
 R3=10 kΩ  
 R4, R5, R6, R14, R19, R24=301 kΩ, 1%  
 R7, R12, R17, R22, R27, R32, R37=51.1 kΩ, 1%  
 R8, R13, R18, R23, R28, R33, R38=4.7 MΩ  
 R9=309 kΩ, 1%  
 R10, R34=18.2 kΩ, 1%  
 R11=619 kΩ, 1%  
 R15, R20, R25=17.8 kΩ, 1%  
 R16, R21, R26=604 kΩ, 1%  
 R29=294 kΩ, 1%  
 R30=17.4 kΩ, 1%  
 R31=590 kΩ, 1%  
 R35=6.49 kΩ, 1%  
 R36=118 kΩ, 1%  
 R44, R45=390 Ω  
 R46=1.0 kΩ, 1%  
 R47=30.9 kΩ, 1%  
 R48-R57=330 Ω  
 R58=1 MΩ  
 R59=68 kΩ  
 R60=2.2 Ω  
 P1=47 kΩ preset  
 P2=2.5 kΩ preset

### Capacitors:

C1, C5, C6=12 nF  
 C2=33 nF  
 C3, C11, C12=1.8 nF  
 C4, C7, C10, C13, C16, C19, C24=100 nF  
 C8, C9=4.7 nF  
 C14, C15=680 pF\*  
 C17, C18=270 pF\*  
 C20, C21, C22=470 pF\*  
 C29=100 pF  
 C30=1 nF  
 C31-C40, C44=47 nF, ceramic  
 C41, C42, C43, C45, C46=100 nF, ceramic  
 \*polystyrene, axial

### Semiconductors:

D1, D2, D4, D7, D10, D13, D16, D19, D22=1N4148  
 D3, D5, D6, D8, D9, D11, D12, D14, D15, D17, D18, D20, D21, D23=BAT85  
 IC1=TL081  
 IC2-IC5=TL084  
 IC6, IC7=4051  
 IC8=4060  
 IC9=TLC272  
 IC10=UDN2585A  
 IC11, IC12=LM3915

### Miscellaneous:

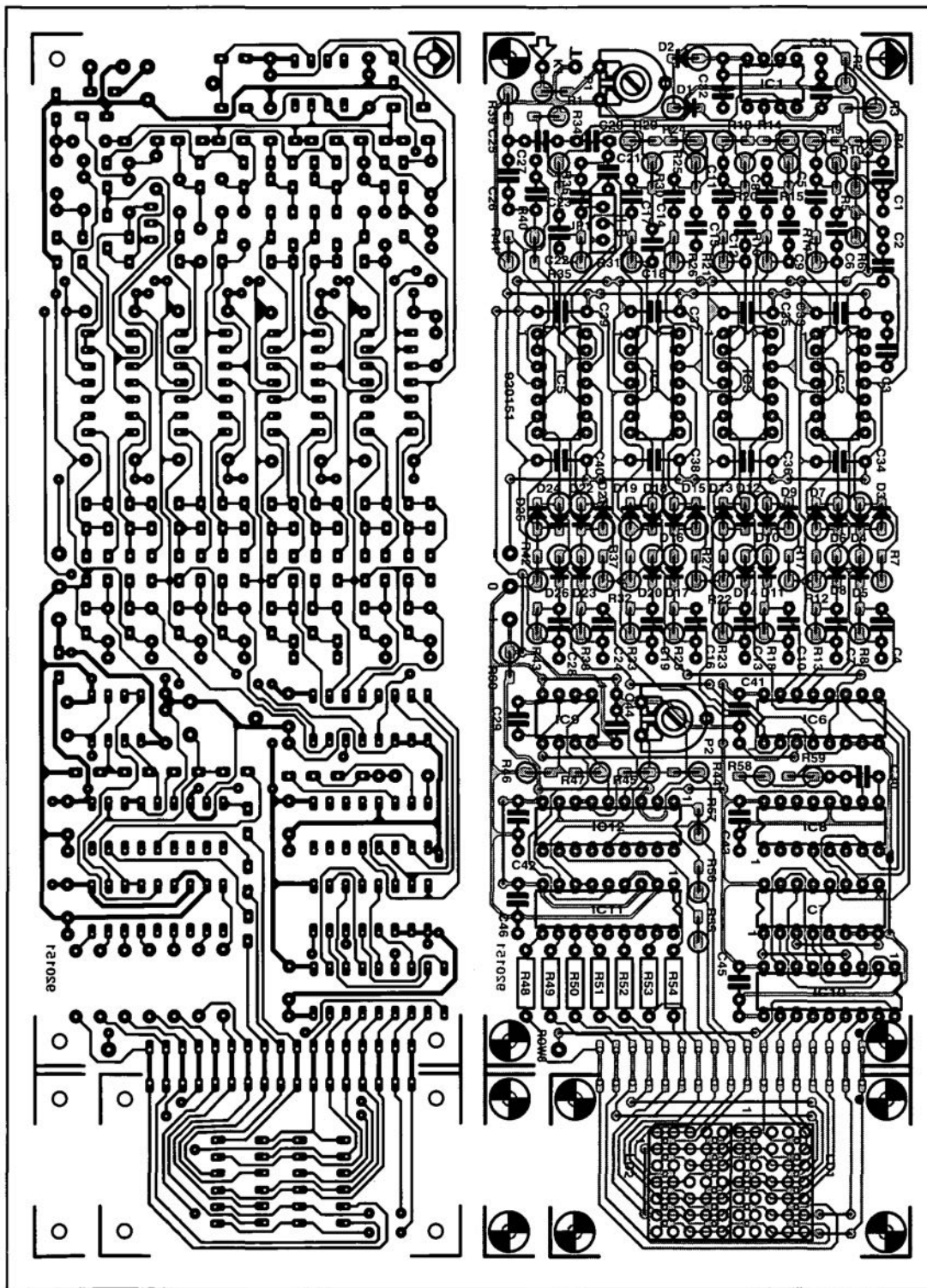
JP1=terminal strip with 3-way jump lead  
 K1=audio socket  
 LD1, LD2=display with 5×7 matrix, e.g., Kingbright Type TC07-11EWA (larger types: TC20-11EWA; 5×8:TC24-11EWA  
 PCB Type 920151 (see p. 70)

Filter	$f_c$ or $f_s$	Component values
IC <sub>2d</sub>	57 Hz	R4=267 k $\Omega$ ; R5, R6=249 k $\Omega$ ; C1=22 nF; C2=120 nF; C3=1 nF
IC <sub>2a</sub>	113 Hz	R9=274 k $\Omega$ ; R10= 11.8 k $\Omega$ ; R11=549 k $\Omega$ C5, C6=18 nF
IC <sub>3d</sub>	255 Hz	R14=324 k $\Omega$ ; R15=13.7 k $\Omega$ ; R16=649 k $\Omega$ ; C8, C9=6.8 nF
IC <sub>3a</sub>	577 Hz	R19=294 k $\Omega$ ; R20=12.4 k $\Omega$ ; R21=590 k $\Omega$ ; C11, C12=3.3 nF
IC <sub>4d</sub>	1030 Hz	R24=287 k $\Omega$ ; R25=12.1 k $\Omega$ ; R26=576 k $\Omega$ ; C14, C15=1.5 nF
IC <sub>4a</sub>	2940 Hz	R29=280 k $\Omega$ ; R30=12.1 k $\Omega$ ; R31=562 k $\Omega$ ; C17, C18=680 pF (polystyrene)
IC <sub>5d</sub>	6650 Hz	C20=309 k $\Omega$ ; R34=13.3 k $\Omega$ ; R35=619 k $\Omega$ ; R36=wire bridge; C22=not used; C21, C23=270 pF (polystyrene) Place JP1 in position B
IC <sub>5a</sub>	13600 Hz	R39=11.8 k $\Omega$ ; R40=2.37 k $\Omega$ ; R41=294 k $\Omega$ C25-C27=470 pF (polystyrene)
IC <sub>5b</sub>		R42=51.1 k $\Omega$ ; R43=4.7 M $\Omega$ ; C28=100 nF;

## Calibration

Connect the meter to a point in the amplifier where a strong signal is present; this is normally the loudspeaker terminal in an output amplifier. Make sure that the amplifier is fully driven. Turn P<sub>1</sub> so that IC<sub>1</sub> is just not overdriven. If an oscilloscope is not available, connect a multimeter, set to the 10 V a.c. range, to the output of IC<sub>1</sub>. If this is an inexpensive digital multimeter, use a low-frequency input signal, say, a couple of hundred hertz. Turn P<sub>1</sub> slowly till the meter reads 9.5 V r.m.s. Then, using an input signal at a frequency in the centre of the pass-band, say, 130 Hz or 340 Hz, adjust P<sub>2</sub> until the entire associated LED bar just lights. ■

Table 1. Component values and frequencies for eight filter sections.



R30=17.4 k $\Omega$ , 1%  
 R31=590 k $\Omega$ , 1%  
 R35=6.49 k $\Omega$ , 1%  
 R36=118 k $\Omega$ , 1%  
 R44, R45=390  $\Omega$   
 R46=1.0 k $\Omega$ , 1%  
 R47=30.9 k $\Omega$ , 1%  
 R48-R57=330  $\Omega$   
 R58=1 M $\Omega$   
 R59=68 k $\Omega$   
 R60=2.2  $\Omega$   
 P1=47 k $\Omega$  preset  
 P2=2.5 k $\Omega$  preset

**Capacitors:**

C1, C5, C6=12 nF  
 C2=33 nF  
 C3, C11, C12=1.8 nF  
 C4, C7, C10, C13, C16, C19,  
 C24=100 nF  
 C8, C9=4.7 nF  
 C14, C15=680 pF\*  
 C17, C18=270 pF\*  
 C20, C21, C22=470 pF\*  
 C29=100 pF  
 C30=1 nF  
 C31-C40, C44=47 nF, ceramic  
 C41, C42, C43, C45, C46=  
 100 nF, ceramic  
 \*polystyrene, axial

**Semiconductors:**

D1, D2, D4, D7, D10, D13, D16,  
 D19, D22=1N4148  
 D3, D5, D6, D8, D9, D11, D12,  
 D14, D15, D17, D18, D20,  
 D21, D23=BAT85  
 IC1=TL081  
 IC2-IC5=TL084  
 IC6, IC7=4051  
 IC8=4060  
 IC9=TLC272  
 IC10=UDN2585A  
 IC11, IC12=LM3915

**Miscellaneous:**

JP1=terminal strip with 3-way  
 jump lead  
 K1=audio socket  
 LD1, LD2=display with 5x7  
 matrix, e.g., Kingbright Type  
 TC07-11EWA (larger types:  
 TC20-11EWA;  
 5x8:TC24-11EWA  
 PCB Type 920151 (see p. 70)

Fig. 4. The printed-circuit board for the VU meter.

# Electricity from the wind

By Dr K.A. Nigim

Since the early 1890s, man has pioneered the technique of converting wind power into useful electricity. The development of engineering skills and the steady consumption of energy has speeded the development of the farm windmill into aerodynamically shaped turbines.

From the twenties, power from the wind was the main source of energy supply to rural areas worldwide. The modest reliability and social acceptability of the wind spinners encouraged researchers as well as environmentalists to seek ways to upgrade and increase the produced energy.

The energy crisis of the seventies revived the interest in wind power, and dozens of small wind machine manufacturers have started research into the means of increasing the generated capacity by introducing larger turbines and new designs.

Now, there are 45 companies worldwide specialized in manufacturing wind energy generators (WEGs) ranging from 100 W windmills (to charge 12 V batteries) to 4 MW windmills for direct connection to the national electricity network.

## Types of windmill

Practically, windmills are classified into two categories:

1. horizontal axis wind turbines (HAWT);
2. vertical axis wind turbines (VAWT).

Both categories are shown in Fig. 1. There are several shapes, each having its own merits and requiring certain strengths of wind speed to start spinning.

There are as many as 31 types of turbine, all serving to convert the kinetic energy of the moving air to an energy associated with a mechanical motion, which in turn is converted into electricity by an electrical generator.

Each turbine model will have the capability of producing electrical power,  $P_w$  as given by the equation

$$P_w = K_w \cdot C_p \cdot R^2 \cdot V^3,$$

where

$K_w$  is constant =  $0.5\pi \cdot A_d$  (air density);  
 $C_p$  is power coefficient, whose value depends on the shape of the turbine used; for example, it is equal to 0.45 for a two-bladed turbine as shown in Fig. 2;  
 $R$  is the radius of the area swept by the blades;  
 $V$  is the free stream wind speed.

This equation gives the value of the

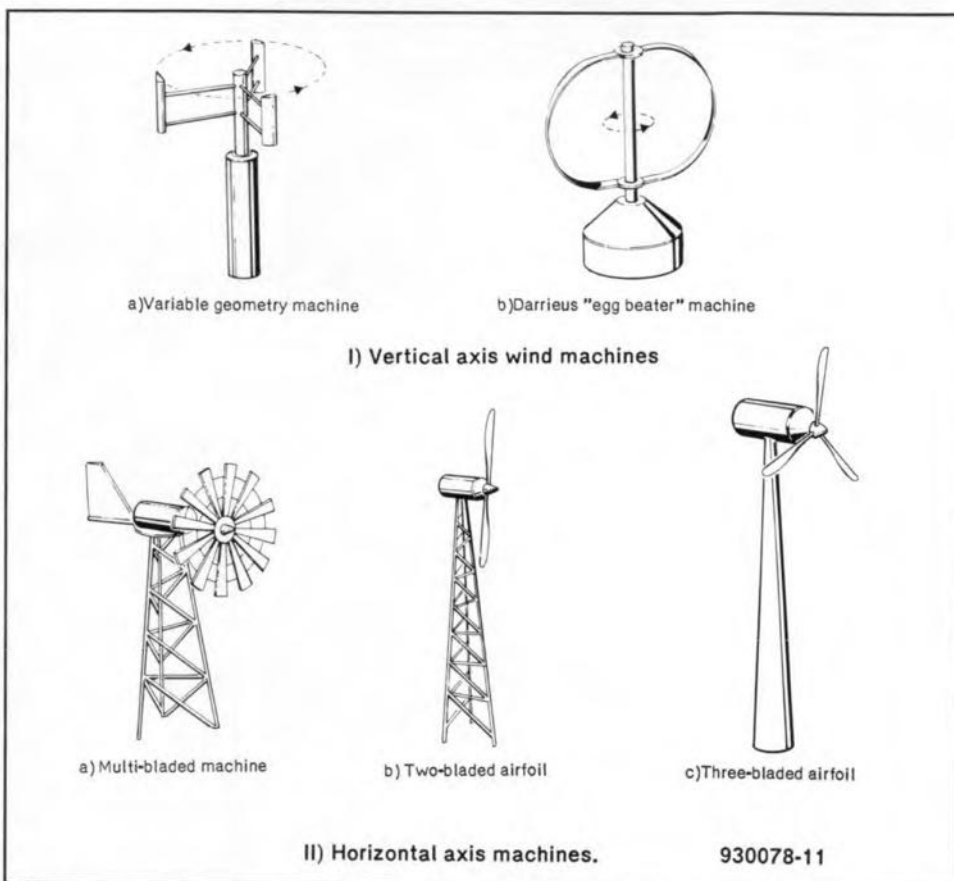


Fig. 1. Vertical axis and horizontal axis wind machines.

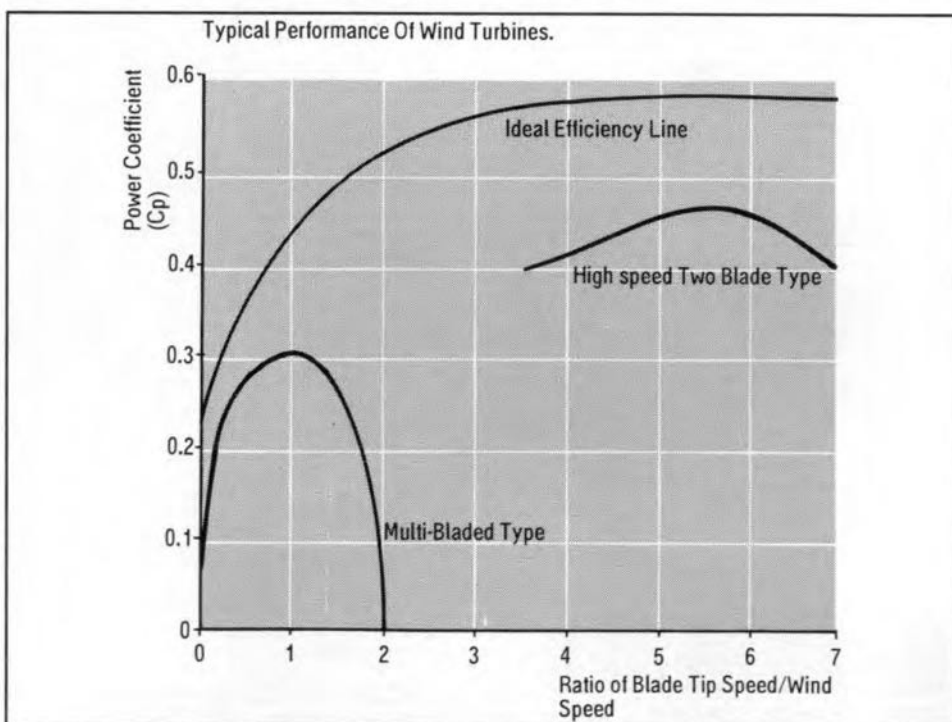


Fig. 2. Typical performance curves of wind turbines.



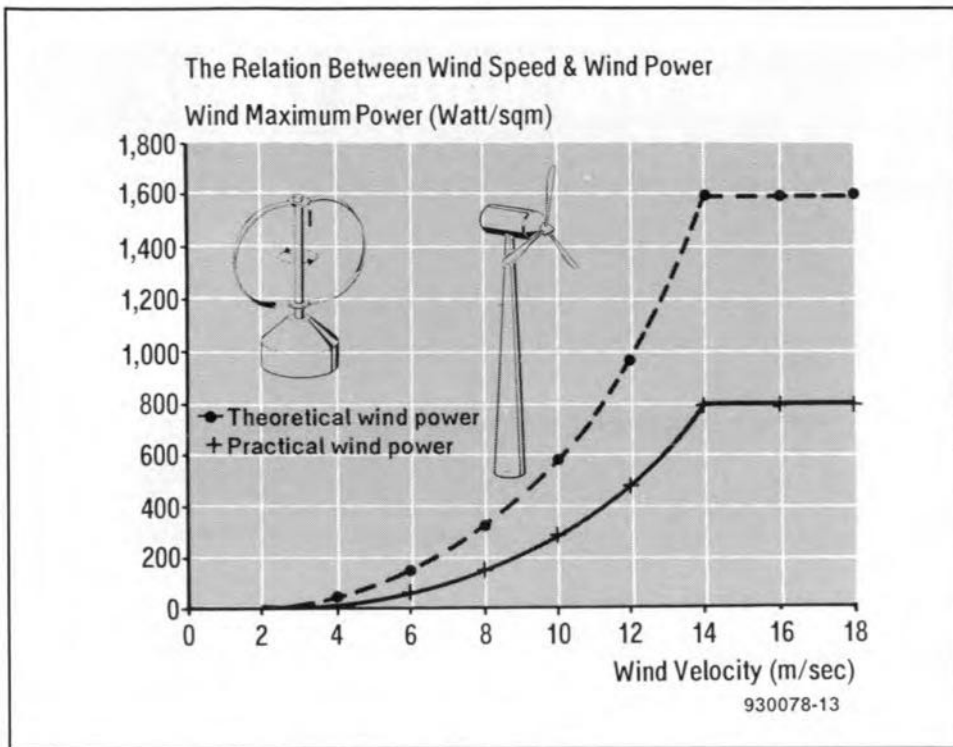


Fig. 3. Relation between wind speed and wind power.

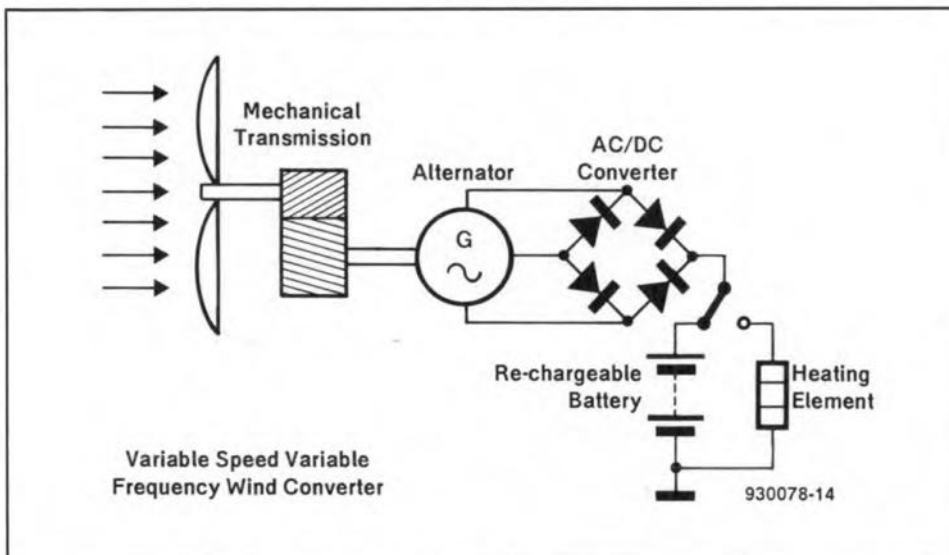


Fig. 4. Variable speed, variable frequency wind convertor.

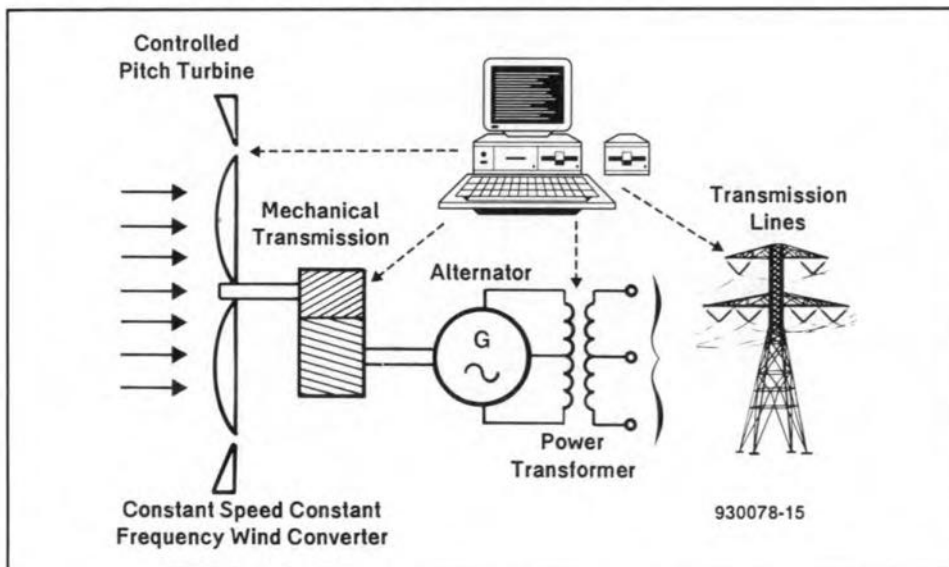


Fig. 5. Constant speed, constant frequency wind convertor.

maximum attainable power from a turbine. Owing to aerodynamic factors and other mechanical restraints, the power extracted is much smaller. A well-designed windmill achieves outputs that are 50–70% of the maximum theoretical power.

The dependence of power upon the cubic value of wind speed, as shown in Fig. 3, tends to limit the useful energy that can be extracted at low speeds. This fact presents a serious drawback to the use of wind converters in low wind-speed areas. On the other hand, gales are not welcome either, since they impose a danger to the mechanical parts of the wind turbines.

To overcome the unsteady nature of wind speeds, wind turbines are planted in groups located strategically around the selected site, which is known as a wind farm. In this way, a continuous supply of power may reasonably be expected at all times.

### Wind power to electricity

Horizontal and vertical axis wind turbines with rotor diameters of 60–100 m (200–300 ft), feeding electricity into the national grid systems, are now in operation at many sites in Europe and the USA. The various schemes for interconnecting the generated electricity with power lines or for the supply of isolated communities can be classified into three groups:

- a. variable speed, variable frequency (VSVF);
- b. constant speed, constant frequency (CSCF);
- c. variable speed, constant frequency (VSCF).

### VSVF generation

In this group, the generated output power is of variable voltage and frequency, so that the quality of the produced electricity is not suitable for household electricity supply. The turbine is coupled either to an alternator or to a DC generator and supplies energy to insensitive loads such as heaters.

One practical realization of this group is to use a 12 V permanent magnet alternator to charge a battery. Figure 4 shows a schematic of the essential parts needed to convert wind power to a useful DC battery charger. Windmills in this group are of relatively simple design.

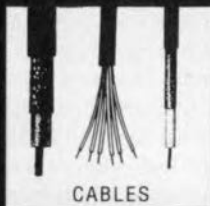
### CSCF generation

The usual approach to provide a constant frequency alternating electric power is to drive the generator at constant shaft speed, thus producing output power at constant frequency. This is a must for trading in electricity with the public and other generating companies.

In most constant-speed drive systems, a control mechanism is necessary to control the speed of the rotating shaft. One way to regulate fluctuation of the shaft speed is to use a hydraulically operated pitch controller to adjust the pitch of the turbine blades so that the input power is held fairly constant.

The technology and degree of refine-

**Call us now! We have the widest range of components available - At competitive prices!**



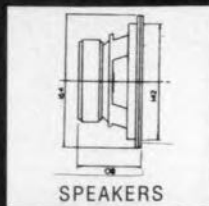
CABLES



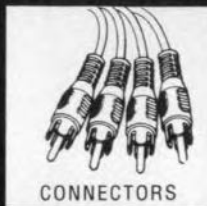
CAPACITORS



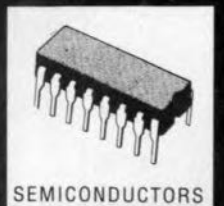
VIDEO HEADS



SPEAKERS



CONNECTORS



SEMICONDUCTORS

**CRICKLEWOOD**  
ELECTRONICS

Cricklewood Electronics Ltd. 40 Cricklewood Broadway, London NW2 3ET.  
Telephone: 081 452 0161 Faxsimile: 081 208 1441

All Major Credit Cards Accepted



ment involved in this scheme add to the initial costs of the windmill and it is, therefore, considered only for large wind turbines. Electricity is produced with two types of electrical machine as shown in Fig. 5. The electrical section is the standard type without the use of any power electronic devices.

### VSCF generation

VSCF generating systems are those that have no pitch control mechanism fitted. Such a system is defined as an assembly of rotating electrical machinery, assisted by power equipment that is capable of converting the variable speed of the rotating mechanical energy into standard electrical energy of constant frequency, meeting the generating companies' trading rules.

There are various successfully operating schemes that use standard electrical machinery whose output is controlled by power electronic devices that are controlled by microprocessors. Figure 6 shows a schematic diagram of a system widely used all over the world.

### The future

Already there is 324 MW of wind turbine generating capacity in the European Community. The greatest share of this is contributed by Denmark, which produces 1% of its electricity demand from the wind, with a target of increasing this to 20% by the turn of the century.

The Netherlands has similar plans. Enthusiasts in the UK, the area in the EC most exposed to wind, want to erect wind farms across the country and even out at sea to produce pollution-free electricity.

In the USA, special tax breaks have assisted in the creation of vast areas of the Californian desert to be planted with two and three bladed wind turbines. However, the technology used in many of these erected prototypes was not good enough and, although the windmills are still running, very little electricity is produced economically.

The experience of harnessing the wind is well shared by many developed countries. Geographic and demographic conditions pre-

vent many developing countries from installing a country-wide national grid for electricity distribution. The availability of windy sites is, therefore, greatly appreciated. Small-scale, isolated wind turbines are erected in the nearest suitable place. Integration between wind converters and conventional diesel engines is proving to be an economical solution to the need of continuous electricity demand.

Owing to the small size and/or the remote location of such power stations, the generating costs are markedly higher than the cost in interconnected national networks.

The present cost of electricity produced by wind generators in good wind sites is 2 to 3 times as high as that produced by conventional power stations. However, electricity from the wind is an environment-friendly energy source in spite of the noise the turbines produce during a breezy night.

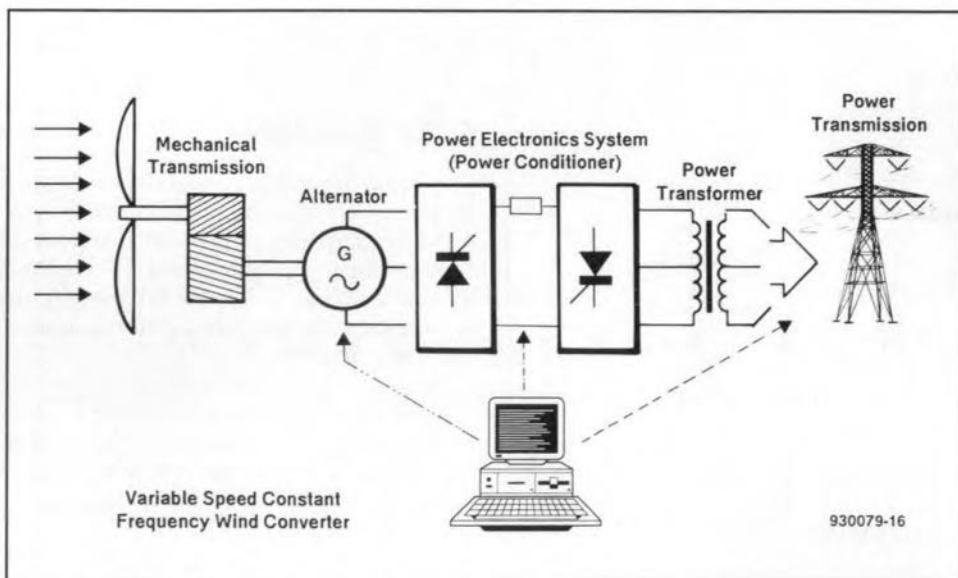


Fig. 6. Variable speed, constant frequency wind convertor

# INEXPENSIVE PHASE METER

Design by F. Hueber

The phase meter presented is based on just two CMOS ICs and a liquid-crystal display (LCD) to make it affordable with even the tightest budget.

The block schematic of the phase meter is shown in Fig. 1. Two amplifiers convert the input signal into a rectangular voltage that controls an edge-sensitive SR bistable (flip-flop). The average output of the bistable – between zero and the supply voltage – is directly proportional to the phase shift (0–360°). The measurement whose phase shift with respect to the reference signal at input B is to be determined is applied to input A. Every time the reference signal starts the positive half of its period, the leading edge of signal 1 sets the bistable. The bistable is reset when the phase-shifted signal at A starts the positive half of its period. In this way, the output of the bistable remains high longer the more the phase shift, that is, the average output voltage, increases. This is shown by timing diagrams 1 and 2 in Fig. 1.

Timing diagram 3 shows the situation when the phase shift is 0° or a multiple of 360°. In those cases, it may happen that sometimes the leading edge of input A occurs first and at other times that of the reference signal. This will cause the output of the bistable to fluctuate between zero and the supply voltage. The meter will then give an undefined or instable reading because the average voltage cannot be exactly zero (0°) or the supply voltage (360°). This is one of the (small) prices to be paid for simplicity.

Another is that when the input signals are removed when the bistable is set, the meter reading remains at 360°. This error may be obviated by first removing the reference signal (B) and then the signal from A.

## Circuit description

The two input channels are virtually identical—see Fig. 2. Only capacitors  $C_1$ ,  $C_7$  and  $C_9$  differ from their counterparts in the other channel. These capacitors serve to synchronize the phase pattern in the two channels.

Since the two channels are near-identical, channel B only will be discussed.

The signal—input at B—is applied to the circuit via  $C_1$ , shunted by calibration capacitor  $C_9$ , which prevents direct voltage being applied to the meter. Resistor  $R_2$  and diodes  $D_1$  and  $D_2$  provide protec-

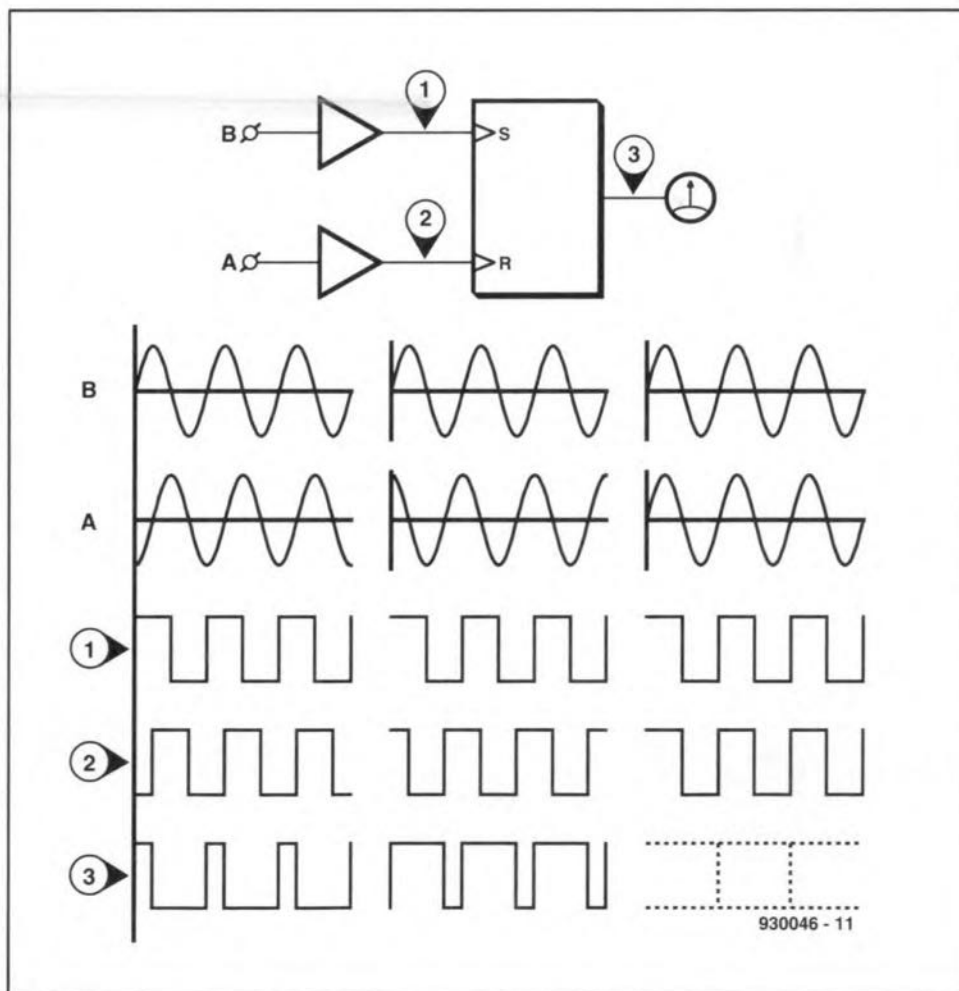


Fig. 1. The principle of the phase meter is quite simple.

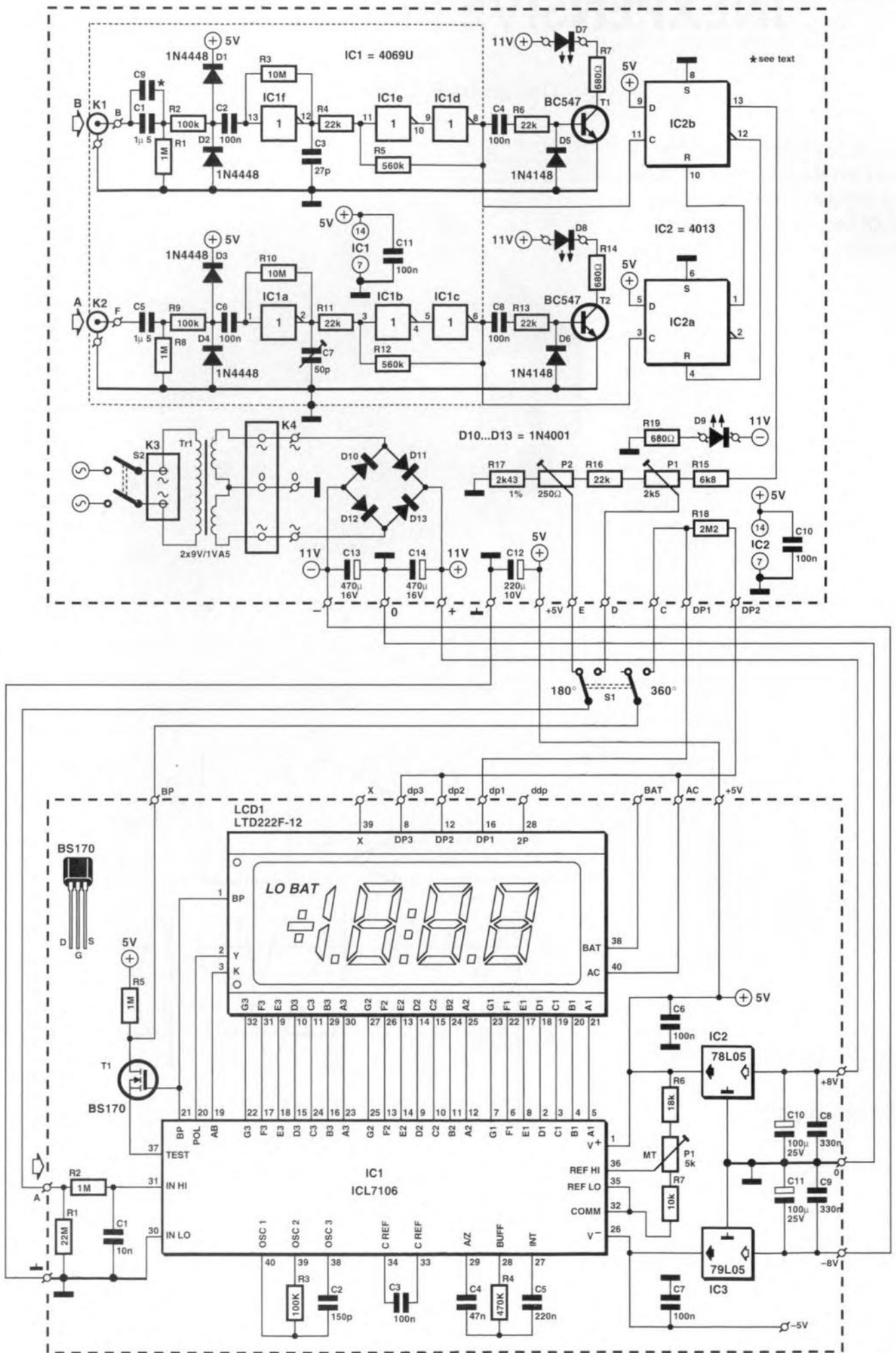


Fig. 2. Circuit diagram of the complete phase meter.

tion against too high alternating voltages at the input.

The signal is then applied to inverter IC<sub>1f</sub>, which is not buffered, so it can be converted into a linear amplifier. In fact, IC<sub>1f</sub> is arranged as an inverting amplifier, whose amplification is set to about  $\times 10$  by R<sub>2</sub> and R<sub>3</sub>. This arrangement is not immediately recognizable owing to the protection diodes. Capacitor C<sub>2</sub> prevents any direct voltage generated by the protection circuit reaching IC<sub>1f</sub>.

In contrast to that of a standard opamp, the input impedance of IC<sub>1f</sub> is not easily determined. This is because of the protection circuit (which has a lower impedance at high voltages) and also since the inverter is a less ideal amplifier than an opamp. The input impedance varies between 200 k $\Omega$  and 300 k $\Omega$ , which is in most cases high enough to prevent loading of the circuit on test.

The amplifier is followed by a Schmitt trigger that converts the amplified signal to a neat rectangular signal. The trigger is formed by two series-connected inverters, IC<sub>1d</sub> and IC<sub>1e</sub> that have been provided with a measurement coupling via R<sub>4</sub> and R<sub>5</sub>.

The signal is subsequently applied to bistable IC<sub>2B</sub> directly and to T<sub>1</sub> via C<sub>4</sub> and R<sub>6</sub>. The transistor is switched on briefly at each leading edge by the charging current through C<sub>4</sub> and this causes D<sub>7</sub> to light. This indicates that the signal is suitable for driving the bistable. If the LED goes out or flickers, the signal is too small or something else prevents the Schmitt trigger from regular toggling.

As already stated, the difference between the two channels is confined to a couple of capacitors that enable the phase behaviour in the two channels to be identical, or nearly so, over as large a frequency range as possible. This is particularly important at the extremes of the range, because where the frequency response

starts to roll off, phase shift ensues. This does no harm as long as the shift is the same in both channels and this is ensured by the calibration points.

The lower cut-off point is determined by the input circuit. Since the value of capacitors normally has a greater tolerance (usually 20%) than that of resistors, capacitors are used for calibrating. To that end, C<sub>1</sub> may be shunted by C<sub>9</sub>, which compensates small differences in value between C<sub>1</sub> and C<sub>5</sub> (C<sub>1</sub> and C<sub>5</sub> are compared and the smaller is fitted as C<sub>1</sub>).

The upper cut-off point is determined primarily by parasitic capacitances in the inverters, but also by the small differences in the switching thresholds of the Schmitt triggers (bear in mind that the resistors have a tolerance of about 5%). The latter effect is particularly noticeable at high frequencies. The overall effect is compensated by C<sub>3</sub> and C<sub>7</sub>.

The SR bistable is not a standard component, but is composed of two D-type bistables with reset input, IC<sub>2A</sub> and IC<sub>2B</sub>. The D-bistables are interconnected in such a manner that every time one of them is set (the D inputs are permanently high), the other is reset. Just as the usual edge-triggered SR bistable, the present one has a non-permitted state and this occurs when two leading edges appear simultaneously. In that state, it is impossible to say whether the circuit interprets this as a set or a reset. This is the cause of the fact that, in theory, the meter has no stable null and cannot stably indicate multiples of 360° (which the meter 'sees' as 0°). This sounds worse than what happens in practice, because a few tenths of a degree are sufficient to give a stable display. Unreliable display of the phase shift occurs mainly when the frequency of the input signal is not stable (jitter).

The phase angle is displayed by an LCD that was also used for the 'inductance/capacitance meter' published last year<sup>1</sup>. This shows, by means of filter R<sub>7</sub>-C<sub>1</sub>, the average value of the output voltage of the bistable.

Owing to the sensitivity of the DVM module and the fact that two meter ranges are required, the output voltage must be lowered to a suitable level. This is done with the aid of potential divider R<sub>15</sub>-R<sub>17</sub>-P<sub>1</sub>-P<sub>2</sub>. From that divider, the signal is applied to the meter via one contact of range switch S<sub>1</sub>. The other contact of this switch switches the decimal point to the backplane signal (AC) via R<sub>18</sub>; it is on when it is connected to inverted backplane signal (BP).

The power supply uses the voltage regulators in the DVM module. Thus, the output of the mains transformer is taken from the transformer board to the phase meter where it is rectified and buffered and then applied to the regulators in the DVM module, which hold the

voltage steady at  $\pm 5$  V. That voltage is then returned to the phase meter board. Note that the regulators can easily cope with the 11 V unregulated input, although the connections on the DVM module state 8 V.

Since the circuit draws only a small current, it is also possible to power it by two 9-V batteries. That saves a transformer and some other components. To reduce the current even further, high-efficiency LEDs should be used. The series resistors must then be increased to 3.9 k $\Omega$ .

## Construction

The printed circuit board for the phase meter and transformer is shown in Fig. 4. This board may be cut into two if, for instance, the transformer is not used. Even if the board is used as shown, it is advisable, because of the weight of the transformer, to use eight screws to fasten it. This results in a rather more rigid construction.

The input circuits must be screened along the dashed lines. The four soldering pins at the corners make this an easy operation. The lid should not be fitted until the calibration has been carried out (possible placing of C<sub>9</sub>). It is advisable to drill a hole in the lid through which C<sub>7</sub> can be adjusted. Because of the screen, it is best to connect the screened wires to K<sub>1</sub> and K<sub>2</sub> at the underside of the board. This must be done, of course, before the board is fitted into the enclosure.

The values of capacitors C<sub>1</sub> and C<sub>5</sub> must be checked with a capacitance meter. The larger value should be used in the C<sub>5</sub> position. The difference between the two values is compensated by C<sub>9</sub>. To start with, make the value of this capacitor the same as the difference; the optimum value can be determined during the calibration.

The PCB for the meter module is shown in Fig. 5. Start with placing the wire bridges, because at a later stage that may be next to impossible. Place IC<sub>1</sub> in a low-profile socket, so that the display neatly fits over it. In case this proves troublesome, insert an extra terminal strip into the terminal strip of the display, so that the LCD sits slightly higher.

Because of the intricate routing of the supply lines, it is advisable to check them thoroughly and to measure the voltage at various positions after the supply has been switched on.

Strictly speaking, the LEDs should not light when the supply is switched on, but the sensitive input channels may well pick up some noise, which is then processed as 'input'. This property may be used to advantage by touching the live input terminal with a finger. If the input channels function correctly, the associated LED should light. With S<sub>1</sub> in position 180°, the decimal point before the

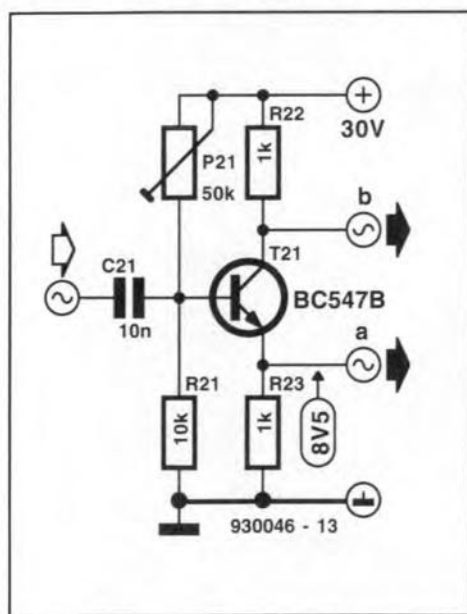


Fig. 3. Auxiliary circuit for calibrating the phase meter.

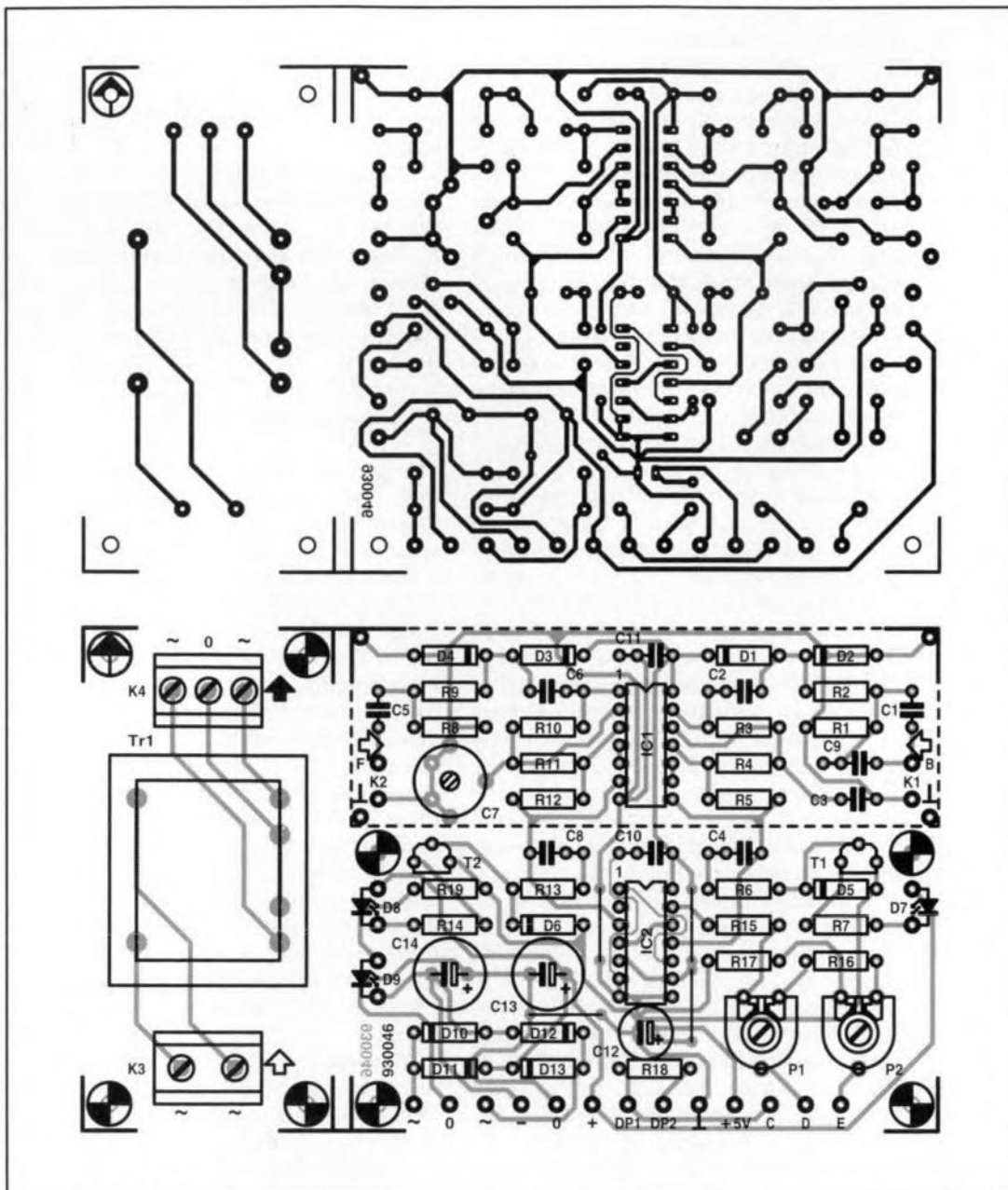


Fig. 4. Printed-circuit board for the phase meter and power supply. If necessary, the board is easily cut into two.

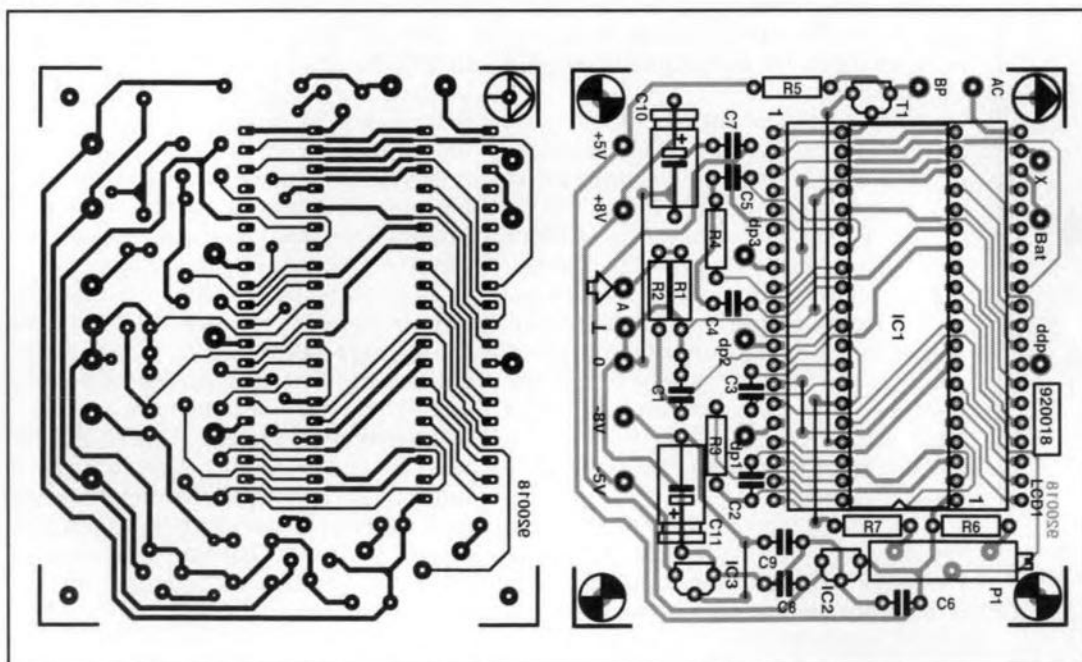


Fig. 5. Printed-circuit board for the meter module.

## PARTS LIST (Phase Meter)

### Resistors:

R1, R8 = 1 M $\Omega$   
 R2, R9 = 100 k $\Omega$   
 R3, R10 = 10 M $\Omega$   
 R4, R6, R11, R13, R16 = 22 k $\Omega$   
 R5, R12 = 560 k $\Omega$   
 R7, R14, R19 = 680  $\Omega$   
 R15 = 6.8 k $\Omega$   
 R17 = 2.43 k $\Omega$ , 1%  
 R18 = 2.2 M $\Omega$   
 P1 = 2.5 k $\Omega$  preset  
 P2 = 250  $\Omega$  preset

### Capacitors:

C1, C5 = 1.5  $\mu$ F, MKT  
 C2, C4, C6, C8, C10, C11 = 100 nF  
 C3 = 27 pF  
 C7 = 50 pF trimmer  
 C9 = see text  
 C12 = 220  $\mu$ F, 10 V, radial  
 C13, C14 = 470  $\mu$ F, 16 V, radial

### Semiconductors:

D1-D4 = 1N4448 or 1N4148  
 D5, D6 = 1N4148  
 D7-D9 = LED, red  
 D10-D13 = 1N4001  
 T1, T2 = BC547  
 IC1 = 4069U  
 IC2 = 4013

### Miscellaneous:

K1, K2 = BNC plug  
 K3 = 2-way terminal block, pitch 7.5 mm  
 K4 = 3-way terminal block, pitch 5 mm  
 S1 = DPCO switch  
 S2 = double pole mains switch  
 Tr1 = mains transformer, 2x9 V, 1.5 A  
 Enclosure 210x80x160 mm (8 1/4x3 3/8x6 5/16 in)  
 PCB Type 930046 (p. 70)  
 Front panel foil 930046-F (p. 70)

## (Meter module)

### Resistors:

R1 = 22 M $\Omega$   
 R2, R5 = 1 M $\Omega$   
 R3 = 100 k $\Omega$   
 R4 = 470 k $\Omega$   
 R6 = 18 k $\Omega$   
 R7 = 10 k $\Omega$   
 P1 = 10-turn preset, 5 k $\Omega$

### Capacitors:

C1 = 10 nF  
 C2 = 150 pF  
 C3, C6, C7 = 100 nF  
 C4 = 47 nF  
 C8, C9 = 330 nF  
 C10, C11 = 100  $\mu$ F, 25 V, radial

### Semiconductors:

T1 = BS170  
 IC1 = ICL7106  
 IC2 = 78L05  
 IC3 = 79L05

### Miscellaneous:

LCD1 = 3 1/2 digit LCD  
 40-pin low profile IC socket  
 2x20-way terminal strip  
 PCB Type 920018 (see p. 70)

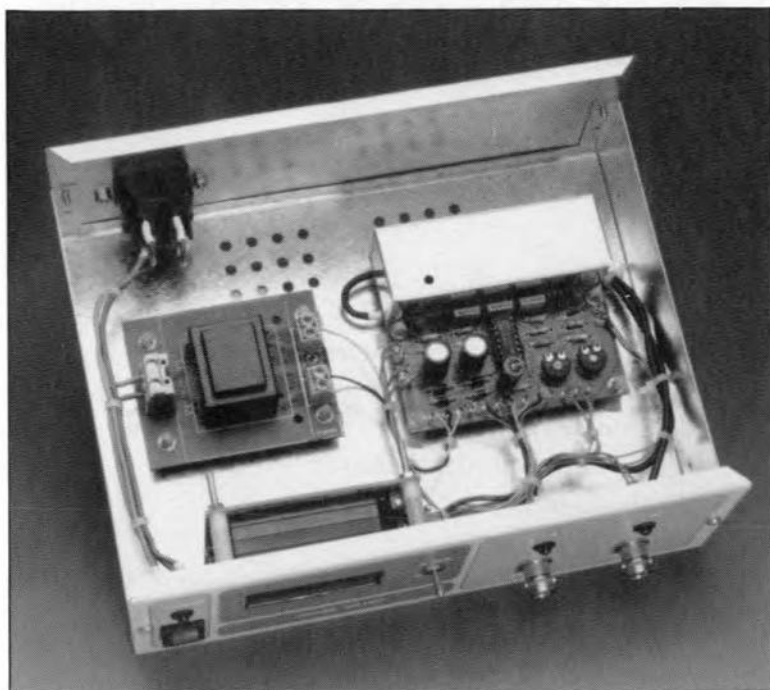


Fig. 6. Inside view of the completed phase meter.

last digit of the display should light. With a signal at input A (and input B short-circuited), the meter should read  $0^\circ$ . With a signal at input B (and input A short-circuited) and  $S_1$  in position  $360^\circ$ , adjust  $P_1$  until the meter reads  $360^\circ$ .

Preset  $P_2$  ( $180^\circ$  range) may be adjusted in a number of ways, but at all times with a 1000 Hz signal. One way is to use the  $360^\circ$  range as reference and to shift the signal by about  $180^\circ$  with the aid of an RC network. The preset is then adjusted until the meter readings in the  $180^\circ$  range and the  $360^\circ$  range are the same.

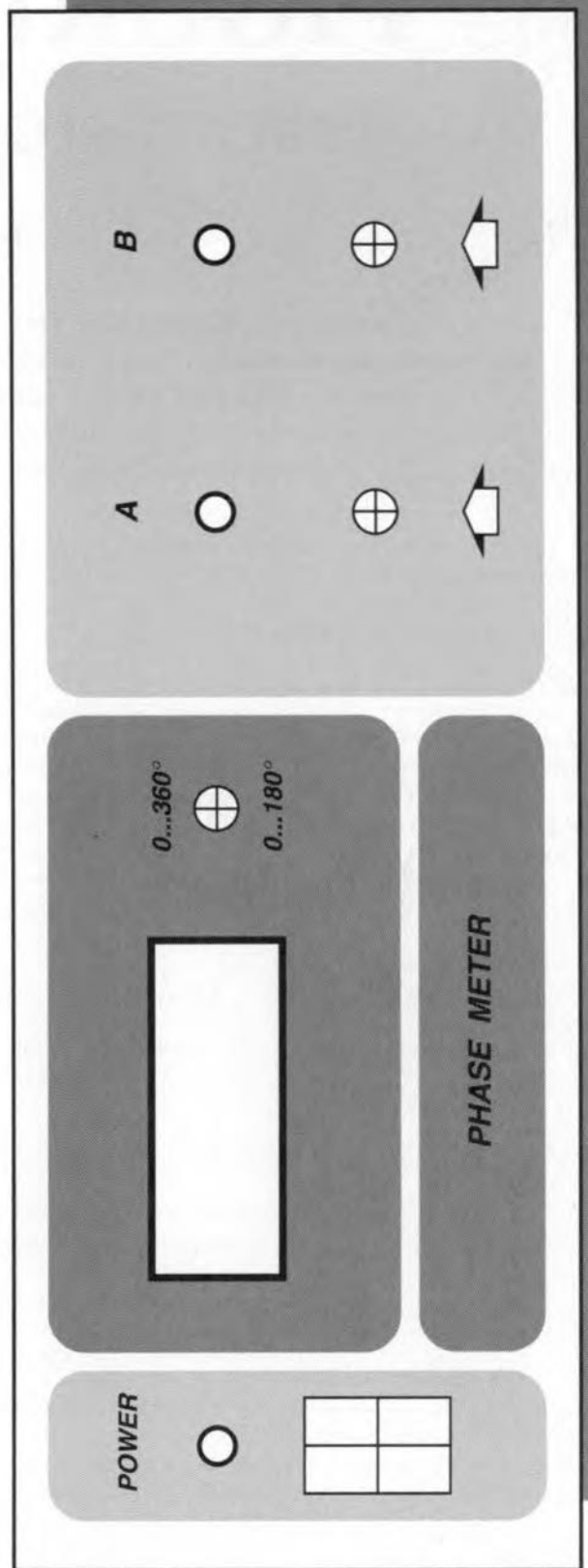
Another way is to use a signal source that can provide an output signal and its inverse (which is the same as one that is shifted by  $180^\circ$ ). Again, adjust  $P_2$  until the meter reads  $180^\circ$ .

A third method makes use of the auxiliary circuit in Fig. 3, which provides two signals that are one another's inverse. Adjust  $P_{21}$  in such a manner that the two signals look identical (or nearly so) on an oscilloscope. If an oscilloscope is not available, set  $P_2$  to obtain an emitter voltage of 8.5 V. An input signal of 100 mV is fine. With the auxiliary circuit connected to the phase meter, adjust  $P_2$  for a meter reading of  $180^\circ$ .

To determine the optimum value of  $C_9$  and to adjust  $C_7$ , either a signal source with inverted outputs or the circuit of Fig. 3 is required.

Start with lowering the frequency to between 100 Hz and 50 Hz. If everything is all right, the indicated phase angle ( $S_1$  in position  $180^\circ$ ) should not change by more than a few tenths of a degree. If it is more, the value of  $C_9$  must be made a little lower or higher (this has to be tried out). Do the same with a frequency of 30 Hz. Then, adjust  $C_7$  until the meter reads  $180^\circ$  again. If  $C_7$  cannot be made

Fig. 7. The front panel foil for the phase meter is available through our Readers' services (see page 70).



small enough, the value of  $C_3$  must be increased slightly. If  $C_7$  cannot be made large enough, shunt  $C_3$  with a small, say, 27 pF, capacitor.

Finally, carry out these tests at a few different frequencies to make sure that everything works all right. Readjust the relevant controls where necessary. Put the lid on the screening of the input circuits and close the enclosure. [930046]

#### References

1. 'Inductance-capacitance meter', *Elektor Electronics*, March, April 1992.

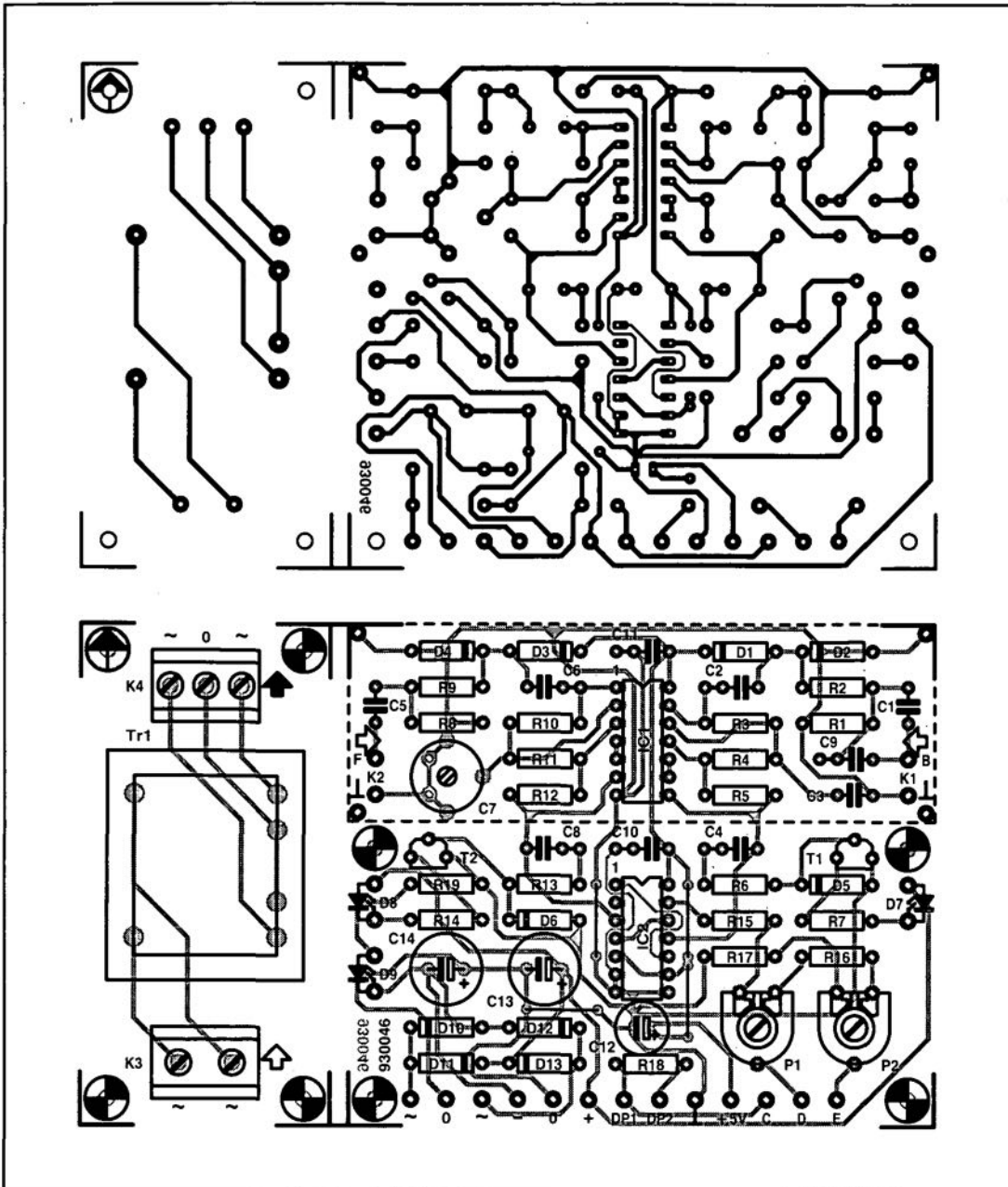


Fig. 4. Printed-circuit board for the phase meter and power supply. If necessary, the board is easily cut into two.

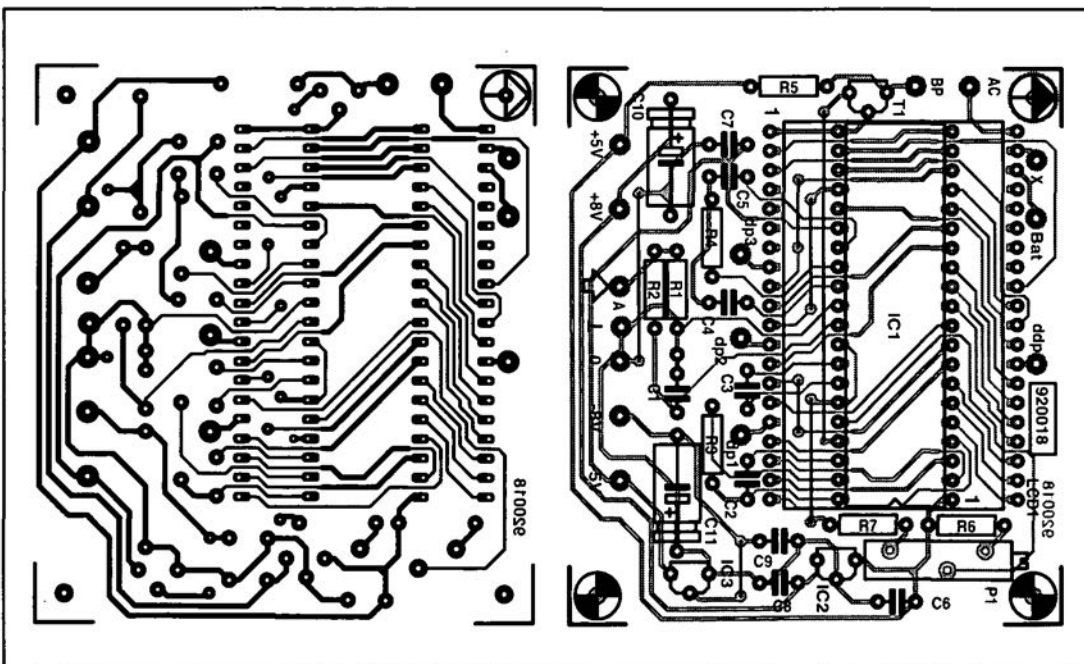


Fig. 5. Printed-circuit board for the meter module.

**PARTS LIST**  
(Phase Meter)

- Resistors:**  
 R1, R8 = 1 MΩ  
 R2, R9 = 100 kΩ  
 R3, R10 = 10 MΩ  
 R4, R6, R11, R13, R16 = 22 kΩ  
 R5, R12 = 560 kΩ  
 R7, R14, R19 = 680 Ω  
 R15 = 6.8 kΩ  
 R17 = 2.43 kΩ, 1%  
 R18 = 2.2 MΩ  
 P1 = 2.5 kΩ preset  
 P2 = 250 Ω preset

- Capacitors:**  
 C1, C5 = 1.5 μF, MKT  
 C2, C4, C6, C8, C10, C11 = 100 nF  
 C3 = 27 pF  
 C7 = 50 pF trimmer  
 C9 = see text  
 C12 = 220 μF, 10 V, radial  
 C13, C14 = 470 μF, 16 V, radial

- Semiconductors:**  
 D1-D4 = 1N4448 or 1N4148  
 D5, D6 = 1N4148  
 D7-D9 = LED, red  
 D10-D13 = 1N4001  
 T1, T2 = BC547  
 IC1 = 4069U  
 IC2 = 4013

- Miscellaneous:**  
 K1, K2 = BNC plug  
 K3 = 2-way terminal block, pitch 7.5 mm  
 K4 = 3-way terminal block, pitch 5 mm  
 S1 = DPCO switch  
 S2 = double pole mains switch  
 Tr1 = mains transformer, 2×9 V, 1.5 A  
 Enclosure 210×80×160 mm (8 1/4×3 3/8×6 5/16 in)  
 PCB Type 930046 (p. 70)  
 Front panel foil 930046-F (p. 70)

(Meter module)

- Resistors:**  
 R1 = 22 MΩ  
 R2, R5 = 1 MΩ  
 R3 = 100 kΩ  
 R4 = 470 kΩ  
 R6 = 18 kΩ  
 R7 = 10 kΩ  
 P1 = 10-turn preset, 5 kΩ

- Capacitors:**  
 C1 = 10 nF  
 C2 = 150 pF  
 C3, C6, C7 = 100 nF  
 C4 = 47 nF  
 C8, C9 = 330 nF  
 C10, C11 = 100 μF, 25 V, radial

- Semiconductors:**  
 T1 = BS170  
 IC1 = ICL7106  
 IC2 = 78L05  
 IC3 = 79L05

- Miscellaneous:**  
 LCD1 = 3 1/2 digit LCD  
 40-pin low profile IC socket  
 2×20-way terminal strip  
 PCB Type 920018 (see p. 70)



# FIGURING IT OUT

## PART 6 – FREQUENCIES AND FILTERS

By Owen Bishop

This series is intended to help you with the quantitative aspects of electronic design: predicting currents, voltage, waveforms, and other aspects of the behaviour of circuits.

Our aim is to provide more than just a collection of rule-of-thumb formulas.

We will explain the underlying electronic theory and, whenever appropriate, render some insights into the mathematics involved.

In Part 5 we looked at what happens when an alternating pd is applied to an inductor. In Fig. 43, the applied pd is given by

$$U = U_0 \cos \omega t, \quad [\text{Eq. 31}]$$

where  $U_0$  is the peak pd and  $\omega$  is the angular frequency (more about this in a moment). We then showed that the current through the inductor is given by

$$I = I_0 \sin \omega t. \quad [\text{Eq. 32}]$$

We compared these equations to demonstrate the facts that  $I$  has the same frequency as  $U$ , but lags behind  $U$  by  $\pi/2$  radian.

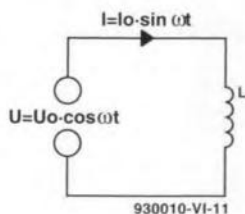


Fig. 43

First to clarify the quantity  $\omega$ . This is related to frequency by the equation

$$\omega = 2\pi f,$$

where  $\omega$  is in radian per second. Equation 31 could equally well be written as  $U = U_0 \cos 2\pi ft$ . In many instances, particularly when dealing with audio circuits,  $f$  is a more convenient quantity to use. However, it is often easier to deal with the single symbol  $\omega$  than the multiple  $2\pi f$  when integrating or differentiating, so we shall use either way of expressing frequency, depending on circumstances.

During the discussion of the

equations above, we derived an equation for  $I$ , in which

$$I = (U/\omega L) \sin \omega t.$$

At the time we said that the expression in brackets represents the peak value,  $I_0$ , of a sinusoidally varying current, immediately replacing the expression by  $I_0$  to produce Eq. 32. Now we will take time to look at this bracketed expression more closely. The expression gives the value of the peak current as

$$I_0 = U_0/\omega L.$$

This has the same form as the well-known equation for resistance:

$$I = U/R$$

and demonstrates that  $\omega L$  is the equivalent of resistance. It is the **inductive reactance** of the inductor and has the symbol  $X_L$ :

$$X_L = \omega L. \quad [\text{Eq. 33}]$$

Like resistance, inductive reactance is one of the elements of the total **impedance** of a circuit and is expressed in ohm ( $\Omega$ ). Equation 33 shows that inductive reactance is proportional to inductance, as would be expected. The equation also shows that, unlike resistance, it is proportional to frequency: as the frequency increases, so does the inductive reactance.

Example: calculate the reactance of a coil,  $L = 0.1$  mH, given a signal of (a) 100 Hz; (b) 1 MHz.

$$\begin{aligned} \text{(a)} \quad \omega &= 2\pi f = 200\pi = 628 \text{ rad s}^{-1}. \\ X_L &= 628 \times 0.1 \times 10^{-3} = 0.0628 \Omega. \end{aligned}$$

$$\begin{aligned} \text{(b)} \quad \omega &= 2\pi \times 10^6 = 6.28 \times 10^6 \text{ rad s}^{-1}. \\ X_L &= 6.28 \times 10^6 \times 0.1 \times 10^{-3} = 628 \Omega. \end{aligned}$$

### Capacitive reactance

In Part 5 we also showed that, if a capacitor is being charged with a sinusoidally varying pd (Fig. 44), the current flowing into the capacitor is:

$$I = C(dU/dt).$$

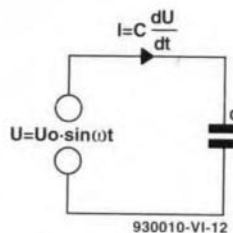


Fig. 44

Differentiating  $U_0 \sin \omega t$  as one of the standard differentials, we find:

$$I = C(\omega U_0 \cos \omega t).$$

As  $C$ ,  $\omega$  and  $U_0$  are all constants, we can replace their product with a single constant. The equation for current is, in fact, a cosine equation, where the single constant is  $I_0$ , the peak current. In other words,

$$I_0 = \omega C U_0.$$

The argument follows the same lines as that above, leading to the conclusion that the **capacitive reactance** is given by

$$X_C = 1/\omega C. \quad [\text{Eq. 34}]$$

Equation 34 shows that  $X_C$  has features that are the opposite of those of  $X_L$ . It is **inversely** proportional to both capacitance and frequency. The higher the frequency, the lower the capacitive reactance. This is another example of a pair of duals.

Example: calculate the reac-

tance of a capacitor,  $10 \mu\text{F}$ , given a signal of (a) 100 Hz, (b) 1 MHz.

$$\begin{aligned} \text{(a)} \quad \omega &= 628 \text{ rad s}^{-1}, \text{ as above.} \\ X_C &= 1/(628 \times 10 \times 10^{-6}) = 159 \Omega. \end{aligned}$$

$$\begin{aligned} \text{(b)} \quad \omega &= 6.28 \times 10^6 \\ X_C &= 1/(6.28 \times 10^6 \times 10 \times 10^{-6}) = 0.0159 \Omega. \end{aligned}$$

### Total impedance

The calculations above are for purely inductive and purely capacitive circuits, as illustrated by Fig. 43 and 44. Now, to examine what happens in a circuit in which all three elements are present in series, as in Fig. 45.

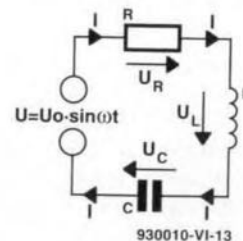


Fig. 45

Two facts are clear:

(a) The instantaneous current,  $i$ , through each of  $L$ ,  $C$ ,  $R$ , and the source is the same. If it were not, it would imply that current was leaking out of, or into, the circuit at some point.

(b) KVL applies to the instantaneous pds. The equation for the loop is:

$$U = U_R + U_L + U_C.$$

There are several ways of analysing the changing pds and currents in the circuit. Techniques using complex numbers or differential equations will be considered in a later issue. Here we adopt an approach that relies on geometry. The dif-

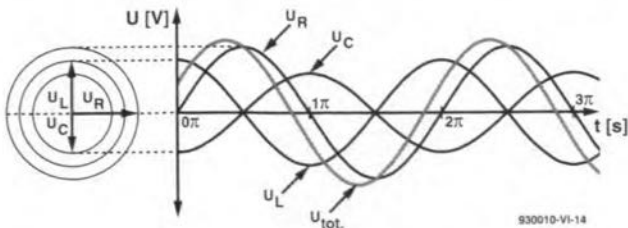


Fig. 46

difficulty with analysing this circuit is that the changing pds are usually not in phase with each other. The graphs of Fig. 46 show their relationships, with  $U_L$  leading  $U_R$  by  $\pi/2$  and  $U_C$  lagging  $U_R$  by the same amount.

The current is in phase with  $U_R$ , since the pd across a resistor and the current through it are always in phase. The three vectors on the left represent the pds at the instant corresponding to the extreme left of the graph. The relative lengths of the vectors depend on the impedances found in a particular circuit at a given frequency. Their relative directions, however, are always as shown in the figure.

Comparison with the graph shows that these vectors represent **peak** pds. As time passes, that is, as we move toward the right-hand end of the graph, we can imagine this array of vectors rotating anticlockwise (with angular velocity  $\omega$ ), each vector remaining the same length and the angles between them remaining unchanged. The pds peak in order:  $U_L$ , then  $U_R$ , and finally  $U_C$ . This can be seen by examining the curves in Fig. 46. Since the three vectors retain their relative magnitude and keep in phase with each other, we can add them for the position shown on the left of Fig. 46, knowing that rotation does not affect the result.

Figure 47 shows the pds added by vector addition. The first step is to add  $U_L$  and  $U_C$ , which is easy because they lie in exactly opposite direction ( $U_C$  is negative). Call their resultant the **reactance voltage**,  $U_X$ . This leaves us just two vectors,  $U_R$  and

$U_X$ , which are summed by drawing the diagonal of the vector rectangle. Since the vectors represent peak pds, the length of  $U$  represents the peak pd of the source.  $U_R$  is in phase with the current (as always), so it is clear from Fig. 47 that  $U$  is **not** in phase with  $I$ . This is the effect of the action of the capacitor and inductor. The **phase angle**,  $\phi$ , in this example is positive (a lead) but, if  $U_C$  had been greater than  $U_L$ , it would have been negative (a lag).

Looking again at Fig. 46, it can be seen that  $U_R$  is the dominant pd in this particular circuit.  $U_L$  and  $U_C$  are very similar in magnitude and, since they are out of phase with each other (leading and lagging  $U_R$  by  $90^\circ$ ) they almost cancel each other out. The  $U_{tot}$  curve in Fig. 46 is plotted by summing the point values calculated for the other three curves. Its peak value is slightly greater than that of  $U_R$ , and it leads  $U_R$  by a small phase angle, both features confirming the results of Fig. 47.

Since all the quantities are represented geometrically, it is easy to discover the equations that relate them. Figure 48 is the key diagram for all such calculations. In this diagram, the vectors represent impedances, not pds. Because the current is the same for all elements, a diagram of impedance vectors has the same proportions and angles as a diagram of pd vectors. The difference is just a matter of scale. In Fig. 48 the relative lengths of vectors differ from those in Fig. 47, which represent a circuit with different values of  $R$ ,  $L$ , and  $C$ .

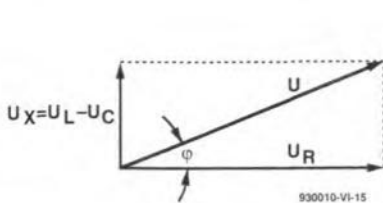


Fig. 47

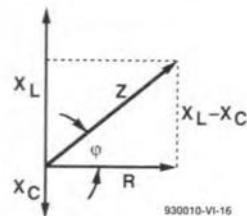


Fig. 48

Given the values of  $R$ ,  $L$ , and  $C$ , the first step is to calculate  $X_L$  and  $X_C$ , using equations 33 and 34. Then we can draw a sketch of the vectors (as in Fig. 48) and find:

1. The **total impedance**,  $Z$ : apply the Pythagoras theorem to the triangle enclosed by the vectors  $R$ ,  $(X_L - X_C)$ , and their resultant  $Z$ .

$$Z = \sqrt{R^2 + (X_L - X_C)^2} \quad [\text{Eq. 35}]$$

2. The **phase angle**,  $\phi$ .

$$\phi = \tan^{-1}[(X_L - X_C)/R] \quad [\text{Eq. 36}]$$

Note that since the calculations depend solely on the **proportions** of the rectangle, not on its absolute dimensions, the equations are independent of the magnitudes of the pds or the current. The circuit behaves the same, irrespective of the magnitude of the signal.

**Example.** Given  $R=100 \Omega$ ,  $L=100 \text{ mH}$ , and  $C=22 \mu\text{F}$ , connected in series, calculate their total impedance and the phase angle when the signal frequency is 500 Hz.

$$\begin{aligned} \omega &= 2\pi f = 1000\pi = 3141.6 \text{ rad s}^{-1}; \\ R &= 100 \Omega; \\ X_L &= 3141.6 \times 100 \times 10^{-3} = 314.16 \Omega; \\ X_C &= 1/(3141.6 \times 22 \times 10^{-6}) = \\ &= 1/0.069115 = 14.469 \Omega; \\ X_L - X_C &= 299.69 \Omega. \end{aligned}$$

$$\therefore Z = \sqrt{(100^2 + 299.1^2)} = 315.4 \Omega;$$

$$\phi = \tan^{-1} 299.1/100 = 1.25 \text{ rad.}$$

### What about j?

If you are reading this article in conjunction with an electrical or electronics textbook, you may have found that the text quotes the reactance of an inductor as  $j\omega L$  and that of the capacitor as  $-j/\omega C$ . The symbol  $j$  is used when expressing complex numbers and this will be explained in a future issue. For the moment, take  $+j$  to indicate that inductive reactance leads the current, and  $-j$  to indicate that capacitive reactance lags it. At present we are using the geometrical technique in which lead and lag are clear from the sketch of the vectors.

### Sinusoidal or not?

All the discussions so far have assumed that the source pd or the current varies in time according to a sine (or cosine) function. What happens if the waveform is not sinusoidal? What about

square waves or sawtooth waves, for example? As we shall see later in the series, all periodic waves can be treated as if they were the sum of a number of sine waves of various amplitudes with related frequencies. For example, the sawtooth wave of Fig. 49 is the sum of a sequence of terms which goes like this:

$$y = 3\pi - 6\sin t - 3\sin 2t - 2\sin 3t - \dots - (6/n)\sin nt$$

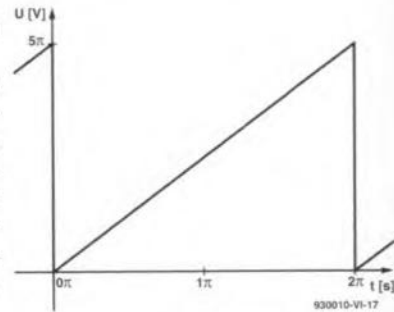


Fig. 49

The greater the number of terms summed, the more accurately the curve comes to look like a sawtooth wave. If we want to know how a circuit will behave with a sawtooth input, we analyse the waveform into its sinusoidal components, and calculate the impedances and phase angles for each component separately, as above. Then we sum the results. This may involve a lot of calculations, but it can be done, especially with the aid of a computer.

### Simpler circuits

Equations 35 and 36 cater for circuits in which all three kinds of impedance are present. If one source of impedance is absent, or so small that it can be ignored, we use the same two equations putting the absent impedance equal to zero. Consider the network of Fig. 50.

Since  $L$  equals zero (assuming that the self-inductance of the connecting wires and the leads of the capacitor is so small

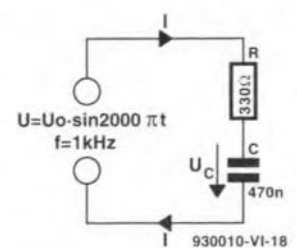


Fig. 50

that it can be ignored), the equations simplify to

$$Z = \sqrt{R^2 + X_C^2};$$

$$\phi = \tan^{-1} -X_C/R.$$

Given the values shown in Fig. 50:

$$\omega = 2000\pi = 6283.2 \text{ rad s}^{-1};$$

$$X_C = 1/(6283.2 \times 470 \times 10^{-9}) = 338.6 \Omega.$$

$$\therefore Z = \sqrt{330^2 + 338.6^2} = 472.8 \Omega.$$

$$\phi = \tan^{-1}(-338.6/330) = -0.80 \text{ rad}.$$

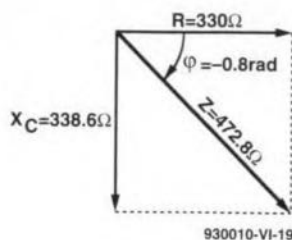


Fig. 51

Figure 51 shows the vectors. The current lags  $0.80 \text{ rad}$  (about  $45^\circ$ ) behind the pd. Since the same current flows through all components, the impedance vectors are proportional to the pd vectors. Thus,  $Z$  is proportional to the total pd applied to the network at any instant. The pd across the capacitor is proportional to  $X_C$ , and it can be seen that this pd lags about  $45^\circ$  behind the pd applied to the network.

We can also calculate the peak value of the alternating signal across the capacitor. Consider Fig. 50 to be that of a potential divider circuit. The current through  $R$  and  $C$  are equal (of course, no current actually passes through  $C$ , but current flowing to one plate is matched by current flowing from the other). Thus, the pd developed across  $R$  and across  $C$  is proportional to their impedances. The pd across  $C$  is calculated as for a potential divider. Taking pds at their peak values:

$$U_C = U(X_C/Z) = U(338.6/472.8) = 0.716U_0,$$

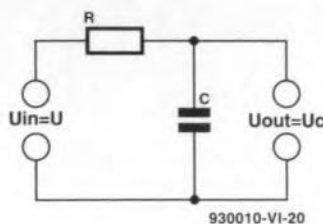


Fig. 52

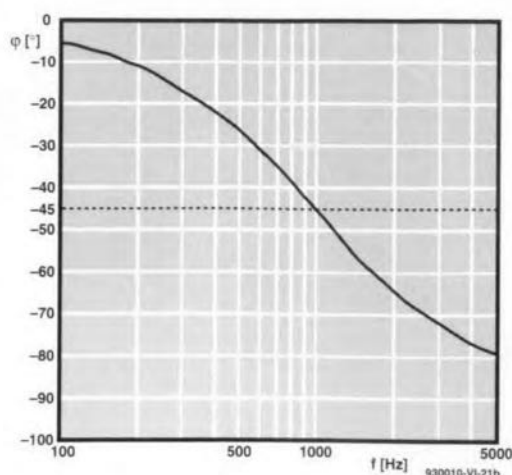
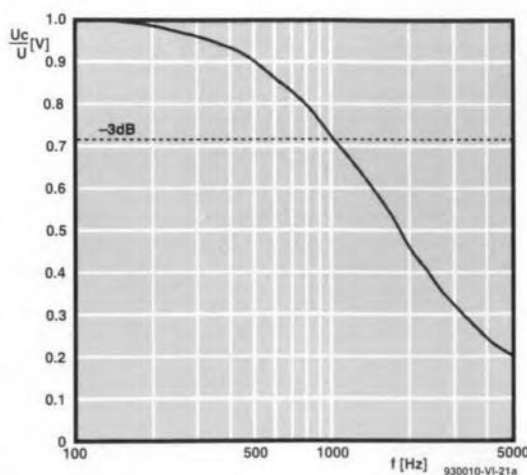


Fig. 53

or

$$U_C/U = 0.716.$$

Redraw Fig. 50 as in Fig. 52; call the total pd the **input pd**,  $U_{in}$ ; and call the pd across the capacitor the **output pd**,  $U_{out}$ .  $U_{out}$  is about 0.7 of  $U_{in}$ . The network attenuated the signal by roughly 0.3. The calculation assumes that the current drawn from the network by any load is insignificant.

## Frequency dependence

The calculations for Fig. 50 can be repeated for lower and higher frequencies and graphs plotted to relate phase lag and signal attenuation to frequency. As these graphs show (Fig. 53), phase lag approaches zero at low frequency and approaches  $-90^\circ$  at high frequencies. Remember that here we are considering the angle between  $U$  and  $U_C$  (or between  $Z$  and  $X_C$ ), not the angle between  $U$  and  $U_R$ . Attenuation approaches zero at low frequencies and gradually becomes more important at high frequencies. In fact, this network is a **low-pass filter**. The frequency chosen for the worked example (1000 Hz) is very close to what is known as the  $-3 \text{ dB}$  point. This is the frequency (1026 Hz for the specified component values) at which the output is 0.707 of the input (equivalent to a power attenuation of  $-3 \text{ dB}$  or 50%), and the phase lag is exactly  $45^\circ$ . It is the frequency at which  $X_C$  is equal to  $R$ , giving us the approximately  $45^\circ$  triangle of Fig. 51. We can find a formula for this frequency by equating  $R$  and  $X_C$ :

$$R = X_C = 1/\omega C = 1/2\pi f C.$$

Rearranging gives:

$$f = 1/2\pi RC.$$

**Example.** Find the  $-3 \text{ dB}$  point for a low-pass filter in which  $R=150 \Omega$  and  $C=2.2 \mu\text{F}$ .

$$f = 1/(2\pi \times 150 \times 2.2 \times 10^{-6}) = 482 \text{ Hz}.$$

## Other filters

The filter of Fig. 52 is converted to a high-pass filter simply by interchanging the resistor and capacitor. The vector diagram remains unchanged, but  $U_{out}$  is now the pd across the resistor. Thus, output **leads** input by  $45^\circ$  when  $R$  and  $X_C$  are equal and by greater or lesser amounts when the frequency is lower or higher. The  $-3 \text{ dB}$  point or **cut-off frequency** is calculated as for the low-pass filter.

A high-pass filter may also be constructed by substituting an inductor for the capacitor in Fig. 52. The  $-3 \text{ dB}$  point of such a filter occurs when  $R=X_L$ , so that at that point  $f=1/2RL$ .

A resistor, inductor and capacitor may be combined in a filter network such as that in Fig. 54. The output is the pd across the resistor. It is left to the reader to calculate  $U_{out}$  for a num-

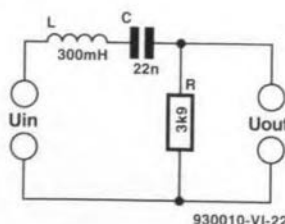


Fig. 54

ber of different frequencies in the range 100 Hz to 10 kHz, to observe the response, and say what type of filter this is. (Answer next month).

## Test yourself

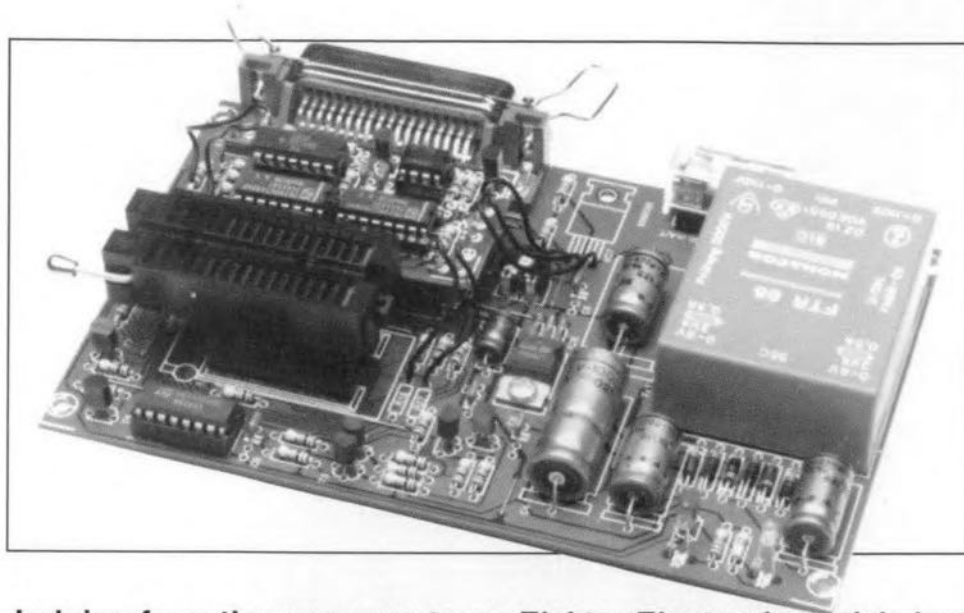
1. Calculate the angular velocity  $\omega$  for a signal of frequency 350 Hz.
2. What is the reactance of a  $33 \mu\text{H}$  inductor at (a) 50 Hz, (b) 10 MHz?
3. What is the reactance of a  $120 \mu\text{F}$  capacitor at (a) 2 Hz, (b) 10 kHz?
4. Draw the vector diagram for the circuit of Fig. 47, given that  $R=680 \Omega$ ,  $L=0.3 \text{ H}$ ,  $C=1 \mu\text{F}$ , and the signal frequency is 250 Hz.
5. Calculate the cut-off frequency for a low-pass filter in which  $R=12 \text{ k}\Omega$  and  $C=2.2 \mu\text{F}$ .
6. Given a  $10 \text{ k}\Omega$  resistor, what value capacitor is needed to form high-pass filter with its  $-3 \text{ dB}$  point at 500 kHz?

Answers will be given in next month's instalment.

## Answers to Test yourself (Part 5)

1.  $U=L(-0.5)=-0.05 \text{ V}$ . A constant back e.m.f. in the direction opposing the reduction of current.
2.  $U=0.2 \times -2e^{-2} = 7.33 \text{ mA}$ .
3.  $I=10000 \times [t^2]_0 = 0.09 \text{ A}$ . The constant of integration  $C/L$  cancels out when we evaluate the definite integral.

# GAL PROGRAMMER UPGRADE



Judging from the response to an *Elektor Electronics* article last year describing a low-cost GAL programmer, it looks like many of you have recognized the power of GALs, and have started programming these interesting devices. This article answers many readers' requests for a hardware extension plus upgraded software that allows more GAL types, including the industry standard 22V10, to be programmed.

Design by M. Nosswitz

AFTER some research into the programming algorithms of a number of relatively new GALs, the designer found out that only very small modifications were required to the original GAL programmer (Ref. 1) to enable it to handle even more GAL types.

The differences in GAL programming algorithms often concern the programming voltage and the signal timing. Hence, the two main programmer upgrades are (1) a variable programming voltage source and (2) modifications to the control software to implement the (complex) timing of the programming signals, and the variable programming voltage. The software automatically adapts to the GAL type in question, hence changes to the programming algorithms are transparent to the user.

In addition to GAL types 16V8(A) and 20V8(A), the upgraded GAL programmer is also capable of handling the B versions of these GALs, the 22V10, 20RA10 and the GAL6001. Programming the 6001 takes about one minute, which, admittedly, is not fast, but still useful. As regards the programming ability of different GAL brands (a subject on which we have received many letters), please do remem-

ber that the GAL programmer can only handle GALs manufactured by **Lattice**, **National Semiconductor** and **SGS/Thomson**.

## Hardware extension

Everyone who has successfully built the original GAL programmer should be encouraged to upgrade it with the present hardware extension. The circuit diagram shows that the extension is relatively simple. Circuits IC<sub>1</sub> and IC<sub>2</sub> (Type 4094s) together form an 8-bit shift register. The output of IC<sub>2</sub> drives IC<sub>3</sub>, a digital-to-analogue converter (DAC) Type ZN426. The DAC supplies an output voltage between 0.63 V and 1.92 V, which is programmable in steps of 20 mV. The DAC output voltage is applied to IC<sub>4</sub>, a Type CA3140 BiFET opamp, which replaces the LM317 voltage regulator originally fitted in the circuit. Apart from removing the LM317 from the board, the voltage divider around it has to be changed also. Resistor R<sub>27</sub> (270 Ω) is changed into 22 kΩ, and R<sub>26</sub> (2.7kΩ) into 1.8kΩ. Finally, preset P<sub>1</sub> (1 kΩ) is

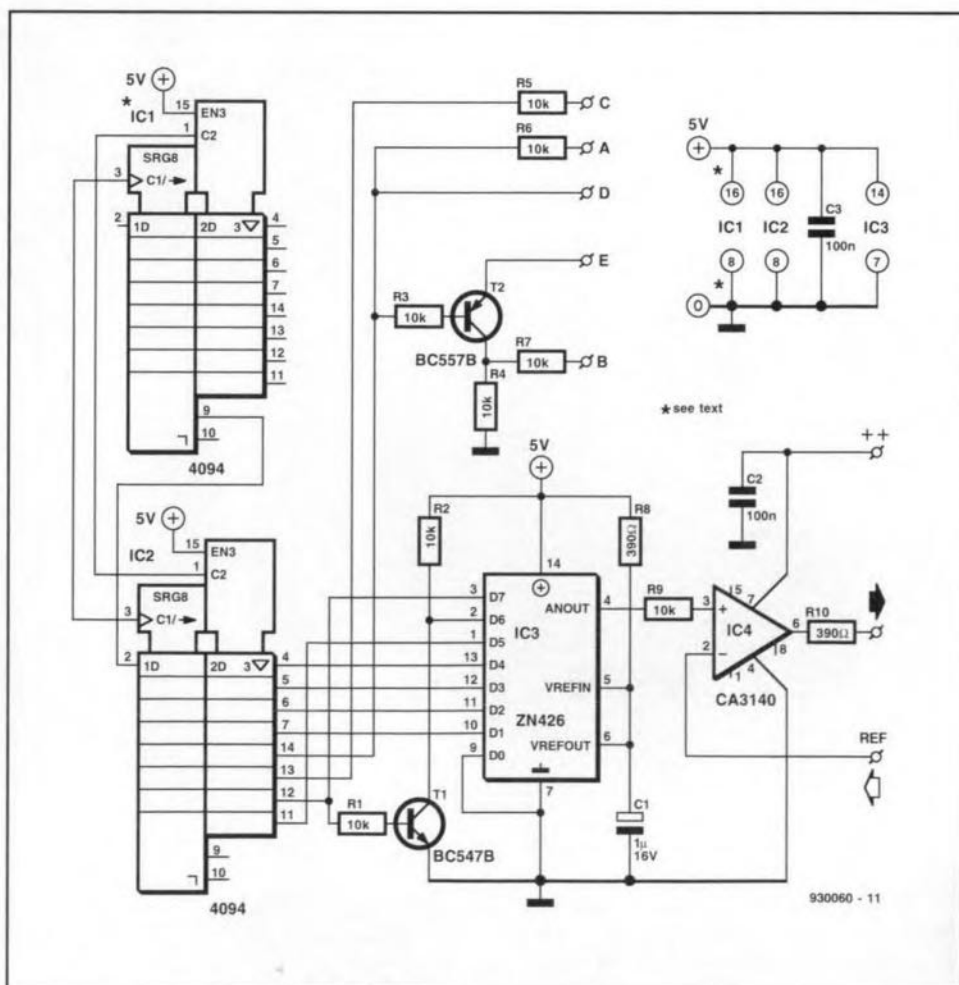


Fig. 1. Circuit diagram of the GAL programmer extension.

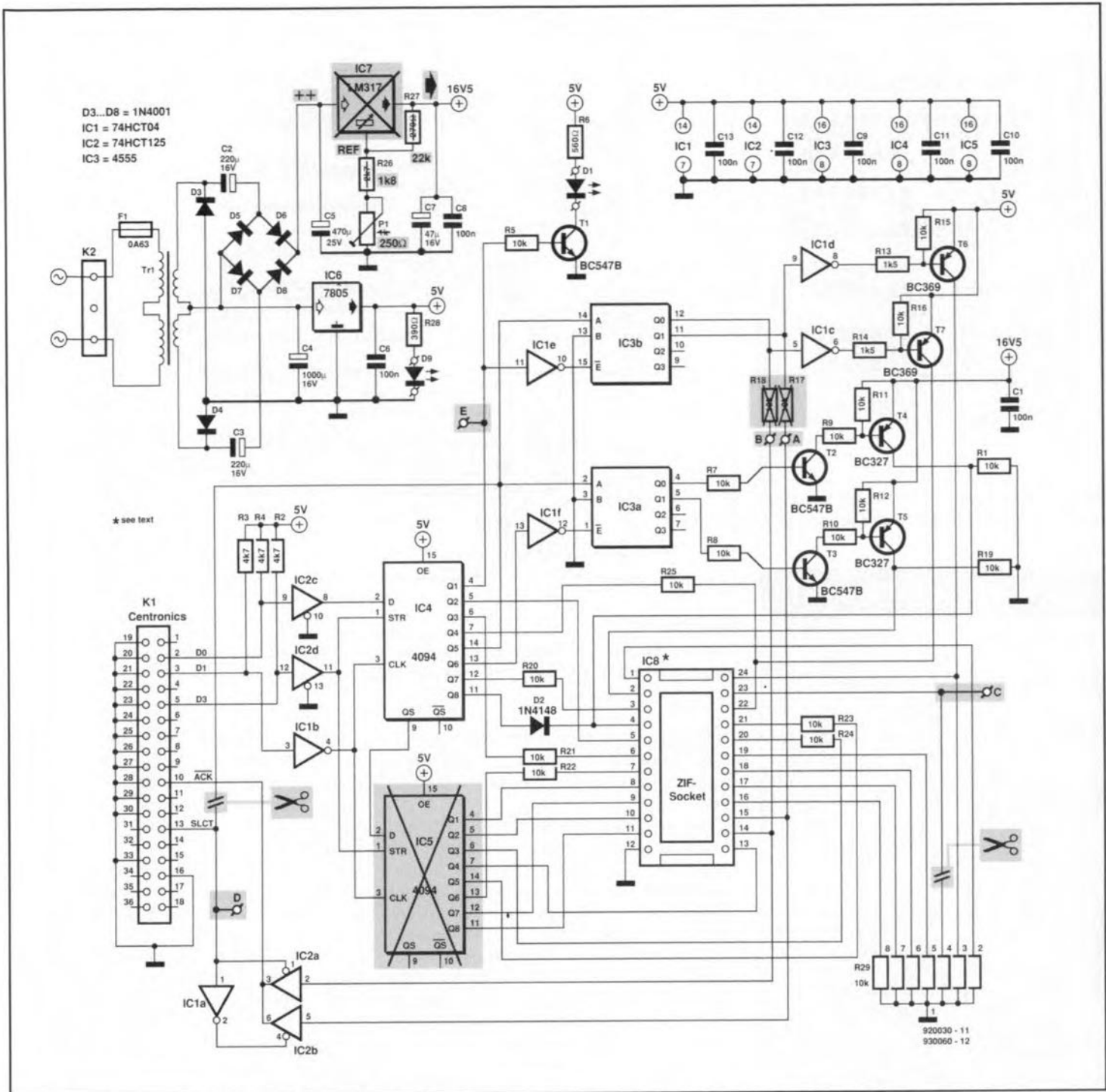


Fig. 2. This diagram shows where the original GAL programmer has to be modified to enable the extension to be integrated.

changed into 250 Ω (or 220 Ω). The opamp ensures a programming voltage range from 8 V to 23.75 V. For the sake of clarity, Fig. 2 shows the original circuit diagram with the modifications in shaded blocks.

The small board that contains the additional circuitry is fitted as an extension on to the main board. IC5 (a 4094) is removed from the main board, and replaced by the (extended) pins of the socket for IC1 on the extension board. This IC takes over the function of IC5 on the main board, and at the same time provides the connection of the supply voltage. IC2 on the extension board becomes the third element in the shift register consisting of IC4

on the main board, and IC1 and IC2 on the extension board. The third element is required to copy and latch the control word that represents the variable programming voltage. Furthermore, a number of output signals of IC2, marked A through E, are sent into the circuit. These signals are under software control, and, therefore, of little interest to the user.

### Construction

As already mentioned, the extension board is plugged into the empty socket in position IC5 on the main board. The track layout and component overlay of the extension board are given in Fig. 3.

IC1 on the extension board is mounted into two IC pin rows with extra long pins, or a wire-wrap socket. The long pins are pushed through the holes in the extension board, soldered at the track side, and inserted into the socket in position IC5 on the GAL programmer main board. First, however, the extension board has to be populated. Fit eight solder pins where the wires between the extension board and the main board are to be connected. Once the extension board is complete, you can proceed with the modifications to the main board.

Remove IC7 from the main board, and solder three lengths of insulated wire in the open PCB holes. Next, re-

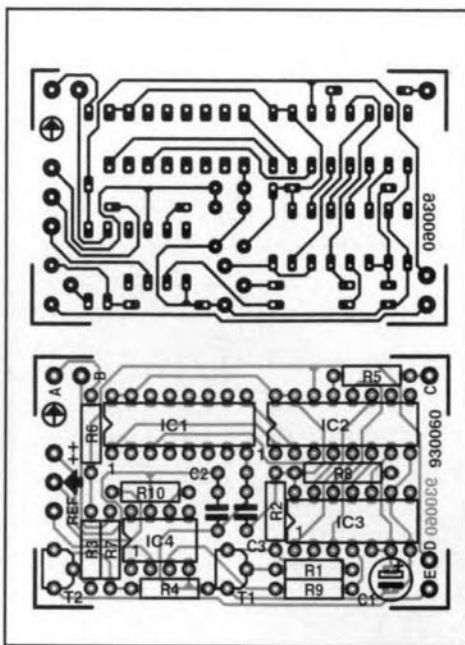


Fig. 3. Track layout (mirror image) and component overlay of the extension board.

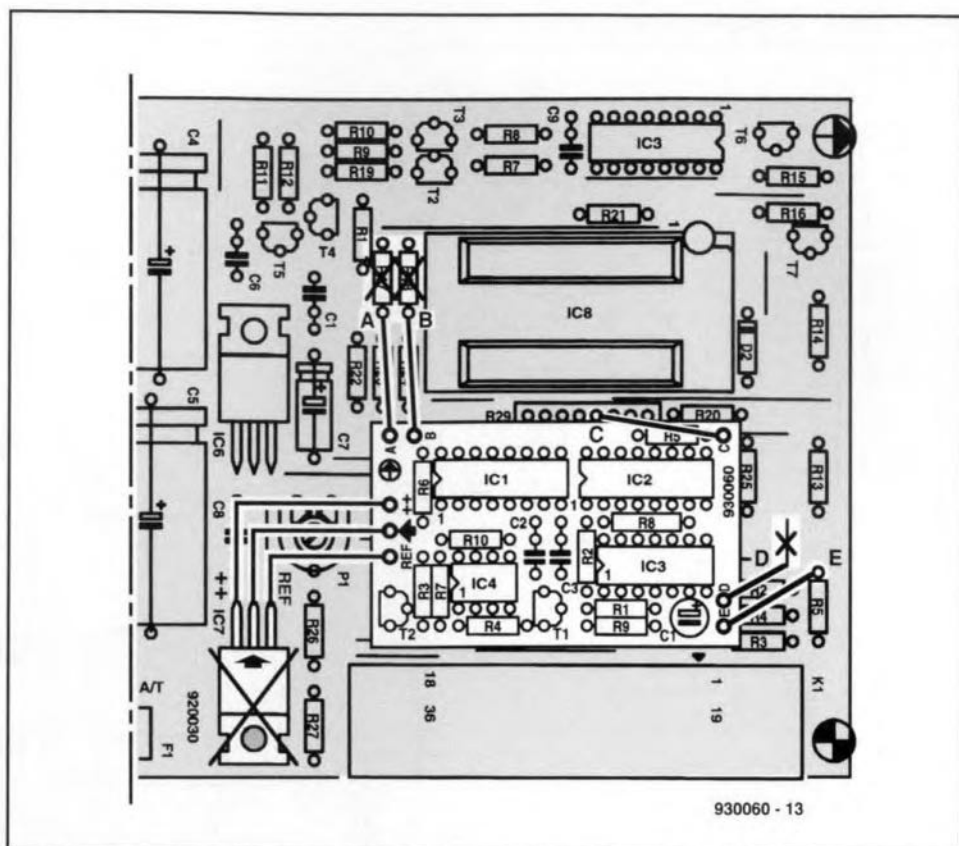


Fig. 4. This diagram tells you which components have to be changed on the main board, which wire link is removed, and where the eight wires are connected.

## COMPONENTS LIST

### Resistors:

8	10 k $\Omega$	R1-R7;R9
2	390 $\Omega$	R8;R10

### Capacitors:

1	1 $\mu$ F 16V tantalum	C1
2	100nF ceramic	C2;C3

### Semiconductors:

1	BC547B	T1
1	BC557B	T2
2	4094	IC1;IC2
1	ZN426	IC3
1	CA3140	IC4

### Miscellaneous:

- 1 DIL-16 wire-wrap socket, or two 8-way IC pin strips with long pins
- 1 Printed circuit board, order code 930060 (see page 70)
- 1 Software on disk, order code 1701 or 1881 (see page 70)

move resistors R17 and R18 from the board, and solder two wires into the holes nearest R23 and R24. The next job is a little more difficult: pin 4 of array R29 has to be disconnected from the PCB, and a short wire is inserted into the hole. If you find it difficult to actually pull the array pin out of the PCB hole, you may also cut it off (using a pair of precision pliers), and pull the remaining wire out of the PCB hole (while heating it with the solder iron, of course). Next, remove the wire link between R5 and R13, and fit a wire into the hole near R2/R5. The last wire is connected to the side of R5 that is close to the wire link you have just removed.

Replace resistor R27 by a 22-k $\Omega$  type, resistor R26 by a 1.8-k $\Omega$  type, and preset P1 by a 250- $\Omega$  (or 220- $\Omega$ ) type.

After plugging the extension board on to the main board, connect the eight wires to the appropriate solder pins. The drawing in Fig. 4 shows which components must be removed, and which connections are to be made.

That concludes the modification work, and only leaves preset P1 to be adjusted, which requires the use of the new GAL programmer software (ver-

sion 6.65 or later). Once you have the program running on your PC, type a colon (:) followed by a carriage return. Next, measure the voltage at pin 2 of the ZIF socket, and adjust P1 until you measure 16.5 V.

Finally, if you foresee programming GAL6001's, it may be necessary to replace the 7805 on the main board by a low-drop regulator such as the L4941BV or the L4940V5. This prevents thermal overloading of the regulator, which would cause the supply voltage to drop below about 4.75 V. In

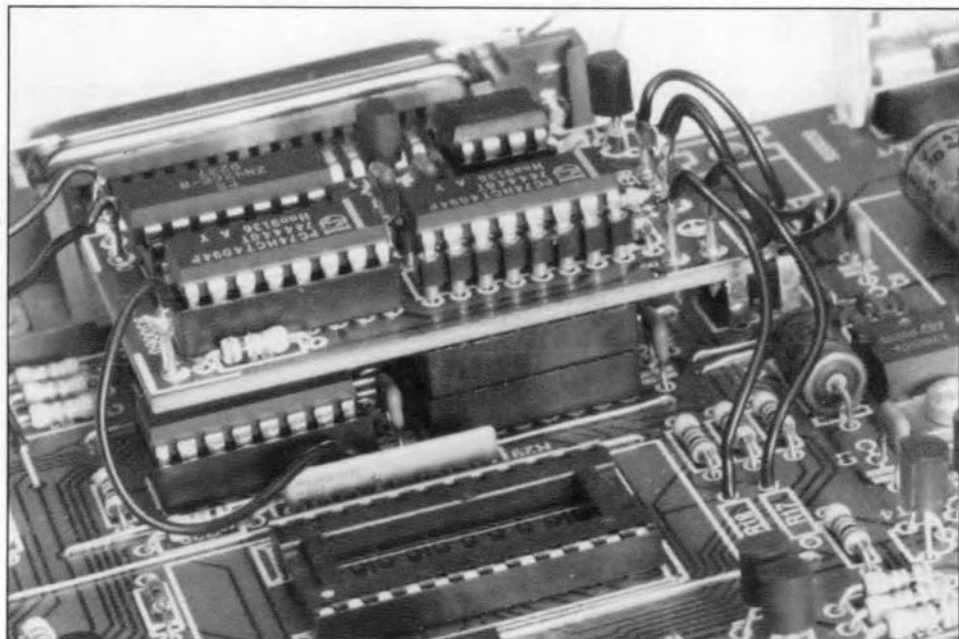


Fig. 5. Prototype of the extension board, plugged into the socket for IC5 on the main board.

some cases, this is harmful for the GAL6001.

## New software

The new features of the GAL programmer call for revisions to the existing control software. From the publication date of this article, the new version (6.65) of the GAL programmer software is supplied as Readers Services item 1701, which includes National Semiconductors's Opal Jr. demonstration software. Those of you who already have Opal Jr. may order the updated GAL programmer software only as item 1881 (one disk).

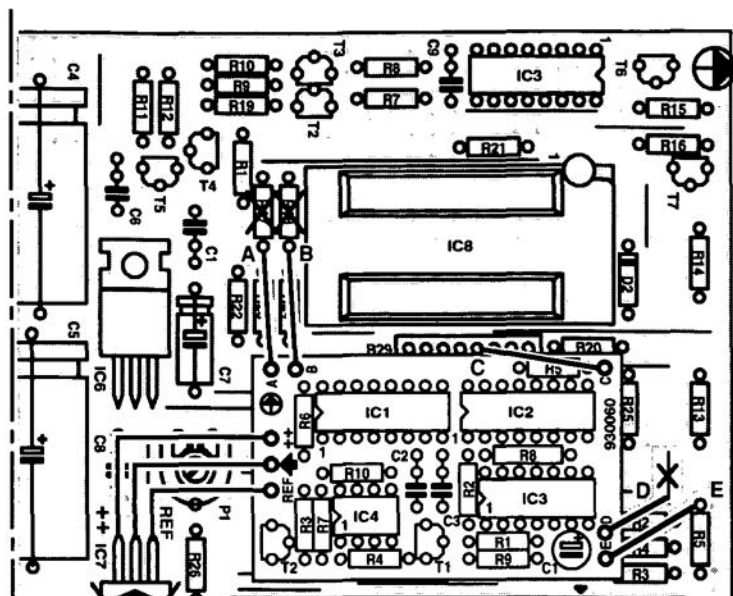
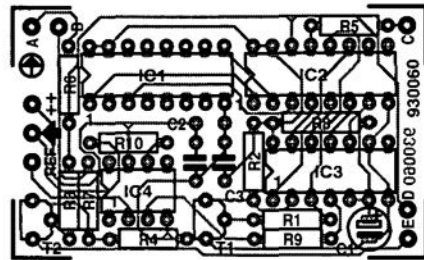
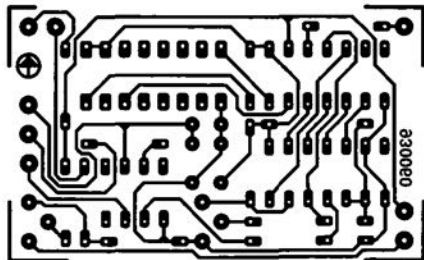
Finally, the new GAL programmer software includes a modified configuration file, called GAL665.CFG. This file, and the associated comment, is shown in Fig. 6. ■

```
GAL665.cfg
{license number}
{user number}
$3bc Address of Centronics port for GAL data exchange
1 GAL extension board no=0 yes=1
1 Change PES (program counter) no=0 yes=1
0 Switch for general RESET (EPROM, PROM, GAL) no=0 yes=1
1 Check if GAL hardware accessible no=0 yes=1
0 Select set security bit at power-up no=0 yes=1
1 Basic GAL type selection (16V8=1, 20V8=2, 16V8A=3, 20V8A=4,
75 beep length in ms 20V8A/B=4, 22V10=5, 6001=6, 20RA10=7)
2000 error beep frequency in Hz
2000 error display time in ms
1 Background colour Text (blue)
7 Foreground colour Text (bright grey)
5 Background colour Error reports (magenta)
7 Foreground colour Error reports (bright grey)
5 Background colour Letters (magenta)
15 Foreground colour Figures (white)
7 Background colour Selection window (bright grey)
1 Foreground colour Selection window (blue)
5 Background colour Selection bar (magenta)
14 Foreground colour Selection bar (yellow)
4 Background colour Changed cells (red)
7 Foreground colour Changed cells (bright grey)
5 Top of paper margin (in lines) (printing)
8 Left margin (printing)
```

Fig. 6. GAL programmer version 6.65 configuration file listing.

### Reference:

1. GAL programmer. *Elektor Electronics* May 1992.





# GAL PROGRAMMER SOFTWARE FOR AMIGA

SOFTWARE to control the GAL programmer is now also available for the Amiga series of computers. The Amiga software consists of two programs, AmiGAL and AmiBURN, with associated (extensive) documentation files that can be printed from disk. The disk also contains an installation instruction file.

AmiGAL is a GAL logic function editor, while AmiBURN is the actual programming software. Interestingly, AmiGAL is capable of generating JEDEC files, and has a built-in Minterms (minimal terms) generator that can help you reduce complex logic equations into a form suitable for implementation with the aid of GAL cells. AmiBURN reads the files produced by AmiGAL (or any other program capable of outputting JEDEC format files), and sets up the programming conditions required for the selected GAL. Functions like making master GALs, actuating the read protection in a GAL, device copying, producing cell hard copies, and much more, are available.

AmiGAL and AmiBURN are fully menu-driven, and make full use of the Amiga's graphics power. They can be run on all types of Amiga with 512 KBytes of memory or more. Before running the software, a small hard-



ware modification is required: pins 10 and 11 of the Centronics connector must be interconnected. Fortunately, this modification still allows the programmer to be used with a PC. The

Amiga GAL programmer software may be ordered through our Readers Services as item **1841** (see page 70). ■

# DIGITAL FREQUENCY READOUT FOR VHF/UHF RECEIVER

g260014 - IA

The wideband AM/FM receiver<sup>1</sup> described last month is not complete without a dial that tells you the transmit frequency of the station you are listening to. Such a tuning dial is described here — it takes the form of a sensitive 4-digit frequency meter with a preset option and a maximum input frequency of well over 30 MHz. Also suitable for general use in your workshop!

Design by L. Pijpers

THE circuit diagram of the frequency meter (Fig. 1) is not too complex, which is mainly by virtue of the use of an integrated counter/display driver Type ICM72117AIP1 from Harris Semiconductor. The display circuit is shown separately in Fig. 2.

The function of the ICM72117AIP1 is changed from a counter only into a frequency meter by IC5 and IC6d. The timebase consists of a crystal oscillator, X1-IC2, and a divider chain, IC2, IC3 and IC5. The input signal arrives at divider IC4 via a transistor preamplifier, T1. The digitized and scaled down input signal is applied to the counter IC input (pin 8) via gate IC6d, which functions as an electronic switch. IC6d is enabled during the gate time (measurement period) by pin 12 of IC5. Diodes D1-D16 serve to give to the counter a certain preset value — this will be reverted to below.

The time base pulse that controls the closing of IC6d must be accurately

times to ensure the correct gate time for the counter. The timing diagram of the timebase generator, IC5, is shown in Fig. 3. The numbers 0-9 at the left of the diagram represent the Q outputs of IC5. As indicated, these outputs go high successively on each pulse applied to the clock (CLK) input. The CO (carry out) output of IC5 is high when one of the outputs Q0-Q4 is high also. The CO output is low during the rest of the time, i.e., when one of the outputs Q5-Q9 is high. This means that the CO output supplies a symmetrical rectangular signal whose frequency equals  $\frac{1}{10}$ th that of the input clock signal. When the CO output of IC5 is high, IC6d is enabled, so that the count pulses arriving via T1 and IC4 are fed to the count (CNT) input of IC1. The number of pulses counted during the gate time is stored in a 4-digit counter contained in IC1.

When the gate time has elapsed, the count value is fed to the 4-digit LED

display. This happens when output Q5 of IC5 goes high, whereupon IC6a supplies a 'low' to the store input of IC1.

The counter memory is cleared (reset to zero) at the start of every count cycle by a logic 'high' on Q7 of IC5, which is fed to the RESET\ input via inverter IC6b. The counter preset value defined with the aid of diodes D1-D16 is loaded into the counter when output Q8 of IC5 pulls the 'load counter' (LC) input of IC1 logic 'high'.

The input of the frequency meter is connected to prescaler output 'F' or 'G' of the Philips TV tuner in the VHF/UHF receiver. To refresh your memory, this tuner output supplies the local oscillator (LO) frequency divided by 256. The signal level is about  $1 V_{pp}$ , which is too small to drive the digital frequency meter directly. Furthermore, the signal edges are not steep enough. These problems are resolved by the circuit around transistor T1, which acts as a preamplifier and signal shaper that turns the prescaler output signal into a neat rectangular wave with a level of  $5 V_{pp}$ , suitable for driving the clock input of counter IC4.

IC4 divides its input signal by  $2^7$ , which gives a total LO frequency scale factor of  $2^{15}$  ( $2^8 \times 2^7$ ). This means that the highest frequency at pin 13 of IC6d is about 30 kHz.

To obtain a readout in megahertz ( $10^6$  Hz), a timebase of  $1 \times 10^{-6}$  s is required, which means that the period of the gate signal is  $2 \times 10^{-6}$  s, or 0.5 MHz. This is achieved with the aid of dividers contained in IC2, IC3a and IC3b, which scale the 8-MHz clock signal generated by the oscillator in IC2 down by a factor  $2^{19}$  ( $2^3 \times 2^{1 \times 15}$ ). Note, however, that the timebase signal is divided by 10 in IC5 before it is available at the CO output. Although this results in a display reading that is ten times too high, it increases the counter accuracy, and is simple to correct visually by lighting the decimal point on



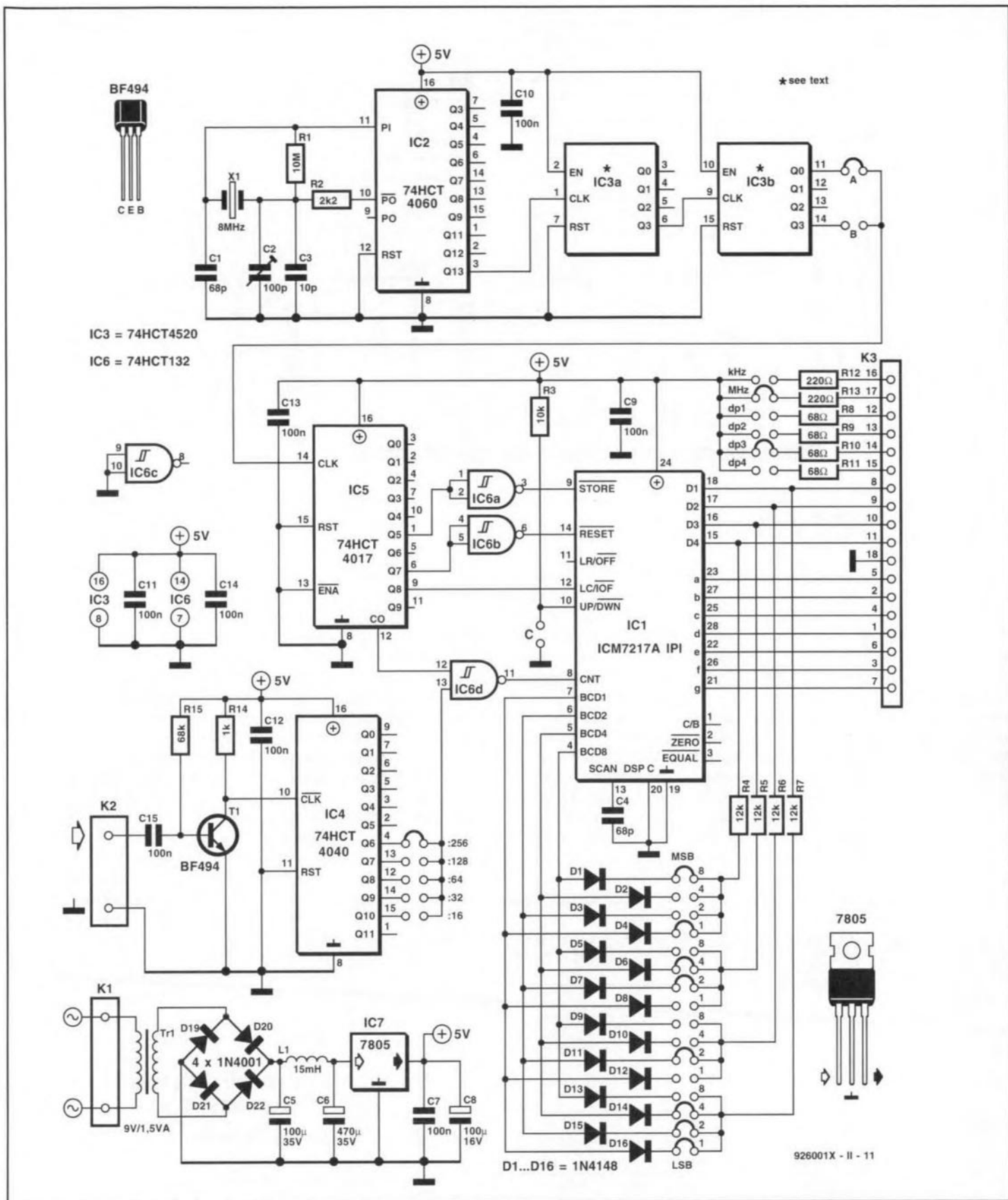


Fig. 1. Circuit diagram of the counter/power supply section. Diodes D1 through D16 serve to program a frequency off-set.

display LD3 — a simple solution, achieved by fitting jumper JP3.

**Preset**

When all jumpers are fitted as indicated in the circuit diagram, the frequency meter will indicate the frequency (in MHz) received on the

VHF/UHF receiver. To enable the frequency meter to display the frequency of the received signal rather than that of the local oscillator, it is programmed with an off-set of 37.3 MHz. In other words, the counter's preset must be used to subtract 37.3 from the frequency applied to its input. In

practice, this is achieved by loading a preset value, which causes the counter to start at a value other than 0. The preset value has to be set separately, with the aid of diodes, for each display digit:

LD1 (MSD): D13-D16

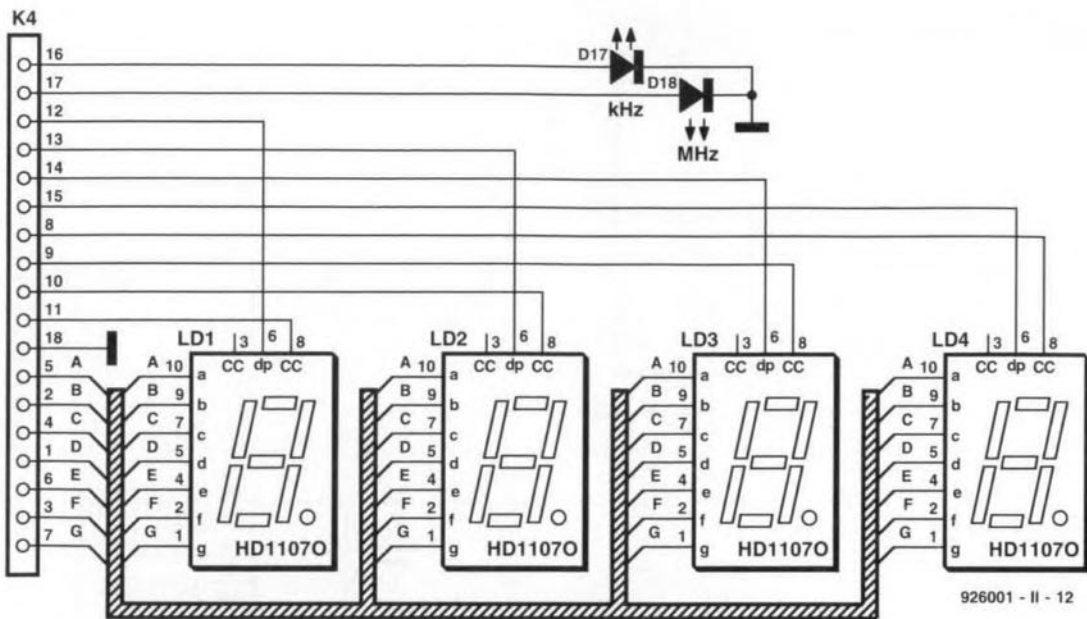


Fig. 2. Circuit diagram of the display section.

LD2	D9-D12
LD3	D5-D8
LD4 (LSD)	D1-D4

Although the four diodes associated with each digit allow a maximum preset of  $2^4=16$ , in practice, only the values 0 through 9 will be useful. If no jumper is fitted for a certain digit, this results in a '0', or 'no off-set'. The digit preset value is binary coded. Examples: a '3' is programmed by fitting jumpers 1 and 2, a '4' by fitting jumper 3 only, and a '7' by fitting jumpers 4, 2 and 1. Programming a

certain preset means that you have to fit the correct jumper combination for each preset. While this is straightforward with positive presets, negative presets, as required for the VHF/UHF receiver, call for a simple calculation. The instruction is simple; starting from four zeros on the display, put a '1' ahead of them (for borrowing), subtract the off-set frequency, and program the result with the aid of the diodes. So, for a LO off-set of 37.3 MHz ('373' without the decimal point), the preset value becomes

$$10000 - 373 = 9627,$$

which is programmed by fitting the preset jumpers as indicated in the circuit diagram, Fig. 1. The other jumpers are also in the positions as required for the VHF/UHF receiver: dp3 for the decimal point on LD3, the 'MHz' jumper, jumper 'A' with IC3b to set the correct timebase, and the '256' jumper with IC4 to match the +256 prescaler in the VHF/UHF tuner. The other jumpers are for tuners that have different prescaling factors.

Jumper 'C' defines the count direction (up or down). For the VHF/UHF receiver, the readout should increase with a higher LO frequency. This means that the counter must count 'UP', hence jumper 'C' must not be fitted. The 'DOWN' mode is used with receivers whose intermediate frequency is higher than the signal frequency and the local oscillator frequency.

### General-purpose frequency meter

As already mentioned, the present circuit is perfect for use as a general purpose frequency meter. Since this function does not require a counter off-set, none of the diodes D1-D16 must be fitted. Also, IC3 (a dual binary counter/divider Type 74HCT4520) must be replaced with a dual decimal counter Type 74HCT4518. No modifications are required to the printed circuit board, which is suitable for both ICs. The 4518 is virtually identical to the 4520, only the signal at output Q3 is divided by 10 rather than by 16.

For frequencies from 0.01 MHz to

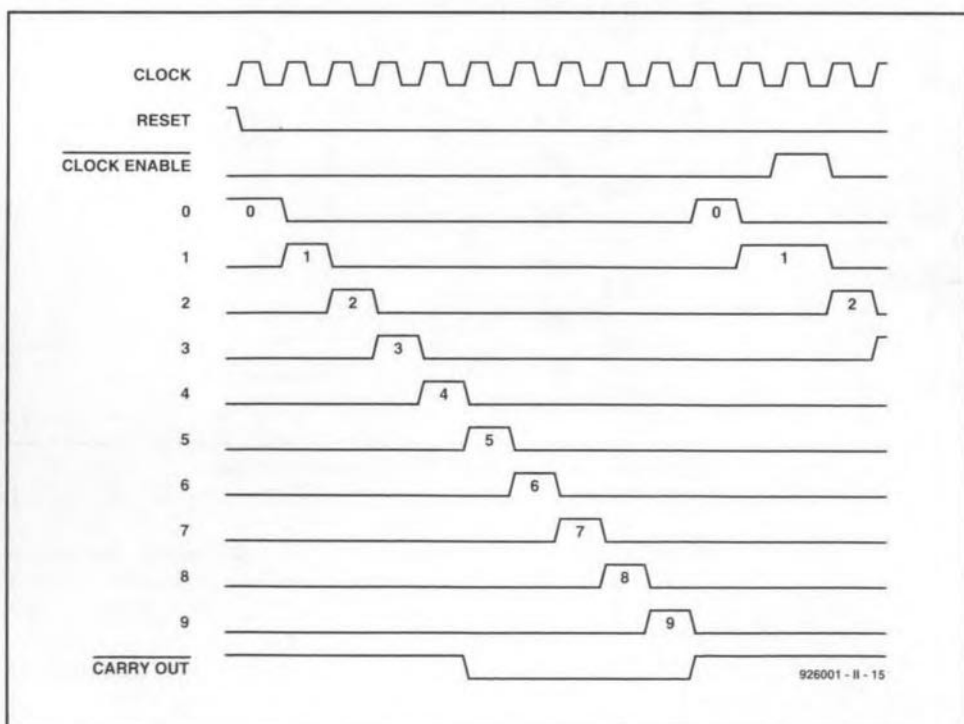


Fig. 3. Timing diagram of the counter control signals.

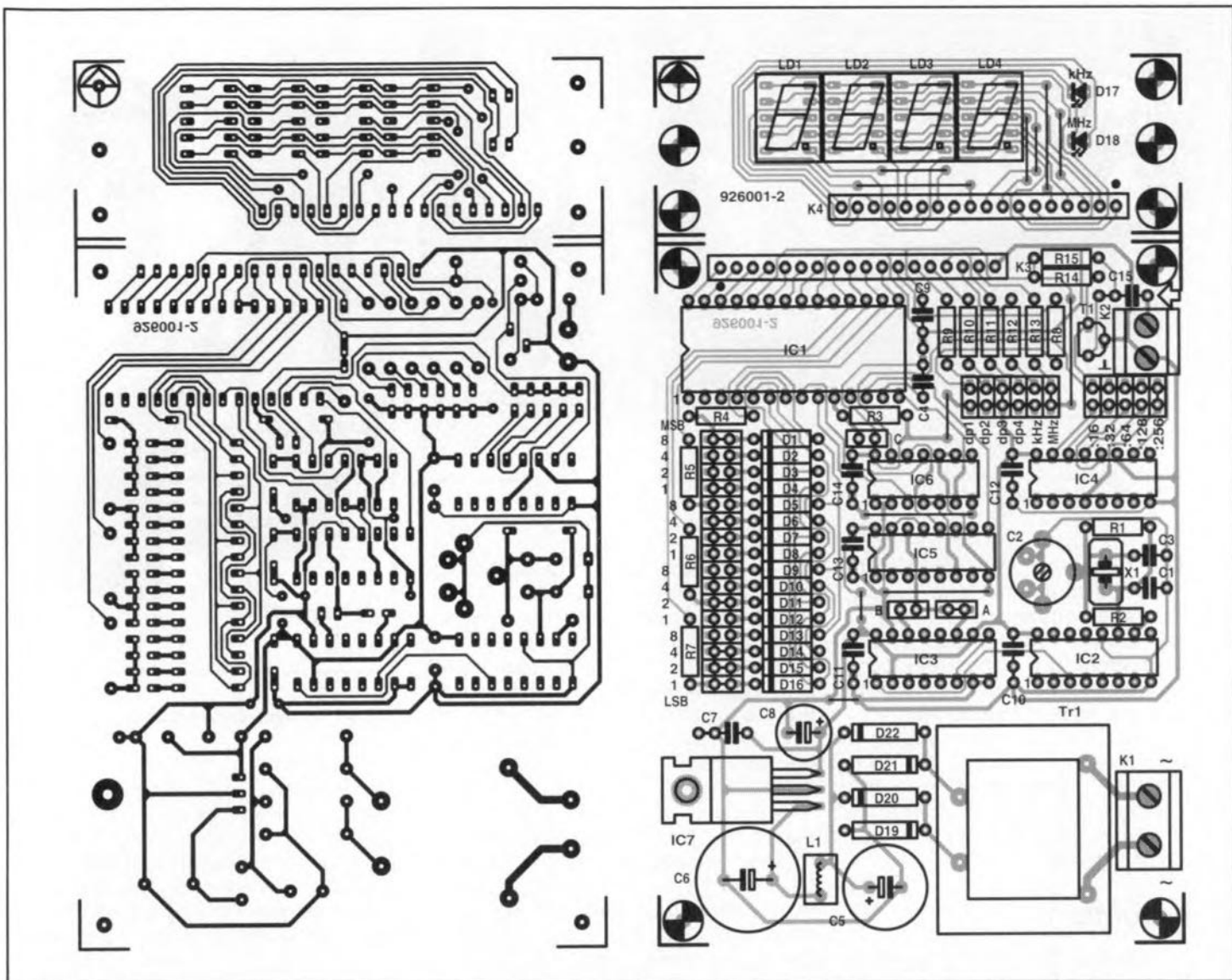


Fig. 4. Track layout (mirror image) and component mounting plan of the printed circuit board designed for the frequency meter.

### COMPONENTS LIST

**Resistors:**

1	10MΩ	R1
1	2kΩ	R2
1	10kΩ	R3
4	12kΩ	R4-R7
4	68Ω	R8-R11
2	220Ω	R12;R13
1	1kΩ	R14
1	68kΩ	R15

**Capacitors:**

2	68pF	C1;C4
1	100pF trimmer	C2
1	10pF	C3
1	100μF 35V radial	C5
1	470μF 35V radial	C6
8	100nF	C7;C9-C15
1	100μF 16V radial	C8

**Inductors:**

1	15mH	L1
---	------	----

**Semiconductors:**

16	1N4148	D1-D16
2	LED, red, 3mm	D17;D18

4	1N4001	D19-D22
1	BF494	T1
1	ICM7217A-IP1*	IC1
1	74HCT4060	IC2
1	74HCT4520	
	(see text)	IC3
1	74HCT4040	IC4
1	74HCT4017	IC5
1	74HCT132	IC6
1	7805	IC7
4	HD11070**	LD1-LD4

**Miscellaneous:**

1	8-MHz quartz crystal	X1
1	9V/1.5VA PCB mount mains transformer, e.g., Monacor VTR1109	Tr1
1	double-pole mains switch	S1
1	2-way PCB terminal block, pitch 7.5mm	K1
1	2-way PCB terminal block, pitch 5mm	K2
1	18-way SIL socket	K3
1	18-way SIL header, angled	K4
1	Metal enclosure 80×150×132mm,	

e.g., Telet\*\*\* LC740  
 1 Printed circuit board 926001-2 (see page 70)

\* Electromail (0536) 204555; fax (0536) 405555.

\*\* ElectroValue (0784) 433603; fax: (0784) 435216.

\*\*\* C-1 Electronics fax (+31) 45 241877.

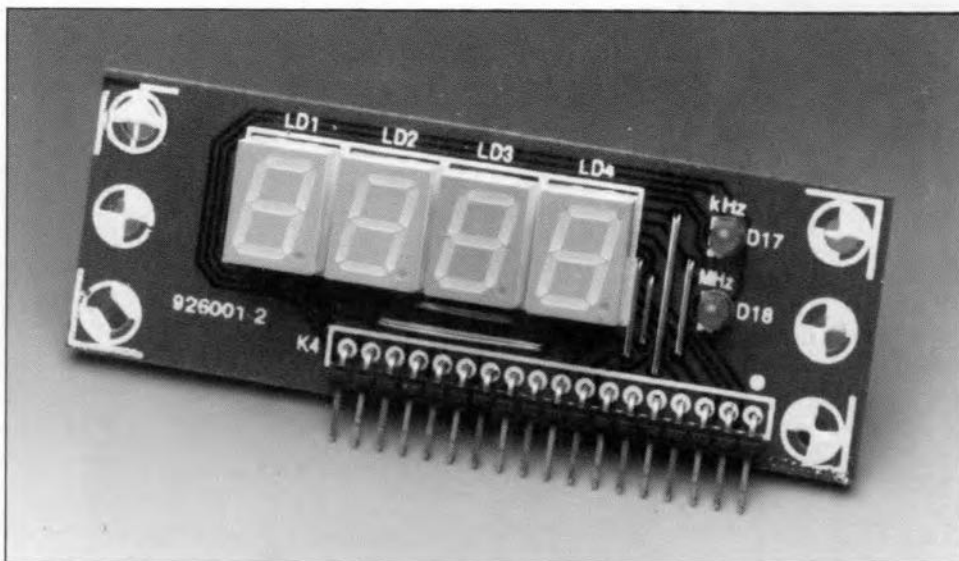


Fig. 5. Completed display board.

30 MHz, fit jumper 'A' with IC3, the ':16' jumper with IC4, the 'dp2' jumper, and the 'MHz' jumper. Depending on the maximum frequency that T1 and IC4 can handle, the highest input frequency that can be measured may be considerably higher than 30 MHz.

If you want to use the counter to measure relatively low frequencies (1 to 9999 kHz), fit jumper 'B' with IC3, and jumper ':32' with IC4. Also fit either the 'dp4' and 'kHz', or the 'dp1' and 'MHz' jumpers.

## Construction

The printed circuit board designed for the frequency meter is available ready made through our Readers Services (see page 70). Those of you who have the means to make their own PCBs will find the artwork in Fig. 4. Before you start fitting parts, cut the board to separate the counter/supply section (Fig. 6) from the display section (Fig. 5).

Start the construction of the main board with the resistors, capacitors, the transformer, the crystal and the solder pins. Be sure not to damage the plastic foil trimmer (C2, near the crystal) by overheating its pins. The voltage regulator, IC7, does not need a heat-sink, and may be bolted straight on to the board. As shown by the photographs of the prototype, the display board is connected to the main board with the aid of an angled pin header and a mating socket.

The completed counter/supply board is mounted on to the bottom cover of the enclosure using PCB spacers, bolts and nuts. Great attention should be paid to the insulation of the parts, wires and terminals that are at mains potential. Also be sure to use a properly rated dual-pole mains switch.

The prototype has two 50-Ω BNC input sockets — one on the front, and

one of the rear panel. The one on the rear panel serves to connect the instrument to the VHF/UHF receiver, while the one on the front is for 'general use'. The two coax input cables are simply soldered in parallel with K2 (braids to ground; cores to C15).

If the frequency readout is used for one application only, the jumpers may be replaced by wire links. Alternatively, the jumpers may be replaced by DIP switch blocks connected to short lengths of flatcable. This allows you to switch quickly between two applications. The coax cable between the VHF/UHF receiver and the frequency meter should be kept as short as possible.

To prevent IC5 being damaged by static discharges, jumpers should not be removed or fitted with the circuit switched on. Also do not forget to discharge yourself (by touching the case) before touching any part of the circuit.

Adjusting C2 will hardly ever be required, since the error caused by a deviation from 8 MHz is negligible at a

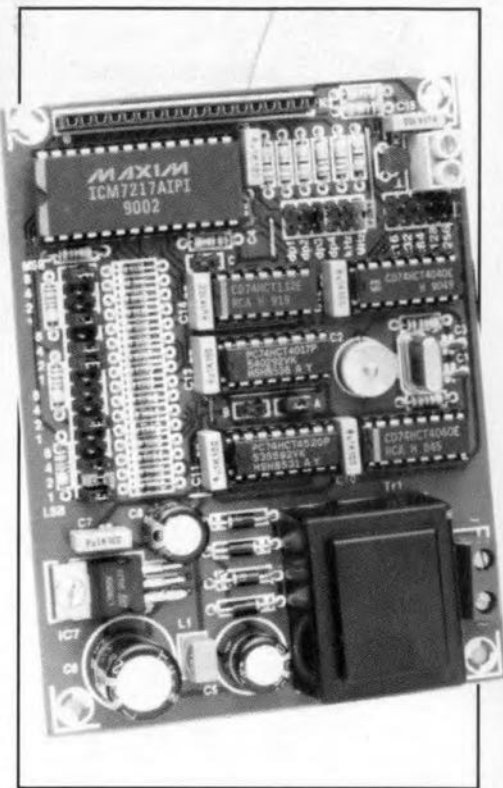


Fig. 6. Completed main board.

few kilohertz only. However, if you have the means to do so, feel free to adjust the trimmer for a clock frequency of 8 MHz exactly. Alternatively, tune the receiver to an accurately known frequency, and adjust C2 until the corresponding readout is obtained. ■

## Reference:

1. VHF/UHF receiver, *Elektor Electronics* May 1992.

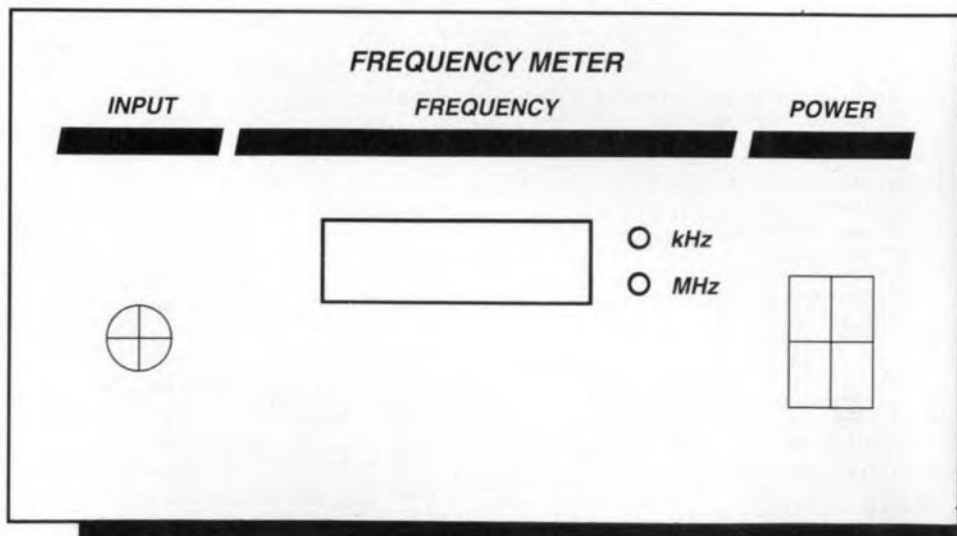


Fig. 7. Suggested front panel layout.

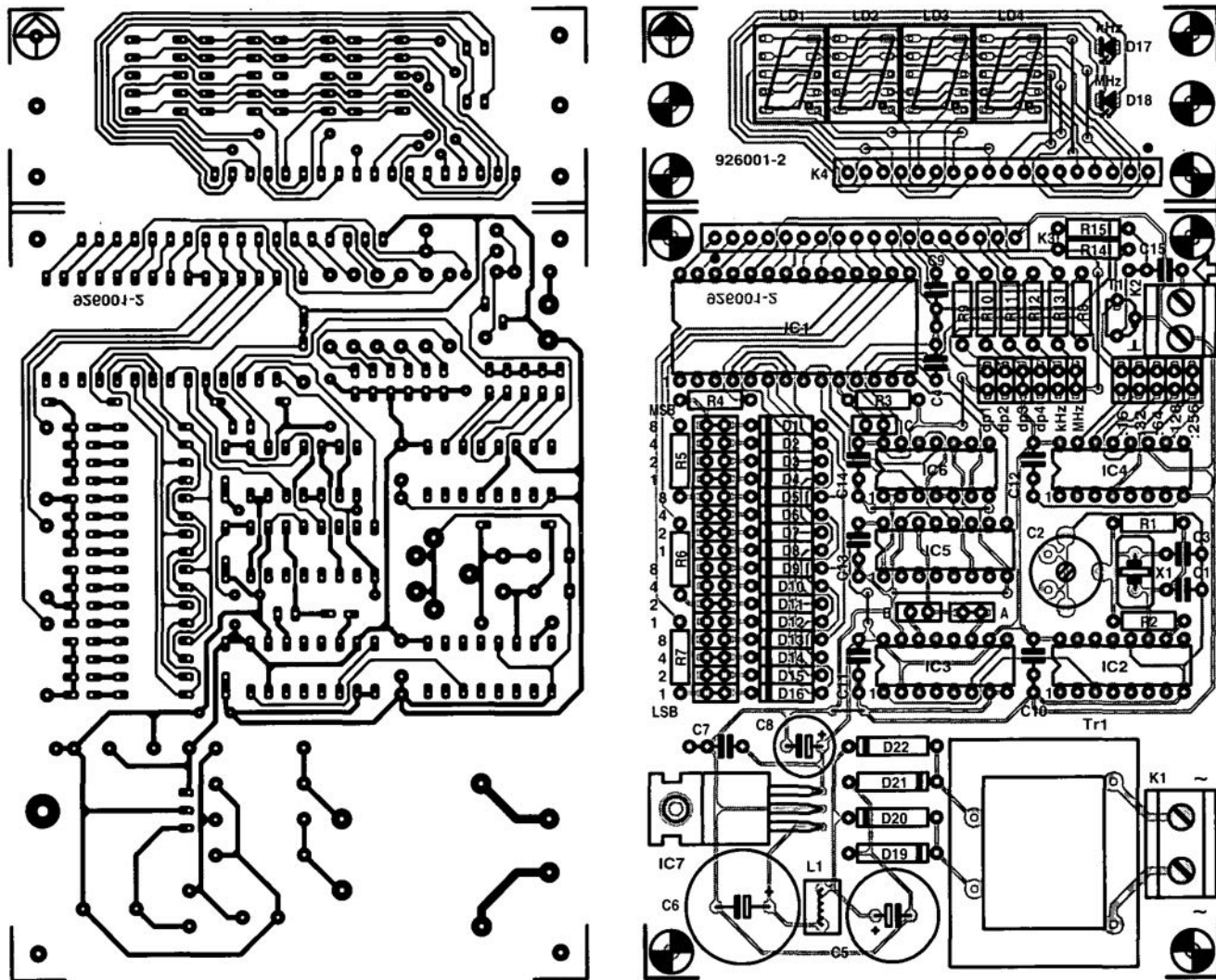


Fig. 4. Track layout (mirror image) and component mounting plan of the printed circuit board designed for the frequency meter.

# MAKING SENSE OF MEASUREMENTS (PART 2)

By Joseph J. Carr

In Part 1 of this two-part article we looked at the subject of measurement variation, and determined that most processes naturally vary according to the **normal distribution curve**, also known as the 'bell shaped' curve. We also discussed the ideas of precision and accuracy, and the different types of measurement (direct, indirect and null). In this final instalment we will discuss measurement errors and some of the arithmetic needed to overcome these difficulties. First, let us look at the various types of measurement error and their sources.

## Theoretical error

All measurements are based on some measurement theory that predicts how a value will behave when a certain measurement procedure is applied. The measurement theory is usually based on some theoretical model of the phenomenon being measured, i.e. an intellectual construct that tells us something of how that phenomenon works. It is often the case that the theoretical model is valid only over a specified range of the phenomenon. For example, nonlinear phenomena that have a quadratic, cubic or exponential function can be treated as a straight line linear function over small, selected, sections of the range. Electronic sensor outputs often fall into this class.

Alternatively, the actual phenomenon may be terribly complex, or even chaotic, under the right conditions, so the model is therefore simplified for many practical measurements. An equation that is used as the basis for a measurement theory may be only a first order approximation of the actual situation. For example, consider the **mean arterial pressure** (MAP) that is often measured in clinical medicine and medical sciences research situations. The MAP approximation equation used by clinicians is:

$$\bar{P} = \text{Diastolic} + \frac{\text{Systolic} - \text{Diastolic}}{3} \quad [3]$$

This equation is really only an approximation (and holds true mostly for well people, not some sick people on whom it is applied) of the equation that expresses the mathematical integral of the blood pressure over a cardiac cycle. That is, the time average of the arterial pressure. The actual expression is written in the

notation of calculus, which is beyond the math abilities of many of the people who use the clinical version above:

$$\bar{P} = \frac{1}{T} \int P dt. \quad [4]$$

The approximation works well, but is subject to greater error owing to the theoretical simplification of the first equation. Incidentally, if you work your way through most of undergraduate and all of graduate school repairing medical and scientific instruments, like I did, then you will understand that it does no good to tell an irate Intensive Care Unit (ICU) nurse that the MAP reading on an instrument is correct when it differs from her calculated value. The actual measured MAP is based on the integral calculus equation (an electronic Miller integrator circuit is used), while her calculated value is based on the simplification. Because some patients lack a considerable part of the time dependent pressure curve (which is sometimes why they are in the hospital), the actual MAP will be lower than the approximation value. Sometimes heat, fire and smoke flow from the tender, loving care hands of ICU nurses!

## Static errors

Static errors include a number of different sub-classes that are all related in that they are always present even in unchanging systems (thus are not dynamic errors). These errors are not functions of the time or frequency variation.

**Reading errors.** These errors result from misreading the display output of the sensor system. An analog meter uses a pointer to indicate the measured value. If the pointer is read at an angle other than straight on, a **parallax reading error** occurs. Another reading error is the **interpolation error**, i.e., an error made in guessing the correct value between two calibrated marks on the meter scale (Fig. 8). Still another reading error occurs if the pointer on a meter scale is too broad, and covers several marks at once.

A related error seen in digital readouts is the **last digit bobble** error. On digital displays, it is often the case that the least significant digit on the display will flip back and forth between two val-

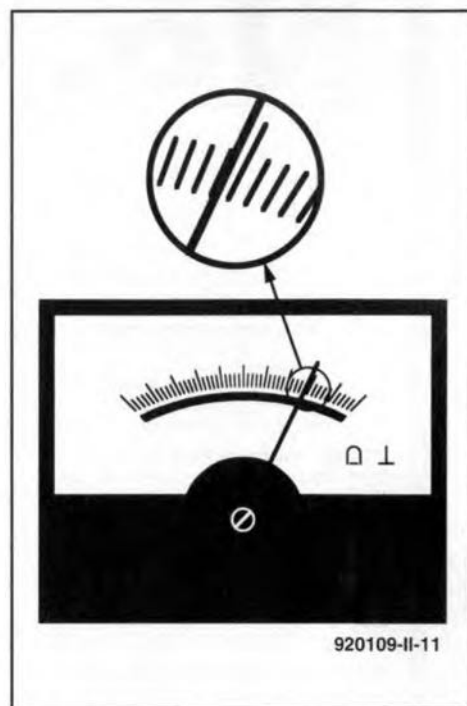


Fig. 8. Analogue meter pointers can suffer both parallax and interpolation of reading errors.

ues. For example, a digital voltmeter might read '12.24' and '12.25' alternately, depending on when you looked at it, despite the fact that absolutely no change occurred in the voltage being measured. This phenomenon occurs when the actual voltage is between the two indicated voltages. Error and uncertainty in the system will make a voltage close to 12.245 V bobble back and forth between the two permissible output states (12.24 and 12.25) on the meter. An example where 'bobble' is of significant concern is the case where some action is taken when a value changes above or below a certain amount — and the digital display bobbles above and below the critical threshold.

**Environmental errors.** All sensors and instruments operate in an environment, which sometimes affect the output states. Factors such as temperature (perhaps the most common error producing agent), pressure, electromagnetic fields, and radiation must be considered in some electronic sensor systems.

**Characteristic errors.** These static errors are still left after reading errors and environmental errors are accounted.



When the environment is well within the allowable limits and is unchanging, when there is no reading error, there will be a residual error remaining that is a function of the measurement instrument or process itself. Errors found under this category include zero offset error, gain error, processing error, linearity error, hysteresis error, repeatability error, resolution error and so forth.

Also included in the characteristic error are any design or manufacturing deficiencies that lead to error. Not all of the 'ticks' on the ruler are truly 1.0000 inch apart at all points along the ruler. While it is hoped that the errors are random, so that the overall error is small, there is always the possibility of a distinct bias or error trend in any measurement device.

For digital systems one must add to the resolution error a **quantization error** that emerges from the fact that the output data can only take on certain discrete values. For example, an 8-bit analogue-to-digital converter allows 256 different states, so a 0 to 10 V range is broken into 256 discrete values in 39.06 mV steps. A potential that is between two of these steps is assigned to one or the other according to the rounding protocol used in the measurement process. An example is the weight sensor that outputs 8.540 V, on a 10-V scale, to represent a certain weight. The actual 8-bit digitized value may represent 8.502, 8.541, or 8.580 V because of the ±0.039 V quantization error.

**Dynamic errors**

Dynamic errors arise when the measurement is changing or in motion during the measurement process. Examples of dynamic errors include the inertia of mechanical indicating devices (such as analog meters) when measuring rapidly changing parameters. There are a number of limitations in electronic instrumentation that fall into this category, as you will find out by consulting any competent book on the subject.

**Instrument insertion error**

A fundamental rule of making engineering and scientific measurements is that **the measurement process should not significantly alter the phenomenon being measured**. Otherwise, the measurement is actually the altered situation, not the original situation that is of true interest. Examples of this error are found in many places. One such is the fact that pressure sensors tend to add volume to the system being measured, so slightly reduce the pressure indicated below the actual pressure. Similarly, a flow meter might add length, a different pipe diameter, or turbulence to a system being measured. A voltmeter with a low

impedance of its own could alter resistance ratios in an electrical circuit and produce a false reading (Fig. 9). This problem is seen when using cheap analogue volt-ohm-milliammeters (VOMs), that have a low sensitivity hence a low impedance ( $R_m$  in Fig. 9), to measure a voltage in a circuit. The meter resistance  $R_m$  is effectively shunted across the circuit resistance across which the voltage appears.

Instrument insertion errors can usually be minimized by good instrument design and good practices. No measurement device has zero effect on the system being measured, but one can reduce the error to a very small value by appropriate selection of methods and devices.

**Dealing with measurement errors**

Measurement error can be minimized through several methods, some of which are lumped together under the rubric 'procedure' and others under the legend 'statistics'.

Under 'procedure' one can find methods that will reduce, or even minimize, error contributions to the final result. For example, in an electrical circuit, use a voltmeter that has an extremely high input impedance compared with circuit resistances. The idea is to use an instrument (whether a voltmeter, a pressure meter or whatever) that least disturbs the thing being measured.

A way to reduce total error is to use several different instruments to measure the same parameter. In Fig. 10 we see an example where the current flow in a circuit is being measured by three different ammeters: M1, M2 and M3. Each of these instruments will produce a result that contains an error term de-correlated

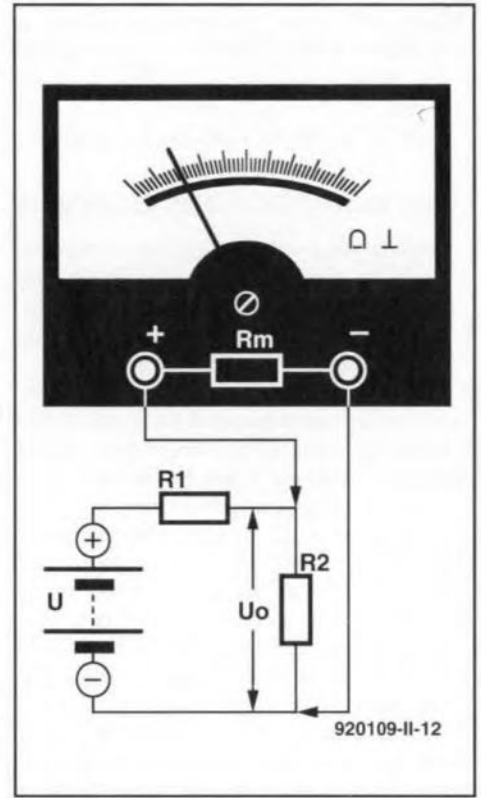


Fig. 9. If a low-impedance VOM is used to measure voltages in a circuit, it can load the circuit and produce an erroneous reading. This is an example of an instrument insertion error.

from the error of the others and not biased (unless, by selecting three identical model meters we inherit the characteristic error of that type of instrument). We can estimate the correct value of the current flow rate by taking the average of the three:

$$M_0 = \frac{M_1 + M_2 + M_3}{3} \quad [5]$$

One must be careful to either randomize

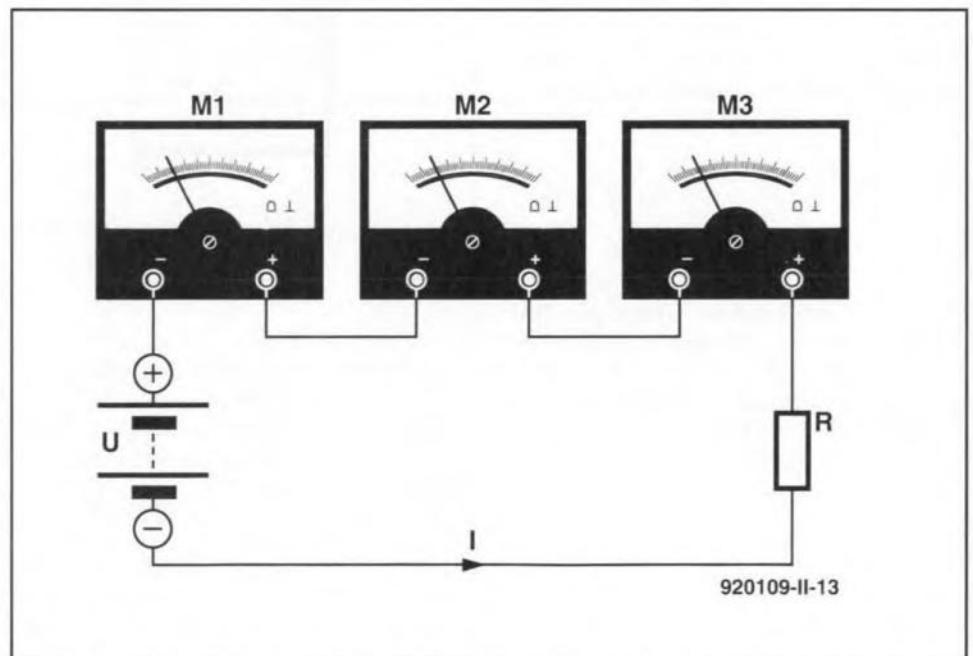


Fig. 10. Use of multiple instruments, and then averaging the results, can reduce error.

the system in cases where the sensor or instruments used tend to have large error terms biased in one direction, or calibrate the average error so that it may be subtracted from of the final result.

## Error contributions analysis

An **error analysis** should be performed in order to identify and quantify all contributing sources of error in the system. A determination is then made regarding the randomness of those errors, and a **worst case analysis** is made. Under the worst case, one assumes that all of the component errors are biased in a single direction and are maximized. We then attempt to determine the consequences (to our purpose for making the measurement) if these errors line up in that manner, even if such an alignment is improbable. The worst case analysis should be done on both the positive and negative side of the nominal value. An **error budget** is then created to allocate an allowable error to each individual component of the measurement system in order to ensure that the overall error is not too high for the intended use of the system.

If errors are independent of each other, and are random rather than biased, and if they are of the same order of magnitude, then one can find the **root of the sum of the squares** (RSS) value of the errors, and use it as a composite error term in planning a measurement system. The RSS error is:

$$\epsilon_{\text{rms}} = \sqrt{\sum \epsilon_i^2} \quad [6]$$

The RSS error term is a reasonable estimate or approximation of the combined effects of the individual error components.

A collection of repetitive measurements of a phenomenon can be considered a sampled population, and treated as such. If we take  $N$  measurements ( $M_1$  through  $M_n$ ) of the same parameter, and then average them we get:

$$\bar{M} = \frac{M_1 + M_2 + M_3 + \dots + M_n}{N} \quad [7]$$

The average value obtained in Eq. [7] is the **mean arithmetic average**. This value is usually reported as the correct value for the measurement, but when taken alone does not address the issue of error. For this purpose we add a fudge factor by quoting the **standard error** of the mean, or

$$\sigma_m = \frac{\sigma_m}{\sqrt{N}} \quad [8]$$

which is reported in the result as:

$$M = \bar{M} \pm \sigma_m \quad [9]$$

Any measurement contains error, and this procedure allows us to estimate that error, and thereby understand the limitations of that particular measurement.

## Operational definitions in measurement

Some measurement procedures suggest themselves immediately from the nature of the phenomenon being measured. In other cases, however, there is a degree of ambiguity in the process, and it must be overcome. Sometimes the ambiguity results from the fact that there are many different ways to define the phenomenon, or perhaps no way is established. In cases such as these, one might wish to resort to an **operational definition**, i.e., a procedure that will produce consistent results from measurement to measurement, or when measurements are taken by different experimenters.

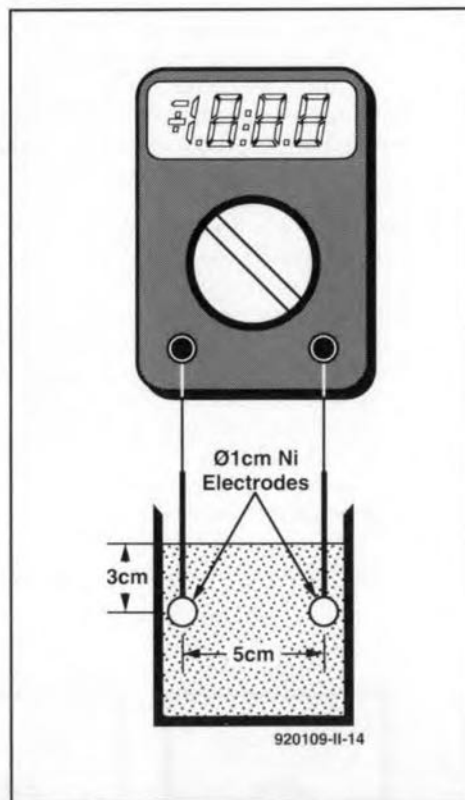


Fig. 11. Example of an 'operational definition'.

An operational definition, therefore, is a procedure that must be followed, and specifies as many factors as are needed to control the measurement so that changes can be properly attributed only to the unknown variable. The need for operational definitions (as opposed to absolute) definitions arises from the fact that things are only rarely so neat and clean as to suggest their own natural definition; ambiguity reigns. By its very definition, the operational definition does

not ask 'true' or 'false' questions, but rather it asks 'what happens under given sets of assumptions or conditions'. What an operational definition can do for you, however, is to standardize a measurement in clear and precise way so that it remains consistent across numerous trials. Operational definitions are used extensively in science and technology. When widely accepted, or promulgated by a recognized authority, they are called **standards**.

An operational definition should embrace what is measurable quantitatively, or at least in non-subjective terms. For example, in measuring the 'saltiness' of saline solution (salt water), one might taste it and render a subjective judgement such as 'weak' or 'strong'. Alternatively, one can establish an operational definition that calls for you to measure the electrical resistance of the saline under certain specified conditions:

1. immerse two 1-cm diameter circular nickel electrodes, spaced 5 cm apart and facing each other, to a depth of 3 cm into a 500-ml beaker of the test solution.
2. Bring the solution to a temperature of 4 °C.
3. Measure the electrical resistance ( $R$ ) between the electrodes using a Snotz Model 1120 digital ohmmeter.
4. Find the conductance ( $G$ ) by taking the reciprocal of resistance ( $G = 1/R$ ).

You can probably come up with a better definition of the conductance of saline solution that works for some peculiar situation. Keep in mind that only rarely does a preferred definition suggest itself naturally.

The use of operational definitions results in both strengths and weaknesses. One weakness is that the definition might not be honed fine enough for the purpose at hand. Sociologists and psychologists often face this problem because of difficulties in dealing with non-linearities such as human emotions. But such problems also point to a strength. We must recognize that scientific truth is always tentative, so we must deal with uncertainties in experimentation. Sometimes, the band of uncertainty around a point of truth can be reduced by using several operational definitions in different tests of the same phenomenon. By taking different looks from different angles, we may get a more refined idea of what is actually happening.

When an operational definition becomes widely accepted, and is used throughout an industry, it may become part of a formal **standard** or test procedure. You may, for example, see a procedure listed as 'performed in accordance with NIST XXXX.XXX<sup>1</sup>' or 'ANSI Standard XXX.'<sup>2</sup> These notations mean that whoever made the measurement fol-

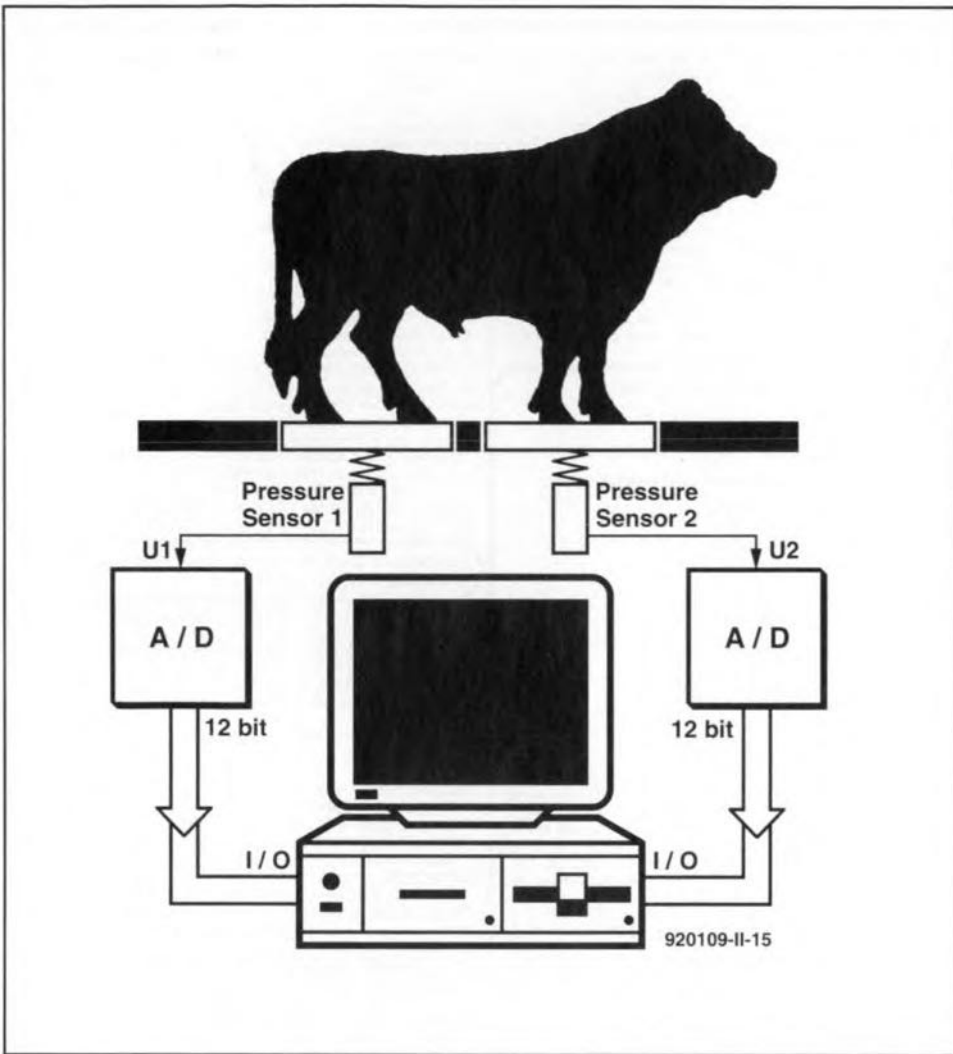


Fig. 12. Instrument for weighing a bull.

lowed one or another of a published standard.

### Weighing a cow

Now let us get back to the issue of weighing a cow on an electronic scale. The main problem is that the cow will not stand still long enough to make a static measurement. As a result, it is necessary to use statistical methods to weigh the animal. Figure 12 shows the cattle scale seen by my electronically literate political aide. The animal stands on two platforms, one for the front legs and another for the rear legs, that are each connected to an electronic pressure sensor. The voltage outputs of each sensor ( $U_1$  and  $U_2$ ) are each approximately equal to half the weight of the animal. Therefore, the sum of  $U_1$  and  $U_2$  is proportional to the total weight of the animal.

These voltages ( $U_1$  and  $U_2$ ) are converted to binary numbers by the analogue-to-digital (A-D) converters, and input to a desktop computer. Because very fast A-D converters are now available, it is possible to take several thousand samples of the two half weights in the ten to twenty seconds the animal is held on the scale. The average of each is taken, along with the error factor, and

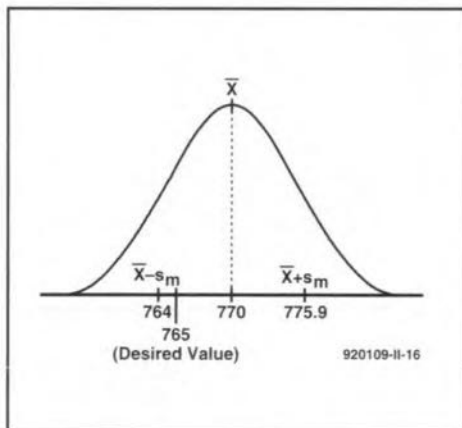


Fig. 13. Plot of oven test data showing error limits.

they are then added together. As long as the error factor is less than the desired resolution, the scale's reading is accepted.

Now let us take a look at another situation that involves ambiguous measurements.

### Did it pass the test?

An adhesives curing oven is supposed to have an equilibrium temperature of

765 °F after 10 minutes. A test technician inserted an electronic thermometer and a timer to take the temperature measurement after exactly ten minutes; the oven was allowed to cool back to room temperature between trials. She took 20 measurements and found the mean to be 770 °F with a standard deviation of 26.2. Did this oven pass the test? The situation is shown in Fig. 13 — the answer seems to be: yes. Why? Because the error term represented by the standard error of the mean (shown as  $\pm s_m$  in Fig. 13) encompasses the desired value of 765 despite the dispersion of the data. We can only claim that the test is failed if the desired value is outside these limits. ■

#### Notes:

1. NIST is the National Institute for Standards and Technology, formerly called National Bureau of Standards.
2. ANSI is the American National Standards Institute.

# 'SMARTWATCH' REAL-TIME CLOCK FOR 80C32 COMPUTER

A 'Smartwatch' real-time clock is described that provides a time/date indication and a stopwatch function on the *Elektor Electronics* 80C32 single-board computer<sup>1,2</sup>.

Design by W. Hackländer

DALLAS Semiconductor's 'Smartwatch' Type DS1216C is a real-time clock IC which is, unusually, housed in a 28-way IC socket. The device is pin compatible with 64-kBit and 256-kBit static CMOS RAMs, and is simply inserted between the RAM on the 80C32 computer and its socket. The 'intelligent socket' between the RAM and the processor contains a clock circuit, a Lithium battery and a power supply controller for the CMOS RAM. The Lithium battery contained in the DS1216C doubles as a RAM backup for the computer, which means that the existing 3.6-V battery and battery holder board may be removed from the board.

## Smartwatch intelligent socket

With the exception of pins 20 and 28, the 'intelligent socket' (Fig. 1) connects all RAM pins directly to the corre-

sponding PCB holes. The DS1216C may be used with all static RAMs organized as  $8\text{ k} \times 8$  or  $32\text{ k} \times 8$ . Its principal feature, the real-time clock, counts hundredths of a second, seconds, minutes, hours, days, months and years, and automatically updates the date information. The clock error is less than  $\pm 1$  minute per month, and the clock takes leap years into account. Both 12-hour (AM/PM) and 24-hour time indications are possible.

Communication with the clock starts with pattern recognition. This is achieved by sending 64 successive write cycles to port DQ0. The 64-bit datastream is compared with a fixed pattern (Fig. 2), which arranges the bits into eight bytes (groups of 8 bits). This results in a byte pattern as shown to the right in Fig. 2. The probability of an identical datastream intended for the RAM is smaller than 1 in 1019 instances. The 64-bit pattern is followed by 64 further read or write cycles to set

or read the clock. RAM access is disabled during these operations. Any write instruction to the RAM that actuates CE\ (chip enable) and OE\ (output enable) starts the pattern recognition operation by setting up a pointer to the first of the 64 bits in the comparison register. Obviously, the next 64 write operations that enable the CPU to access the clock end up in the RAM also. Consequently, one address in the RAM should be reserved for use as a kind of scratch pad, and the clock should be accessed via this address.

The pattern recognition that selects the clock is a sequential (bit-by-bit) operation. The DS1216C compares the first write instruction with bit 0 of the 64-bit pattern register. If the bits match, the pointer is increased to bit 1, and waits for the next instruction. This continues until all 64 bits have been compared, or the first mismatch occurs, when the pointer is 'frozen', and the clock ignores all further write instructions. If a read operation occurs during the pattern recognition, the comparison is terminated, and the pointer reset.

The clock is accessible when a sequence of 64 bits received via DQ0 matches the clock selection pattern, whereupon the next 64 bits can be read from, or written to, DQ0. This is

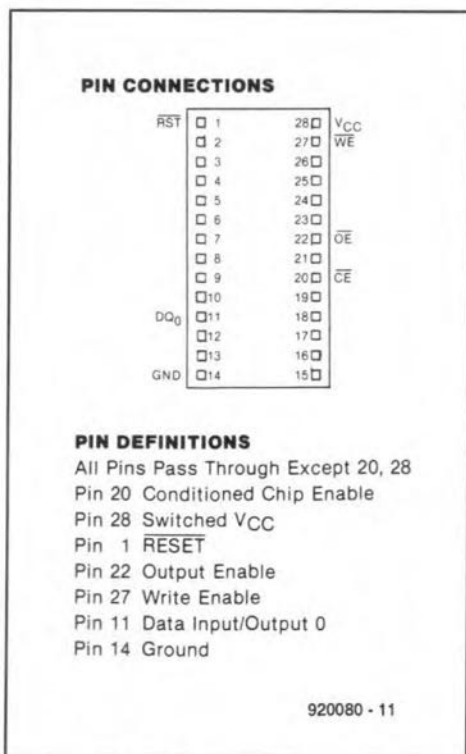


Fig. 1. DS1216C Smartwatch pin-out (courtesy Dallas Semiconductor).

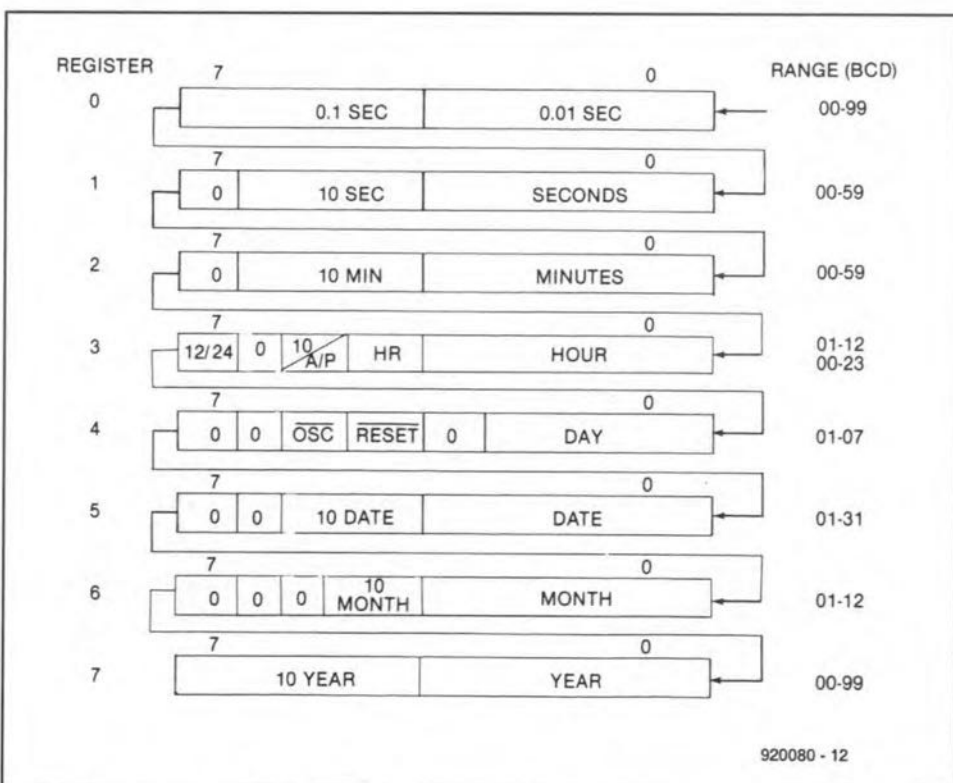


Fig. 2. Smartwatch register definition.

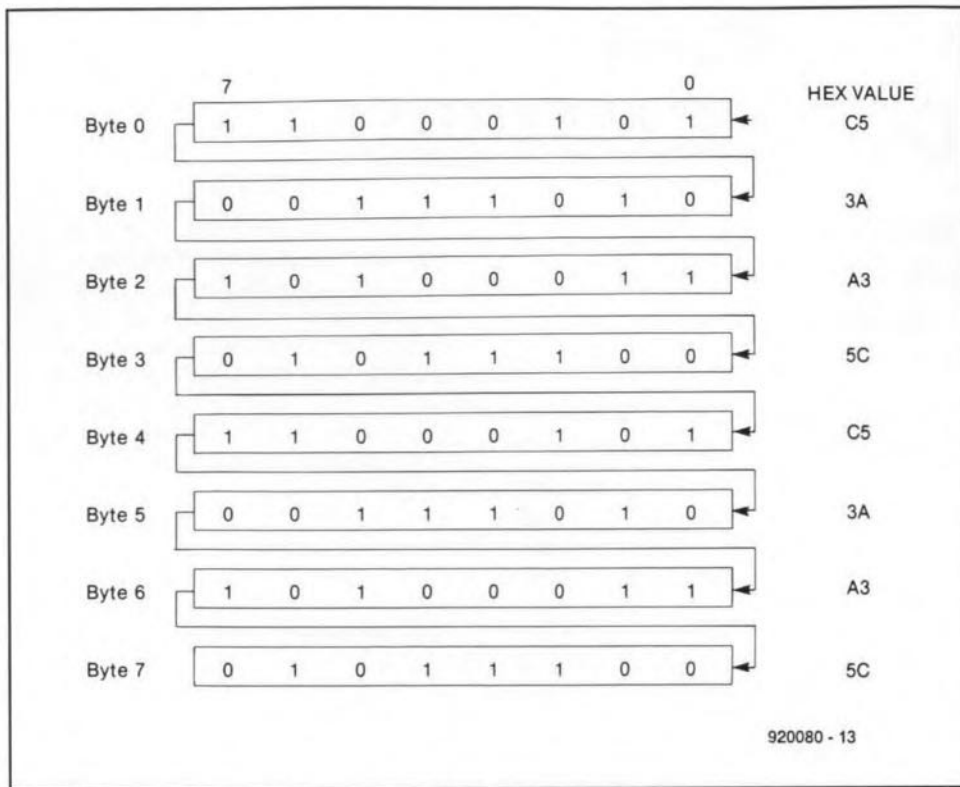


Fig. 3. Smartwatch comparison register definition.

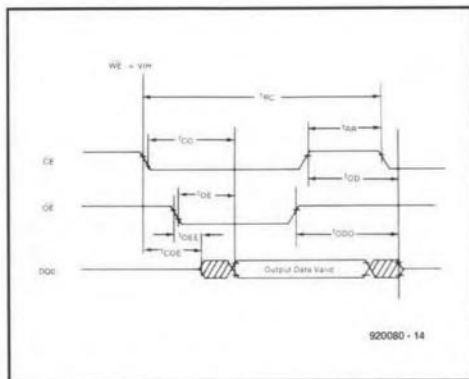


Fig. 4. Timing diagram — read cycle to Smartwatch.

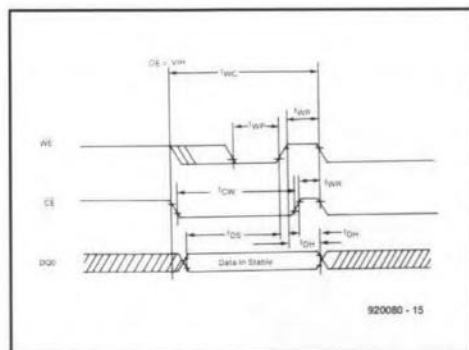


Fig. 5. Timing diagram — write cycle to Smartwatch.

achieved by pulling OE\ (read clock) or WE\ (set clock) low. The timing for read and write cycles is shown in Fig. 3. Instructions to addresses outside the RAM range may occur during the pattern recognition or the data exchange with the clock.

The time information is organized in

eight 8-bit registers (Fig. 4). These bits appear serially on port DQ0. Since it is not possible to write or read individual bits, data exchange between the CPU and the clock should always be organized in groups of eight bits at a time. The register data are BCD coded.

The internal organization of the clock registers is fairly simple: with the exception of register 4, all registers are divided into two 4-bit sections, each of which allows decimal numbers 0 through 9 to be represented. Some bits are fixed as a '0', and can not be changed into '1' by writing to the clock. An example is found in register 6a, which should only contain decimal '0' or '1'.

Registers 4a and 3a are exceptions. Bit 7 of the hours register (3) selects between 12-hour (AM/PM) and 24-hour time indication. A high in this bit location selects the 12-hour clock, when bit 5 is the AM/PM indicator. In 24-hour indication mode, bit 5 represents the second tens-of-hours bit (20-23 hours).

Finally, a word about the RESET and OSC bits, numbers 4 and 5, in the days register. Both control 'active low' functions. If bit 5 is programmed low, the data exchange is interrupted, but the register contents are retained. Bit 4 controls the internal oscillator. The DS1216C is supplied with the OSC bit set, i.e., '1', to save battery power while the device is not in use. The bit must be made low to get the clock to tick.

The operation of the battery backup system is simple. The DS1216C compares the voltage on the Vcc line of the

80C32 board with the voltage supplied by its internal Lithium battery, and switches the RAM from mains supply to battery supply as soon as Vcc drops below the battery voltage. The voltage drop across the electronic switch used to accomplish this is only 0.2 V.

The DS1216C also features a power-fail detection circuit that continuously monitors the supply voltage line for dips. As soon as the supply voltage drops below 4.25 V, the IC switches to 'emergency supply' from the internal battery. While in battery backup mode, the DS1216C keeps the RAM's CE\ line logic high, so that the memory is write-protected. Normally, this control line follows the CE\ signal to the DS1216C within 20 ns.

## DS1216C and 80C32 computer

The DS1216C is simply inserted between the RAM and its IC socket, while D4 is replaced by a wire link. After changing the monitor EPROM, the following example programs may be loaded:

### CLKTST.HEX

start address

```
4100 Interrogate clock status on or off
4200 Switch on clock
4300 Switch off clock
4400 Clock setting demo, change date from 31.12.1991 to 1.1.1992
```

### EBTST5A.HEX

```
4100 Start melody in loudspeaker, stopwatch function
```

These example programs display their results on the LCD. ■

### References:

- 80C32/8052AH-BASIC single board computer. *Elektor Electronics* May 1991.
- 8051/8032 Assembler. A course in 8 instalments. *Elektor Electronics* February through November 1992.

### Note:

Dallas Semiconductor distributors in the UK are

Dialogue Distribution, Top House, 403 London Road, Camberley, Surrey GU15 3HL. Telephone (0276) 682001. Fax (0276) 683722.

Joseph Electronics Ltd., 2 The Square, Broad Street, Birmingham B15 1AP. Telephone (02164) 36999.

DS1216C SMARTWATCH software for Elektor Electronics 80C32 computer

### 1. Smartwatch address assignment

```
CLKADDR EQU 03FFFH ;Smartwatch dummy address
```

### 2. Eight registers assigned in internal RAM.

Registers for intermediate storage of data exchanged between CPU and Smartwatch. 80C32 board RAM definitions including eight RTC registers.

#### ; RAM definitions

```
;
; ORG 030H
COMMAND: DS 1 ;for MON call, MUST be address 030H!
CNT1: DS 1
HEXLEN: DS 1
HEXSUM: DS 2
;
dBYTES EQU 5 ;must be 5, loop unrolling used;
;
dREG1: DS dBYTES
dACCU: DS dBYTES
;
PWSAV: DS 1 ;used for snapshot and MON
ACCSAV: DS 1
DPHSAV: DS 1
DPLSAV: DS 1
;
; arithmetic storage
;
top EQU dREG1 ;overlay 2 bytes
next EQU dREG1+2 ;overlay 2 bytes
;
FAC1 EQU top ;overlay factors for 16*16 bit
FAC2 EQU next ;overlay
DIVI EQU FAC2 ;overlay divisor for 32/16 bit division
QUOT EQU FAC1 ;overlay quotient for 32/16 bit divis.
PROD EQU dACCU ;overlay 5 bytes (4+ ext.) for division
DIVCNT: DS 1
;
; date and clock storage
;
CLOCK: DS 4 ;Smartwatch, Time
DAY_NR: DS 1 ;Smartwatch, Day of Week (+OSC/RES-Bits)
DATE: DS 3 ;Smartwatch, Date
;
Rtop EQU $
;
```

### 3. Command codes assignment

Allow the courseware RAM to access Smartwatch via courseware EPROM. All relevant EMON51 codes are listed; additions are marked.

#### ; function codes for MON calls

```
;
ccCHR EQU 001H
ccSTXT EQU 002H
ccBYTE EQU 003H
ccHEX16 EQU 004H
ccdR016 EQU 005H
ccdR032 EQU 006H
cchR016 EQU 007H
cchR032 EQU 008H
;
ccGETC EQU 010H
ccTSTC EQU 011H
ccGET16 EQU 012H
ccGET10 EQU 013H
ccGETU EQU 014H
;
ccSNAP EQU 020H
ccLTIME EQU 021H
ccSTIME EQU 022H
;
ccCLKREQ EQU 030H **** New
ccCLKRUN EQU 031H **** New
ccCLKSTP EQU 032H **** New
ccCLK_WR EQU 033H **** New
ccCLK_RD EQU 034H **** New
;
ccLINK EQU 040H
;
ccADD EQU 050H
ccSUB EQU 051H
ccMUL EQU 052H
ccDIV EQU 053H
ccABS EQU 054H
ccNEG EQU 055H
;
```

4. Embedding the above command codes into the EPROM jump table in EMON51. Refer to the program section 'main monitor service routine'. For clarity lines before and after the insertion are given also.

```
.....
ttGETU: CJNE A,#ccGETU,ttLINK
LJMP GETUPC
ttLINK: CJNE A,#ccLINK,ttCLKEQ
LJMP LINK1
ttCLKEQ: CJNE A,#ccCLKREQ,ttCLKRUN
LJMP CLKREQ
ttCLKRUN: CJNE A,#ccCLKRUN,ttCLKSTOP
LJMP CLK_ON
ttCLKSTP: CJNE A,#ccCLKSTP,ttCLKWR
LJMP CLKOFF
ttCLKWR: CJNE A,#ccCLK_WR,ttCLK_RD
LJMP CLKWR
ttCLKRD: CJNE A,#ccCLK_RD,ttADD
LJMP CLKRD
ttADD: CJNE A,#ccADD,ttSUB
LJMP rADD16
.....
.....
```

### 5. The actual program

This program arranges the data exchange between 8051 and the Smartwatch module. In the EMON51 monitor, it is located between routines "snap" and "Arithmetic routines".

```
;
;***** Routines for Smartwatch DS 1216C *****
;
;----- Clear and switch off clock (OSC bit)
CLKOFF: LCALL C_REGO ;Clear storage register
MOV DAY_NR,#00110000B ;Oscillator off, RES passive
SJMP CLK_WR
;
;----- Clear and switch on clock (OSC bit)
CLK_ON: LCALL C_REGO ;Clear storage register
MOV DAY_NR,#00010000B ;Oscillator on, RES passive
;
;----- convey data from internal RAM to clock
CLK_WR: LCALL C_OPEN ;convey code word
;
MOV DPTR,#CLKADDR ;Smartwatch dummy address
MOV R0,#CLOCK ;Pointer to storage register
MOV R7,#8 ;8 Bytes
MOV R6,#8 ;8 Bits
MOV A,@R0 ;Read byte
WRBYTE: @DPTR,A ;Clock write pulse
RR A ;Bit 1 --> Bit 0
DJNZ R6,WRBIT ;8 Bits written?
INC R0 ;Next register
DJNZ R7,WRBYTE ;8 Bytes written?
NOP
RET
;
;----- Get clock status (OSC bit)
CLKREQ: ACALL CLK_RD ;Read hours register
MOV A,DAY_NR ;Fetch control register
JB ACC.5,C_OFF ;Bit 5 set (clock off)?
;
MOV DPTR,#C_TXT1 ;Monitor report, clock active
LCALL STXT
RET
;
C_OFF: MOV DPTR,#C_TXT2 ;Monitor report, clock passive
LCALL STXT
RET
;
C_TXT1: DB 'Smartwatch active',13,10,0
C_TXT2: DB 'Smartwatch passive',13,10,0
;
;----- Transfer clock data to internal RAM
UHR_RD: LCALL C_REGO ;Clear storage register
LCALL C_OPEN ;Convey code word
MOV DPTR,#CLKADDR ;Dummy address
MOV R0,#CLOCK ;Pointer to lowest storage reg.
MOV R7,#8 ;8 Bytes
MOV R6,#8 ;8 Bits
RDBYTE: MOV A,@DPTR ;Clock read pulse
RRC A ;Bit 0 --> C bit
MOV A,@R0 ;Read register
RRC A ;C bit --> bit 7
MOV @R0,A ;Write register
DJNZ R6,RDBIT ;8 Bits read?
INC R0 ;Next byte
DJNZ R7,RDBYTE ;8 Bytes read
NOP
RET
;
;----- Enable access to clock (64-bit code word)
C_OPEN: MOV DPTR,#CLKADDR ;Dummy address
MOVX A,@DPTR ;Initialize clock
MOV DPTR,#C_CODE
MOV R7,#8 ;8 Bytes
MOV R6,#8 ;8 Bits
CDBYTE: CLR A
MOVC A,@A+DPTR ;Fetch constant
PUSH DPH ;Save string pointer (DPTR)
PUSH DPL
MOV DPTR,#CLKADDR ;Dummy address
CDBIT: MOVX @DPTR,A ;Clock write pulse
RR A ;Bit 1 --> Bit 0
DJNZ R6,CDBIT ;8 Bits written?
POP DPL ;Restore string pointer
POP DPH
INC DPTR ;Next constant
DJNZ R7,CDBYTE ;8 Bytes (64 bits) transf'd?
NOP
RET
;
C_CODE: DB 0C5H,03AH,0A3H,05CH,0C5H,03AH,0A3H,05CH
;
;----- Clear 8 registers in internal RAM
C_REGO: CLR A
MOV R7,#8
MOV R0,#CLOCK
ALL_0: MOV @R0,A
INC R0
DJNZ R7,ALL_0
NOP
RET
;
```

## I<sup>2</sup>C interface for PCs

**February 1992**

The PCD8584 used in this project is no longer manufactured by Philips Semiconductors, and replaced by the PCF8584. This is a fully compatible IC and only improved as regards the 4-wire long-distance mode, which did not work correctly on the PCD8584.

## Real-time clock for 80C32 computer

**June 1993**

Contrary to what is implied by the description of the parallel connection of the SmartWatch IC pins with the EPROM pins, pin 1 of the SmartWatch

# CORRECTIONS AND UPDATES

should be connected separately to +5V, for instance, to EPROM pin 28, via a short wire. This is necessary because pin 1 on the SmartWatch is 'reset', while on the EPROM it is address line A14, which may be made high by 'high' addressing or glitches, causing the clock to be reset.

## VHF-low converter

**June 1993**

The parts list should be corrected to

read:

1	2 $\mu$ H2	L3
1	0 $\mu$ H1	L5

The circuit diagram is correct. The sub-1 $\mu$ H chokes used in this project are available from, among others, Cricklewood Electronics.

## 1.2 GHz multifunction frequency meter

**December 1992**

The recommended LCD module Type LTN211-F10 is no longer manufactured by Philips Components, and may be replaced by the compatible types LM016L from Hitachi, or the LM16A21 from Sharp.

# ELECTROMAGNETIC COMPATIBILITY (2)

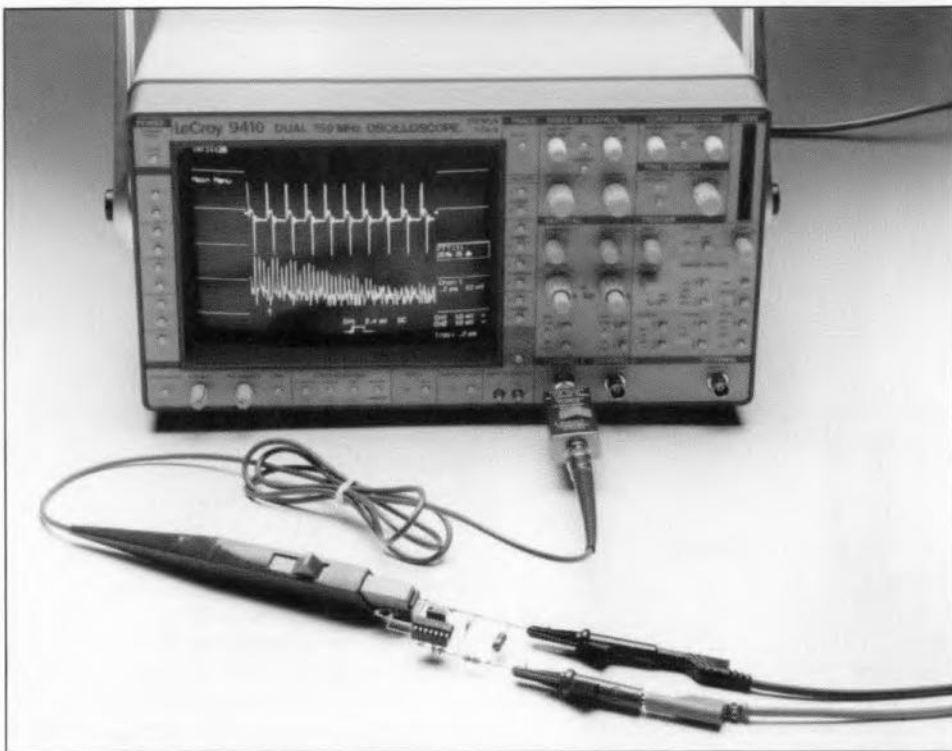
## From theory to practice

By J. Ruiters

As already stated in Part 1 of this two-part article, the EMC Directive must be taken into consideration when the marketing, and thus the design, specification is drawn up. This makes it far cheaper for the final product to meet the EMC guidelines than taking corrective measures in the later stages of the production process.

Although much work has been done by, for instance, the Department of Trade & Industry, The Institution of Electrical Engineers, and organizations like ERA Technology, in informing industry and all who are affected by the Directive, the practical application of EMC is still in its infancy. This is mainly because of the great variety of possible compatibility problems: after all, each design is different from the next, each product may be used in a different environment. On top of that, there are specific requirements for specific systems. Here are a few guide lines for designers.

- **Design on the basis of representative models.** In other words, use models that are characteristic of reality. Too often designers take decisions on the basis of analyses on non-valid models. If, therefore, a design decision does not yield the desired effect or result, the conclusion must be that the model used was not, or only partly, correct.
- **Always consider component properties as a function of frequency.** This rule applies to the range 0 Hz to 12 GHz. For instance, in an optoisolator common-mode signals are converted to differential-mode signals; this process, in EMC terms, is frequency-dependent. Another example is that one metre of yellow/green earth wire (as found in mains cable) represents an inductance of 1  $\mu$ H (this will be reverted to later). At 10 MHz, this gives an impedance of 63  $\Omega$ , which



shows that much equipment cannot be made EMC approved by just 'earthing it properly'.

Figure 7 shows that the behaviour of electrolytic capacitors is strongly frequency-dependent: above about 10 kHz, an electrolytic capacitor is no longer a capacitor, but an inductor. This fact is important in decoupling power supply lines for high frequencies.

- **Think in terms of current.** It is well known that in a closed circuit current can flow even though the circuit is not connected to a voltage source. If such a circuit is placed in a varying magnetic field, a current equal to  $-1/R \cdot d\phi/dt$  flows. This makes it clear that each measured potential difference (pd) is determined partly by the meter leads and the magnetic flux,  $d\phi$ , which (accidentally) is enclosed by these leads. It is, therefore, virtually impossible to conform to the EMC Directive on the basis of voltage considerations.

Even a more fundamental consideration of 'potential difference' leads to a preference of thinking in terms of current. From Maxwell's Second Law, which is applicable to each and every electromagnetic phenomenon, it follows that at frequencies that are not zero the potential difference between two points is dependent on the route along which the

electric field is integrated. Strictly speaking, therefore, potential difference has meaning only in the context of electrostatic fields. Note that Kirchhoff's Second Law ( $\sum U=0$ ) is merely a special case of Maxwell's Second Law ( $\sum U=-d\phi/dt$ ) and is, therefore, often not sufficiently accurate. However, Kirchhoff's First Law ( $\sum I=0$ ) is always valid. In other words, voltage does not always have a rational physical meaning, whereas current does.

### Properties of current

From what has been said, it is important to be well aware of a number of properties of current. In the first place: **currents always flow in closed circuits (loops)**. This is an important fact, because it is these loops that determine the emission and susceptibility to interference of an electronic circuit. It also explains why earthing does not always have the desired effect. After all, a current will flow to earth only if it cannot flow elsewhere. Mother earth is definitely not a bottomless pit into which we can dump all our interfering signals.

**Each and every current sets up an electromagnetic field.** A current-carrying conductor is always surrounded by a magnetic field ( $H$ ), while as a result of the charge on the conductor an electric field ( $B$ ) ensues between the conductor and its

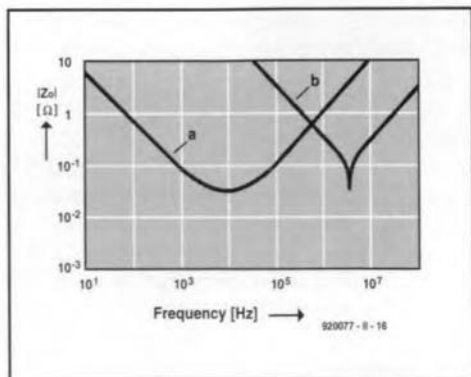


Fig. 7. Impedance as a function of frequency, (a) of a 2200  $\mu$ F capacitor, and (b) of a 470 pF ceramic capacitor.



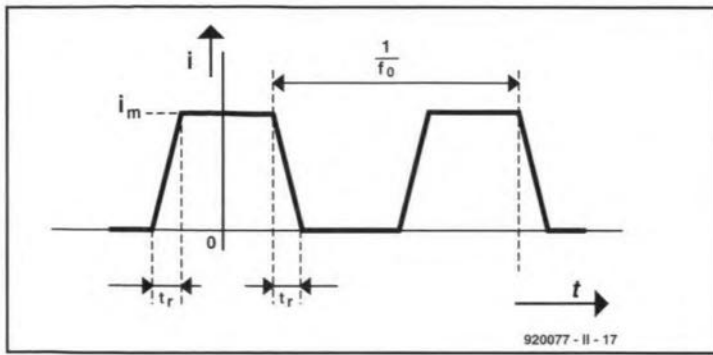


Fig. 8. True rectangular waveforms cannot be attained; the usual shape is trapezoidal as shown (slightly exaggerated).

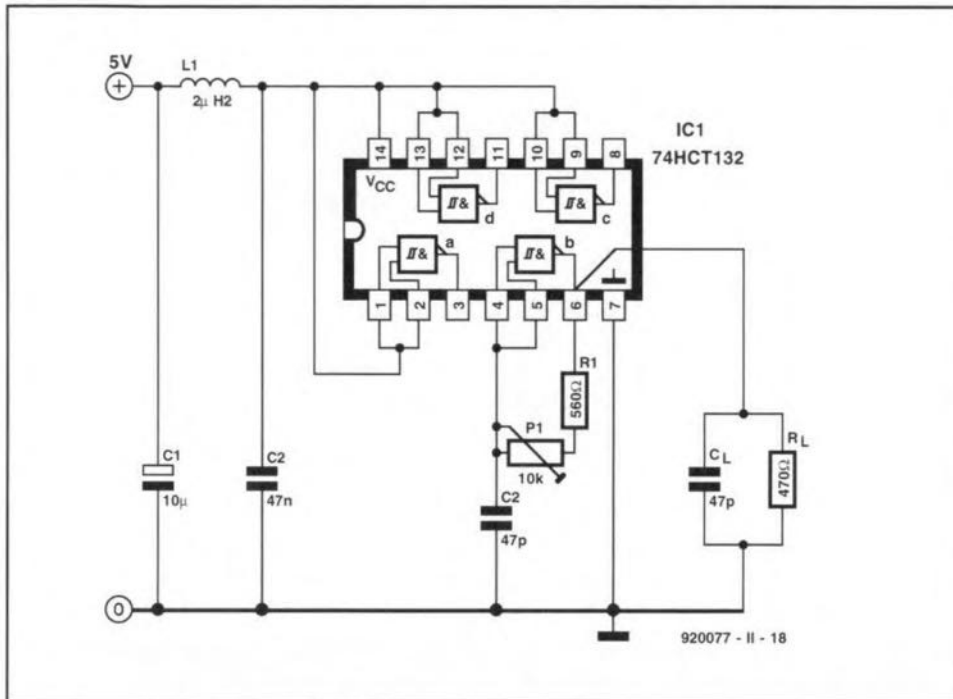


Fig. 9. In this digital oscillator, several currents have been measured. The measurement set-up is as shown in the introductory photograph.

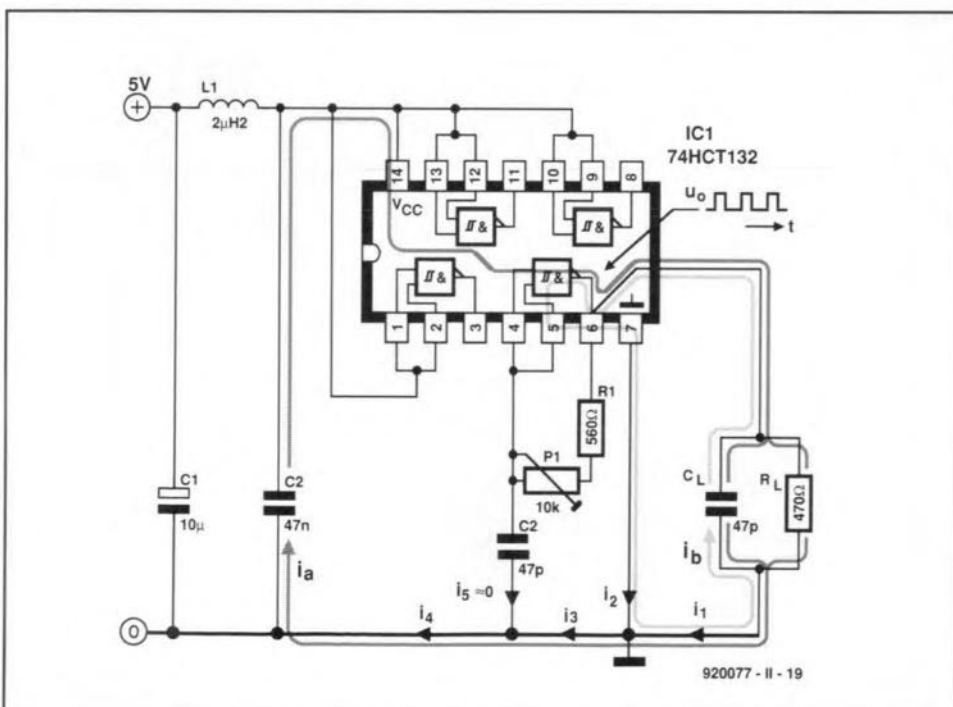


Fig. 10. The radiation of the oscillator is determined by currents  $i_a$  and  $i_b$ .

environment. The electromagnetic field causes the conductor to have not only resistance, but also several parasitic properties, such as inductance ( $1 \text{ nH mm}^{-1}$ ) and capacitance (read: coupling) to its ambience. The electromagnetic fields cause couplings over (electrically) short distances: cross talk.

To be able to predict the electrical behaviour of a design on the basis of a (low-frequency) network model (the CAD drawing, for instance), these field effects must be taken into account by adding to the model the correct parasitic components and sources.  $E$ -field couplings (interfaces) are indicated by parasitic  $C$ s (important in, for instance, cross talk in high-impedance clock circuits), and  $H$ -field couplings by parasitic  $M$ s (mutual inductance) or  $L$ s (self inductance).

It is obvious that a knowledge of these matters is of importance in the design of printed-circuit board layouts. Many current CAD programs were written before the EMC Directive was formulated, so that, in order to comply with EMC guide lines, many critical tracks (usually about half of the total) must be laid manually by the designer.

## Low and high frequency

Network theory enables the designer to approximate physical reality with models by replacing the  $E$ - and  $H$ -fields by impedances. It must be borne in mind, however, that the familiar low-frequency approximation is permitted only if the length,  $\ell$ , of the current loop is small with respect to the wavelength  $\lambda = 3 \cdot 10^8 f^{-1}$ . In words, the low-frequency approximation is valid for small systems only, that is, systems that satisfy the rule of thumb  $\ell \leq \lambda/10$ . Even then, as has already been hinted at, a low-frequency analysis will already lose much of its value if the effects of the  $E$ - and  $H$ -fields are not, or insufficiently, specified in the network elements (for instance, because it was assumed that there are no fields around or between the connecting wires).

In the case of a large electrical system ( $\ell \geq \lambda/10$ ), that is, a high-frequency system, the designer must apply transmission line theory (characteristic impedance, reflections, standing waves, and so on).

## Designing current loops

The electric field strength around a current-carrying circuit (read: small magnetic dipole) is directly proportional to the area of the loop in which the conductive or capacitive displacement currents flow. The maximum radiated field,  $E_m$ , at a distance  $r$  from a small current loop through which a trapezoidal current flows (see Fig. 8), is estimated from:

$$E_m = 2Z_0 S / \pi r c^2 f_0 i_m / t_r \quad [\text{V m}^{-1}]$$

where  $Z_0$  is the radiation resistance in

air ( $377 \Omega$ ),  $S$  is the area of the current loop,  $c$  is the speed of propagation of electromagnetic waves ( $3 \cdot 10^8 \text{ m s}^{-1}$ ),  $f_0$  is the frequency of the trapezoidal current,  $i_m$  is the pulse magnitude, and  $t_r$  is the first transition duration (rise time). The expression applies to a distant-field situation, which assumes that the observer distance,  $r > \lambda / 2\pi$ .

The wavelength  $\lambda = 3 \cdot 10^8 / f$  is thus a yardstick of whether the approximation formula may or may not be used. It is important to note that  $\lambda$  is not the fundamental frequency, but the harmonic nearest to  $1/\pi t$  Hz. This is because the electric field strength reaches its highest value with harmonics around this spectral cut-off point.

That the area,  $S$ , in the above expression must include the entire loop is made clear by considering a Schmitt trigger oscillator (see Fig. 9), which is based on a Type 74HCT132 NAND gate. The oscillator frequency can be varied with  $P_1$  over the range 1–10 MHz.

Capacitor  $C_1$  and low-pass filter  $L_1$ - $C_2$  bound the emission area in the direction of the power supply. Because of  $L_1$ ,  $C_1$ , and  $C_2$ , the spectrum of the supply current (to the left of  $L_1$ ) consists of low-frequency components that do not contribute to the radiation.

Because of the load on the gate,  $R_L$ - $C_L$ , two current loops ensue that determine the radiation. The first, indicated in Fig. 10 by  $i_a$ , carries the sum of the currents through  $R_L$ , the charging current of  $C_L$ , and the switching current of the IC. The second mesh current,  $i_b$ , is characterized by the displacement current that arises as a result of  $C_L$  discharging at the instant the output of IC<sub>1b</sub> goes low.

The current waveforms,  $i_1$ - $i_3$ , mea-

sured with a current probe are shown sequentially in Fig. 11. Note that  $i_5$  is negligibly small, whence  $i_4 \approx i_3$ . Note also that the amplitude of the currents (and thus the strength of the radiated field) is determined by  $C_L$  and not by  $R_L$ . In practice,  $C_L$  consists of the sum of the wiring capacitance, and the input capacitance of the digital circuit.

Characteristic values for the IC are:  $t = 3 \text{ ns}$ ,  $i_m = 40 \text{ mA}$  and  $S = 25 \text{ cm}^2$ . Substituting these values in the radiation formula, it is possible to estimate the maximum field to be expected at a distance of 10 m from the oscillator. From this, it appears that the radiation limit of  $30 \mu\text{V m}^{-1}$  is already reached at an oscillator fre-

quency of 3.3 MHz. The harmonics responsible for the limit to be exceeded lie above  $1/\pi t$ , that is, 106 MHz, or from the 33rd harmonic up ( $1/\pi t f_0$ ).

To keep the radiation from current loops within bounds, a well thought out PCB design is imperative. Particularly effective is a board with a reference plane or reference grid. On such a board, the main part of the return current flows underneath the supply line (in agreement with the minimum-flux principle, this is the route of least impedance). A further benefit is that this also gives the smallest possible area of the current loop. All these measures reduce the radiation. On single-sided boards and double-sided

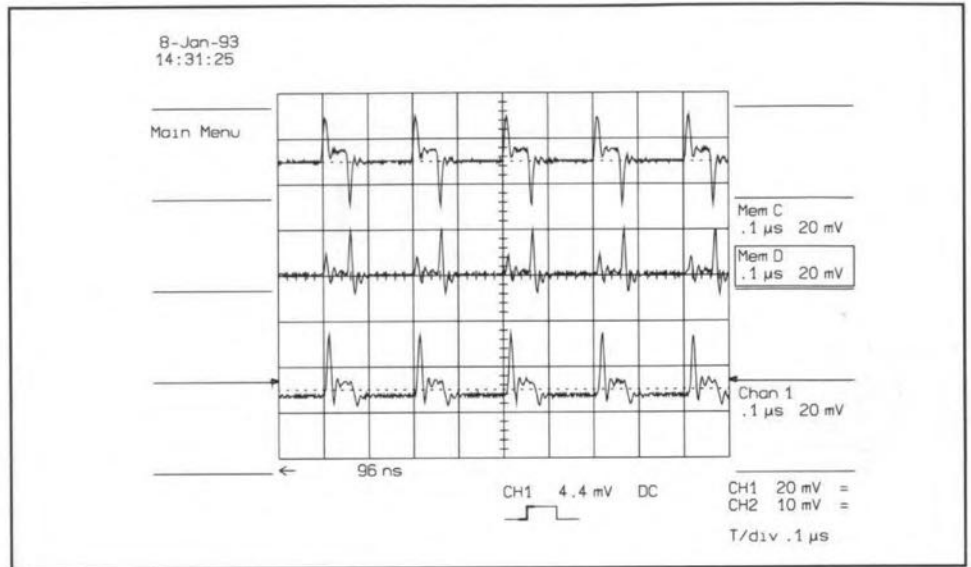


Fig. 11. The output current of the IC, 1, consists of the charging and discharge current of  $C_L$  B and the current through  $R_L$ . The current in the earth conductor, 2, consists of the discharge current of  $C_L$  and the switching current of the IC itself. The current in the large loop is equal to currents 1 and 2.

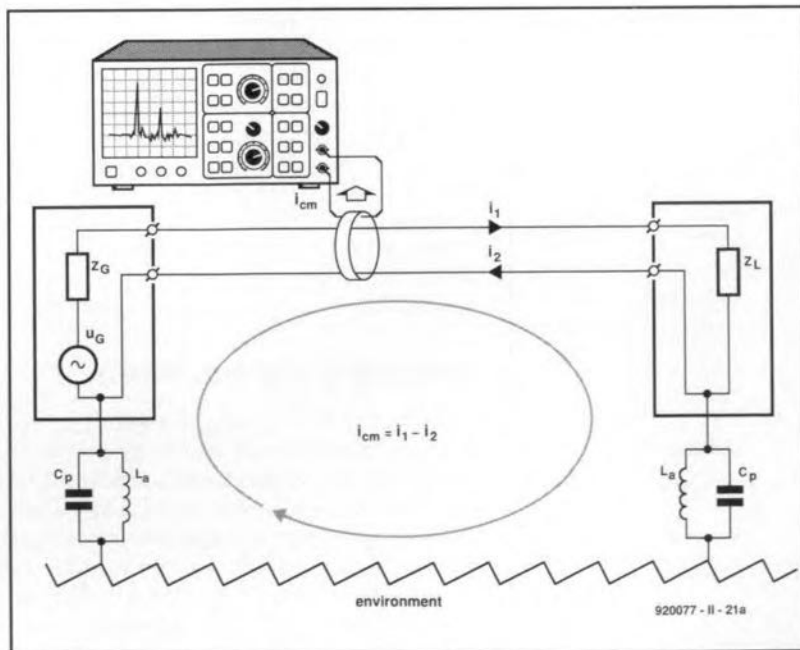


Fig. 12. Common-mode currents occur as the result of a coupling between the circuit and its environment. They may be measured with an HF tong-test ammeter and a spectrum analyser. The coupling is represented here by parasitic capacitances  $C_p$  and earth connections  $L_a$ .

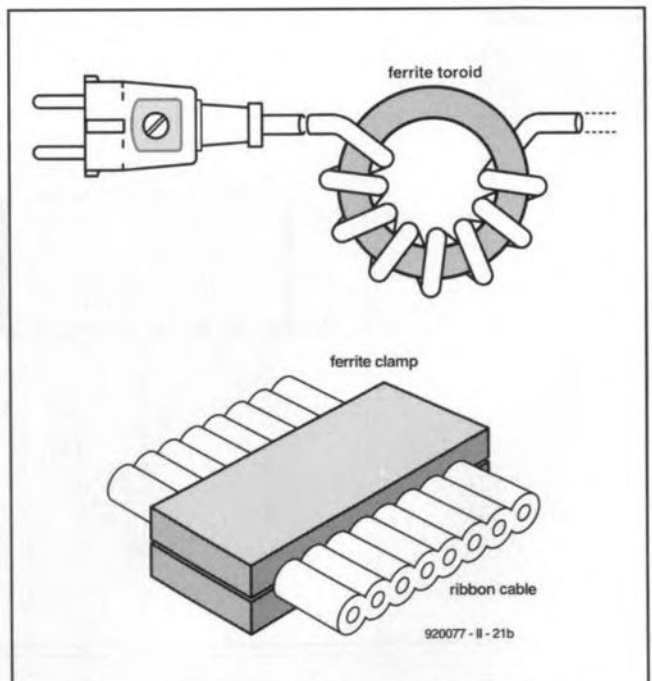


Fig. 13. Radiation may be reduced by ferrite materials like a clamp around a flatcable or the mains cable wound around a ferrite toroid.

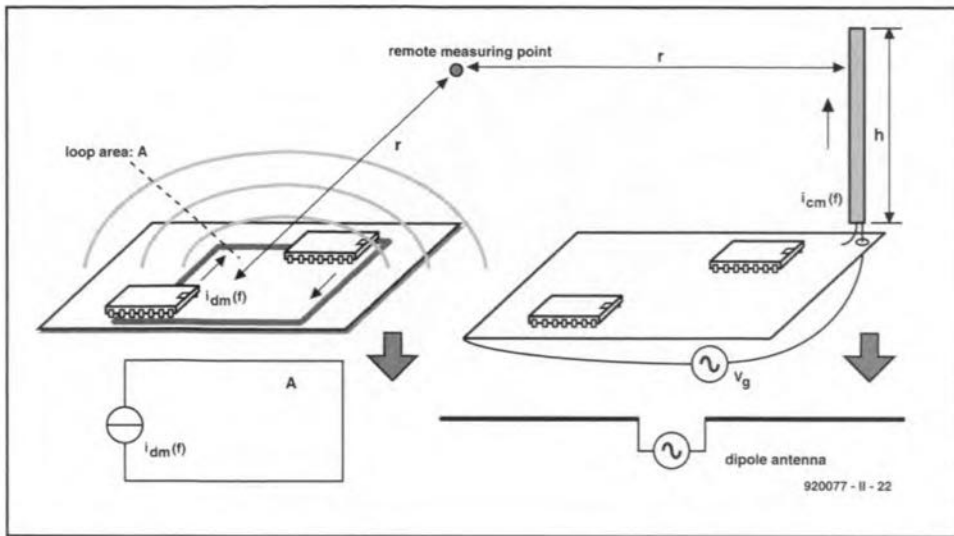


Fig. 14. Energy transfer by radiation. Differential mode radiation (left) is a result of the (wanted) current through an electrically small loop. Common-mode radiation (right) results from an (unwanted) antenna current through the cables.

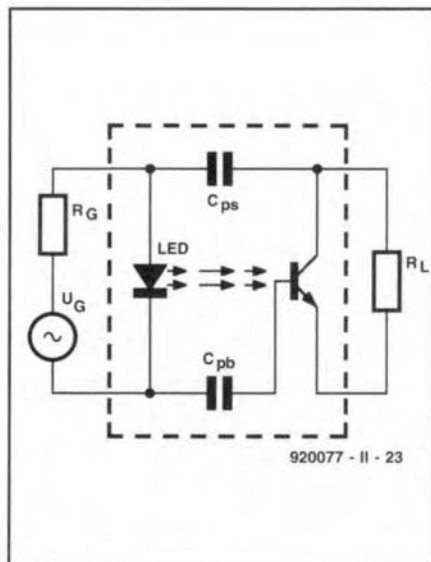


Fig. 15. Parasitic capacitances  $C_{pb}$  and  $C_{ps}$  cause the conversion in the optoisolator of CM signals into DM signals.

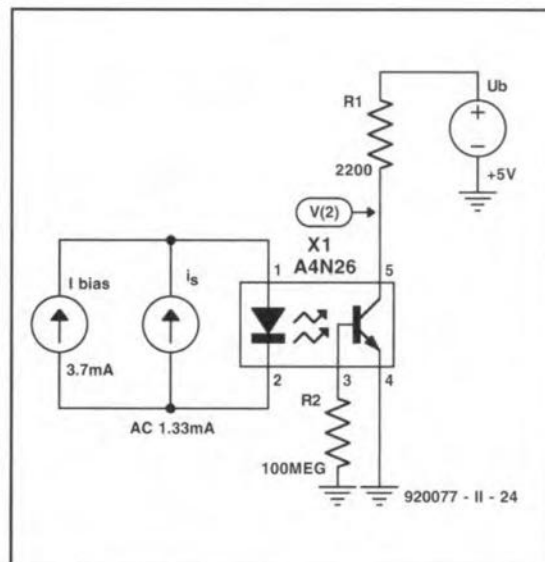


Fig. 16. Pspice model of the electrically isolated data connection in Fig. 15.

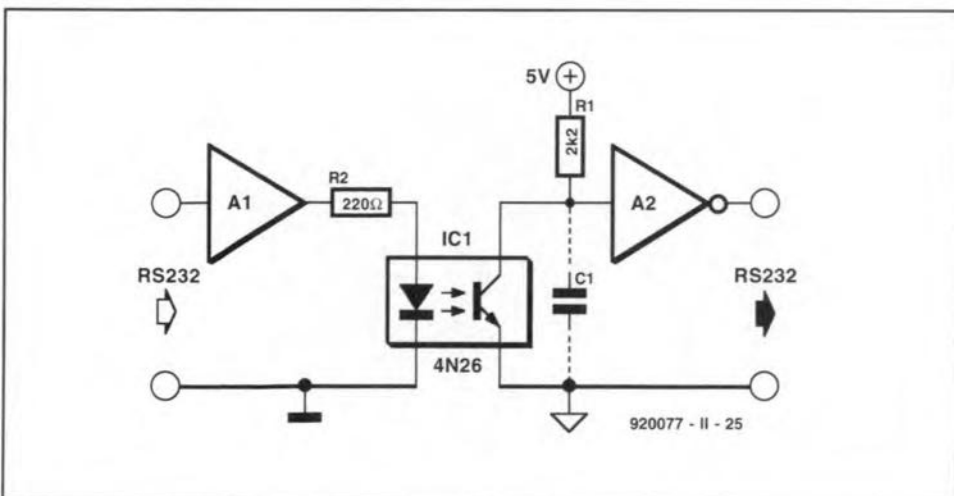


Fig. 17. Basic circuit of an electrically isolated data connection.

ones without a reference grid, the current-loop areas may be kept small by keeping the distance between the supply and return conductors small.

Also, it is advisable never to use faster logic circuits than is necessary: a higher  $t_r$  will after all cause a lower  $E_m$ . Furthermore, it is clear from the radiation formula that the clock frequency should be as low as possible. The phenomenon that  $E_m$  is directly proportional to the clock is a consequence of the fact that the amplitude of the harmonic near to  $1/\pi t$  is directly proportional to  $f_0$ . Since the electric-field strength is directly proportional to the amplitude of the current, it is also directly proportional to  $f_0$ .

## Beware of common-mode currents

A current loop always maintains a coupling with its surroundings, either by conduction or by radiation. 'Surroundings' include objects such as a metal table top, a central heating radiator, an earthing point, and so on. It all depends on which coupling predominates at a given frequency. Owing to the coupling to the surroundings, common-mode currents, also called asymmetrical currents, arise—see Fig. 12. Unfortunately, common-mode currents often flow through conductors (supply cables), whose dimension is of the same order as the wavelength: for instance,  $106 \text{ MHz} = 2.8 \text{ m}$ . This means that in electronic systems whose dimensions are much smaller than the wavelength of the signals, the cables connected to the system radiate more than the tracks on the PCB. Therefore, **the radiation of most products is determined by the magnitude of the high-frequency common-mode currents flowing in the cables.**

The CM currents may be measured with an HF tong-test ammeter and a spectrum analyser. In the design stages this test and the rule of thumb  $I_{CM} < 5 \mu\text{A}$  gives a good idea of whether the radiation will be higher or lower than the legal limit of  $30 \mu\text{V m}^{-1}$ . If, in the prototype, the measured CM current through one of the cables (mains lead, cable to printer, signal cables) is greater than  $5 \mu\text{A}$ , the final product will almost certainly exceed the maximum permissible radiation.

The radiation can be reduced by inserting a high CM impedance in the current path. For example, a ferrite clamp may be placed around a flatcable as shown in Fig. 13. The same drawing shows how the CM currents in a mains lead may be reduced by winding the lead through a ferrite toroid.

Figure 14 shows two other ways via which interference may be transferred through radiation.

## Design example

An optoisolator can often be used to put

some of the rules stated into practice. It is an analogue device that is frequently used with digital hardware. In such cases, the optoisolator is controlled digitally, so that, at least from a functional point of view, its output is also digital.

A suitable optoisolator for use in EMC designs is shown in Fig. 15. As usual in such a device, the signal transfer is effected by light. Capacitors  $C_{pb}$  and  $C_{ps}$  show, however, that there is another, spurious coupling between input and output. The effect of these parasitic capacitances has been investigated with a simulation program, Pspice. A setup with which this program can be used is shown in Fig. 16. This model is derived from the electrically isolated data connection in Fig. 17.

In Fig. 16, the optoisolator has been set to its linear operating range with a direct current of 3.7 mA. This value has been determined empirically and ensures that a direct voltage, whose level is equal to half the supply voltage, is present at the output. To enable the differential mode to differential mode transfer,  $u_{out}/i_s = V(2)/i_s$ , to be computed, an alternating current source, providing 1.33 mA, has been added at the input. With Pspice this source can be frequency-swept and the amplitude characteristic shown in Fig. 18 calculated. The most important datum to be gleaned from the characteristic is that the bandwidth for the wanted signal transfer is about 25 kHz.

In practice, the electrically isolated data connection will be affected by the common mode source of interference across the optoisolator. To study the effect of this, a voltage source,  $u_{CM}$ , and two 50- $\Omega$  impedances have been added to the model in Fig. 19. Since the optoisolator is not ideal ( $C_{ps}$  and  $C_{pb}$ ), part of  $u_{CM}$  will appear at the output. This is awkward, because this interference signal is in series with the output voltage. If the level of the interference is (relatively) high, it is possible that gate A2 (read: wideband amplifier) produces erroneous logic levels during the transition from one to the other. This comes down to insufficient immunity. Note that this transition in EMC literature is called common-mode/dif-

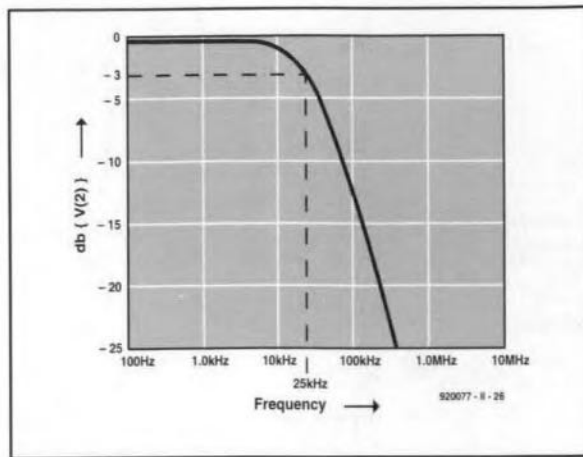


Fig. 18. The simulated DM-DM characteristic according to Fig. 16.

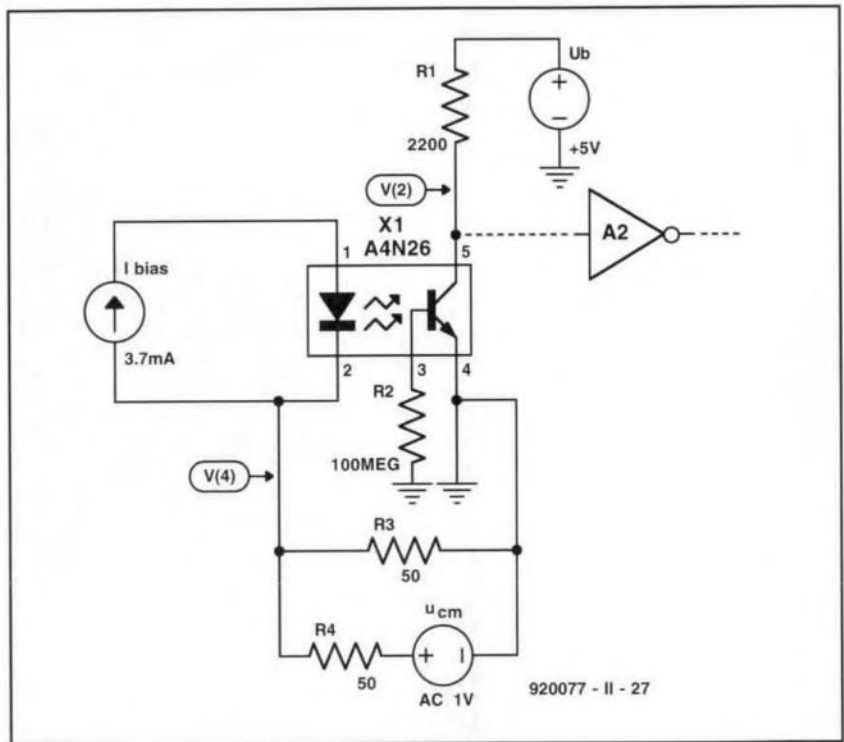


Fig. 19. To compute the CM-DM transfer, voltage source  $u_{CM}$  was added to the model in Fig. 16.

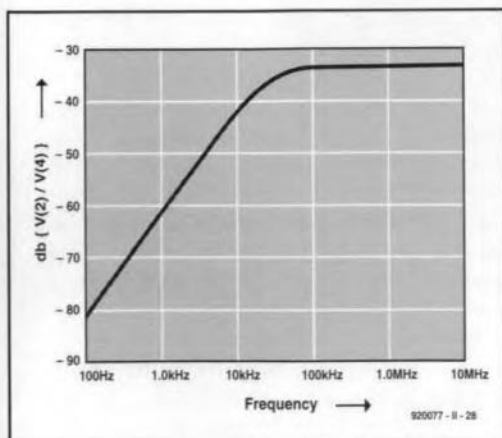


Fig. 20. CM-DM transfer characteristic computed from the setup in Fig. 19.

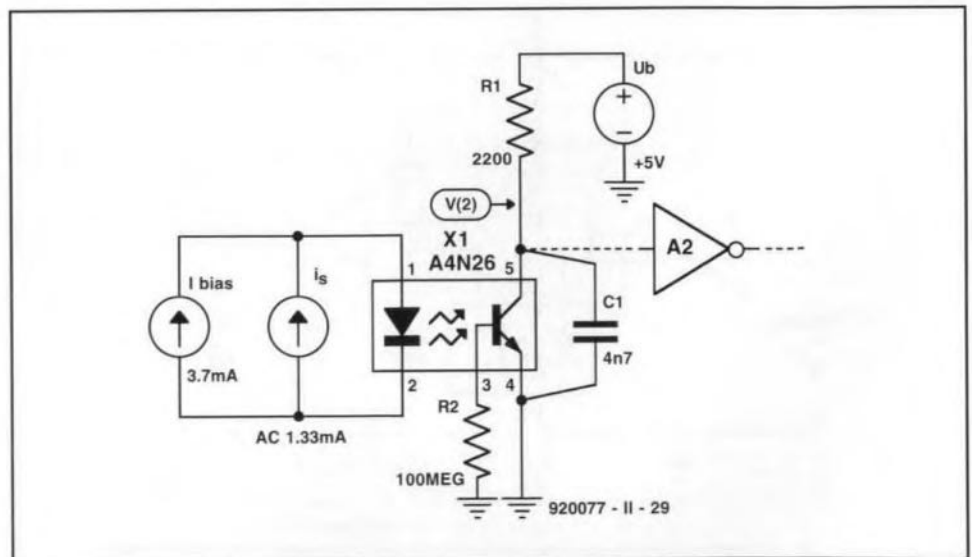


Fig. 21. Capacitor  $C_1$  reduces the DM transfer at high frequencies.

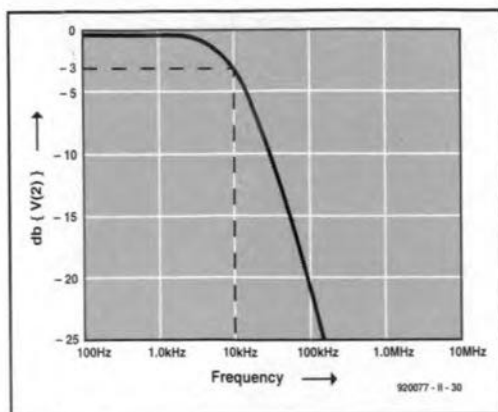


Fig. 22. The DM-DM characteristic for the set-up in Fig. 21.

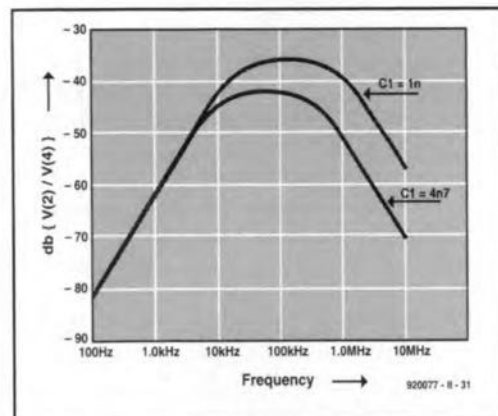
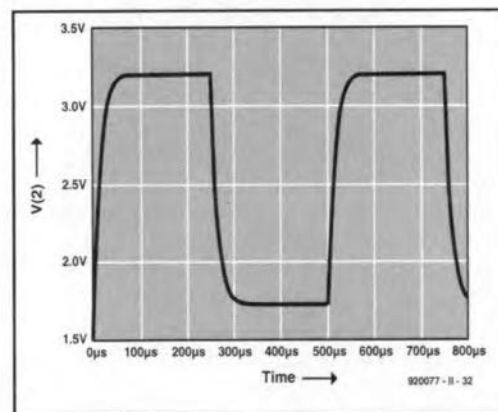


Fig. 23. The CM-DM transfer characteristic for Fig. 21 with different values for  $C_1$ .



ferential mode (CM-DM) transition.

The quality of an optoisolator, as far as immunity is concerned, is a measure of the degree to which CM signals are suppressed. The characteristic calculated on the basis of the model in Fig. 19 is shown in Fig. 20. This indicates that the suppression of CM signals reduces with rising frequency. Again, this is awkward, because, in practice,  $u_{CM}$  contains primarily HF (>1 MHz) components. The characteristic can, however, be improved greatly by reducing the bandwidth of the optoisolator. This is done in Fig. 21 by shunting the switching transistor with a 4.7 nF capacitor. This reduces the bandwidth to about 10 kHz—see Fig. 22; the CM suppression for high frequencies is thereby increased. The CD-DM characteristic for the model in Fig. 21 with shunt capacitors of 1 nF and 4.7 nF is given in Fig. 23. It is clear from the curves that the CM suppression is inversely proportional to the bandwidth.

When the electrically isolated data connection in Fig. 17 operates at a bandwidth (BW) of 10 kHz, the first transition duration (rise time),  $t_s$ , of the pulses at the output of the optoisolator is  $t_s = 0.35/BW = 35 \mu s$ . The maximum input frequency at which a correct digital signal can be measured at the collector of the phototransistor is, by rule of thumb,  $BW/5 = 2 \text{ kHz}$ . The output signal simulated with Pspice is shown in Fig. 24; the model is given in Fig. 25. The circuit is thus suitable for use in an RS232 connection with baud rates up to 4000 Bd (which coincides with the frequency limit of 2 kHz). A complete design was published earlier this year\*.

\*Electrically isolated RS232 interface. *Elektor Electronics*, March 1993.

Fig. 24. Characteristic of the output voltage with a channel bandwidth of 10 kHz and a rectangular (2 kHz) input current.

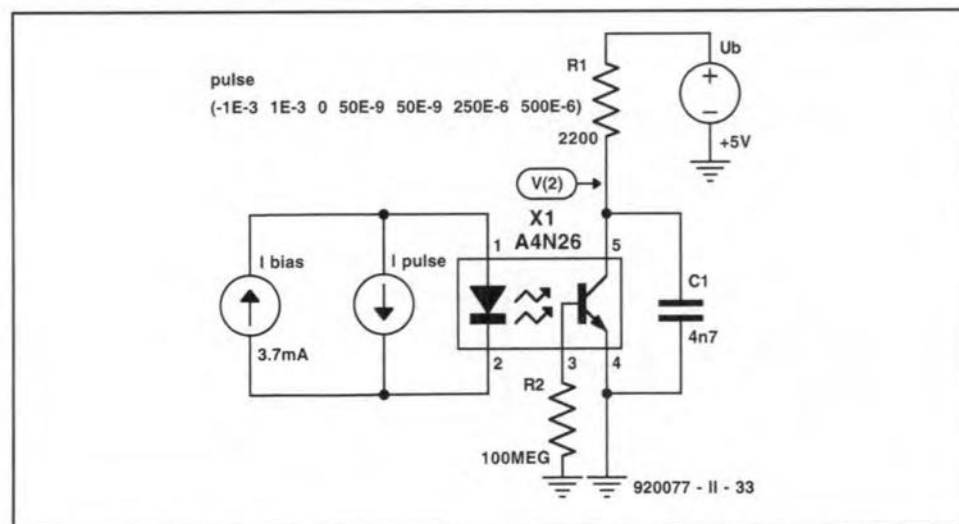


Fig. 25. Model used by Pspice for computing the characteristic in Fig. 24.

### Further reading:

*Electronic system design: interference and noise control techniques*, ISBN 0-13-252 123-7, by J.R. Barnes, Prentice Hall, 1987.

*Interference-free electronics: design and applications*, ISBN 0-86238-255-6, by S. Benda, Chartwell Bratt, 1991.

*Electromagnetic compatibility: Europe*, ISBN 0-580-20917-2, British Standards Institution, 1992.

*EMC: electromagnetic theory to practical design*, ISBN 0-471-82878-X, by P.A. Chatterton & M.A. Holden, Wiley, 1992.

*ZZAAP! taming ESD, RFI and EMI*, ISBN 0-12-189930-6, by M.B. Corp, Academic, 1990.

*Electromagnetic compatibility: bibliography and information pack (2nd Edition)*, ISBN 0-85296-495-1, by J. Coupland & P. Fountain, IEE Technical Information Unit, 1993.

*Grounding for the control of EMI*, ISBN 0-932 263-17-8, by H.W. Denny, Don White Consultants, 1989.

*Electromagnetic compatibility in radio engineering*, ISBN 0-444-99722-9, by W. Rotkiewicz (ed), Elsevier Scientific, 1982.

*Electromagnetic compatibility: applied principles of cost-effective control of electromagnetic interference and hazards*, ISBN 0-8247-1887-9, by H.M. Schlicke, Marcel Dekker, 1982.

*Electromagnetic compatibility handbook*, ISBN 0-442-28903-0, by J.L.N. Violette, D.R.J. White & M.F. Violette, Van Nostrand, 1987.

Designers may also note that Rohde & Schwarz's Type ESHS 10 and ESVS 10 test receivers are now available from Livingstone Hire. These instruments meet the measurement requirements of European EMC Standards incl. 55 011 to 55 022, ETS, FCC, VCCI and VDE 0871 to 0879. Full information on these versatile instruments from Livingstone Hire, Livingstone House, Queens Road, Teddington TW11 0LB, England. Telephone (0)81 943 5151; Fax (0)81 977 6431.

# CW COMPATIBLE T/R SWITCH

The use of CW (morse) on a high-power transmitter/receiver presents a serious risk of burned antenna (coax) relay contacts or destruction of a GaAs FET preamplifier. Fortunately, that problem can be overcome quite easily at a very small outlay with the circuit described here.

Design by Pedro Wyns, ON4AWQ

ALTHOUGH a number amateur radio magazines have recently carried designs that ensure that antenna relays change before the transmitter is powered, most of these circuits are suitable for 'phone' (voice) transceivers only. Just in case you did not know, early switching of the antenna relay is necessary to protect the expensive and

highly sensitive GaAs FET preamplifier(s) against the huge power produced by the transmitter.

The trouble starts if you want to use a commercial VHF or UHF transceiver for high-power, high-speed CW modes such as Meteor-scatter, Tropo-DX or EME (earth-moon-earth). These modes require high transmitter power levels

and extremely sensitive preamplifiers. Unfortunately, most commercial transceivers have a built-in COR (carrier operated relay), which powers the transmitter the instant the morse key is pressed, not allowing sufficient time for the antenna relay to switch over.

The circuit shown here is connected between the microphone, CW key and the transceiver. The operation of the circuit is quite simple: in 'phone' mode, the antenna relay is energized the instant the PTT switch on the microphone is pressed. The transmitter, however, is switched on a little later by a timer built around Schmitt-trigger NAND gate IC1c. When the PTT switch is released, the reverse takes place: the transmitter is switched off immediately, while the relay is de-energized a little later because of the delaying action of gate IC1d.

When CW is used, the key signals are blocked by wired-AND gate IC1a-T2 until the delay introduced by timer IC1c has elapsed (approx. 200 ms). The circuit around IC1b provides a 'hang' time of about 2 seconds to prevent relay clatter while the transmitter is being keyed. Transistor T4 is a darlington type to enable relays 'outside' the transceiver to be controlled also. If this is not required, the BD675 may be replaced by a BC547. Note that the collector of T5 is supplied via the coil of the Tx/Rx relay in the transceiver. ■

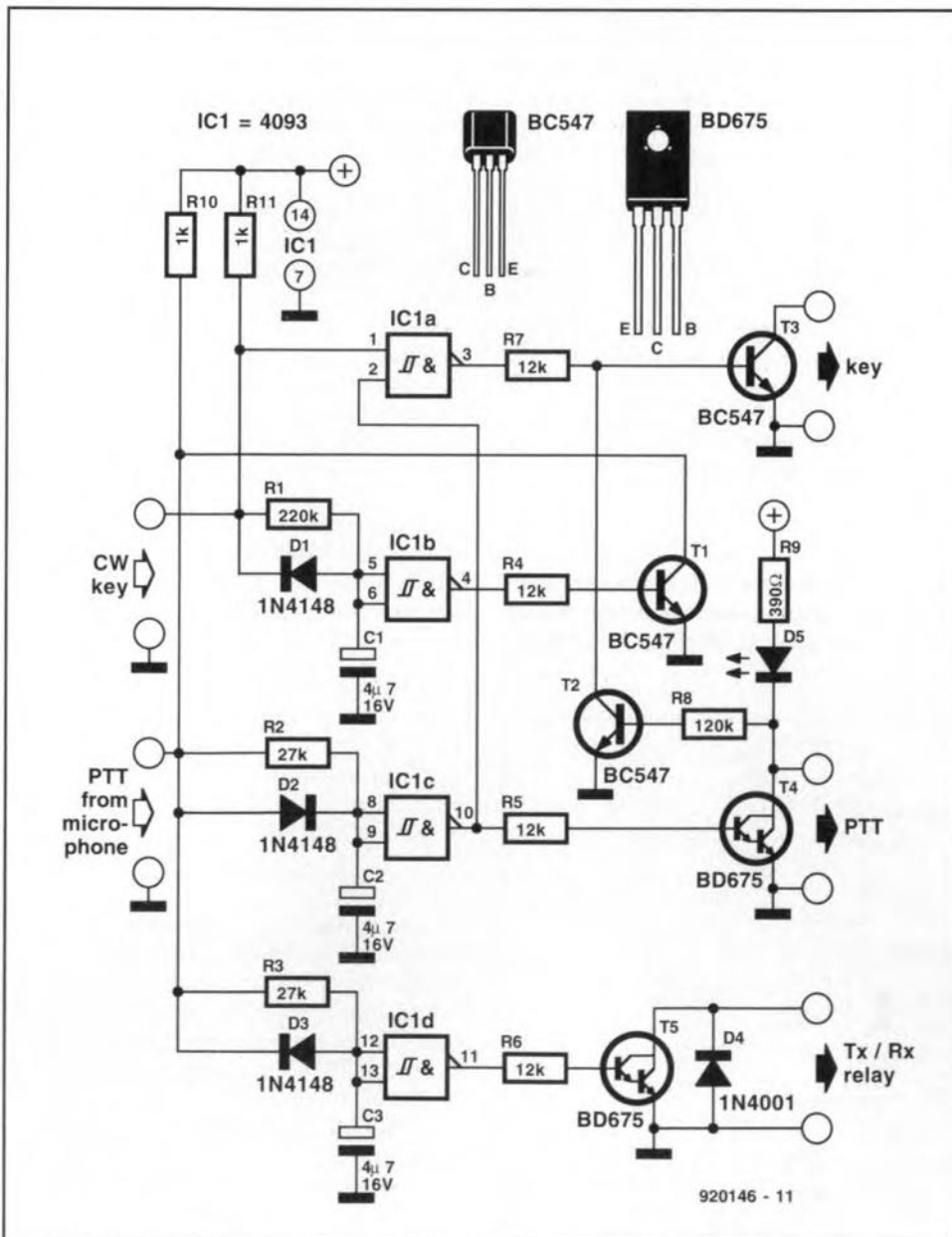


Fig. 1. Circuit diagram of the transmit/receive switch

**A two-monthly column by Keith Hamer and Garry Smith**

SEVERAL intense tropospheric openings punctuated the bleakness of February and March. Signals were plentiful in Band III and at UHF, particularly on February 14th when many French, German and Benelux stations emerged at considerable strength.

By comparison, Band I reception was relatively quiet, apart from several sustained sporadic-E openings in the latter half of February. Other Band-I activity was due to meteor-scatter and auroral activity.

**Reception reports**

Andrew Jackson of Birkenhead has written to say that tropospheric reception conditions were excellent during February. The most productive day was Sunday 14th when most of the 'usual' signals were around plus some new ones. Transmissions received in clear colour included RTBF-1 (Belgium) on channel E57, RTBF-TELE 21 on channel E60, and Canal Plus (France) on channel E63. The 'VOX-Koeln' FuBK test card was received on the 5th and the 13th, and this was also strong. Sporadic-E activity occurred on February 15th at 2037h with prolonged reception from a German ARD-1 transmitter on channel E2.

Andrew has been monitoring the new Irish TV channel allocations from the Kippure transmitter on a daily basis. RTE-1 can be good at times although co-channel interference from the Maghera transmitter does occur. Signals from the Band-I channel B Maghera outlet have also been available during tropospheric activity.

On the 14th, a strange-looking test pattern was present on channel E11 for most of the day and well into the evening. It resembled the FuBK pattern, but had a distinctive central 'window'; there was no identification. This was subsequently identified as 'Canal Plus Belgique' on test from the Leglise transmitter, which once broadcast RTBF-1 programmes.

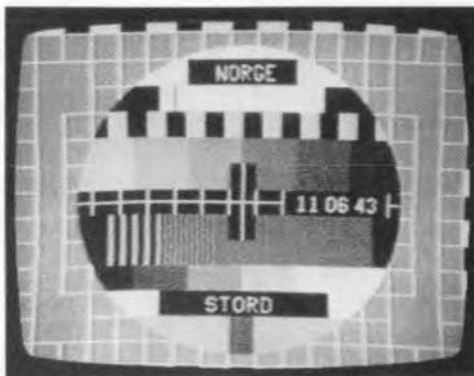
Davis Asher of Wrexham has only DX-ed at UHF so far, but plans are afoot to install VHF equipment in the near future. His successes include several Dutch and German outlets, with the reception of almost perfect Teletext from the Nederland-3 network. Unfortunately, Nederland-2 on channel 27 is now blocked by a local relay station. His equipment consists of a 10-element wide-band aerial, aligned East North-East.

This is fed into a home-brew mast-head amplifier with 15-20 dB gain. A Goodmans 20-inch Teletext receiver and Goodmans 2500 VCR completes the set-up.

Stephen Michie of Bristol found that early February was active with sporadic-E on the 2nd from Hungary. Reception consisted of a tennis match and later the PM5544 test pattern with the identification 'MTV-1' at the top, and 'Budapest' in the lower black rectangle. There was enhanced tropospheric reception on at least seven days, with the weekend of the 13/14th being the most active. One German station was transmitting the FuBK test pattern with the inscription 'ARD 1 PROG' and the date and digital clock below the central block. There was an unidentified German signal on channel E36 which was possibly RTL PLUS from Dusseldorf. Stephen found that March was very quiet with only the daily signals from the Goes transmitter, and the occasional reception from Lopik (both outlets are located in the Netherlands).

Iain Menzies of Aberdeen has been monitoring the HF bands to evaluate the MUF (maximum usable frequency) and the reception conditions in general. On 24th February, a station in Michigan reported a MUF of 46 MHz. Sporadic-E signals were noted two days later at 1900h UTC on channel R1, almost totally masked by baby alarms! On the 27th on 28 MHz between 0830h and 1030h UTC, Australia was heard at S9+ with several FM transmissions at over 30 MHz. Unfortunately, the MUF did not reach TV frequencies.

During the first five days of March, South African stations reported working as far North as Brittany. On March 11th,



The PM5534 test card from the Stord transmitter (30 kW ERP channel E5) in Norway, received in Derby via Sporadic-E.

an aurora produced G1 and G stations with excellent results from the Lerwick beacon. The usual beacon received via auroral activity was not heard. During the same opening, weak unidentified signals were present on TV channels E2 and R1. On 12th March at 1930h UTC the Lerwick beacon was received again via Aurora, but this time there were no TV signals. The MUF has since been extremely poor. Even 28 MHz has been a struggle at times!

According to Simon Hamer of New Radnor in Powys, the weather forecast on Scottish TV is sponsored by *Kwik-Fit*, and not *Legal and General*. Grampian ITV's clock resembles the old TVS one, though blue and white. The identification in red and white on the Danish PM5534 test pattern is, according to Simon, to tie in with their national flag.

Simon has confirmed that RTL-2 is now operational on the Astra 1A satellite, replacing Screensport. RTL-2 is a spin-off from RTL Plus, but more family-oriented and without 'adult' films. The RTL-2 news is called *Action News*. This service is also available on Eutelsat II F1.

Simon has also advised that various BBC Radio broadcasts can now be found on the UK Gold transponder of the Astra 1B, using the Wegener Panda-1® system. The satellite subcarriers transmit the BBC World Service on 7.38 MHz, Radio 4 (long wave version) on 7.56 MHz, Radio 1 on 7.74 MHz and Radio 5 on 7.92 MHz.

**Log for February**

**02.02.93:** Norwegian PM 5534 test pattern via meteor scatter propagation on channel E3 at 0815h UTC, plus unidentified signals on channel E2. Sporadic-E signals from Hungary were noted between 1145h and 1330h UTC.

**13.02.93:** Sporadic-E activity at 1235h on channel E3. The unidentified reception consisted of an historical play.

**15.02.93:** Strong sporadic-E signals from Germany on channel E2 at 2037h UTC.

**18.03.93:** A small sporadic-E opening from Denmark on channel E3 at 0730h UTC. Also, meteor scatter activity noted on channel R2 at 0750h.

**26.02.93:** Unidentified sporadic-E signals on R1 at 1900h.

Tropospheric reception from France, Eire, Belgium, Germany and the Netherlands was noted on the following dates during February: 1st, 4th, 5th, 9th, 10th, 13th, 14th and 15th. In addition, Luxembourg and Denmark were logged on the 14th.

**Log for March**

**09.03.93:** SVT-1 (Sweden) on channel E6 and SVT-2 E30 via tropospheric propagation.

**11.03.93:** Unidentified signals on channels E2 and R1 via auroral activity.

**14.03.93:** Serbia on channel E3 plus unidentified signals on R2 (meteor scatter).

**18.03.93:** Sporadic-E reception from Germany on channel E2 and Denmark E3.

**20.03.93:** Unidentified FuBK test pattern on channel E2 via meteor scatter at 0825h.

The DX-TV logs were kindly supplied by the following enthusiasts: Andrew Jackson (Birkenhead), Simon Hamer (New Radnor), Iain Menzies (Aberdeen) and Stephen Michie (Bristol).

### 1993 Sporadic-E Season

This is now underway and should last from May to September. An in-depth look at sporadic-E reception was featured in the February 1993 issue of *Elektor Electronics*. To briefly recap, throughout the summer, signals can be received in Band I from transmitters located at distances in excess of 1,100 km. The basic equipment required for reception consists of a tuner covering Band-I channels (48-70 MHz) plus an aerial, such as a dipole with a total length of approximately 2.8 metres.

The modified MP3 converters mentioned in the previous column have all been sold, but several readers have been in contact who purchased the basic unit. Even in their original form they are suitable for sporadic-E work, provided they have Band-I coverage. With the original 5.5-MHz ceramic sound filters fitted, the TV sound from most countries in Western Europe will be heard.

### Service information

**Portugal:** Since its launch in mid-1992, RAP International (RTPi) has been broadcasting for 42 hours per week, taking the best Portuguese programmes from among the four RAP channels (RAP-1 and RAP-2 in Portugal, RAP-Madeira and RAP-Azores). In addition, there are regular news programmes and live football coverage. RTPi also produces a daily news magazine that serves as an interface among the many Portuguese communities throughout the world.

**France:** Canal Plus is gradually introducing a new scrambling system in an attempt to make pirate decoders unusable. The new scrambling system, called 'Syster', has been developed in Switzerland. It is a technically more sophisticated system than 'Discret 1', which was originally adopted for Canal Plus transmissions. It is hoped that the new system will offer greater security, and will be more difficult to 'hack'.

**Belgium:** The Canal+ programme is now aired from the Leglise transmitter on channels E11 and E63. A colour test card with a small but distinctive 'window' in the centre has been used for recent tests. No identification is shown.

### TV systems

During the recent periods of enhanced tropospheric reception conditions, tuning through the UHF band on a normal TV set may have revealed several foreign stations dotted about the band. Given favourable conditions, some of these would be complete with Teletext information. However, the biggest mystery for the viewer is the absence of sound. This is due to the differences in TV systems adopted by various countries, for example, in the UK and Eire the sound carrier sits at 6 MHz above the vision carrier, whereas in countries such as Belgium and Germany the carrier off-set is only 5.5 MHz. In Eastern Europe and the CIS the spacing is 6.5 MHz.

The FM intercarrier sound system is used by every country throughout the world, apart from France and Monaco where AM sound continues to be used. With the intercarrier system, both the sound and vision IF signals are handled by the vision detector, the resultant beat frequency (the frequency difference) being fed into the sound IF stages which respond to either 5.5, 6.0 or 6.5 MHz signals.

The characteristics that make up a TV system can be divided into five main elements: (1) the number of scan lines; (2) positive or negative vision modulation; (3) FM or AM sound; (4) the sound subcarrier off-set; (5) the colour system. Any combination of these can make up a TV system.

Many different systems were originally adopted in Europe. Even during the early eighties there were at least four different line standards in use: 405 by the UK and Eire; 819 by France and Monaco, 525 by the American forces transmitters, and 625 by other countries. Since the closure of the 405-line system in 1985, only 525-line and 625-line systems exist. Transmissions using 819 lines were phased out a number of years ago.

With the exception of France, Monaco and Luxembourg, negative vision modulation is used worldwide. Positive vision modulation was also used by the UK, Eire and Belgium. If such a transmission is received on a 'normal' set, the pictures tend to resemble a black and white photographic negative, i.e., black areas appear white and vice-versa, when viewed on a UK receiver. The synchronization may also be poor due to the incorrect sense of the video detection.

Amplitude modulation (AM) is used for the sound carrier accompanying positive modulated vision signals. The FM intercarrier system is used elsewhere with four different spacings, depending on the system.

PAL and SECAM colour systems are used throughout Europe. SECAM was adopted by Russia, Eastern-bloc countries and France, while PAL was used elsewhere. Since the recent political changes in Eastern Europe, SECAM is gradually being phased out in favour of the PAL system in some countries. Already the Czech and Slovak republics have initiated this change, and the former East German transmitters have radiated PAL for some time.



The station opening caption of the Dutch third network, photographed by David Glenday in Arbroath.

The 'BRT' header information on the PM5544 test pattern as used by the Flemish-speaking networks now reads 'BRTN'. The lower identification 'TV1' or 'TV2' remains unchanged.

**United Kingdom:** DAB (Digital Audio Broadcasting) test transmissions are due to start in London this summer (they will commence in France during 1994 with ten local programmes in the Paris area). Frequencies around 60 MHz in Band I and 220 MHz in Band III have been chosen, which could present problems for UK DX-ers. The choice of Band I frequencies again demonstrates the irresponsibility shown by the powers-that-be, because it is likely to cause interference to European TV services during periods of Sporadic-E propagation.

**Eire:** The channels used for RTE-1 and Network-2 transmissions from Kippure have changed. RET-1 has moved from channel H to E, and Network-2 from channel J to H. Channel J is no longer used. The E and H pair of channels are also used by other Irish transmitters such as Achill, Castletownbere, Clencolumcille, Kilmacthomas and Suir

Valley.

A new RTE-1 transmitter at Maghera is now operating on channel E with 100 kW ERP, and it seems likely to replace the existing channel B outlet. Network-2 is already broadcast from the Maghera site on channel E. A similar move to channel H for RTE-1 seems a possibility for the low-power Glanmire relay which currently radiates the first programme on channel C and Network-2 on channel E.

**Finland:** MTV, which used to provide programmes for the TV1 and TV2 networks, has transferred its output to the commercial TV3 network, which now covers most of the country. The test card is the FuBK with the 'MTV 3' identification.

The TV1 and TV2 networks have recently undergone a complete face-lift because of this move. TV1 is now described as being modern, international and up-to-date; the TV2 network caters for specialist programmes.

**Germany:** The MDR-3 network is now using the FuBK colour test pattern with the identification 'MDR 3 Dresden'. VOX TV, who were given two terrestrial channels previously occupied by WEST-3, also radiate the FuBK pattern with the identification 'VOX — Koeln'.

This month's service information was kindly supplied by Gösta van der Linden and the Benelux DX club, Netherlands; Bernd Trutenau, Lithuania; Pertti Salonen, Finland; Reflexion Club, Germany; Roger Bunney, UK; Simon Hamer, UK; André Gille, France. Please send any news about DX-TV in your part of the world to: Keith Hamer, 7 Epping Close, Derby DE3 4HR, England.



# 80C32 COMPUTER APPLICATION NOTES - 3

## X2404 EEPROM interfacing to an 8751

Design by Zoran Stojsavljevic

XICOR's X2404 is a 4096-bit serial Electrically Erasable PROM (EEPROM), internally organized as two pages, each containing 256x8 bits. The X2404 features a serial interface and an I2C compatible software protocol that allows it to be operated via a 2-wire bus. The pinning and internal architecture of the IC are given in Fig. 1. The SCL (serial clock) input is used to clock all data into and out of the device. The serial data pin, SDA, is bidirectional, and used to transfer data into and out of the device. SDA is an open-drain output, and may be wire-ORed with any number of open-drain or open-collector outputs to form a bus. Address input A0 is not used by the X2404, although it must be tied to  $V_{SS}$  for proper device operation. Address inputs A1 and A2 are used to set the least-significant two bits of the six-bit slave address assigned to the device. The address inputs are static, and should be tied to logic high or low levels, to give one unique address per device.

The circuit diagram in Fig. 2 shows an example application of the X2404 in a 8751 microcontroller driven racing car computer. The functions of this computer are not our prime concern here, hence the following discussion will concentrate mainly on the way the 8751 and the X2404 are set up to communicate properly. The functions of the four push-buttons are:

- S2: adjust clock;
- S3: display max. rpm during race;
- S4: display max. rpm ever.
- S5: reserved.

The hardware implementation of the X2404 is simplicity itself, being essentially restricted to two lines only. In the application circuit, the X2404 records the highest rpm (revolutions per minute) value of the car engine. This is achieved by reducing the ignition pulses to a suitable level, digitizing (Tx), and feeding them to the P3.2 input of the 8751 microcontroller.

### X2404 device operation

The X2404 supports a bidirectional, bus oriented protocol. This protocol defines any device that sends data on to the bus as a transmitter, and the receiving device as a receiver. The device

Following the eight instalment '8051/8032 assembler course' featured in last year's issues of *Elektor Electronics*, this column presents design ideas, programming examples and hardware experiments based on and around the popular 80C32 single-board computer. All descriptions are kept as brief as possible to ensure that a wide variety of subjects can be presented. Apart from the knowledge you have hopefully gathered from the assembly language course, you will need the following to get going with the application notes: an 80C32 SBC (with extension board) running the EMON51 system monitor from EPROM, and a PC running the EASM51 assembler. Both programs are contained on the assembler course diskette, no. 1661. This month Zoran Stojsavljevic tells us all about 8751-to-EEPROM interfacing.

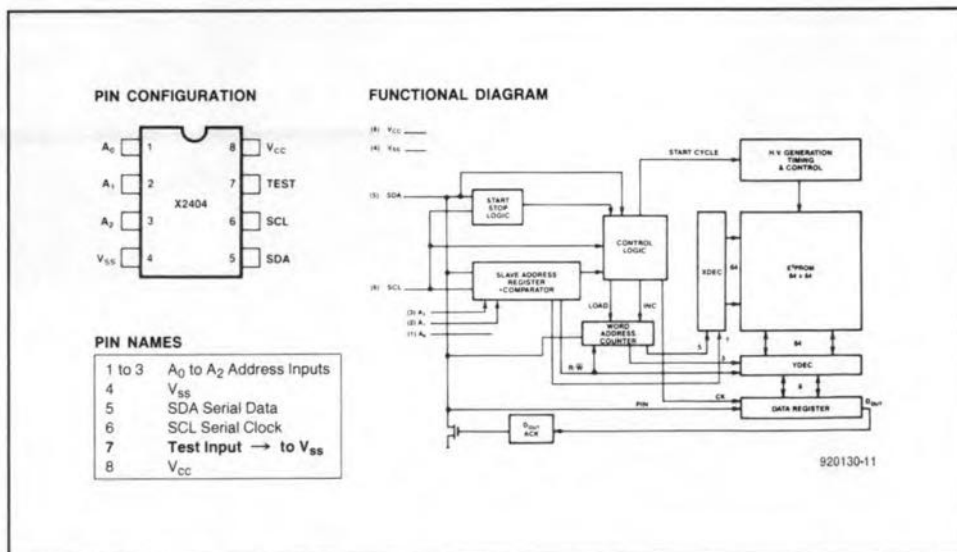


Fig. 1. Pin layout and internal structure of EEPROM X2404.

controlling the data transfer is a master, and the device being controlled is a slave. The master will always initiate data transfers, and provide the clock for both transmit and receive operations. Therefore, the X2404 will be considered a slave in all applications.

Data states on the SDA line can change only when SCL is low. SDA changes during SCL 'high' periods are reserved for indications of start and stop conditions, as illustrated in Fig. 3. All commands are preceded by the start condition, which is a high-to-low transition of SDA when SCL is high. The X2404 continuously monitors the SDA and SCL lines for the start condition, and will not respond to any command until this condition is

satisfied. All communications are terminated by a stop condition, which is a low-to-high transition of SDA when SCL is high. The definitions of the start and stop conditions are illustrated in Fig. 4.

The transmitting device, either a master or a slave, releases the bus after transmitting eight bits. During the ninth clock cycle, the receiver pulls the SDA line low to acknowledge that it received the eight bits of data. The X2404 will always respond with an acknowledge after recognition of a start condition, followed by its slave address. If both the device and a write operation have been selected, the X2404 will respond with an acknowledge on receipt of each subsequent

# SPECTRUM VU METER

Design by T. Giesberts

Making an audio signal visible on a display is something that appeals to many audio & hi-fi enthusiasts. Most commercial audio equipment is now provided with a display in the form of one or more light bars that move in rhythm with the music. The proposed VU meter offers seven or eight bars that each serve a certain part of the audio spectrum.

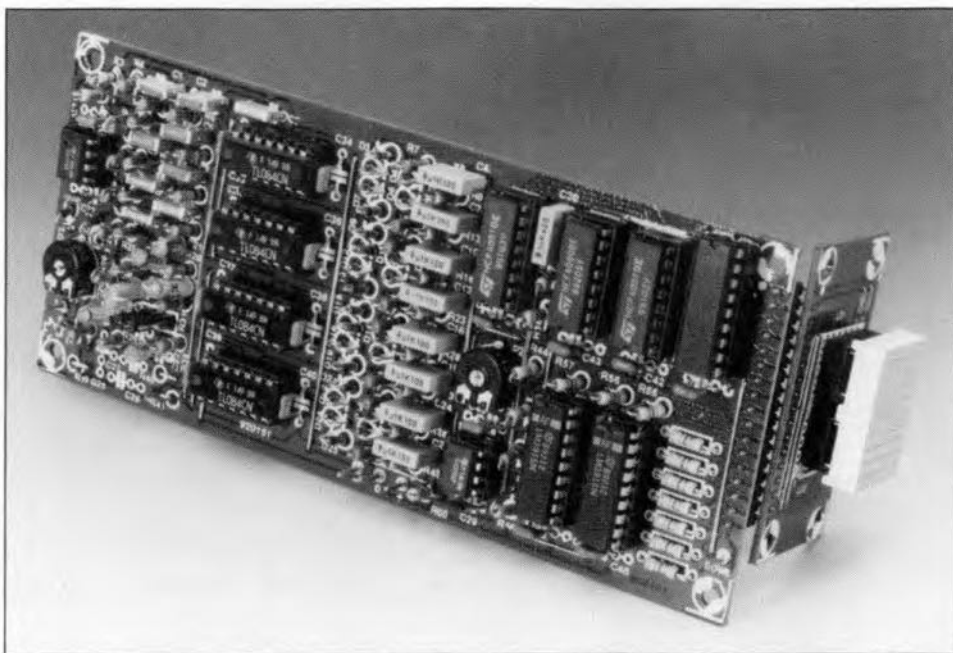
A VU meter used to be a moving-coil meter that indicated the drive power of, for instance, a tape recorder in 'Volume Units'. Modern equipment is normally provided with a VU meter consisting of a bar of small LEDs per channel.

The VU meter described is intended primarily for use with an amplifier and does not only show the strength of the incoming or outgoing signal, but also its spectral distribution. The sound spectrum is divided into seven or eight bands, each of whose strengths is shown on a 10-LED bar. All these LEDs do not present a construction problem, because use is made of two 5x7 or 5x8 matrix displays that are mounted one above the other. These displays are available in various sizes, from 18x26 mm to 61x72 mm.

## Design considerations

The audio input signal is fed to a variable amplifier and then to seven filters (Fig. 1). The eighth filter shown is for use only with large displays that have eight LED bars. The lowest filter is a low-pass section, the five (or six in case of a large display) following ones are band-pass sections, and the highest is a high-pass section. To obtain a good split of the audio spectrum and yet keep the number of components in the filters to a minimum, the cut-off frequencies and Q factors have been chosen to give -10 dB transfer points of adjacent frequencies. That may seem a lot, but it should be borne in mind that the resolution of the display is 3 dB per step at the top and as much as 9 dB per step at the bottom.

To get an even distribution of the audio range of 20 Hz to 20 kHz, the central frequencies of the band-pass filters have been set to 130 Hz, 340 Hz, 880 Hz, 2.3 kHz, and 6 kHz. With a Q factor of 3, the filters interconnect just about at



their -10 dB points.

The cut-off frequency of the low-pass filter is set to 50 Hz and that of the high-pass section to 15 kHz. For small displays, these filters are third-order Butterworth types that fit in well with the band-pass sections, but for large displays their behaviour becomes more of a Chebishev nature.

The filter responses are shown in Fig. 2.

The filter outputs are passed to peak detectors. These are rather more complex than in Fig. 1, but that will be reverted to in the circuit description.

The seven (eight) direct voltages are fed to a multiplexer that passes one of them via buffer-amplifiers to a double comparator-buffer formed by two LED driver ICs. These quasi-series connected ICs enable a range of some 50 dB to be displayed.

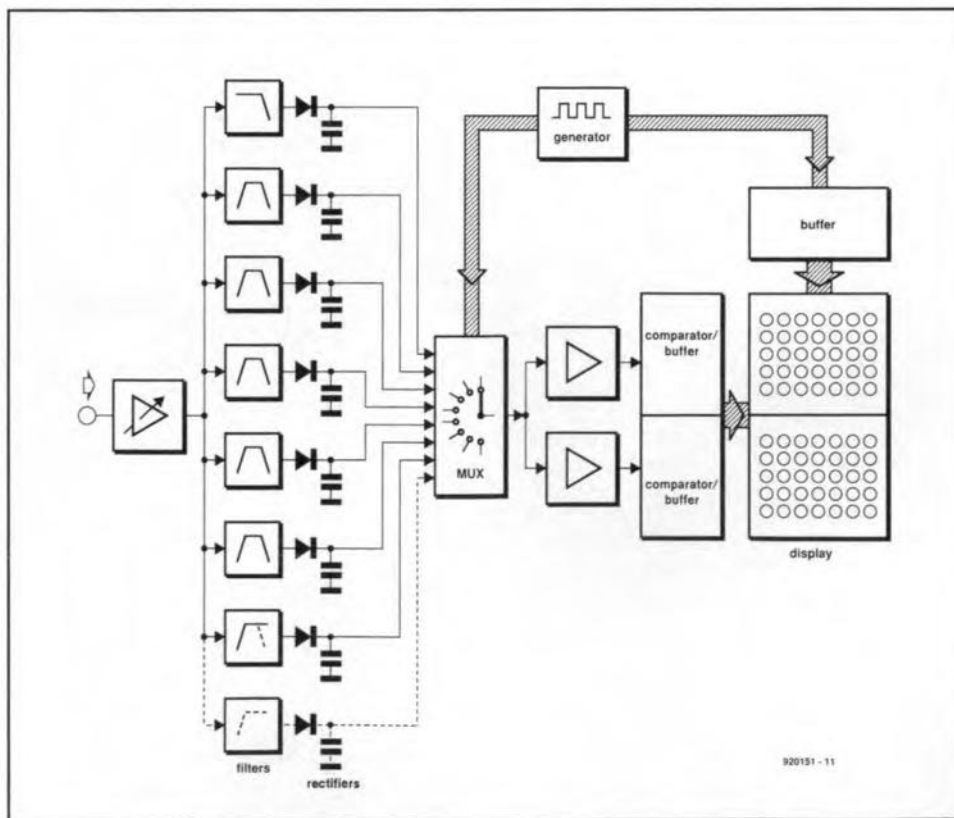


Fig. 1. Block schematic of the VU meter.

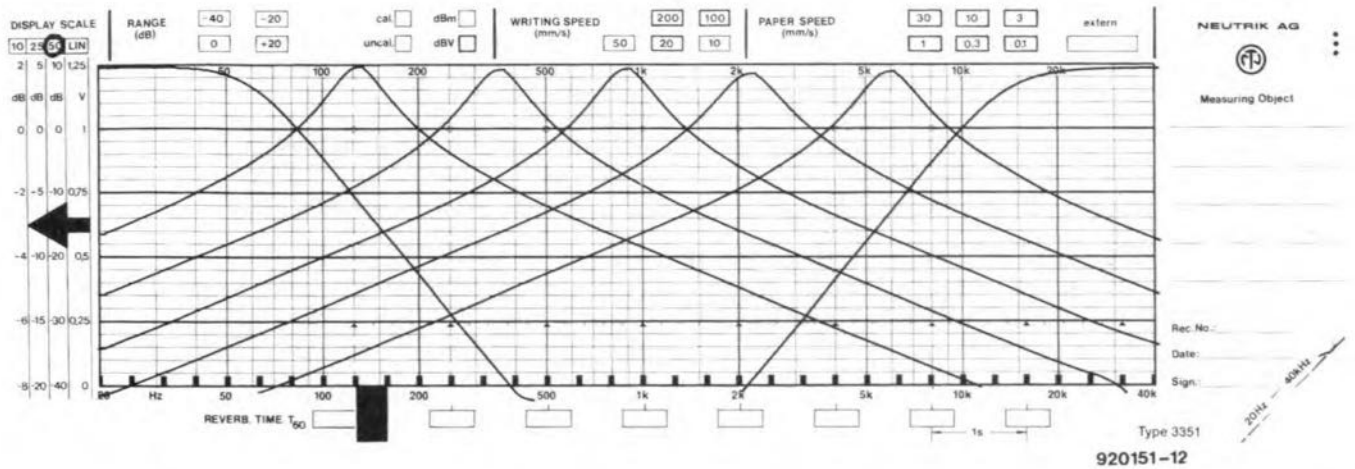


Fig. 2. Response curves of the low-pass, high-pass and band-pass filters when a seven-bar display is used.

A frequency generator provides the clock that switches the multiplexer to each successive direct voltage. At the same time, this signal actuates the LED bar associated with that direct voltage via a number of buffer stages, so that this bar displays only the level monitored at that instant.

### The circuit

The audio input is applied to  $K_1$  (see Fig. 4) and from there to  $IC_1$  via  $P_1$ , which enables it to be attenuated as required. The amplifier has a gain of about 16 dB. The output of  $IC_1$  is fed to the seven or eight filter sections. The multiple feedback band-pass filters are formed by  $IC_{2a}$ ,  $IC_{3d}$ ,  $IC_{3a}$ ,  $IC_{4d}$ , and  $IC_{4a}$ . As already mentioned, their  $Q$  factor is 3.

The third-order low-pass filter, which has a cut-off frequency of 50 Hz, is based on  $IC_{2d}$ .

The third-order high-pass filter, which has a cut-off frequency of 15 kHz, is based on  $IC_{5d}$ .

If a  $10 \times 8$  LED matrix is used, the eighth filter needed is based on  $IC_{5a}$ . In that case, the high-pass filter based on  $IC_{5d}$  is converted to a band-pass section (whence the duplicated component indications; in the  $C_{20}$  position a resistor is then used). Table 1 lists all the component values in case eight filters are used.

The rectifiers are pseudo-active types to ensure proper coverage of the display range of 50 dB. In the prototype, standard passive rectifiers, even Schottky types, gave serious deviations (in some case, a 30 dB signal was attenuated to no less than 12 dB by the rectifier). The design finally chosen consists of a passive rectifier, consisting of a diode ( $D_5$ ,  $D_8$ ,  $D_{11}$ ,  $D_{14}$ ,  $D_{17}$ ,  $D_{20}$ ,  $D_{23}$ ), a capacitor ( $C_4$ ,  $C_7$ ,  $C_{10}$ ,  $C_{13}$ ,  $C_{16}$ ,  $C_{19}$ ,  $C_{24}$ ) and a discharge resistor ( $R_6$ ,  $R_{13}$ ,  $R_{18}$ ,  $R_{23}$ ,  $R_{28}$ ,  $R_{33}$ , and  $R_{38}$ ), coupled with an active compensating

device ( $IC_{2c}$ ,  $IC_{2b}$ ,  $IC_{3c}$ ,  $IC_{3b}$ ,  $IC_{4c}$ ,  $IC_{4b}$ , and  $IC_{5c}$ ).

The active devices compensate the forward bias of the associated diodes as well as the discharge of the capacitors through the diodes when these conduct.

Since each of the ICs, connected in a voltage follower configuration, has negative feedback through two anti-parallel diodes, its output will always be larger by the forward bias of one of the diodes ( $D_3$ ,  $D_6$ ,  $D_9$ ,  $D_{12}$ ,  $D_{15}$ ,  $D_{18}$ ,  $D_{21}$ ) than the input. That bias depends to some extent on the current, which here is determined by the load resistor ( $R_7$ ,  $R_{12}$ ,  $R_{17}$ ,  $R_{22}$ ,  $R_{27}$ ,  $R_{32}$ ,  $R_{37}$ ). The diodes mentioned above are of a type that is identical to the rectifier. The type of the other diode in the feedback loop is not so important.

When the input is small, the drop across  $D_3$ ,  $D_6$ , and so on, may be increased by reducing the value of  $R_7$ ,  $R_{12}$ ,

and so on.

Outputs  $Q_3$ ,  $Q_4$  and  $Q_5$  of oscillator-divider  $IC_8$  switch multiplexer  $IC_6$  at a frequency of about 400 Hz, so that at all times one of the output voltages of the rectifiers is connected to the comparator and drive section,  $IC_9$ ,  $IC_{11}$ ,  $IC_{12}$ .

The same three  $Q$  outputs of  $IC_8$  are also linked to binary-to-decimal converter (BDC)  $IC_7$ . This converter ensures (via a number of buffers contained in  $IC_{10}$ ) that the LED bar associated with the direct voltage output of the multiplexer at that instant is powered.

When all LEDs of a small display with seven bars light, the average current drawn is 263 mA.

The multiplexer is linked to  $IC_{11}$  and  $IC_{12}$  via two opamps,  $IC_{9a}$  and  $IC_{9b}$ . The first serves as a buffer for  $IC_{11}$ , while the second not only buffers the signal to  $IC_{12}$ , but also amplifies it  $\times 32$ .

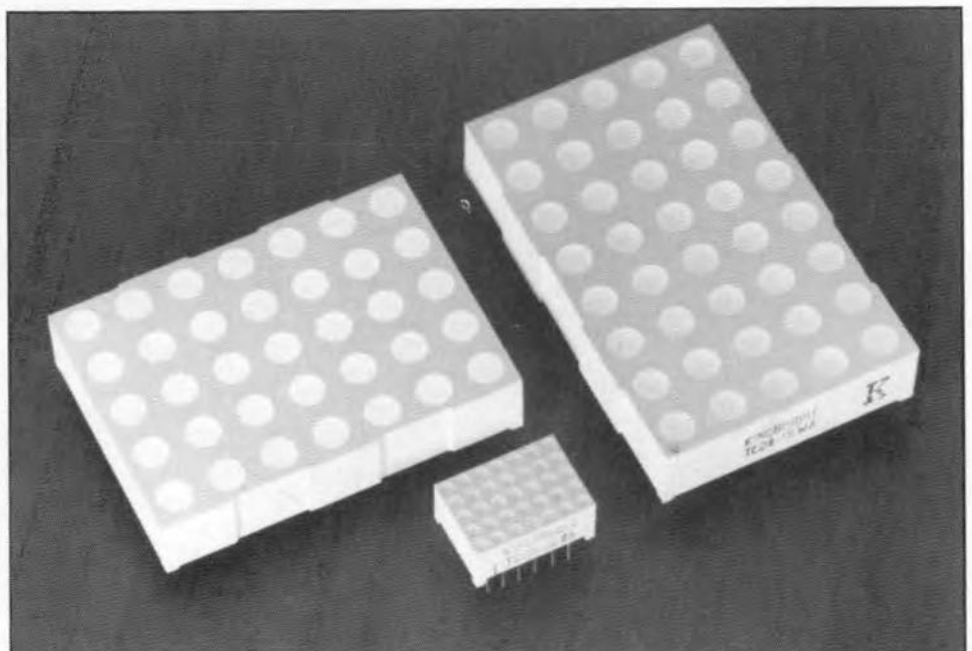


Fig. 3. The displays are available in a variety of sizes.

Circuits IC<sub>11</sub> and IC<sub>12</sub> drive the rows of the display. Each of them contains a 10-step comparator, a variable reference source and a drive circuit for the ten LEDs. Since at the underside of the display larger steps are required than at the top, most outputs of IC<sub>12</sub> are not

used. In that way, the steps on the display are (in dB): 0, -3, -6, -9, -15, -21, -27, -33, -41, and -50.

Resistors R<sub>48</sub>-R<sub>57</sub> serve not so much as current limiters (the outputs of the LM3915s are current sources), but rather as dissipation limiters for the drive transistors contained in IC<sub>11</sub> and IC<sub>12</sub>.

sistors contained in IC<sub>11</sub> and IC<sub>12</sub>.

The power supply needs to provide a stabilized, symmetrical voltage; the positive supply line must be able to deliver a current of at least 330 mA, and the negative line one of about 35 mA.

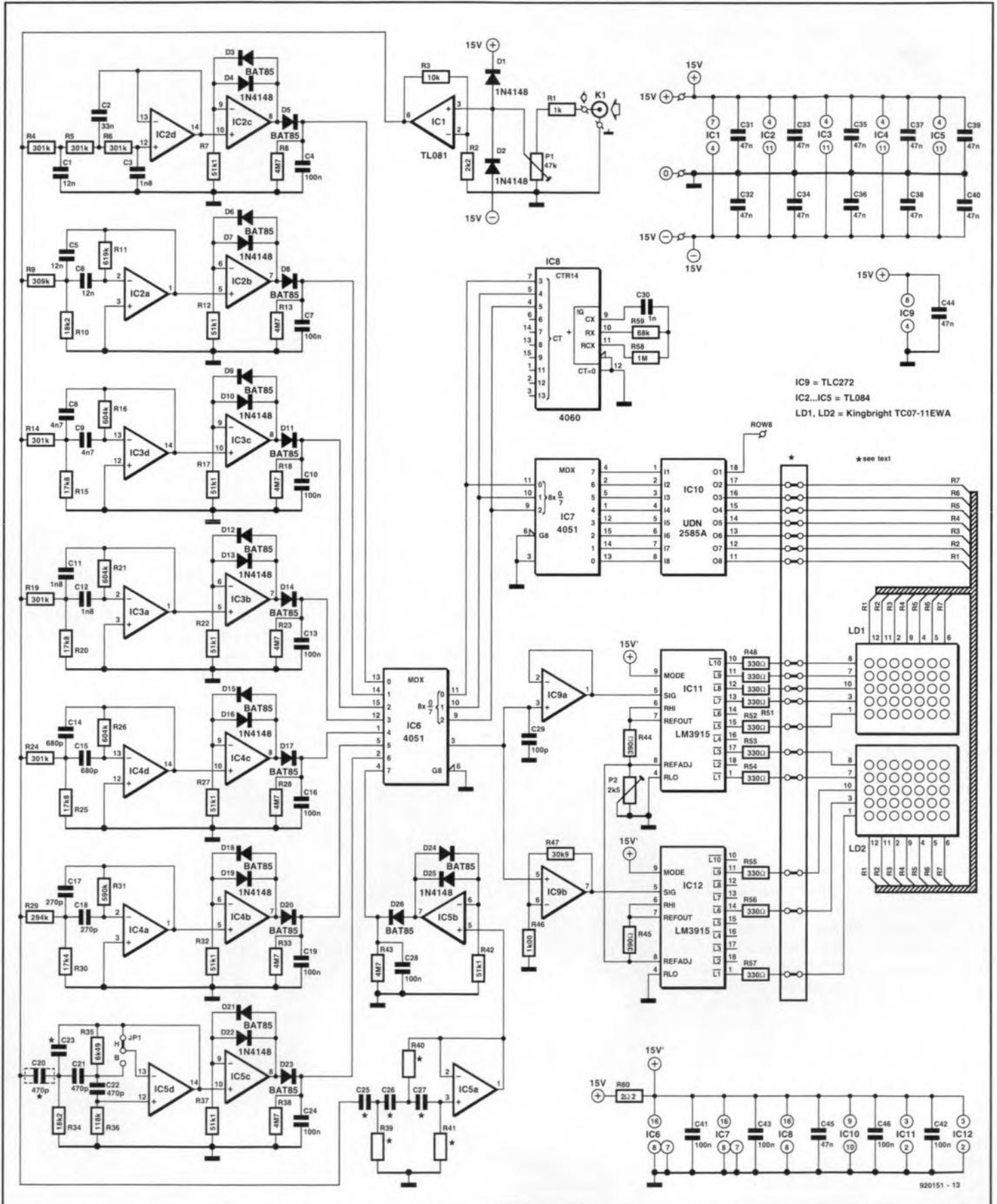


Fig. 4. Circuit diagram of the VU meter.

## Construction

The VU meter is most conveniently built on the printed-circuit board shown in Fig. 5. Start with cutting off the display section if that is to be located elsewhere. Then, all components can be fitted. Note that most resistors and all diodes should be mounted upright. The 270 pF, 470 pF and 680 pF capacitors must be polystyrene types to prevent too high damping of the filters. These capacitors must also be mounted upright.

Once the boards have been completed, they must be interlinked by an angled header (see photograph on p. 8) or 17

discrete, short wires.

The power for the meter may be drawn from the equipment into which it is built, but, owing to the current requirement on the positive line, it is best to build a small, separate supply.

If a larger display is used than shown on the PCB, it must be connected to the board via suitable connectors or half IC sockets. The display section of the board is then useless.

When a small display is used, jumper JP<sub>1</sub> on the board must be placed in position 'H'. Resistors R<sub>41</sub> and R<sub>43</sub> must be replaced by a wire bridge.

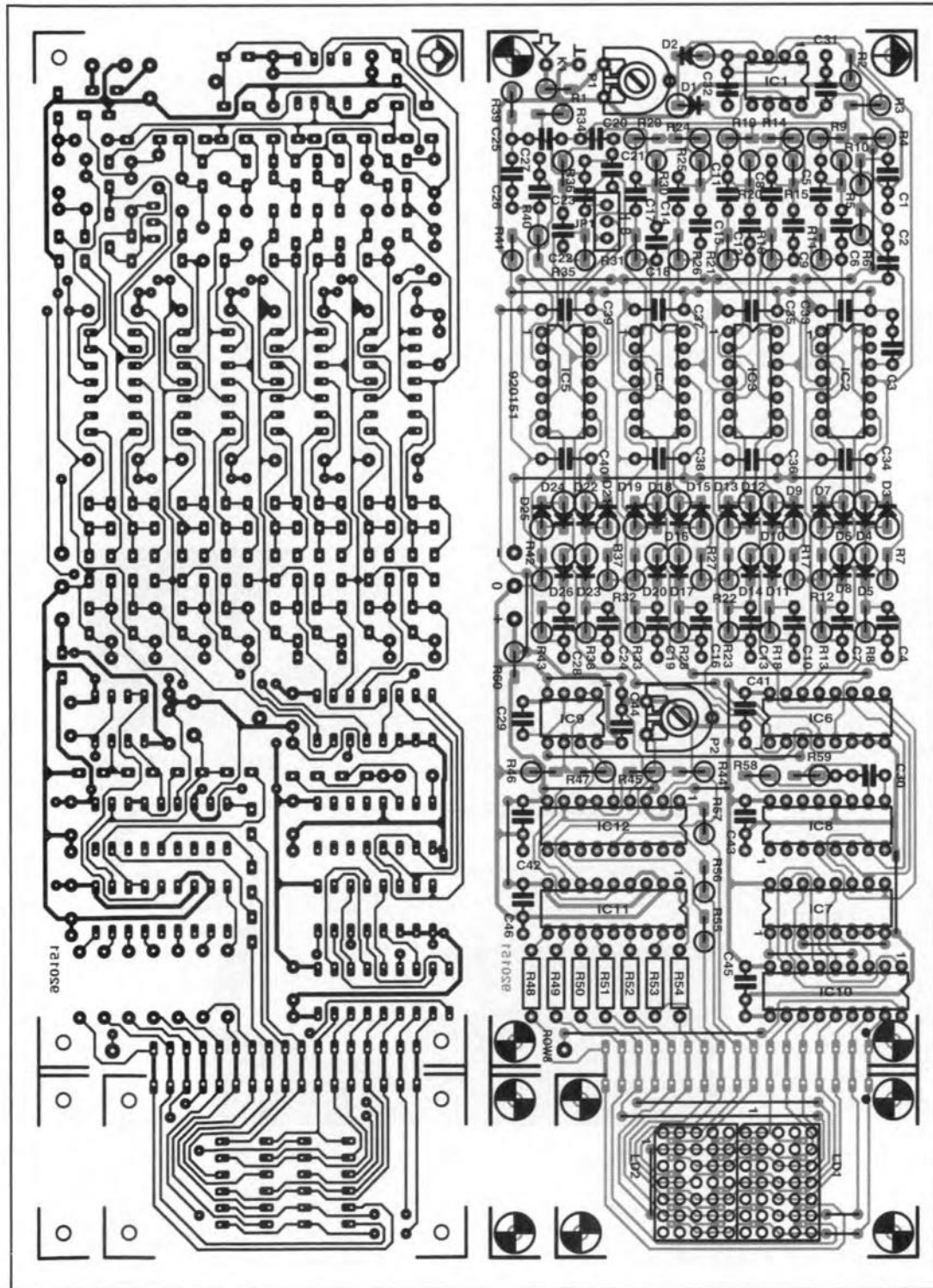


Fig. 4. The printed-circuit board for the VU meter.

## PARTS LIST

### Resistors:

R1=1 kΩ  
 R2=2.2 kΩ  
 R3=10 kΩ  
 R4, R5, R6, R14, R19, R24=301 kΩ, 1%  
 R7, R12, R17, R22, R27, R32, R37=51.1 kΩ, 1%  
 R8, R13, R18, R23, R28, R33, R38=4.7 MΩ  
 R9=309 kΩ, 1%  
 R10, R34=18.2 kΩ, 1%  
 R11=619 kΩ, 1%  
 R15, R20, R25=17.8 kΩ, 1%  
 R16, R21, R26=604 kΩ, 1%  
 R29=294 kΩ, 1%  
 R30=17.4 kΩ, 1%  
 R31=590 kΩ, 1%  
 R35=6.49 kΩ, 1%  
 R36=118 kΩ, 1%  
 R44, R45=390 Ω  
 R46=1.0 kΩ, 1%  
 R47=30.9 kΩ, 1%  
 R48-R57=330 Ω  
 R58=1 MΩ  
 R59=68 kΩ  
 R60=2.2 Ω  
 P1=47 kΩ preset  
 P2=2.5 kΩ preset

### Capacitors:

C1, C5, C6=12 nF  
 C2=33 nF  
 C3, C11, C12=1.8 nF  
 C4, C7, C10, C13, C16, C19, C24=100 nF  
 C8, C9=4.7 nF  
 C14, C15=680 pF\*  
 C17, C18=270 pF\*  
 C20, C21, C22=470 pF\*  
 C29=100 pF  
 C30=1 nF  
 C31-C40, C44=47 nF, ceramic  
 C41, C42, C43, C45, C46=100 nF, ceramic  
 \*polystyrene, axial

### Semiconductors:

D1, D2, D4, D7, D10, D13, D16, D19, D22=1N4148  
 D3, D5, D6, D8, D9, D11, D12, D14, D15, D17, D18, D20, D21, D23=BAT85  
 IC1=TL081  
 IC2-IC5=TL084  
 IC6, IC7=4051  
 IC8=4060  
 IC9=TLC272  
 IC10=UDN2585A  
 IC11, IC12=LM3915

### Miscellaneous:

JP1=terminal strip with 3-way jump lead  
 K1=audio socket  
 LD1, LD2=display with 5×7 matrix, e.g., Kingbright Type TC07-11EWA (larger types: TC20-11EWA; 5×8:TC24-11EWA  
 PCB Type 920151 (see p. 70)

Filter	$f_c$ or $f_s$	Component values
IC <sub>2d</sub>	57 Hz	R4=267 k $\Omega$ ; R5, R6=249 k $\Omega$ ; C1=22 nF; C2=120 nF; C3=1 nF
IC <sub>2a</sub>	113 Hz	R9=274 k $\Omega$ ; R10= 11.8 k $\Omega$ ; R11=549 k $\Omega$ C5, C6=18 nF
IC <sub>3d</sub>	255 Hz	R14=324 k $\Omega$ ; R15=13.7 k $\Omega$ ; R16=649 k $\Omega$ ; C8, C9=6.8 nF
IC <sub>3a</sub>	577 Hz	R19=294 k $\Omega$ ; R20=12.4 k $\Omega$ ; R21=590 k $\Omega$ ; C11, C12=3.3 nF
IC <sub>4d</sub>	1030 Hz	R24=287 k $\Omega$ ; R25=12.1 k $\Omega$ ; R26=576 k $\Omega$ ; C14, C15=1.5 nF
IC <sub>4a</sub>	2940 Hz	R29=280 k $\Omega$ ; R30=12.1 k $\Omega$ ; R31=562 k $\Omega$ ; C17, C18=680 pF (polystyrene)
IC <sub>5d</sub>	6650 Hz	C20=309 k $\Omega$ ; R34=13.3 k $\Omega$ ; R35=619 k $\Omega$ ; R36=wire bridge; C22=not used; C21, C23=270 pF (polystyrene) Place JP1 in position B
IC <sub>5a</sub>	13600 Hz	R39=11.8 k $\Omega$ ; R40=2.37 k $\Omega$ ; R41=294 k $\Omega$ C25-C27=470 pF (polystyrene)
IC <sub>5b</sub>		R42=51.1 k $\Omega$ ; R43=4.7 M $\Omega$ ; C28=100 nF;

## Calibration

Connect the meter to a point in the amplifier where a strong signal is present; this is normally the loudspeaker terminal in an output amplifier. Make sure that the amplifier is fully driven. Turn P<sub>1</sub> so that IC<sub>1</sub> is just not overdriven. If an oscilloscope is not available, connect a multimeter, set to the 10 V a.c. range, to the output of IC<sub>1</sub>. If this is an inexpensive digital multimeter, use a low-frequency input signal, say, a couple of hundred hertz. Turn P<sub>1</sub> slowly till the meter reads 9.5 V r.m.s. Then, using an input signal at a frequency in the centre of the pass-band, say, 130 Hz or 340 Hz, adjust P<sub>2</sub> until the entire associated LED bar just lights. ■

Table 1. Component values and frequencies for eight filter sections.

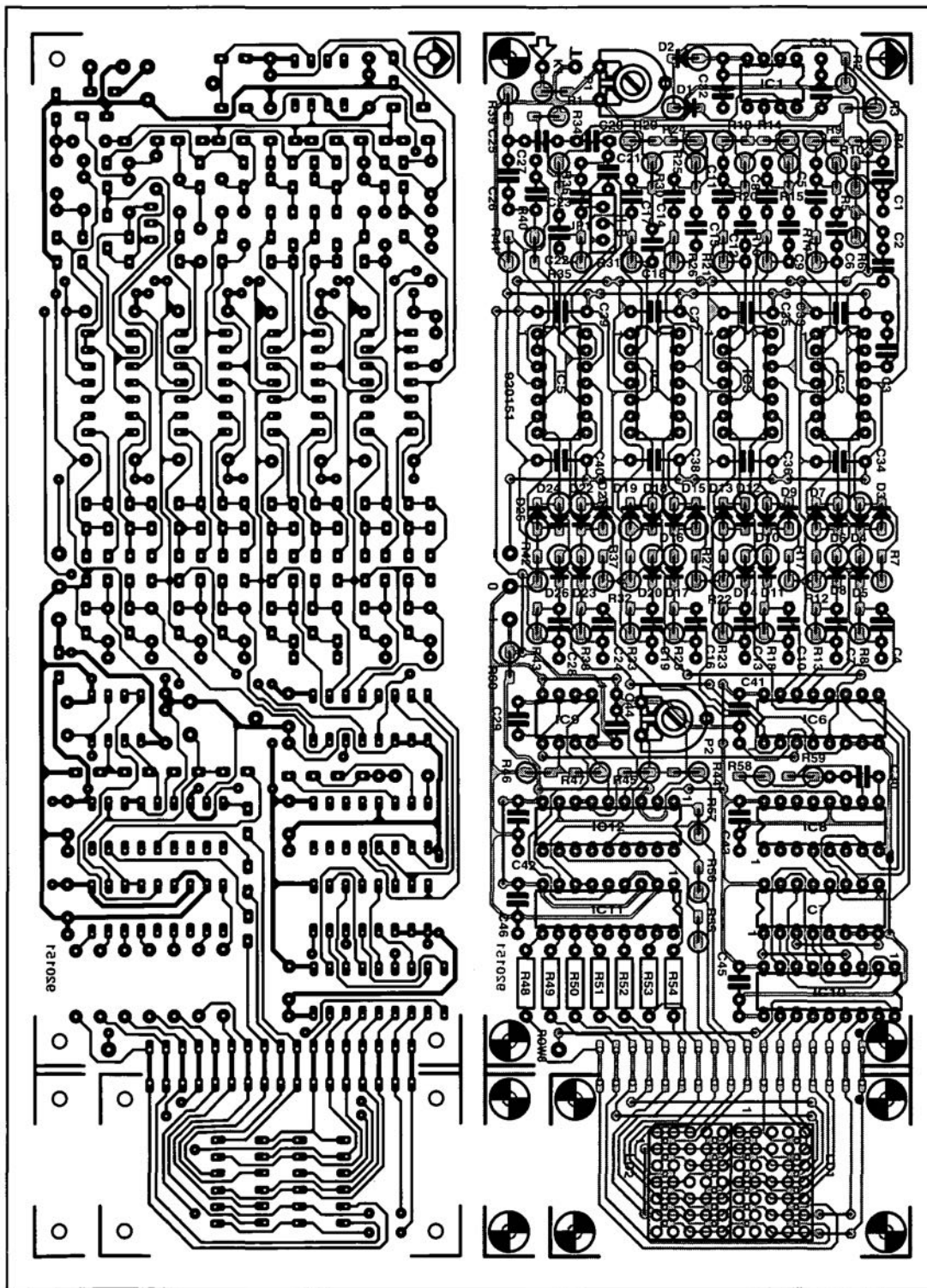


Fig. 4. The printed-circuit board for the VU meter.

R30=17.4 k $\Omega$ , 1%  
 R31=590 k $\Omega$ , 1%  
 R35=6.49 k $\Omega$ , 1%  
 R36=118 k $\Omega$ , 1%  
 R44, R45=390  $\Omega$   
 R46=1.0 k $\Omega$ , 1%  
 R47=30.9 k $\Omega$ , 1%  
 R48-R57=330  $\Omega$   
 R58=1 M $\Omega$   
 R59=68 k $\Omega$   
 R60=2.2  $\Omega$   
 P1=47 k $\Omega$  preset  
 P2=2.5 k $\Omega$  preset

**Capacitors:**

C1, C5, C6=12 nF  
 C2=33 nF  
 C3, C11, C12=1.8 nF  
 C4, C7, C10, C13, C16, C19,  
 C24=100 nF  
 C8, C9=4.7 nF  
 C14, C15=680 pF\*  
 C17, C18=270 pF\*  
 C20, C21, C22=470 pF\*  
 C29=100 pF  
 C30=1 nF  
 C31-C40, C44=47 nF, ceramic  
 C41, C42, C43, C45, C46=  
 100 nF, ceramic  
 \*polystyrene, axial

**Semiconductors:**

D1, D2, D4, D7, D10, D13, D16,  
 D19, D22=1N4148  
 D3, D5, D6, D8, D9, D11, D12,  
 D14, D15, D17, D18, D20,  
 D21, D23=BAT85  
 IC1=TL081  
 IC2-IC5=TL084  
 IC6, IC7=4051  
 IC8=4060  
 IC9=TLC272  
 IC10=UDN2585A  
 IC11, IC12=LM3915

**Miscellaneous:**

JP1=terminal strip with 3-way  
 jump lead  
 K1=audio socket  
 LD1, LD2=display with 5x7  
 matrix, e.g., Kingbright Type  
 TC07-11EWA (larger types:  
 TC20-11EWA;  
 5x8:TC24-11EWA  
 PCB Type 920151 (see p. 70)

# Electricity from the wind

By Dr K.A. Nigim

Since the early 1890s, man has pioneered the technique of converting wind power into useful electricity. The development of engineering skills and the steady consumption of energy has speeded the development of the farm windmill into aerodynamically shaped turbines.

From the twenties, power from the wind was the main source of energy supply to rural areas worldwide. The modest reliability and social acceptability of the wind spinners encouraged researchers as well as environmentalists to seek ways to upgrade and increase the produced energy.

The energy crisis of the seventies revived the interest in wind power, and dozens of small wind machine manufacturers have started research into the means of increasing the generated capacity by introducing larger turbines and new designs.

Now, there are 45 companies worldwide specialized in manufacturing wind energy generators (WEGs) ranging from 100 W windmills (to charge 12 V batteries) to 4 MW windmills for direct connection to the national electricity network.

## Types of windmill

Practically, windmills are classified into two categories:

1. horizontal axis wind turbines (HAWT);
2. vertical axis wind turbines (VAWT).

Both categories are shown in Fig. 1. There are several shapes, each having its own merits and requiring certain strengths of wind speed to start spinning.

There are as many as 31 types of turbine, all serving to convert the kinetic energy of the moving air to an energy associated with a mechanical motion, which in turn is converted into electricity by an electrical generator.

Each turbine model will have the capability of producing electrical power,  $P_w$ , as given by the equation

$$P_w = K_w \cdot C_p \cdot R^2 \cdot V^3,$$

where

$K_w$  is constant =  $0.5\pi \cdot A_d$  (air density);  
 $C_p$  is power coefficient, whose value depends on the shape of the turbine used; for example, it is equal to 0.45 for a two-bladed turbine as shown in Fig. 2;  
 $R$  is the radius of the area swept by the blades;  
 $V$  is the free stream wind speed.

This equation gives the value of the

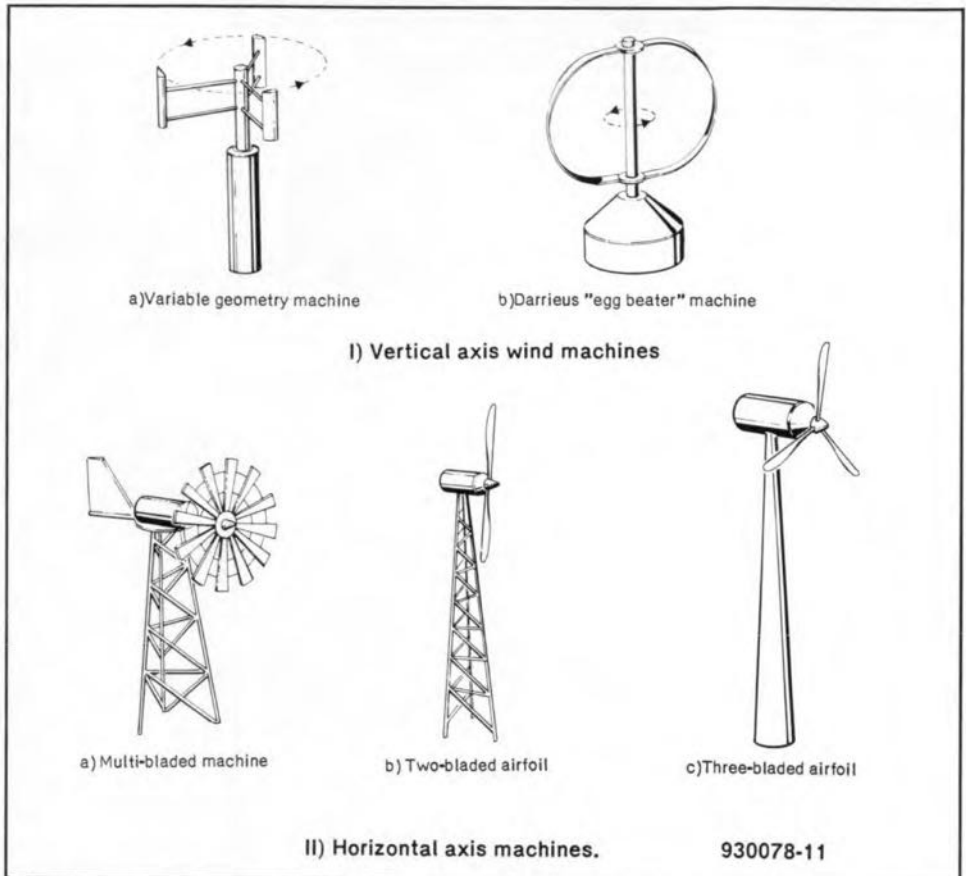


Fig. 1. Vertical axis and horizontal axis wind machines.

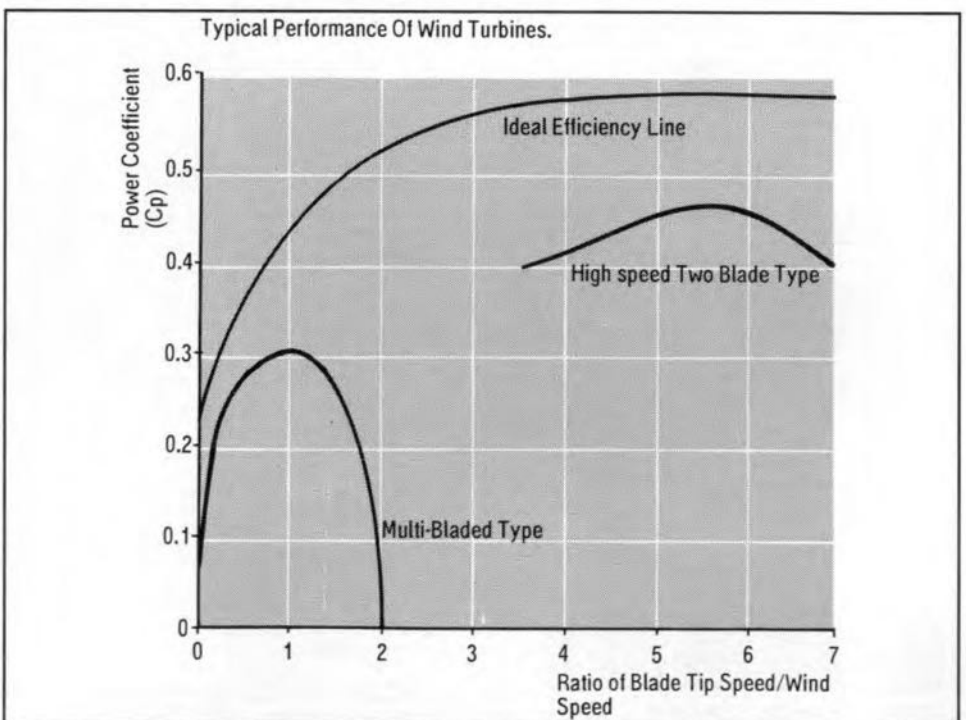


Fig. 2. Typical performance curves of wind turbines.



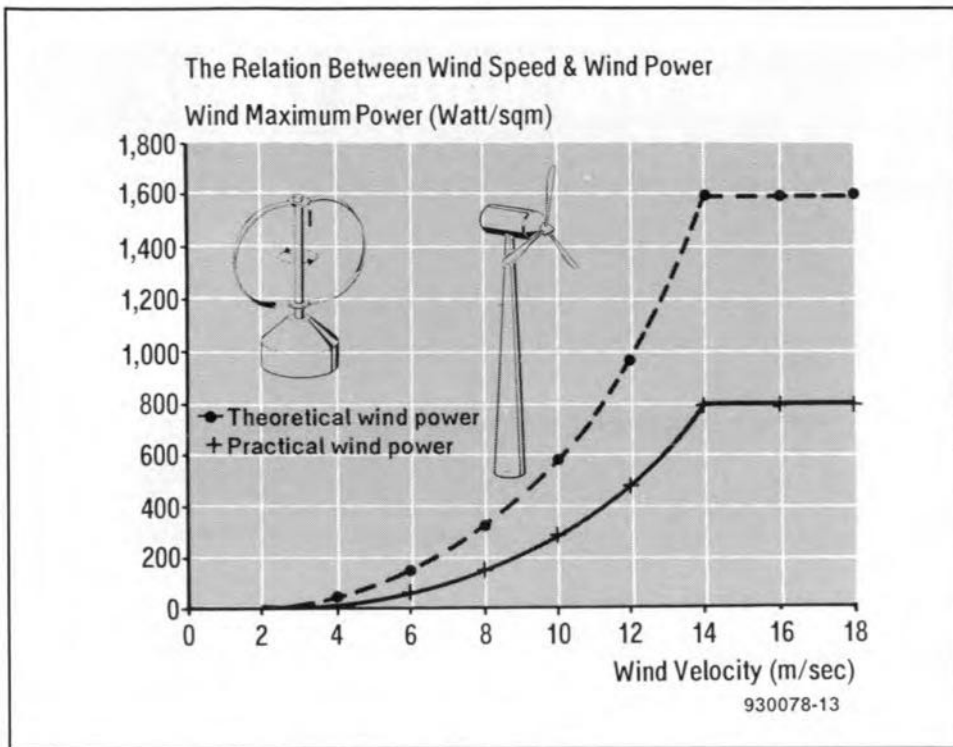


Fig. 3. Relation between wind speed and wind power.

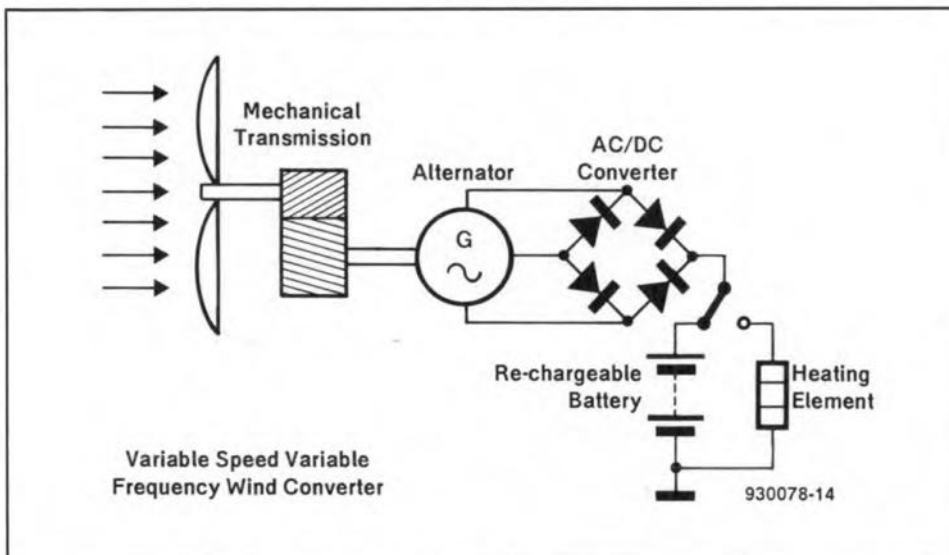


Fig. 4. Variable speed, variable frequency wind convertor.

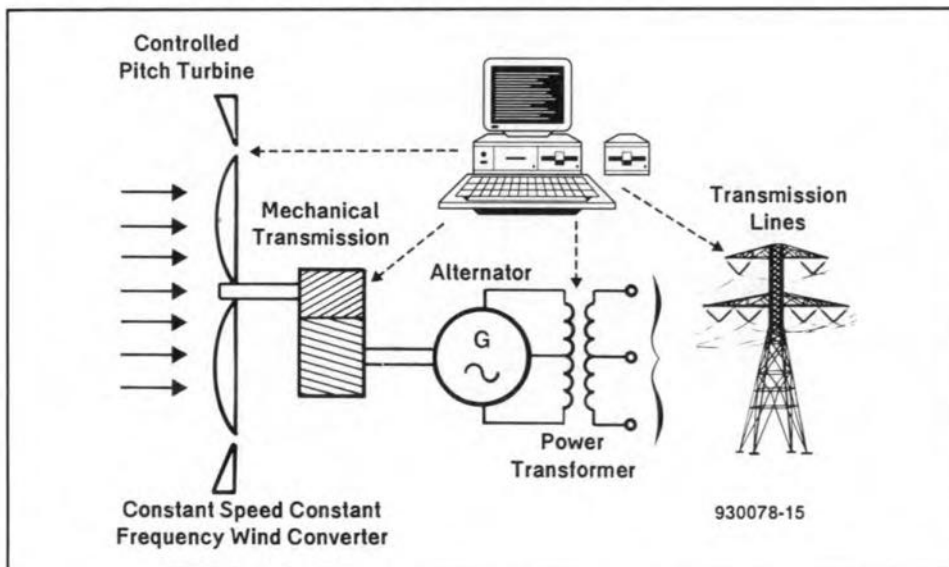


Fig. 5. Constant speed, constant frequency wind convertor.

maximum attainable power from a turbine. Owing to aerodynamic factors and other mechanical restraints, the power extracted is much smaller. A well-designed windmill achieves outputs that are 50–70% of the maximum theoretical power.

The dependence of power upon the cubic value of wind speed, as shown in Fig. 3, tends to limit the useful energy that can be extracted at low speeds. This fact presents a serious drawback to the use of wind converters in low wind-speed areas. On the other hand, gales are not welcome either, since they impose a danger to the mechanical parts of the wind turbines.

To overcome the unsteady nature of wind speeds, wind turbines are planted in groups located strategically around the selected site, which is known as a wind farm. In this way, a continuous supply of power may reasonably be expected at all times.

### Wind power to electricity

Horizontal and vertical axis wind turbines with rotor diameters of 60–100 m (200–300 ft), feeding electricity into the national grid systems, are now in operation at many sites in Europe and the USA. The various schemes for interconnecting the generated electricity with power lines or for the supply of isolated communities can be classified into three groups:

- variable speed, variable frequency (VSVF);
- constant speed, constant frequency (CSCF);
- variable speed, constant frequency (VSCF).

### VSVF generation

In this group, the generated output power is of variable voltage and frequency, so that the quality of the produced electricity is not suitable for household electricity supply. The turbine is coupled either to an alternator or to a DC generator and supplies energy to insensitive loads such as heaters.

One practical realization of this group is to use a 12 V permanent magnet alternator to charge a battery. Figure 4 shows a schematic of the essential parts needed to convert wind power to a useful DC battery charger. Windmills in this group are of relatively simple design.

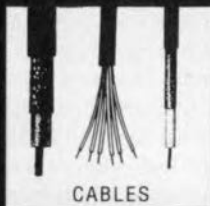
### CSCF generation

The usual approach to provide a constant frequency alternating electric power is to drive the generator at constant shaft speed, thus producing output power at constant frequency. This is a must for trading in electricity with the public and other generating companies.

In most constant-speed drive systems, a control mechanism is necessary to control the speed of the rotating shaft. One way to regulate fluctuation of the shaft speed is to use a hydraulically operated pitch controller to adjust the pitch of the turbine blades so that the input power is held fairly constant.

The technology and degree of refine-

**Call us now! We have the widest range of components available - At competitive prices!**



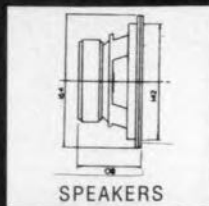
CABLES



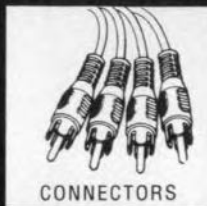
CAPACITORS



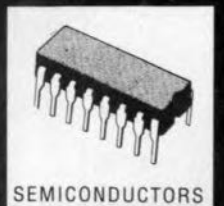
VIDEO HEADS



SPEAKERS



CONNECTORS



SEMICONDUCTORS

**CRICKLEWOOD**  
ELECTRONICS

Cricklewood Electronics Ltd. 40 Cricklewood Broadway, London NW2 3ET.  
Telephone: 081 452 0161 Faxsimile: 081 208 1441

All Major Credit Cards Accepted



ment involved in this scheme add to the initial costs of the windmill and it is, therefore, considered only for large wind turbines. Electricity is produced with two types of electrical machine as shown in Fig. 5. The electrical section is the standard type without the use of any power electronic devices.

### VSCF generation

VSCF generating systems are those that have no pitch control mechanism fitted. Such a system is defined as an assembly of rotating electrical machinery, assisted by power equipment that is capable of converting the variable speed of the rotating mechanical energy into standard electrical energy of constant frequency, meeting the generating companies' trading rules.

There are various successfully operating schemes that use standard electrical machinery whose output is controlled by power electronic devices that are controlled by microprocessors. Figure 6 shows a schematic diagram of a system widely used all over the world.

### The future

Already there is 324 MW of wind turbine generating capacity in the European Community. The greatest share of this is contributed by Denmark, which produces 1% of its electricity demand from the wind, with a target of increasing this to 20% by the turn of the century.

The Netherlands has similar plans. Enthusiasts in the UK, the area in the EC most exposed to wind, want to erect wind farms across the country and even out at sea to produce pollution-free electricity.

In the USA, special tax breaks have assisted in the creation of vast areas of the Californian desert to be planted with two and three bladed wind turbines. However, the technology used in many of these erected prototypes was not good enough and, although the windmills are still running, very little electricity is produced economically.

The experience of harnessing the wind is well shared by many developed countries. Geographic and demographic conditions pre-

vent many developing countries from installing a country-wide national grid for electricity distribution. The availability of windy sites is, therefore, greatly appreciated. Small-scale, isolated wind turbines are erected in the nearest suitable place. Integration between wind converters and conventional diesel engines is proving to be an economical solution to the need of continuous electricity demand.

Owing to the small size and/or the remote location of such power stations, the generating costs are markedly higher than the cost in interconnected national networks.

The present cost of electricity produced by wind generators in good wind sites is 2 to 3 times as high as that produced by conventional power stations. However, electricity from the wind is an environment-friendly energy source in spite of the noise the turbines produce during a breezy night.

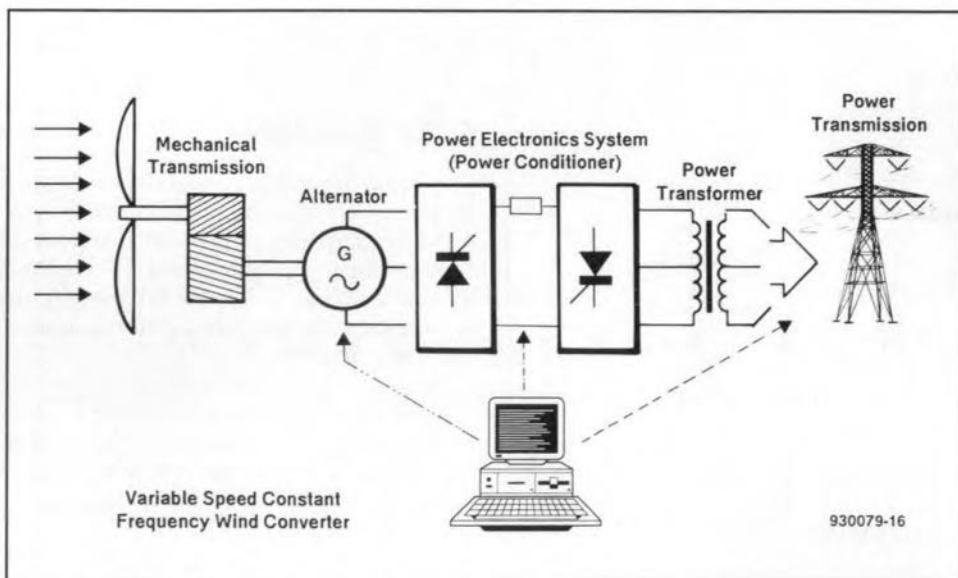


Fig. 6. Variable speed, constant frequency wind convertor

# INEXPENSIVE PHASE METER

Design by F. Hueber

The phase meter presented is based on just two CMOS ICs and a liquid-crystal display (LCD) to make it affordable with even the tightest budget.

The block schematic of the phase meter is shown in Fig. 1. Two amplifiers convert the input signal into a rectangular voltage that controls an edge-sensitive SR bistable (flip-flop). The average output of the bistable – between zero and the supply voltage – is directly proportional to the phase shift (0–360°). The measurement whose phase shift with respect to the reference signal at input B is to be determined is applied to input A. Every time the reference signal starts the positive half of its period, the leading edge of signal 1 sets the bistable. The bistable is reset when the phase-shifted signal at A starts the positive half of its period. In this way, the output of the bistable remains high longer the more the phase shift, that is, the average output voltage, increases. This is shown by timing diagrams 1 and 2 in Fig. 1.

Timing diagram 3 shows the situation when the phase shift is 0° or a multiple of 360°. In those cases, it may happen that sometimes the leading edge of input A occurs first and at other times that of the reference signal. This will cause the output of the bistable to fluctuate between zero and the supply voltage. The meter will then give an undefined or instable reading because the average voltage cannot be exactly zero (0°) or the supply voltage (360°). This is one of the (small) prices to be paid for simplicity.

Another is that when the input signals are removed when the bistable is set, the meter reading remains at 360°. This error may be obviated by first removing the reference signal (B) and then the signal from A.

## Circuit description

The two input channels are virtually identical—see Fig. 2. Only capacitors  $C_1$ ,  $C_7$  and  $C_9$  differ from their counterparts in the other channel. These capacitors serve to synchronize the phase pattern in the two channels.

Since the two channels are near-identical, channel B only will be discussed.

The signal—input at B—is applied to the circuit via  $C_1$ , shunted by calibration capacitor  $C_9$ , which prevents direct voltage being applied to the meter. Resistor  $R_2$  and diodes  $D_1$  and  $D_2$  provide protec-

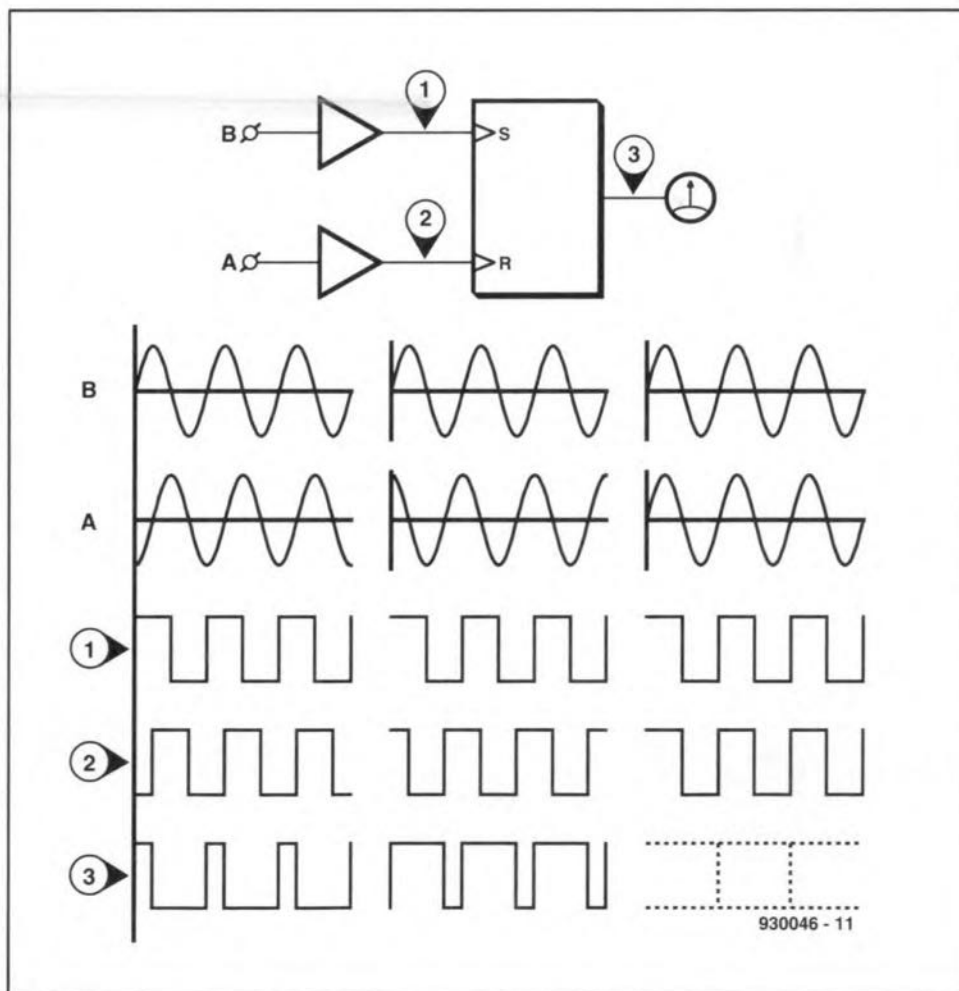


Fig. 1. The principle of the phase meter is quite simple.

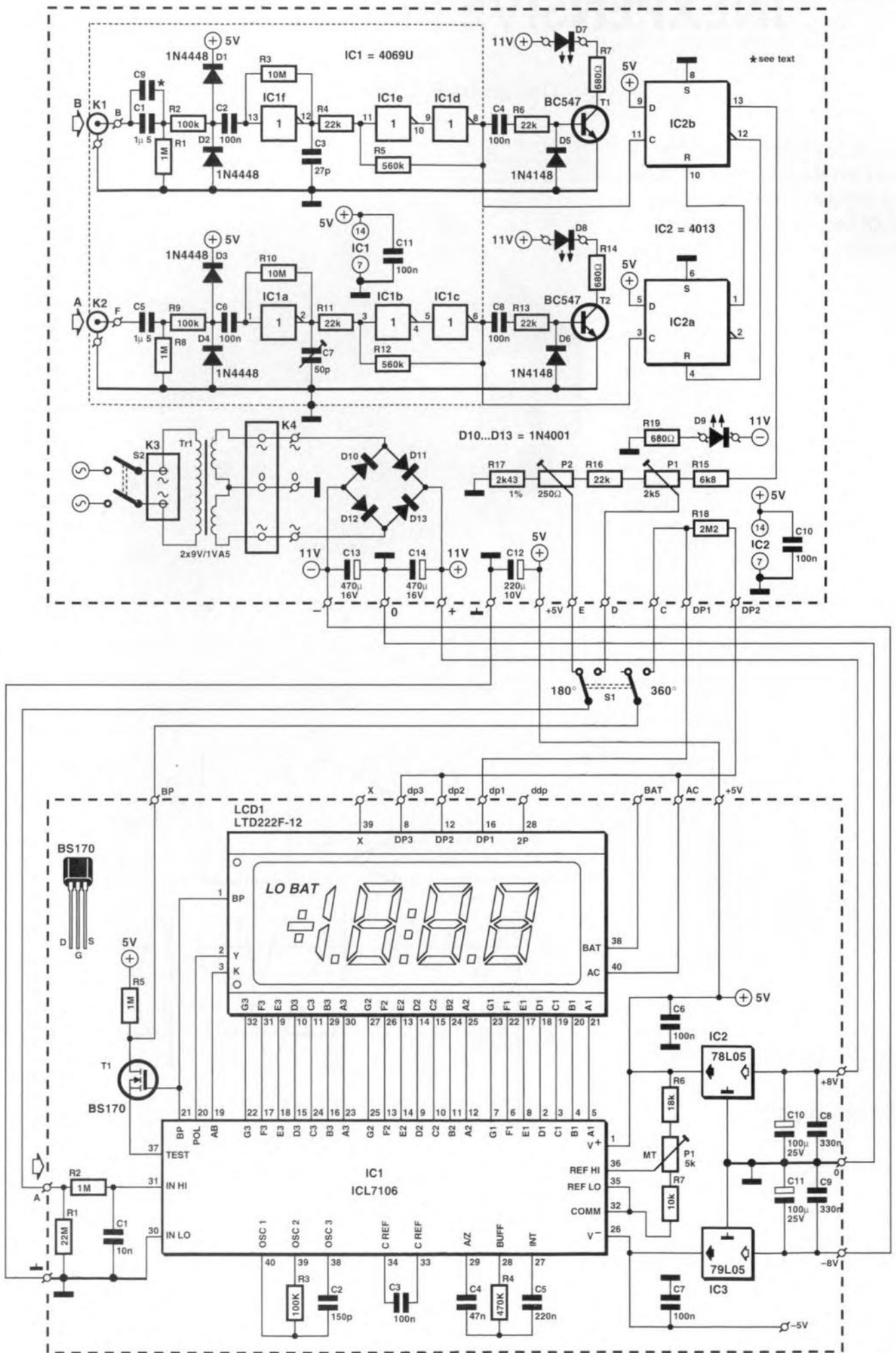


Fig. 2. Circuit diagram of the complete phase meter.

tion against too high alternating voltages at the input.

The signal is then applied to inverter IC<sub>1f</sub>, which is not buffered, so it can be converted into a linear amplifier. In fact, IC<sub>1f</sub> is arranged as an inverting amplifier, whose amplification is set to about  $\times 10$  by R<sub>2</sub> and R<sub>3</sub>. This arrangement is not immediately recognizable owing to the protection diodes. Capacitor C<sub>2</sub> prevents any direct voltage generated by the protection circuit reaching IC<sub>1f</sub>.

In contrast to that of a standard opamp, the input impedance of IC<sub>1f</sub> is not easily determined. This is because of the protection circuit (which has a lower impedance at high voltages) and also since the inverter is a less ideal amplifier than an opamp. The input impedance varies between 200 k $\Omega$  and 300 k $\Omega$ , which is in most cases high enough to prevent loading of the circuit on test.

The amplifier is followed by a Schmitt trigger that converts the amplified signal to a neat rectangular signal. The trigger is formed by two series-connected inverters, IC<sub>1d</sub> and IC<sub>1e</sub> that have been provided with a measurement coupling via R<sub>4</sub> and R<sub>5</sub>.

The signal is subsequently applied to bistable IC<sub>2B</sub> directly and to T<sub>1</sub> via C<sub>4</sub> and R<sub>6</sub>. The transistor is switched on briefly at each leading edge by the charging current through C<sub>4</sub> and this causes D<sub>7</sub> to light. This indicates that the signal is suitable for driving the bistable. If the LED goes out or flickers, the signal is too small or something else prevents the Schmitt trigger from regular toggling.

As already stated, the difference between the two channels is confined to a couple of capacitors that enable the phase behaviour in the two channels to be identical, or nearly so, over as large a frequency range as possible. This is particularly important at the extremes of the range, because where the frequency response

starts to roll off, phase shift ensues. This does no harm as long as the shift is the same in both channels and this is ensured by the calibration points.

The lower cut-off point is determined by the input circuit. Since the value of capacitors normally has a greater tolerance (usually 20%) than that of resistors, capacitors are used for calibrating. To that end, C<sub>1</sub> may be shunted by C<sub>9</sub>, which compensates small differences in value between C<sub>1</sub> and C<sub>5</sub> (C<sub>1</sub> and C<sub>5</sub> are compared and the smaller is fitted as C<sub>1</sub>).

The upper cut-off point is determined primarily by parasitic capacitances in the inverters, but also by the small differences in the switching thresholds of the Schmitt triggers (bear in mind that the resistors have a tolerance of about 5%). The latter effect is particularly noticeable at high frequencies. The overall effect is compensated by C<sub>3</sub> and C<sub>7</sub>.

The SR bistable is not a standard component, but is composed of two D-type bistables with reset input, IC<sub>2A</sub> and IC<sub>2B</sub>. The D-bistables are interconnected in such a manner that every time one of them is set (the D inputs are permanently high), the other is reset. Just as the usual edge-triggered SR bistable, the present one has a non-permitted state and this occurs when two leading edges appear simultaneously. In that state, it is impossible to say whether the circuit interprets this as a set or a reset. This is the cause of the fact that, in theory, the meter has no stable null and cannot stably indicate multiples of 360° (which the meter 'sees' as 0°). This sounds worse than what happens in practice, because a few tenths of a degree are sufficient to give a stable display. Unreliable display of the phase shift occurs mainly when the frequency of the input signal is not stable (jitter).

The phase angle is displayed by an LCD that was also used for the 'inductance/capacitance meter' published last year<sup>1</sup>. This shows, by means of filter R<sub>7</sub>-C<sub>1</sub>, the average value of the output voltage of the bistable.

Owing to the sensitivity of the DVM module and the fact that two meter ranges are required, the output voltage must be lowered to a suitable level. This is done with the aid of potential divider R<sub>15</sub>-R<sub>17</sub>-P<sub>1</sub>-P<sub>2</sub>. From that divider, the signal is applied to the meter via one contact of range switch S<sub>1</sub>. The other contact of this switch switches the decimal point to the backplane signal (AC) via R<sub>18</sub>; it is on when it is connected to inverted backplane signal (BP).

The power supply uses the voltage regulators in the DVM module. Thus, the output of the mains transformer is taken from the transformer board to the phase meter where it is rectified and buffered and then applied to the regulators in the DVM module, which hold the

voltage steady at  $\pm 5$  V. That voltage is then returned to the phase meter board. Note that the regulators can easily cope with the 11 V unregulated input, although the connections on the DVM module state 8 V.

Since the circuit draws only a small current, it is also possible to power it by two 9-V batteries. That saves a transformer and some other components. To reduce the current even further, high-efficiency LEDs should be used. The series resistors must then be increased to 3.9 k $\Omega$ .

## Construction

The printed circuit board for the phase meter and transformer is shown in Fig. 4. This board may be cut into two if, for instance, the transformer is not used. Even if the board is used as shown, it is advisable, because of the weight of the transformer, to use eight screws to fasten it. This results in a rather more rigid construction.

The input circuits must be screened along the dashed lines. The four soldering pins at the corners make this an easy operation. The lid should not be fitted until the calibration has been carried out (possible placing of C<sub>9</sub>). It is advisable to drill a hole in the lid through which C<sub>7</sub> can be adjusted. Because of the screen, it is best to connect the screened wires to K<sub>1</sub> and K<sub>2</sub> at the underside of the board. This must be done, of course, before the board is fitted into the enclosure.

The values of capacitors C<sub>1</sub> and C<sub>5</sub> must be checked with a capacitance meter. The larger value should be used in the C<sub>5</sub> position. The difference between the two values is compensated by C<sub>9</sub>. To start with, make the value of this capacitor the same as the difference; the optimum value can be determined during the calibration.

The PCB for the meter module is shown in Fig. 5. Start with placing the wire bridges, because at a later stage that may be next to impossible. Place IC<sub>1</sub> in a low-profile socket, so that the display neatly fits over it. In case this proves troublesome, insert an extra terminal strip into the terminal strip of the display, so that the LCD sits slightly higher.

Because of the intricate routing of the supply lines, it is advisable to check them thoroughly and to measure the voltage at various positions after the supply has been switched on.

Strictly speaking, the LEDs should not light when the supply is switched on, but the sensitive input channels may well pick up some noise, which is then processed as 'input'. This property may be used to advantage by touching the live input terminal with a finger. If the input channels function correctly, the associated LED should light. With S<sub>1</sub> in position 180°, the decimal point before the

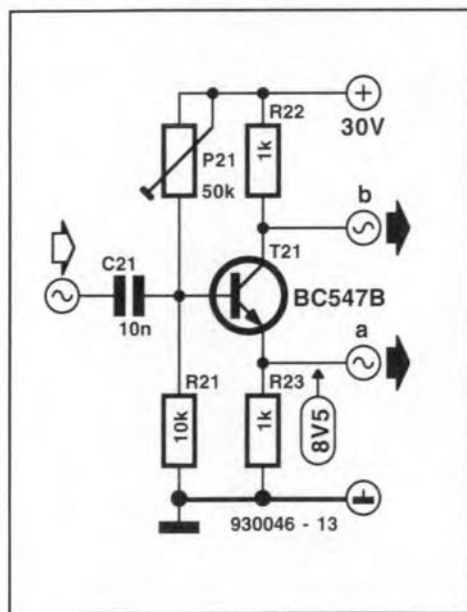


Fig. 3. Auxiliary circuit for calibrating the phase meter.

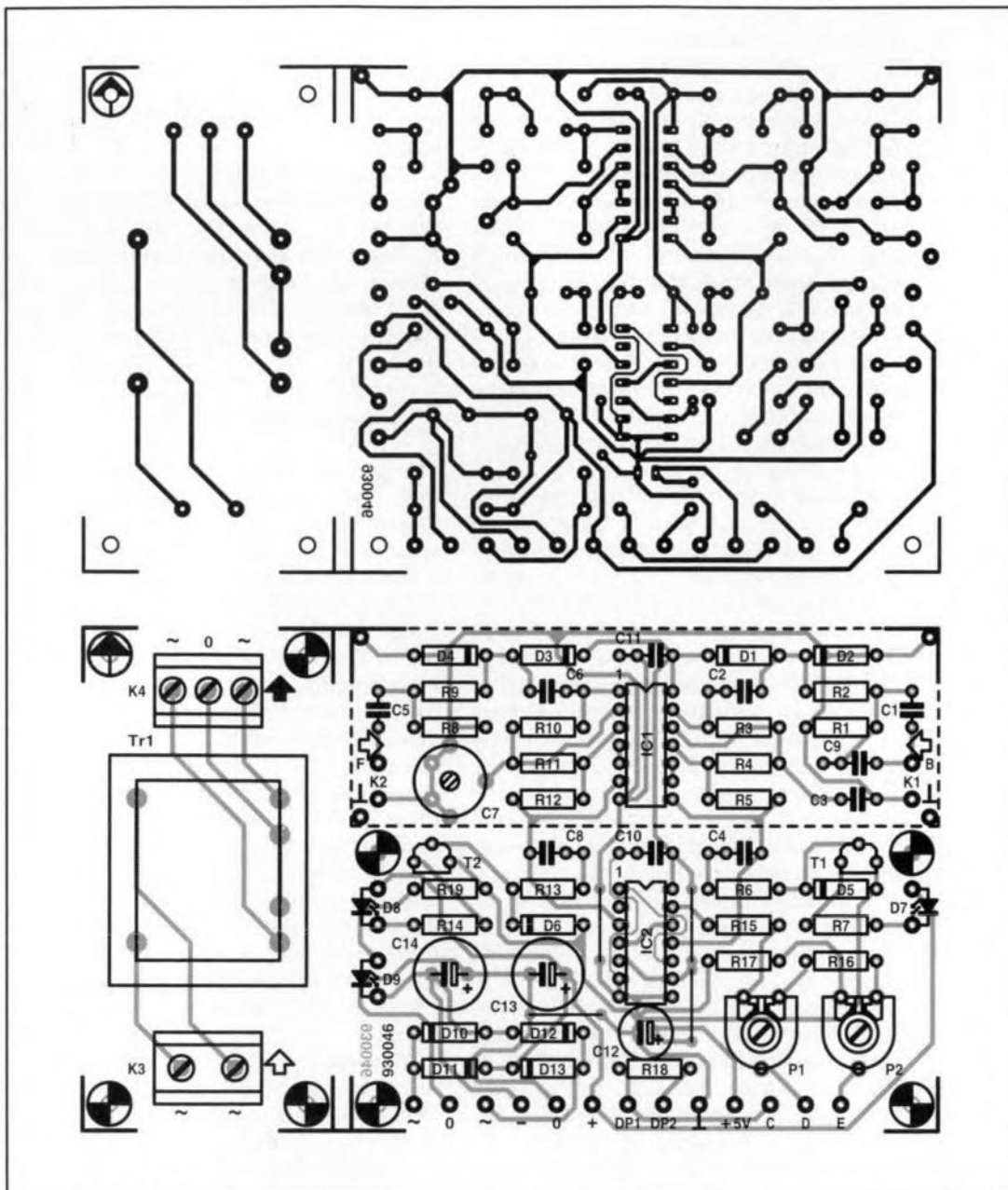


Fig. 4. Printed-circuit board for the phase meter and power supply. If necessary, the board is easily cut into two.

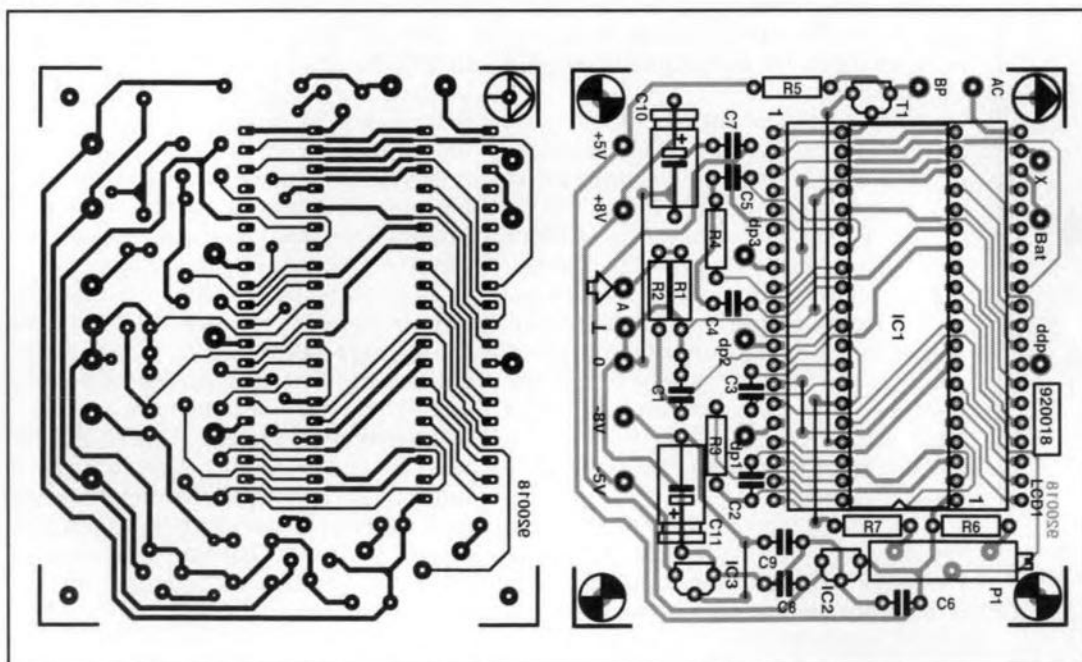


Fig. 5. Printed-circuit board for the meter module.

## PARTS LIST (Phase Meter)

### Resistors:

R1, R8 = 1 M $\Omega$   
 R2, R9 = 100 k $\Omega$   
 R3, R10 = 10 M $\Omega$   
 R4, R6, R11, R13, R16 = 22 k $\Omega$   
 R5, R12 = 560 k $\Omega$   
 R7, R14, R19 = 680  $\Omega$   
 R15 = 6.8 k $\Omega$   
 R17 = 2.43 k $\Omega$ , 1%  
 R18 = 2.2 M $\Omega$   
 P1 = 2.5 k $\Omega$  preset  
 P2 = 250  $\Omega$  preset

### Capacitors:

C1, C5 = 1.5  $\mu$ F, MKT  
 C2, C4, C6, C8, C10, C11 = 100 nF  
 C3 = 27 pF  
 C7 = 50 pF trimmer  
 C9 = see text  
 C12 = 220  $\mu$ F, 10 V, radial  
 C13, C14 = 470  $\mu$ F, 16 V, radial

### Semiconductors:

D1–D4 = 1N4448 or 1N4148  
 D5, D6 = 1N4148  
 D7–D9 = LED, red  
 D10–D13 = 1N4001  
 T1, T2 = BC547  
 IC1 = 4069U  
 IC2 = 4013

### Miscellaneous:

K1, K2 = BNC plug  
 K3 = 2-way terminal block, pitch 7.5 mm  
 K4 = 3-way terminal block, pitch 5 mm  
 S1 = DPCO switch  
 S2 = double pole mains switch  
 Tr1 = mains transformer, 2 $\times$ 9 V, 1.5 A  
 Enclosure 210 $\times$ 80 $\times$ 160 mm (8 $\frac{1}{4}$  $\times$ 3 $\frac{3}{16}$  $\times$ 6 $\frac{5}{16}$  in)  
 PCB Type 930046 (p. 70)  
 Front panel foil 930046-F (p. 70)

## (Meter module)

### Resistors:

R1 = 22 M $\Omega$   
 R2, R5 = 1 M $\Omega$   
 R3 = 100 k $\Omega$   
 R4 = 470 k $\Omega$   
 R6 = 18 k $\Omega$   
 R7 = 10 k $\Omega$   
 P1 = 10-turn preset, 5 k $\Omega$

### Capacitors:

C1 = 10 nF  
 C2 = 150 pF  
 C3, C6, C7 = 100 nF  
 C4 = 47 nF  
 C8, C9 = 330 nF  
 C10, C11 = 100  $\mu$ F, 25 V, radial

### Semiconductors:

T1 = BS170  
 IC1 = ICL7106  
 IC2 = 78L05  
 IC3 = 79L05

### Miscellaneous:

LCD1 = 3 $\frac{1}{2}$  digit LCD  
 40-pin low profile IC socket  
 2 $\times$ 20-way terminal strip  
 PCB Type 920018 (see p. 70)

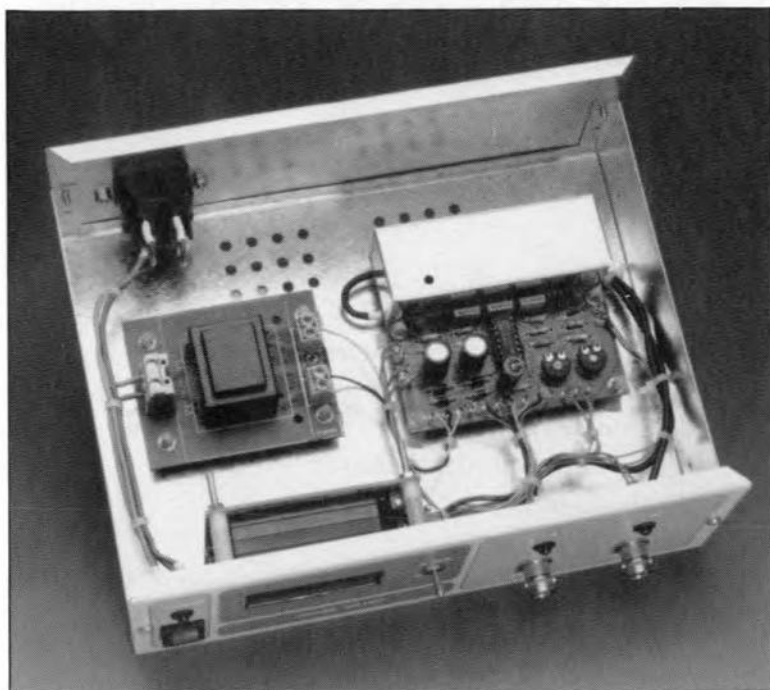


Fig. 6. Inside view of the completed phase meter.

last digit of the display should light. With a signal at input A (and input B short-circuited), the meter should read  $0^\circ$ . With a signal at input B (and input A short-circuited) and  $S_1$  in position  $360^\circ$ , adjust  $P_1$  until the meter reads  $360^\circ$ .

Preset  $P_2$  ( $180^\circ$  range) may be adjusted in a number of ways, but at all times with a 1000 Hz signal. One way is to use the  $360^\circ$  range as reference and to shift the signal by about  $180^\circ$  with the aid of an RC network. The preset is then adjusted until the meter readings in the  $180^\circ$  range and the  $360^\circ$  range are the same.

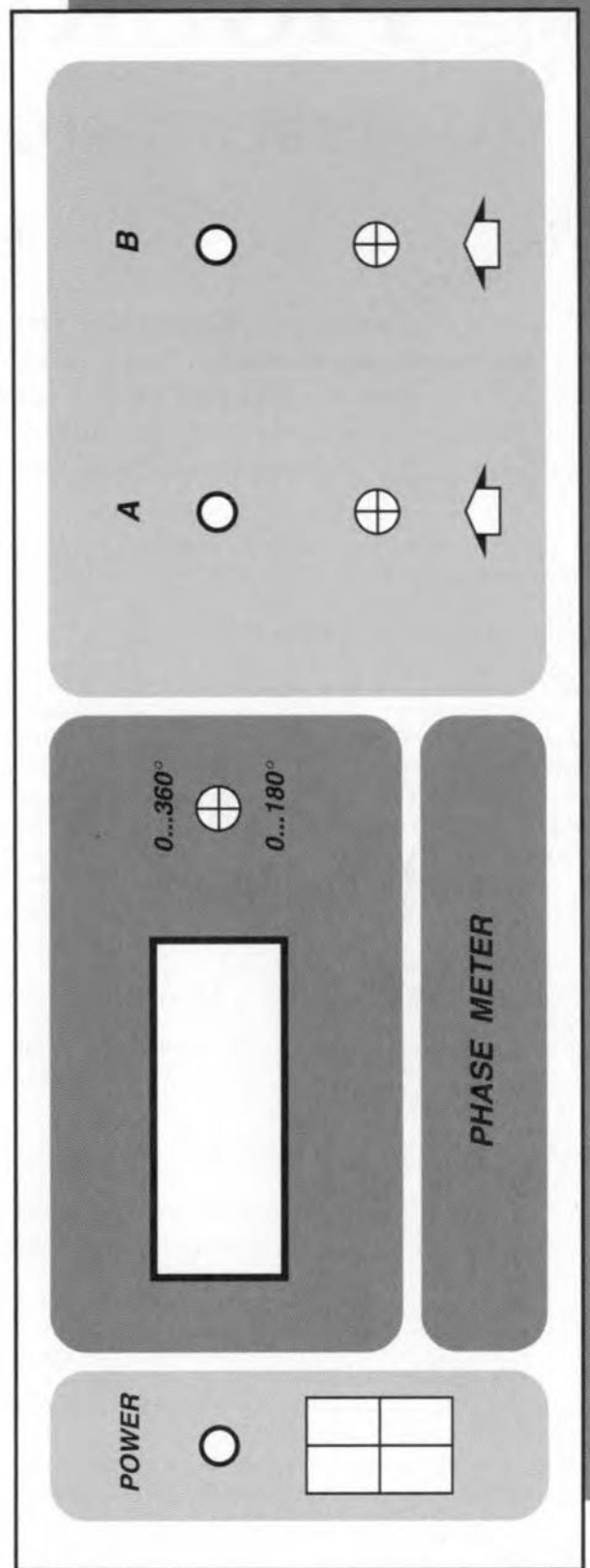
Another way is to use a signal source that can provide an output signal and its inverse (which is the same as one that is shifted by  $180^\circ$ ). Again, adjust  $P_2$  until the meter reads  $180^\circ$ .

A third method makes use of the auxiliary circuit in Fig. 3, which provides two signals that are one another's inverse. Adjust  $P_{21}$  in such a manner that the two signals look identical (or nearly so) on an oscilloscope. If an oscilloscope is not available, set  $P_2$  to obtain an emitter voltage of 8.5 V. An input signal of 100 mV is fine. With the auxiliary circuit connected to the phase meter, adjust  $P_2$  for a meter reading of  $180^\circ$ .

To determine the optimum value of  $C_9$  and to adjust  $C_7$ , either a signal source with inverted outputs or the circuit of Fig. 3 is required.

Start with lowering the frequency to between 100 Hz and 50 Hz. If everything is all right, the indicated phase angle ( $S_1$  in position  $180^\circ$ ) should not change by more than a few tenths of a degree. If it is more, the value of  $C_9$  must be made a little lower or higher (this has to be tried out). Do the same with a frequency of 30 Hz. Then, adjust  $C_7$  until the meter reads  $180^\circ$  again. If  $C_7$  cannot be made

Fig. 7. The front panel foil for the phase meter is available through our Readers' services (see page 70).



small enough, the value of  $C_3$  must be increased slightly. If  $C_7$  cannot be made large enough, shunt  $C_3$  with a small, say, 27 pF, capacitor.

Finally, carry out these tests at a few different frequencies to make sure that everything works all right. Readjust the relevant controls where necessary. Put the lid on the screening of the input circuits and close the enclosure. [930046]

#### References

1. 'Inductance-capacitance meter', *Elektor Electronics*, March, April 1992.

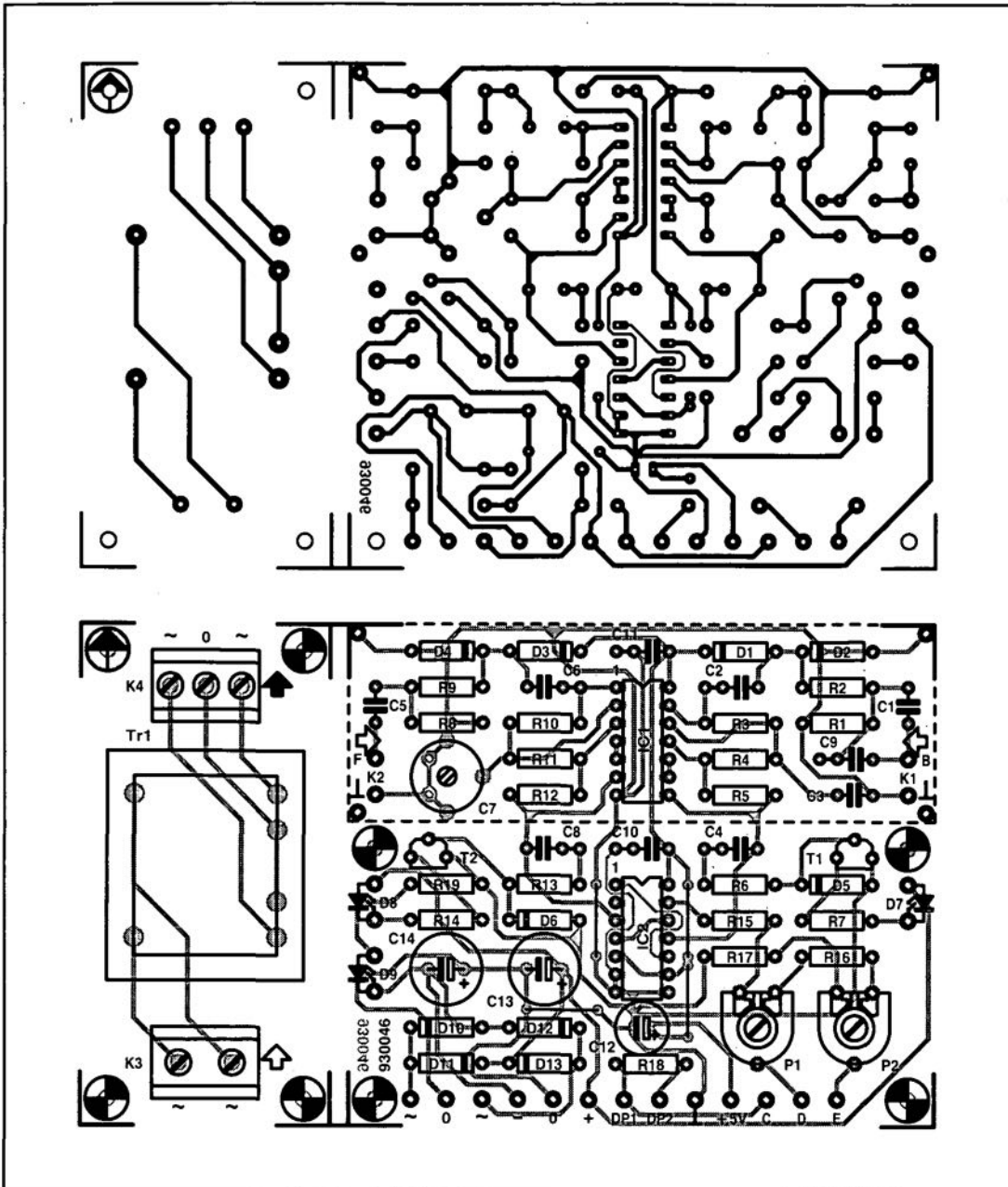


Fig. 4. Printed-circuit board for the phase meter and power supply. If necessary, the board is easily cut into two.

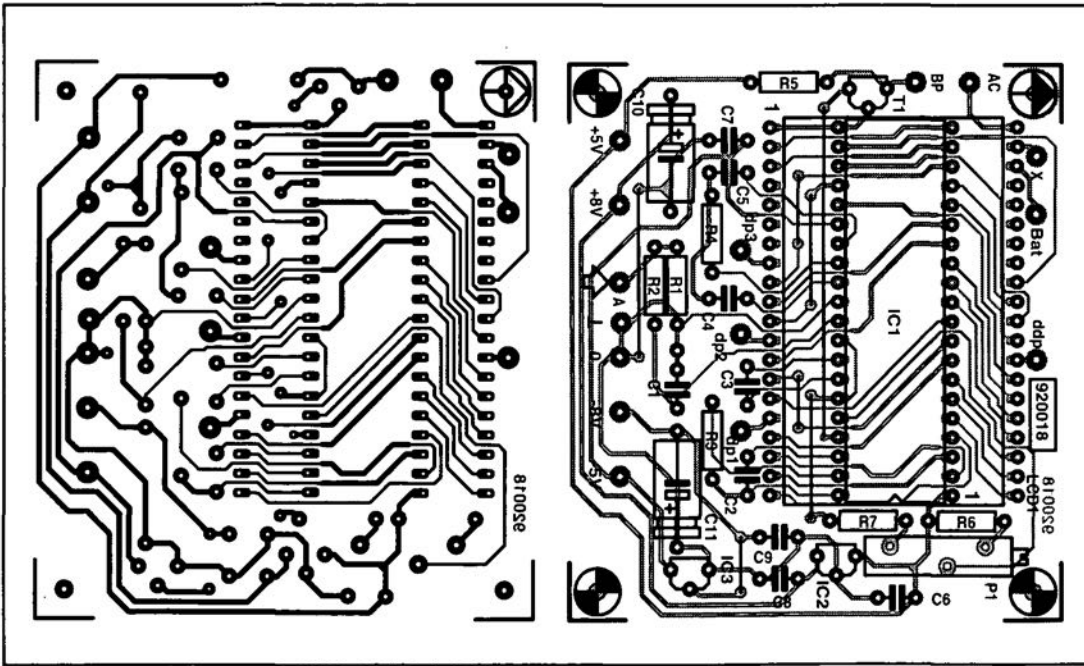


Fig. 5. Printed-circuit board for the meter module.

**PARTS LIST**  
(Phase Meter)

- Resistors:**  
 R1, R8 = 1 MΩ  
 R2, R9 = 100 kΩ  
 R3, R10 = 10 MΩ  
 R4, R6, R11, R13, R16 = 22 kΩ  
 R5, R12 = 560 kΩ  
 R7, R14, R19 = 680 Ω  
 R15 = 6.8 kΩ  
 R17 = 2.43 kΩ, 1%  
 R18 = 2.2 MΩ  
 P1 = 2.5 kΩ preset  
 P2 = 250 Ω preset

- Capacitors:**  
 C1, C5 = 1.5 μF, MKT  
 C2, C4, C6, C8, C10, C11 = 100 nF  
 C3 = 27 pF  
 C7 = 50 pF trimmer  
 C9 = see text  
 C12 = 220 μF, 10 V, radial  
 C13, C14 = 470 μF, 16 V, radial

- Semiconductors:**  
 D1-D4 = 1N4448 or 1N4148  
 D5, D6 = 1N4148  
 D7-D9 = LED, red  
 D10-D13 = 1N4001  
 T1, T2 = BC547  
 IC1 = 4069U  
 IC2 = 4013

- Miscellaneous:**  
 K1, K2 = BNC plug  
 K3 = 2-way terminal block, pitch 7.5 mm  
 K4 = 3-way terminal block, pitch 5 mm  
 S1 = DPCO switch  
 S2 = double pole mains switch  
 Tr1 = mains transformer, 2×9 V, 1.5 A  
 Enclosure 210×80×160 mm (8 1/4×3 3/8×6 5/16 in)  
 PCB Type 930046 (p. 70)  
 Front panel foil 930046-F (p. 70)

(Meter module)

- Resistors:**  
 R1 = 22 MΩ  
 R2, R5 = 1 MΩ  
 R3 = 100 kΩ  
 R4 = 470 kΩ  
 R6 = 18 kΩ  
 R7 = 10 kΩ  
 P1 = 10-turn preset, 5 kΩ

- Capacitors:**  
 C1 = 10 nF  
 C2 = 150 pF  
 C3, C6, C7 = 100 nF  
 C4 = 47 nF  
 C8, C9 = 330 nF  
 C10, C11 = 100 μF, 25 V, radial

- Semiconductors:**  
 T1 = BS170  
 IC1 = ICL7106  
 IC2 = 78L05  
 IC3 = 79L05

- Miscellaneous:**  
 LCD1 = 3 1/2 digit LCD  
 40-pin low profile IC socket  
 2×20-way terminal strip  
 PCB Type 920018 (see p. 70)



# FIGURING IT OUT

## PART 6 – FREQUENCIES AND FILTERS

By Owen Bishop

This series is intended to help you with the quantitative aspects of electronic design: predicting currents, voltage, waveforms, and other aspects of the behaviour of circuits. Our aim is to provide more than just a collection of rule-of-thumb formulas.

We will explain the underlying electronic theory and, whenever appropriate, render some insights into the mathematics involved.

In Part 5 we looked at what happens when an alternating pd is applied to an inductor. In Fig. 43, the applied pd is given by

$$U = U_0 \cos \omega t, \quad [\text{Eq. 31}]$$

where  $U_0$  is the peak pd and  $\omega$  is the angular frequency (more about this in a moment). We then showed that the current through the inductor is given by

$$I = I_0 \sin \omega t. \quad [\text{Eq. 32}]$$

We compared these equations to demonstrate the facts that  $I$  has the same frequency as  $U$ , but lags behind  $U$  by  $\pi/2$  radian.

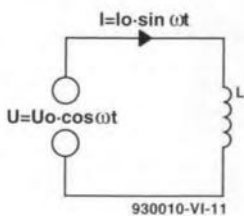


Fig. 43

First to clarify the quantity  $\omega$ . This is related to frequency by the equation

$$\omega = 2\pi f,$$

where  $\omega$  is in radian per second. Equation 31 could equally well be written as  $U = U_0 \cos 2\pi ft$ . In many instances, particularly when dealing with audio circuits,  $f$  is a more convenient quantity to use. However, it is often easier to deal with the single symbol  $\omega$  than the multiple  $2\pi f$  when integrating or differentiating, so we shall use either way of expressing frequency, depending on circumstances.

During the discussion of the

equations above, we derived an equation for  $I$ , in which

$$I = (U/\omega L) \sin \omega t.$$

At the time we said that the expression in brackets represents the peak value,  $I_0$ , of a sinusoidally varying current, immediately replacing the expression by  $I_0$  to produce Eq. 32. Now we will take time to look at this bracketed expression more closely. The expression gives the value of the peak current as

$$I_0 = U_0/\omega L.$$

This has the same form as the well-known equation for resistance:

$$I = U/R$$

and demonstrates that  $\omega L$  is the equivalent of resistance. It is the **inductive reactance** of the inductor and has the symbol  $X_L$ :

$$X_L = \omega L. \quad [\text{Eq. 33}]$$

Like resistance, inductive reactance is one of the elements of the total **impedance** of a circuit and is expressed in ohm ( $\Omega$ ). Equation 33 shows that inductive reactance is proportional to inductance, as would be expected. The equation also shows that, unlike resistance, it is proportional to frequency: as the frequency increases, so does the inductive reactance.

Example: calculate the reactance of a coil,  $L = 0.1$  mH, given a signal of (a) 100 Hz; (b) 1 MHz.

$$\begin{aligned} \text{(a)} \quad \omega &= 2\pi f = 200\pi = 628 \text{ rad s}^{-1}. \\ X_L &= 628 \times 0.1 \times 10^{-3} = 0.0628 \Omega. \end{aligned}$$

$$\begin{aligned} \text{(b)} \quad \omega &= 2\pi \times 10^6 = 6.28 \times 10^6 \text{ rad s}^{-1}. \\ X_L &= 6.28 \times 10^6 \times 0.1 \times 10^{-3} = 628 \Omega. \end{aligned}$$

### Capacitive reactance

In Part 5 we also showed that, if a capacitor is being charged with a sinusoidally varying pd (Fig. 44), the current flowing into the capacitor is:

$$I = C(dU/dt).$$

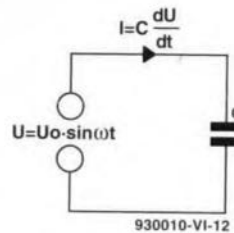


Fig. 44

Differentiating  $U_0 \sin \omega t$  as one of the standard differentials, we find:

$$I = C(\omega U_0 \cos \omega t).$$

As  $C$ ,  $\omega$  and  $U_0$  are all constants, we can replace their product with a single constant. The equation for current is, in fact, a cosine equation, where the single constant is  $I_0$ , the peak current. In other words,

$$I_0 = \omega C U_0.$$

The argument follows the same lines as that above, leading to the conclusion that the **capacitive reactance** is given by

$$X_C = 1/\omega C. \quad [\text{Eq. 34}]$$

Equation 34 shows that  $X_C$  has features that are the opposite of those of  $X_L$ . It is **inversely** proportional to both capacitance and frequency. The higher the frequency, the lower the capacitive reactance. This is another example of a pair of duals.

Example: calculate the reac-

tance of a capacitor,  $10 \mu\text{F}$ , given a signal of (a) 100 Hz, (b) 1 MHz.

$$\begin{aligned} \text{(a)} \quad \omega &= 628 \text{ rad s}^{-1}, \text{ as above.} \\ X_C &= 1/(628 \times 10 \times 10^{-6}) = 159 \Omega. \end{aligned}$$

$$\begin{aligned} \text{(b)} \quad \omega &= 6.28 \times 10^6 \\ X_C &= 1/(6.28 \times 10^6 \times 10 \times 10^{-6}) \\ &= 0.0159 \Omega. \end{aligned}$$

### Total impedance

The calculations above are for purely inductive and purely capacitive circuits, as illustrated by Fig. 43 and 44. Now, to examine what happens in a circuit in which all three elements are present in series, as in Fig. 45.

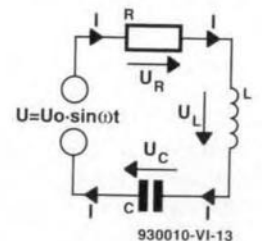


Fig. 45

Two facts are clear:

- The instantaneous current,  $i$ , through each of  $L$ ,  $C$ ,  $R$ , and the source is the same. If it were not, it would imply that current was leaking out of, or into, the circuit at some point.
- KVL applies to the instantaneous pds. The equation for the loop is:

$$U = U_R + U_L + U_C.$$

There are several ways of analysing the changing pds and currents in the circuit. Techniques using complex numbers or differential equations will be considered in a later issue. Here we adopt an approach that relies on geometry. The dif-

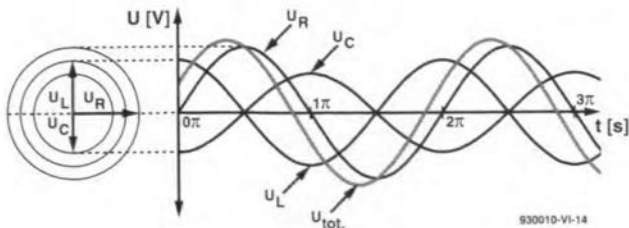


Fig. 46

difficulty with analysing this circuit is that the changing pds are usually not in phase with each other. The graphs of Fig. 46 show their relationships, with  $U_L$  leading  $U_R$  by  $\pi/2$  and  $U_C$  lagging  $U_R$  by the same amount.

The current is in phase with  $U_R$ , since the pd across a resistor and the current through it are always in phase. The three vectors on the left represent the pds at the instant corresponding to the extreme left of the graph. The relative lengths of the vectors depend on the impedances found in a particular circuit at a given frequency. Their relative directions, however, are always as shown in the figure.

Comparison with the graph shows that these vectors represent **peak** pds. As time passes, that is, as we move toward the right-hand end of the graph, we can imagine this array of vectors rotating anticlockwise (with angular velocity  $\omega$ ), each vector remaining the same length and the angles between them remaining unchanged. The pds peak in order:  $U_L$ , then  $U_R$ , and finally  $U_C$ . This can be seen by examining the curves in Fig. 46. Since the three vectors retain their relative magnitude and keep in phase with each other, we can add them for the position shown on the left of Fig. 46, knowing that rotation does not affect the result.

Figure 47 shows the pds added by vector addition. The first step is to add  $U_L$  and  $U_C$ , which is easy because they lie in exactly opposite direction ( $U_C$  is negative). Call their resultant the **reactance voltage**,  $U_X$ . This leaves us just two vectors,  $U_R$  and

$U_X$ , which are summed by drawing the diagonal of the vector rectangle. Since the vectors represent peak pds, the length of  $U$  represents the peak pd of the source.  $U_R$  is in phase with the current (as always), so it is clear from Fig. 47 that  $U$  is **not** in phase with  $I$ . This is the effect of the action of the capacitor and inductor. The **phase angle**,  $\phi$ , in this example is positive (a lead) but, if  $U_C$  had been greater than  $U_L$ , it would have been negative (a lag).

Looking again at Fig. 46, it can be seen that  $U_R$  is the dominant pd in this particular circuit.  $U_L$  and  $U_C$  are very similar in magnitude and, since they are out of phase with each other (leading and lagging  $U_R$  by  $90^\circ$ ) they almost cancel each other out. The  $U_{tot}$  curve in Fig. 46 is plotted by summing the point values calculated for the other three curves. Its peak value is slightly greater than that of  $U_R$ , and it leads  $U_R$  by a small phase angle, both features confirming the results of Fig. 47.

Since all the quantities are represented geometrically, it is easy to discover the equations that relate them. Figure 48 is the key diagram for all such calculations. In this diagram, the vectors represent impedances, not pds. Because the current is the same for all elements, a diagram of impedance vectors has the same proportions and angles as a diagram of pd vectors. The difference is just a matter of scale. In Fig. 48 the relative lengths of vectors differ from those in Fig. 47, which represent a circuit with different values of  $R$ ,  $L$ , and  $C$ .

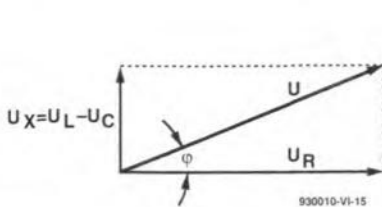


Fig. 47

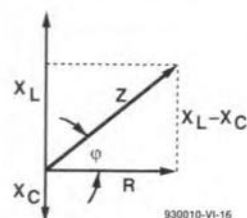


Fig. 48

Given the values of  $R$ ,  $L$ , and  $C$ , the first step is to calculate  $X_L$  and  $X_C$ , using equations 33 and 34. Then we can draw a sketch of the vectors (as in Fig. 48) and find:

1. The **total impedance**,  $Z$ : apply the Pythagoras theorem to the triangle enclosed by the vectors  $R$ ,  $(X_L - X_C)$ , and their resultant  $Z$ .

$$Z = \sqrt{R^2 + (X_L - X_C)^2} \quad [\text{Eq. 35}]$$

2. The **phase angle**,  $\phi$ .

$$\phi = \tan^{-1}[(X_L - X_C)/R] \quad [\text{Eq. 36}]$$

Note that since the calculations depend solely on the **proportions** of the rectangle, not on its absolute dimensions, the equations are independent of the magnitudes of the pds or the current. The circuit behaves the same, irrespective of the magnitude of the signal.

**Example.** Given  $R=100 \Omega$ ,  $L=100 \text{ mH}$ , and  $C=22 \mu\text{F}$ , connected in series, calculate their total impedance and the phase angle when the signal frequency is 500 Hz.

$$\begin{aligned} \omega &= 2\pi f = 1000\pi = 3141.6 \text{ rad s}^{-1}; \\ R &= 100 \Omega; \\ X_L &= 3141.6 \times 100 \times 10^{-3} = 314.16 \Omega; \\ X_C &= 1/(3141.6 \times 22 \times 10^{-6}) = \\ &= 1/0.069115 = 14.469 \Omega; \\ X_L - X_C &= 299.69 \Omega. \end{aligned}$$

$$\therefore Z = \sqrt{(100^2 + 299.1^2)} = 315.4 \Omega;$$

$$\phi = \tan^{-1} 299.1/100 = 1.25 \text{ rad.}$$

### What about j?

If you are reading this article in conjunction with an electrical or electronics textbook, you may have found that the text quotes the reactance of an inductor as  $j\omega L$  and that of the capacitor as  $-j/\omega C$ . The symbol  $j$  is used when expressing complex numbers and this will be explained in a future issue. For the moment, take  $+j$  to indicate that inductive reactance leads the current, and  $-j$  to indicate that capacitive reactance lags it. At present we are using the geometrical technique in which lead and lag are clear from the sketch of the vectors.

### Sinusoidal or not?

All the discussions so far have assumed that the source pd or the current varies in time according to a sine (or cosine) function. What happens if the waveform is not sinusoidal? What about

square waves or sawtooth waves, for example? As we shall see later in the series, all periodic waves can be treated as if they were the sum of a number of sine waves of various amplitudes with related frequencies. For example, the sawtooth wave of Fig. 49 is the sum of a sequence of terms which goes like this:

$$y = 3\pi - 6\sin t - 3\sin 2t - 2\sin 3t - \dots - (6/n)\sin nt$$

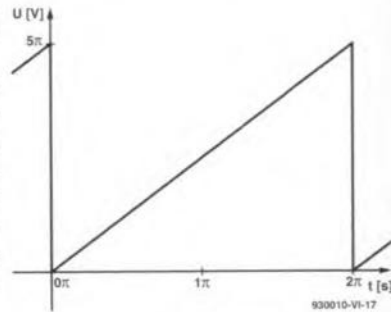


Fig. 49

The greater the number of terms summed, the more accurately the curve comes to look like a sawtooth wave. If we want to know how a circuit will behave with a sawtooth input, we analyse the waveform into its sinusoidal components, and calculate the impedances and phase angles for each component separately, as above. Then we sum the results. This may involve a lot of calculations, but it can be done, especially with the aid of a computer.

### Simpler circuits

Equations 35 and 36 cater for circuits in which all three kinds of impedance are present. If one source of impedance is absent, or so small that it can be ignored, we use the same two equations putting the absent impedance equal to zero. Consider the network of Fig. 50.

Since  $L$  equals zero (assuming that the self-inductance of the connecting wires and the leads of the capacitor is so small

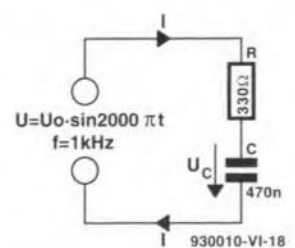


Fig. 50

that it can be ignored), the equations simplify to

$$Z = \sqrt{R^2 + X_C^2};$$

$$\phi = \tan^{-1} -X_C/R.$$

Given the values shown in Fig. 50:

$$\omega = 2000\pi = 6283.2 \text{ rad s}^{-1};$$

$$X_C = 1/(6283.2 \times 470 \times 10^{-9}) = 338.6 \Omega.$$

$$\therefore Z = \sqrt{330^2 + 338.6^2} = 472.8 \Omega.$$

$$\phi = \tan^{-1}(-338.6/330) = -0.80 \text{ rad}.$$

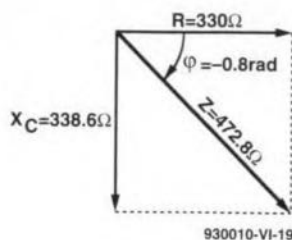


Fig. 51

Figure 51 shows the vectors. The current lags  $0.80 \text{ rad}$  (about  $45^\circ$ ) behind the pd. Since the same current flows through all components, the impedance vectors are proportional to the pd vectors. Thus,  $Z$  is proportional to the total pd applied to the network at any instant. The pd across the capacitor is proportional to  $X_C$ , and it can be seen that this pd lags about  $45^\circ$  behind the pd applied to the network.

We can also calculate the peak value of the alternating signal across the capacitor. Consider Fig. 50 to be that of a potential divider circuit. The current through  $R$  and  $C$  are equal (of course, no current actually passes through  $C$ , but current flowing to one plate is matched by current flowing from the other). Thus, the pd developed across  $R$  and across  $C$  is proportional to their impedances. The pd across  $C$  is calculated as for a potential divider. Taking pds at their peak values:

$$U_C = U(X_C/Z) = U(338.6/472.8) = 0.716U_0,$$

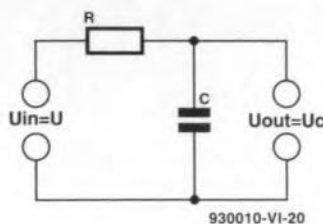


Fig. 52

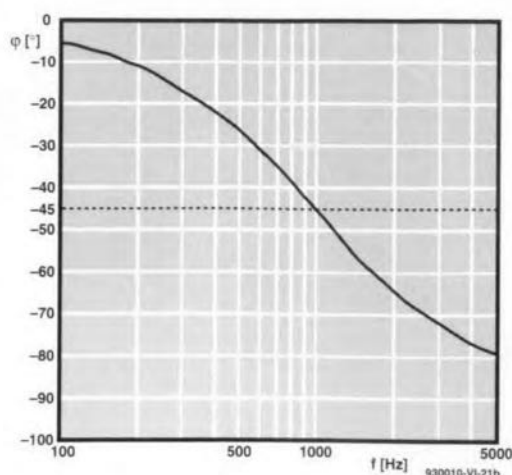
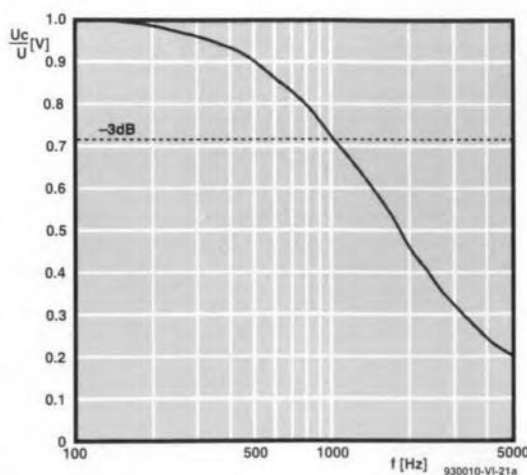


Fig. 53

or

$$U_C/U = 0.716.$$

Redraw Fig. 50 as in Fig. 52; call the total pd the **input pd**,  $U_{in}$ ; and call the pd across the capacitor the **output pd**,  $U_{out}$ .  $U_{out}$  is about 0.7 of  $U_{in}$ . The network attenuated the signal by roughly 0.3. The calculation assumes that the current drawn from the network by any load is insignificant.

## Frequency dependence

The calculations for Fig. 50 can be repeated for lower and higher frequencies and graphs plotted to relate phase lag and signal attenuation to frequency. As these graphs show (Fig. 53), phase lag approaches zero at low frequency and approaches  $-90^\circ$  at high frequencies. Remember that here we are considering the angle between  $U$  and  $U_C$  (or between  $Z$  and  $X_C$ ), not the angle between  $U$  and  $U_R$ . Attenuation approaches zero at low frequencies and gradually becomes more important at high frequencies. In fact, this network is a **low-pass filter**. The frequency chosen for the worked example (1000 Hz) is very close to what is known as the  $-3 \text{ dB}$  point. This is the frequency (1026 Hz for the specified component values) at which the output is 0.707 of the input (equivalent to a power attenuation of  $-3 \text{ dB}$  or 50%), and the phase lag is exactly  $45^\circ$ . It is the frequency at which  $X_C$  is equal to  $R$ , giving us the approximately  $45^\circ$  triangle of Fig. 51. We can find a formula for this frequency by equating  $R$  and  $X_C$ :

$$R = X_C = 1/\omega C = 1/2\pi f C.$$

Rearranging gives:

$$f = 1/2\pi RC.$$

**Example.** Find the  $-3 \text{ dB}$  point for a low-pass filter in which  $R = 150 \Omega$  and  $C = 2.2 \mu\text{F}$ .

$$f = 1/(2\pi \times 150 \times 2.2 \times 10^{-6}) = 482 \text{ Hz}.$$

## Other filters

The filter of Fig. 52 is converted to a high-pass filter simply by interchanging the resistor and capacitor. The vector diagram remains unchanged, but  $U_{out}$  is now the pd across the resistor. Thus, output **leads** input by  $45^\circ$  when  $R$  and  $X_C$  are equal and by greater or lesser amounts when the frequency is lower or higher. The  $-3 \text{ dB}$  point or **cut-off frequency** is calculated as for the low-pass filter.

A high-pass filter may also be constructed by substituting an inductor for the capacitor in Fig. 52. The  $-3 \text{ dB}$  point of such a filter occurs when  $R = X_L$ , so that at that point  $f = 1/2RL$ .

A resistor, inductor and capacitor may be combined in a filter network such as that in Fig. 54. The output is the pd across the resistor. It is left to the reader to calculate  $U_{out}$  for a num-

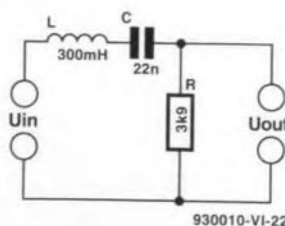


Fig. 54

ber of different frequencies in the range 100 Hz to 10 kHz, to observe the response, and say what type of filter this is. (Answer next month).

## Test yourself

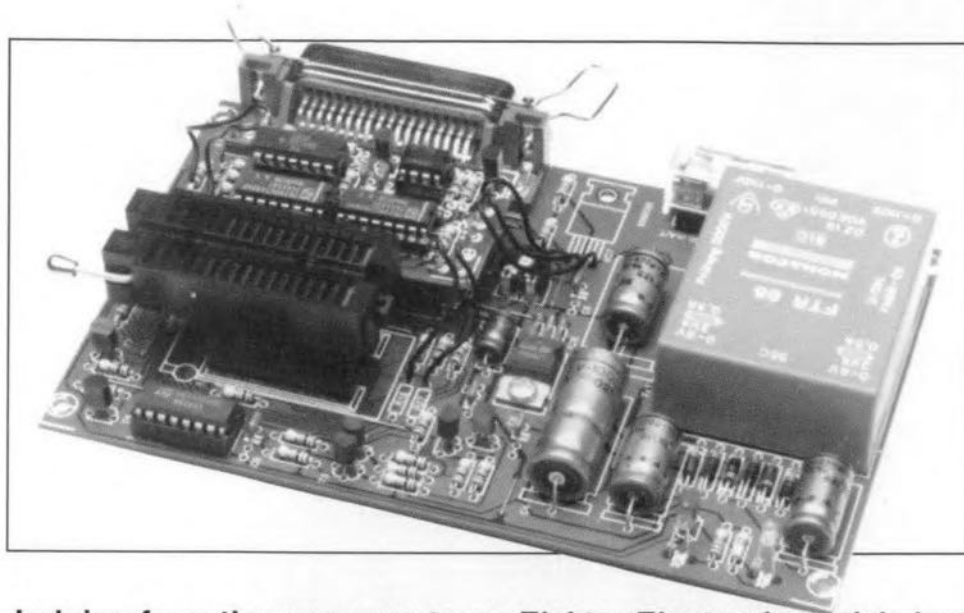
1. Calculate the angular velocity  $\omega$  for a signal of frequency 350 Hz.
2. What is the reactance of a  $33 \mu\text{H}$  inductor at (a) 50 Hz, (b) 10 MHz?
3. What is the reactance of a  $120 \mu\text{F}$  capacitor at (a) 2 Hz, (b) 10 kHz?
4. Draw the vector diagram for the circuit of Fig. 47, given that  $R = 680 \Omega$ ,  $L = 0.3 \text{ H}$ ,  $C = 1 \mu\text{F}$ , and the signal frequency is 250 Hz.
5. Calculate the cut-off frequency for a low-pass filter in which  $R = 12 \text{ k}\Omega$  and  $C = 2.2 \mu\text{F}$ .
6. Given a  $10 \text{ k}\Omega$  resistor, what value capacitor is needed to form high-pass filter with its  $-3 \text{ dB}$  point at 500 kHz?

Answers will be given in next month's instalment.

## Answers to Test yourself (Part 5)

1.  $U = L(-0.5) = -0.05 \text{ V}$ . A constant back e.m.f. in the direction opposing the reduction of current.
2.  $U = 0.2 \times -2e^{-2} = 7.33 \text{ mA}$ .
3.  $I = 10000 \times [t^2]_0 = 0.09 \text{ A}$ . The constant of integration  $C/L$  cancels out when we evaluate the definite integral.

# GAL PROGRAMMER UPGRADE



Judging from the response to an *Elektor Electronics* article last year describing a low-cost GAL programmer, it looks like many of you have recognized the power of GALs, and have started programming these interesting devices. This article answers many readers' requests for a hardware extension plus upgraded software that allows more GAL types, including the industry standard 22V10, to be programmed.

Design by M. Nosswitz

AFTER some research into the programming algorithms of a number of relatively new GALs, the designer found out that only very small modifications were required to the original GAL programmer (Ref. 1) to enable it to handle even more GAL types.

The differences in GAL programming algorithms often concern the programming voltage and the signal timing. Hence, the two main programmer upgrades are (1) a variable programming voltage source and (2) modifications to the control software to implement the (complex) timing of the programming signals, and the variable programming voltage. The software automatically adapts to the GAL type in question, hence changes to the programming algorithms are transparent to the user.

In addition to GAL types 16V8(A) and 20V8(A), the upgraded GAL programmer is also capable of handling the B versions of these GALs, the 22V10, 20RA10 and the GAL6001. Programming the 6001 takes about one minute, which, admittedly, is not fast, but still useful. As regards the programming ability of different GAL brands (a subject on which we have received many letters), please do remem-

ber that the GAL programmer can only handle GALs manufactured by **Lattice**, **National Semiconductor** and **SGS/Thomson**.

## Hardware extension

Everyone who has successfully built the original GAL programmer should be encouraged to upgrade it with the present hardware extension. The circuit diagram shows that the extension is relatively simple. Circuits IC<sub>1</sub> and IC<sub>2</sub> (Type 4094s) together form an 8-bit shift register. The output of IC<sub>2</sub> drives IC<sub>3</sub>, a digital-to-analogue converter (DAC) Type ZN426. The DAC supplies an output voltage between 0.63 V and 1.92 V, which is programmable in steps of 20 mV. The DAC output voltage is applied to IC<sub>4</sub>, a Type CA3140 BiFET opamp, which replaces the LM317 voltage regulator originally fitted in the circuit. Apart from removing the LM317 from the board, the voltage divider around it has to be changed also. Resistor R<sub>27</sub> (270 Ω) is changed into 22 kΩ, and R<sub>26</sub> (2.7kΩ) into 1.8kΩ. Finally, preset P<sub>1</sub> (1 kΩ) is

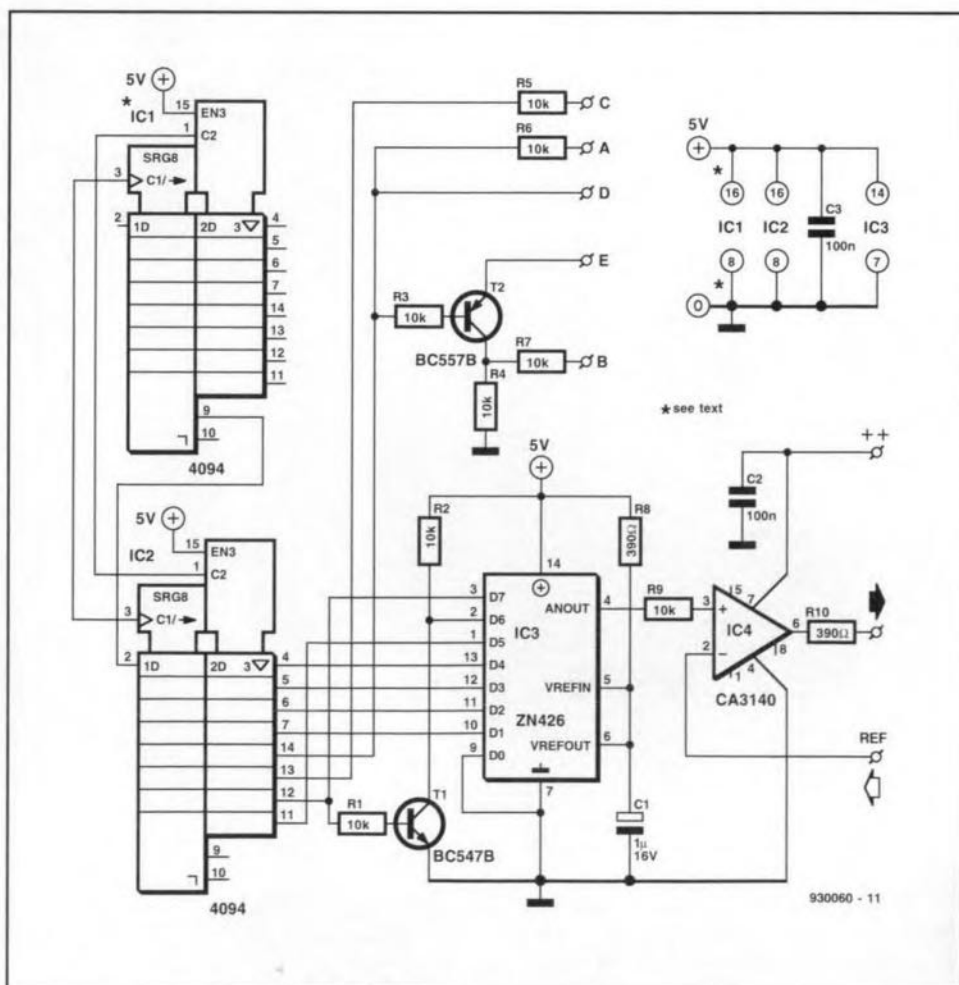


Fig. 1. Circuit diagram of the GAL programmer extension.

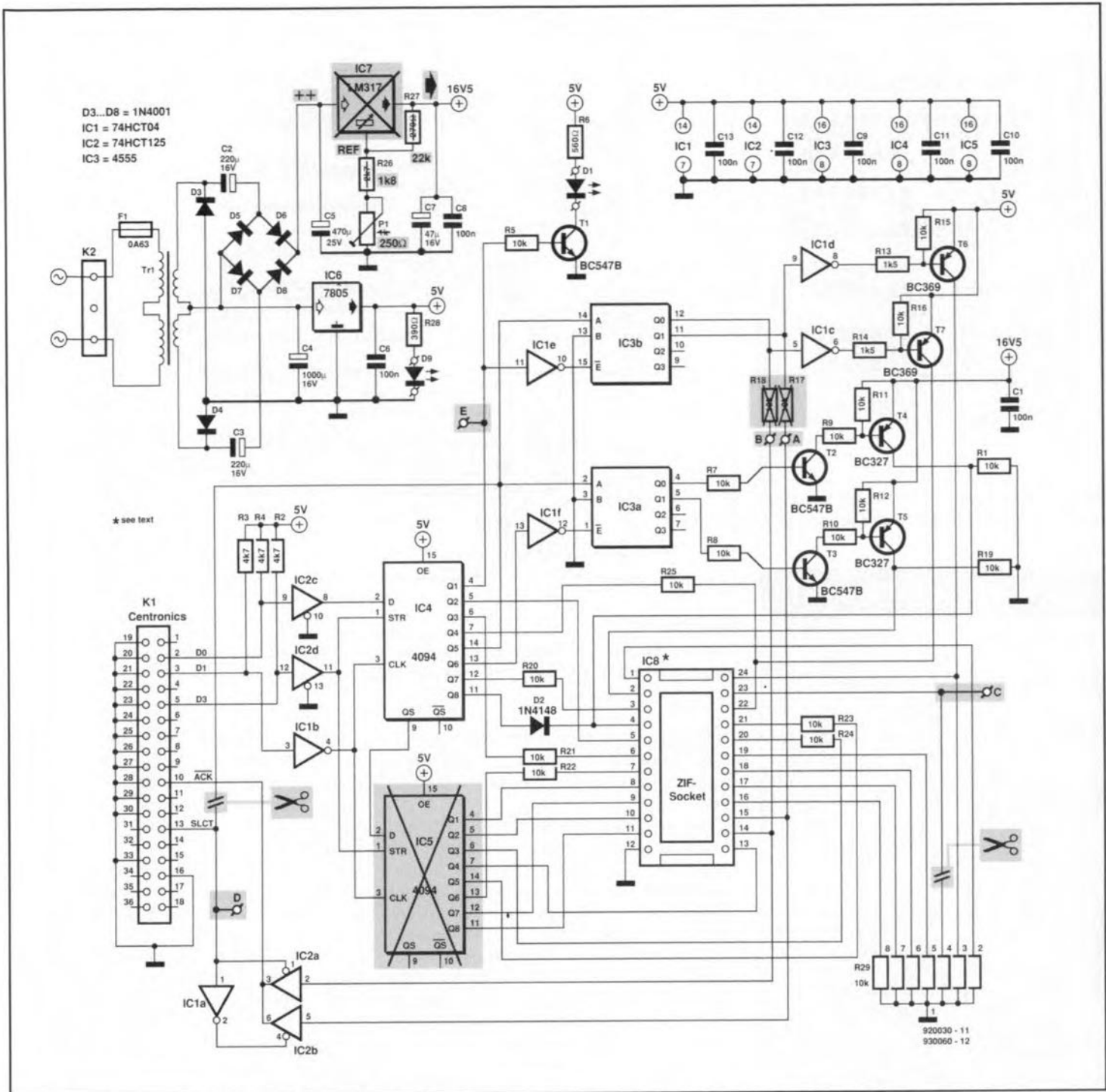


Fig. 2. This diagram shows where the original GAL programmer has to be modified to enable the extension to be integrated.

changed into 250 Ω (or 220 Ω). The opamp ensures a programming voltage range from 8 V to 23.75 V. For the sake of clarity, Fig. 2 shows the original circuit diagram with the modifications in shaded blocks.

The small board that contains the additional circuitry is fitted as an extension on to the main board. IC5 (a 4094) is removed from the main board, and replaced by the (extended) pins of the socket for IC1 on the extension board. This IC takes over the function of IC5 on the main board, and at the same time provides the connection of the supply voltage. IC2 on the extension board becomes the third element in the shift register consisting of IC4

on the main board, and IC1 and IC2 on the extension board. The third element is required to copy and latch the control word that represents the variable programming voltage. Furthermore, a number of output signals of IC2, marked A through E, are sent into the circuit. These signals are under software control, and, therefore, of little interest to the user.

### Construction

As already mentioned, the extension board is plugged into the empty socket in position IC5 on the main board. The track layout and component overlay of the extension board are given in Fig. 3.

IC1 on the extension board is mounted into two IC pin rows with extra long pins, or a wire-wrap socket. The long pins are pushed through the holes in the extension board, soldered at the track side, and inserted into the socket in position IC5 on the GAL programmer main board. First, however, the extension board has to be populated. Fit eight solder pins where the wires between the extension board and the main board are to be connected. Once the extension board is complete, you can proceed with the modifications to the main board.

Remove IC7 from the main board, and solder three lengths of insulated wire in the open PCB holes. Next, re-

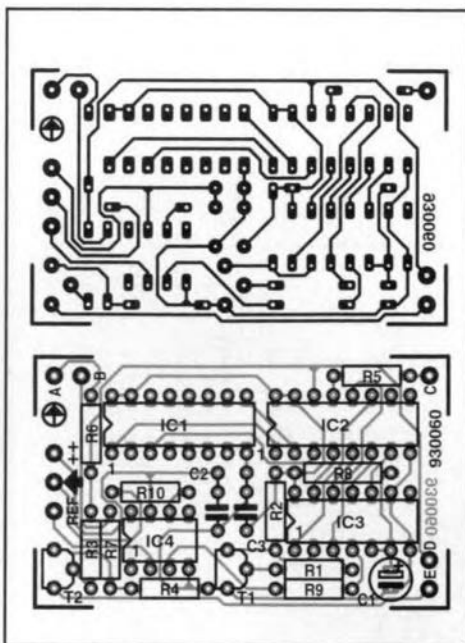


Fig. 3. Track layout (mirror image) and component overlay of the extension board.

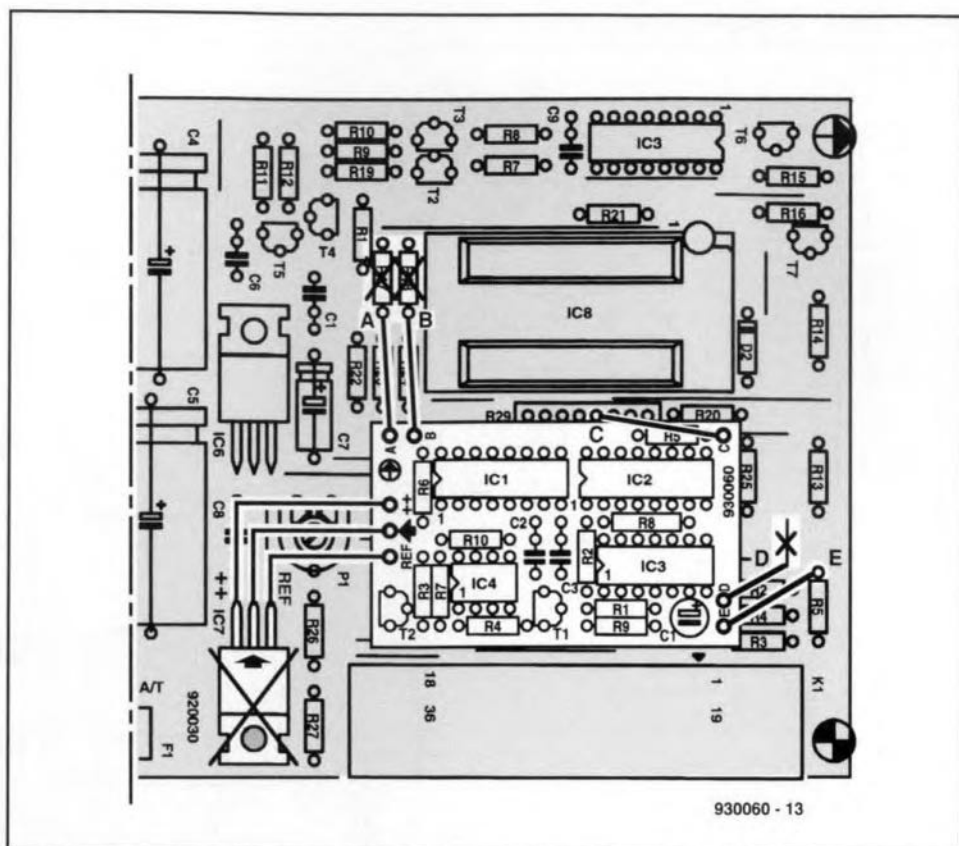


Fig. 4. This diagram tells you which components have to be changed on the main board, which wire link is removed, and where the eight wires are connected.

## COMPONENTS LIST

### Resistors:

8	10 k $\Omega$	R1-R7;R9
2	390 $\Omega$	R8;R10

### Capacitors:

1	1 $\mu$ F 16V tantalum	C1
2	100nF ceramic	C2;C3

### Semiconductors:

1	BC547B	T1
1	BC557B	T2
2	4094	IC1;IC2
1	ZN426	IC3
1	CA3140	IC4

### Miscellaneous:

- 1 DIL-16 wire-wrap socket, or two 8-way IC pin strips with long pins
- 1 Printed circuit board, order code 930060 (see page 70)
- 1 Software on disk, order code 1701 or 1881 (see page 70)

move resistors R17 and R18 from the board, and solder two wires into the holes nearest R23 and R24. The next job is a little more difficult: pin 4 of array R29 has to be disconnected from the PCB, and a short wire is inserted into the hole. If you find it difficult to actually pull the array pin out of the PCB hole, you may also cut it off (using a pair of precision pliers), and pull the remaining wire out of the PCB hole (while heating it with the solder iron, of course). Next, remove the wire link between R5 and R13, and fit a wire into the hole near R2/R5. The last wire is connected to the side of R5 that is close to the wire link you have just removed.

Replace resistor R27 by a 22-k $\Omega$  type, resistor R26 by a 1.8-k $\Omega$  type, and preset P1 by a 250- $\Omega$  (or 220- $\Omega$ ) type.

After plugging the extension board on to the main board, connect the eight wires to the appropriate solder pins. The drawing in Fig. 4 shows which components must be removed, and which connections are to be made.

That concludes the modification work, and only leaves preset P1 to be adjusted, which requires the use of the new GAL programmer software (ver-

sion 6.65 or later). Once you have the program running on your PC, type a colon (:) followed by a carriage return. Next, measure the voltage at pin 2 of the ZIF socket, and adjust P1 until you measure 16.5 V.

Finally, if you foresee programming GAL6001's, it may be necessary to replace the 7805 on the main board by a low-drop regulator such as the L4941BV or the L4940V5. This prevents thermal overloading of the regulator, which would cause the supply voltage to drop below about 4.75 V. In

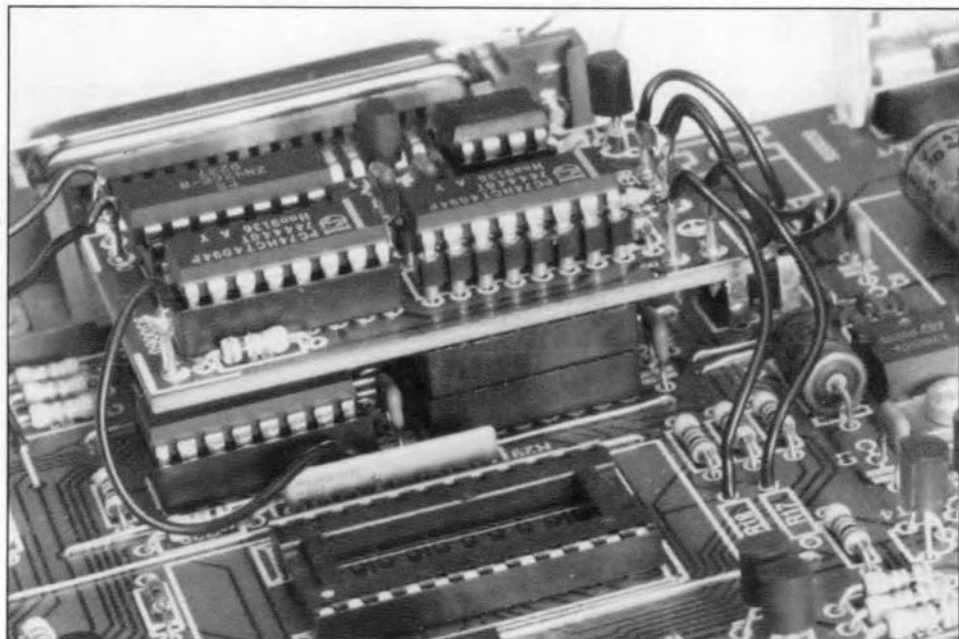


Fig. 5. Prototype of the extension board, plugged into the socket for IC5 on the main board.

some cases, this is harmful for the GAL6001.

## New software

The new features of the GAL programmer call for revisions to the existing control software. From the publication date of this article, the new version (6.65) of the GAL programmer software is supplied as Readers Services item 1701, which includes National Semiconductors's Opal Jr. demonstration software. Those of you who already have Opal Jr. may order the updated GAL programmer software only as item 1881 (one disk).

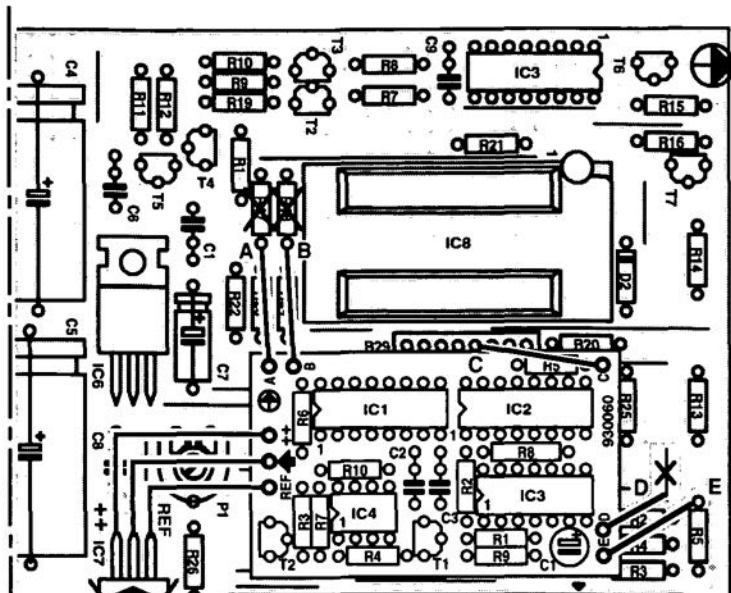
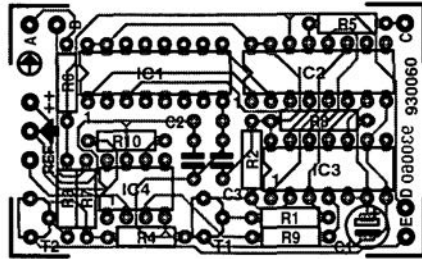
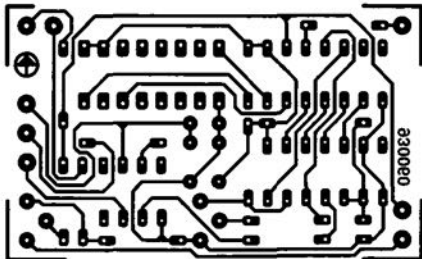
Finally, the new GAL programmer software includes a modified configuration file, called GAL665.CFG. This file, and the associated comment, is shown in Fig. 6. ■

```
GAL665.cfg
{license number}
{user number}
$3bc Address of Centronics port for GAL data exchange
1 GAL extension board no=0 yes=1
1 Change PES (program counter) no=0 yes=1
0 Switch for general RESET (EPROM, PROM, GAL) no=0 yes=1
1 Check if GAL hardware accessible no=0 yes=1
0 Select set security bit at power-up no=0 yes=1
1 Basic GAL type selection (16V8=1, 20V8=2, 16V8A=3, 20V8A=4,
75 beep length in ms 20V8A/B=4, 22V10=5, 6001=6, 20RA10=7)
2000 error beep frequency in Hz
2000 error display time in ms
1 Background colour Text (blue)
7 Foreground colour Text (bright grey)
5 Background colour Error reports (magenta)
7 Foreground colour Error reports (bright grey)
5 Background colour Letters (magenta)
15 Foreground colour Figures (white)
7 Background colour Selection window (bright grey)
1 Foreground colour Selection window (blue)
5 Background colour Selection bar (magenta)
14 Foreground colour Selection bar (yellow)
4 Background colour Changed cells (red)
7 Foreground colour Changed cells (bright grey)
5 Top of paper margin (in lines) (printing)
8 Left margin (printing)
```

Fig. 6. GAL programmer version 6.65 configuration file listing.

### Reference:

1. GAL programmer. *Elektor Electronics* May 1992.





# GAL PROGRAMMER SOFTWARE FOR AMIGA

SOFTWARE to control the GAL programmer is now also available for the Amiga series of computers. The Amiga software consists of two programs, AmiGAL and AmiBURN, with associated (extensive) documentation files that can be printed from disk. The disk also contains an installation instruction file.

AmiGAL is a GAL logic function editor, while AmiBURN is the actual programming software. Interestingly, AmiGAL is capable of generating JEDEC files, and has a built-in Minterms (minimal terms) generator that can help you reduce complex logic equations into a form suitable for implementation with the aid of GAL cells. AmiBURN reads the files produced by AmiGAL (or any other program capable of outputting JEDEC format files), and sets up the programming conditions required for the selected GAL. Functions like making master GALs, actuating the read protection in a GAL, device copying, producing cell hard copies, and much more, are available.

AmiGAL and AmiBURN are fully menu-driven, and make full use of the Amiga's graphics power. They can be run on all types of Amiga with 512 KBytes of memory or more. Before running the software, a small hard-



ware modification is required: pins 10 and 11 of the Centronics connector must be interconnected. Fortunately, this modification still allows the programmer to be used with a PC. The

Amiga GAL programmer software may be ordered through our Readers Services as item **1841** (see page 70). ■

# DIGITAL FREQUENCY READOUT FOR VHF/UHF RECEIVER

g260014 - IA

The wideband AM/FM receiver<sup>1</sup> described last month is not complete without a dial that tells you the transmit frequency of the station you are listening to. Such a tuning dial is described here — it takes the form of a sensitive 4-digit frequency meter with a preset option and a maximum input frequency of well over 30 MHz. Also suitable for general use in your workshop!

Design by L. Pijpers

THE circuit diagram of the frequency meter (Fig. 1) is not too complex, which is mainly by virtue of the use of an integrated counter/display driver Type ICM72117AIP1 from Harris Semiconductor. The display circuit is shown separately in Fig. 2.

The function of the ICM72117AIP1 is changed from a counter only into a frequency meter by IC5 and IC6d. The timebase consists of a crystal oscillator, X1-IC2, and a divider chain, IC2, IC3 and IC5. The input signal arrives at divider IC4 via a transistor preamplifier, T1. The digitized and scaled down input signal is applied to the counter IC input (pin 8) via gate IC6d, which functions as an electronic switch. IC6d is enabled during the gate time (measurement period) by pin 12 of IC5. Diodes D1-D16 serve to give to the counter a certain preset value — this will be reverted to below.

The time base pulse that controls the closing of IC6d must be accurately

times to ensure the correct gate time for the counter. The timing diagram of the timebase generator, IC5, is shown in Fig. 3. The numbers 0-9 at the left of the diagram represent the Q outputs of IC5. As indicated, these outputs go high successively on each pulse applied to the clock (CLK) input. The CO (carry out) output of IC5 is high when one of the outputs Q0-Q4 is high also. The CO output is low during the rest of the time, i.e., when one of the outputs Q5-Q9 is high. This means that the CO output supplies a symmetrical rectangular signal whose frequency equals  $\frac{1}{10}$ th that of the input clock signal. When the CO output of IC5 is high, IC6d is enabled, so that the count pulses arriving via T1 and IC4 are fed to the count (CNT) input of IC1. The number of pulses counted during the gate time is stored in a 4-digit counter contained in IC1.

When the gate time has elapsed, the count value is fed to the 4-digit LED

display. This happens when output Q5 of IC5 goes high, whereupon IC6a supplies a 'low' to the store input of IC1.

The counter memory is cleared (reset to zero) at the start of every count cycle by a logic 'high' on Q7 of IC5, which is fed to the RESET\ input via inverter IC6b. The counter preset value defined with the aid of diodes D1-D16 is loaded into the counter when output Q8 of IC5 pulls the 'load counter' (LC) input of IC1 logic 'high'.

The input of the frequency meter is connected to prescaler output 'F' or 'G' of the Philips TV tuner in the VHF/UHF receiver. To refresh your memory, this tuner output supplies the local oscillator (LO) frequency divided by 256. The signal level is about  $1 V_{pp}$ , which is too small to drive the digital frequency meter directly. Furthermore, the signal edges are not steep enough. These problems are resolved by the circuit around transistor T1, which acts as a preamplifier and signal shaper that turns the prescaler output signal into a neat rectangular wave with a level of  $5 V_{pp}$ , suitable for driving the clock input of counter IC4.

IC4 divides its input signal by  $2^7$ , which gives a total LO frequency scale factor of  $2^{15}$  ( $2^8 \times 2^7$ ). This means that the highest frequency at pin 13 of IC6d is about 30 kHz.

To obtain a readout in megahertz ( $10^6$  Hz), a timebase of  $1 \times 10^{-6}$  s is required, which means that the period of the gate signal is  $2 \times 10^{-6}$  s, or 0.5 MHz. This is achieved with the aid of dividers contained in IC2, IC3a and IC3b, which scale the 8-MHz clock signal generated by the oscillator in IC2 down by a factor  $2^{19}$  ( $2^3 \times 2^{16}$ ). Note, however, that the timebase signal is divided by 10 in IC5 before it is available at the CO output. Although this results in a display reading that is ten times too high, it increases the counter accuracy, and is simple to correct visually by lighting the decimal point on



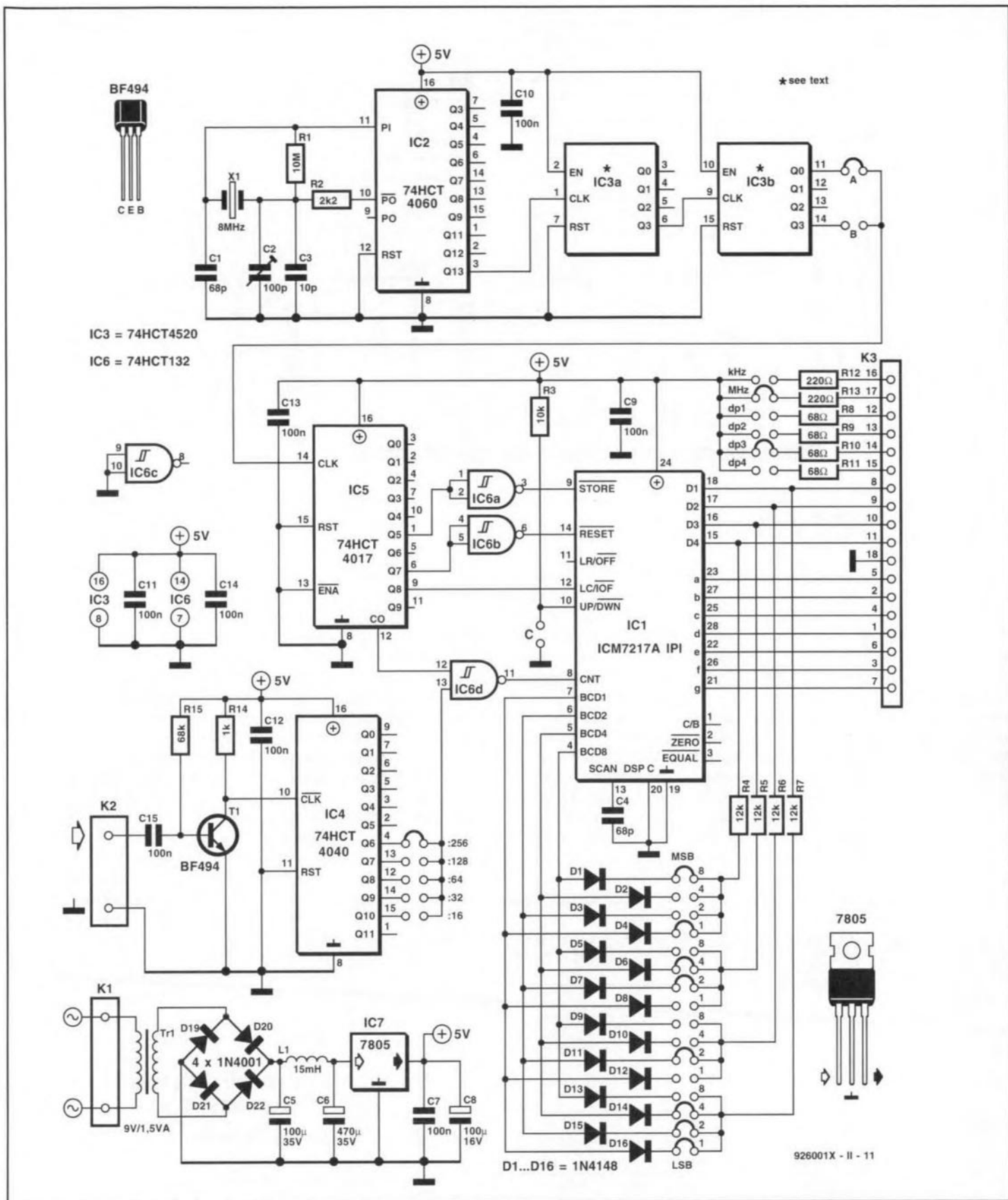


Fig. 1. Circuit diagram of the counter/power supply section. Diodes D1 through D16 serve to program a frequency off-set.

display LD3 — a simple solution, achieved by fitting jumper JP3.

**Preset**

When all jumpers are fitted as indicated in the circuit diagram, the frequency meter will indicate the frequency (in MHz) received on the

VHF/UHF receiver. To enable the frequency meter to display the frequency of the received signal rather than that of the local oscillator, it is programmed with an off-set of 37.3 MHz. In other words, the counter's preset must be used to subtract 37.3 from the frequency applied to its input. In

practice, this is achieved by loading a preset value, which causes the counter to start at a value other than 0. The preset value has to be set separately, with the aid of diodes, for each display digit:

LD1 (MSD): D13-D16

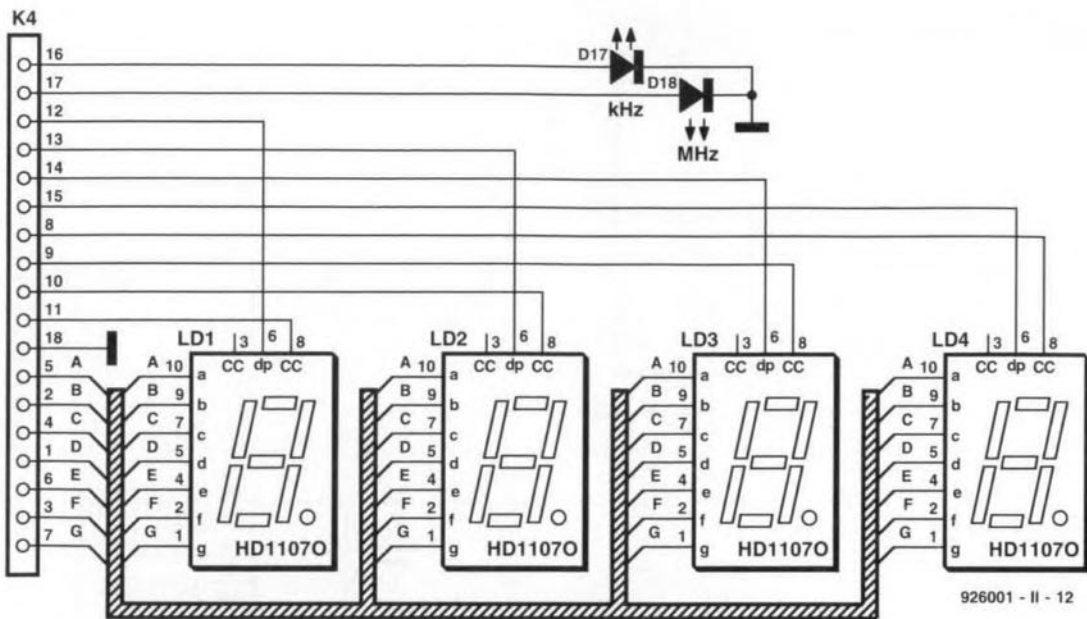


Fig. 2. Circuit diagram of the display section.

LD2	D9-D12
LD3	D5-D8
LD4 (LSD)	D1-D4

Although the four diodes associated with each digit allow a maximum preset of  $2^4=16$ , in practice, only the values 0 through 9 will be useful. If no jumper is fitted for a certain digit, this results in a '0', or 'no off-set'. The digit preset value is binary coded. Examples: a '3' is programmed by fitting jumpers 1 and 2, a '4' by fitting jumper 3 only, and a '7' by fitting jumpers 4, 2 and 1. Programming a

certain preset means that you have to fit the correct jumper combination for each preset. While this is straightforward with positive presets, negative presets, as required for the VHF/UHF receiver, call for a simple calculation. The instruction is simple; starting from four zeros on the display, put a '1' ahead of them (for borrowing), subtract the off-set frequency, and program the result with the aid of the diodes. So, for a LO off-set of 37.3 MHz ('373' without the decimal point), the preset value becomes

$$10000 - 373 = 9627,$$

which is programmed by fitting the preset jumpers as indicated in the circuit diagram, Fig. 1. The other jumpers are also in the positions as required for the VHF/UHF receiver: dp3 for the decimal point on LD3, the 'MHz' jumper, jumper 'A' with IC3b to set the correct timebase, and the '256' jumper with IC4 to match the +256 prescaler in the VHF/UHF tuner. The other jumpers are for tuners that have different prescaling factors.

Jumper 'C' defines the count direction (up or down). For the VHF/UHF receiver, the readout should increase with a higher LO frequency. This means that the counter must count 'UP', hence jumper 'C' must not be fitted. The 'DOWN' mode is used with receivers whose intermediate frequency is higher than the signal frequency and the local oscillator frequency.

### General-purpose frequency meter

As already mentioned, the present circuit is perfect for use as a general purpose frequency meter. Since this function does not require a counter off-set, none of the diodes D1-D16 must be fitted. Also, IC3 (a dual binary counter/divider Type 74HCT4520) must be replaced with a dual decimal counter Type 74HCT4518. No modifications are required to the printed circuit board, which is suitable for both ICs. The 4518 is virtually identical to the 4520, only the signal at output Q3 is divided by 10 rather than by 16.

For frequencies from 0.01 MHz to

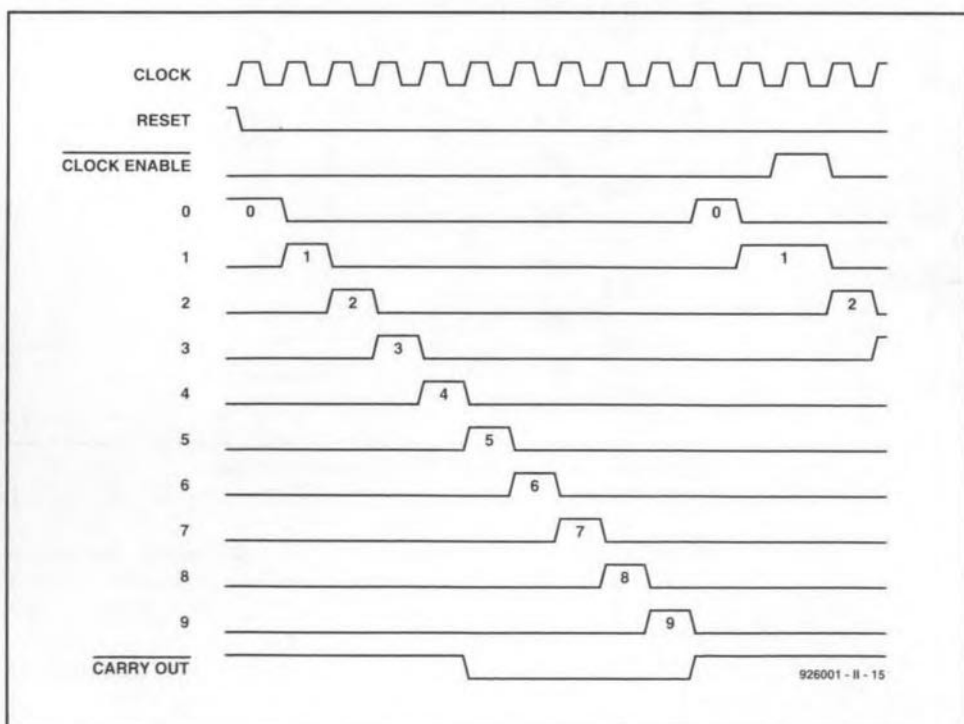


Fig. 3. Timing diagram of the counter control signals.

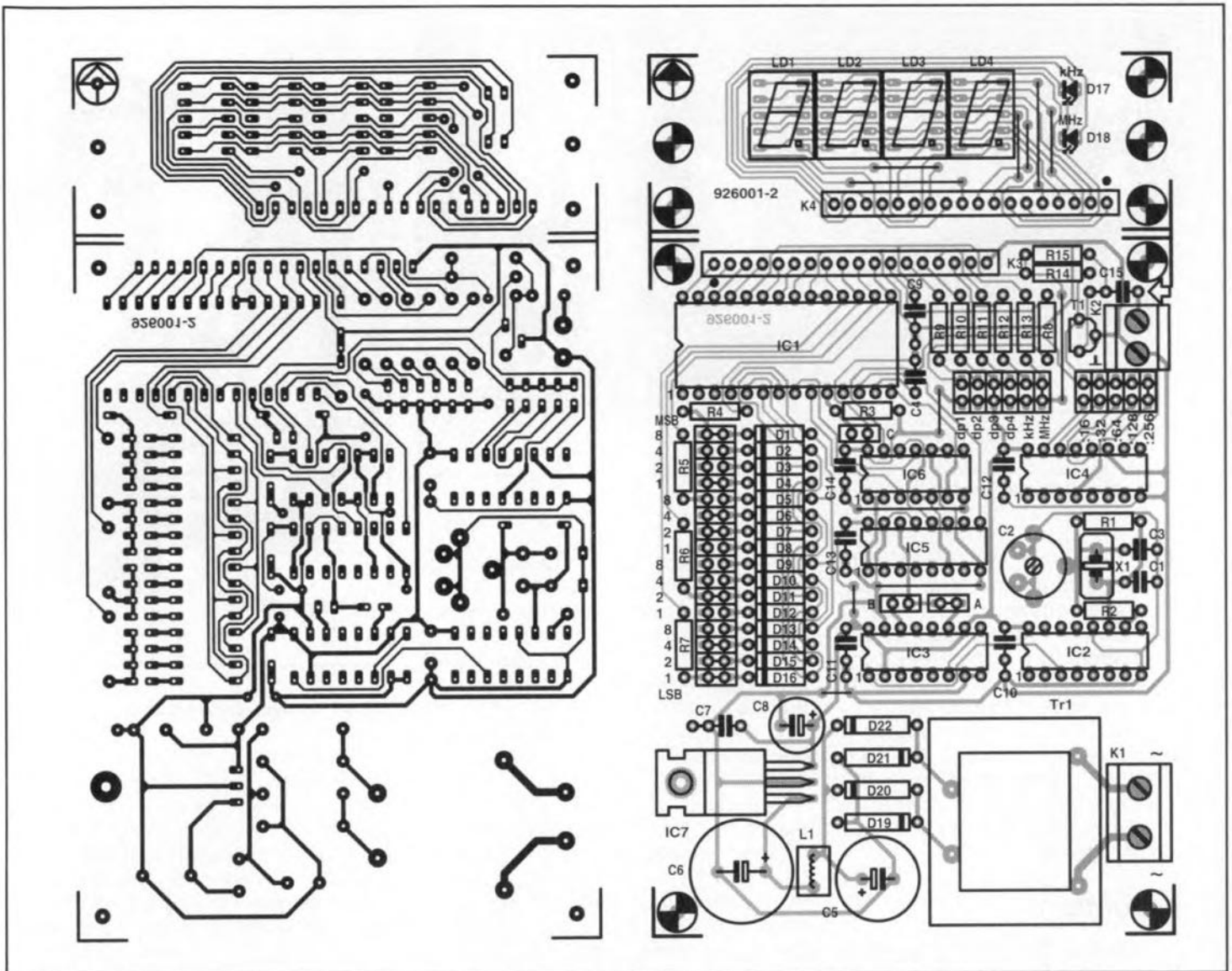


Fig. 4. Track layout (mirror image) and component mounting plan of the printed circuit board designed for the frequency meter.

### COMPONENTS LIST

**Resistors:**

1	10MΩ	R1
1	2kΩ	R2
1	10kΩ	R3
4	12kΩ	R4-R7
4	68Ω	R8-R11
2	220Ω	R12;R13
1	1kΩ	R14
1	68kΩ	R15

**Capacitors:**

2	68pF	C1;C4
1	100pF trimmer	C2
1	10pF	C3
1	100μF 35V radial	C5
1	470μF 35V radial	C6
8	100nF	C7;C9-C15
1	100μF 16V radial	C8

**Inductors:**

1	15mH	L1
---	------	----

**Semiconductors:**

16	1N4148	D1-D16
2	LED, red, 3mm	D17;D18

4	1N4001	D19-D22
1	BF494	T1
1	ICM7217A-IP1*	IC1
1	74HCT4060	IC2
1	74HCT4520	
	(see text)	IC3
1	74HCT4040	IC4
1	74HCT4017	IC5
1	74HCT132	IC6
1	7805	IC7
4	HD11070**	LD1-LD4

**Miscellaneous:**

1	8-MHz quartz crystal	X1
1	9V/1.5VA PCB mount mains transformer, e.g., Monacor VTR1109	Tr1
1	double-pole mains switch	S1
1	2-way PCB terminal block, pitch 7.5mm	K1
1	2-way PCB terminal block, pitch 5mm	K2
1	18-way SIL socket	K3
1	18-way SIL header, angled	K4
1	Metal enclosure 80×150×132mm,	

e.g., Telet\*\*\* LC740  
 1 Printed circuit board 926001-2 (see page 70)

\* Electromail (0536) 204555; fax (0536) 405555.

\*\* ElectroValue (0784) 433603; fax: (0784) 435216.

\*\*\* C-1 Electronics fax (+31) 45 241877.

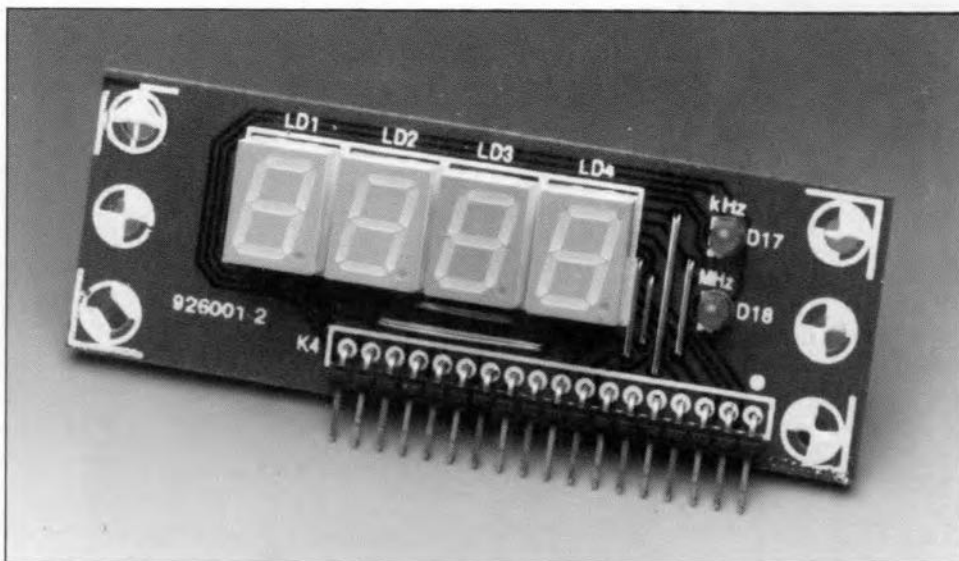


Fig. 5. Completed display board.

30 MHz, fit jumper 'A' with IC3, the ':16' jumper with IC4, the 'dp2' jumper, and the 'MHz' jumper. Depending on the maximum frequency that T1 and IC4 can handle, the highest input frequency that can be measured may be considerably higher than 30 MHz.

If you want to use the counter to measure relatively low frequencies (1 to 9999 kHz), fit jumper 'B' with IC3, and jumper ':32' with IC4. Also fit either the 'dp4' and 'kHz', or the 'dp1' and 'MHz' jumpers.

## Construction

The printed circuit board designed for the frequency meter is available ready made through our Readers Services (see page 70). Those of you who have the means to make their own PCBs will find the artwork in Fig. 4. Before you start fitting parts, cut the board to separate the counter/supply section (Fig. 6) from the display section (Fig. 5).

Start the construction of the main board with the resistors, capacitors, the transformer, the crystal and the solder pins. Be sure not to damage the plastic foil trimmer (C2, near the crystal) by overheating its pins. The voltage regulator, IC7, does not need a heat-sink, and may be bolted straight on to the board. As shown by the photographs of the prototype, the display board is connected to the main board with the aid of an angled pin header and a mating socket.

The completed counter/supply board is mounted on to the bottom cover of the enclosure using PCB spacers, bolts and nuts. Great attention should be paid to the insulation of the parts, wires and terminals that are at mains potential. Also be sure to use a properly rated dual-pole mains switch.

The prototype has two 50-Ω BNC input sockets — one on the front, and

one of the rear panel. The one on the rear panel serves to connect the instrument to the VHF/UHF receiver, while the one on the front is for 'general use'. The two coax input cables are simply soldered in parallel with K2 (braids to ground; cores to C15).

If the frequency readout is used for one application only, the jumpers may be replaced by wire links. Alternatively, the jumpers may be replaced by DIP switch blocks connected to short lengths of flatcable. This allows you to switch quickly between two applications. The coax cable between the VHF/UHF receiver and the frequency meter should be kept as short as possible.

To prevent IC5 being damaged by static discharges, jumpers should not be removed or fitted with the circuit switched on. Also do not forget to discharge yourself (by touching the case) before touching any part of the circuit.

Adjusting C2 will hardly ever be required, since the error caused by a deviation from 8 MHz is negligible at a

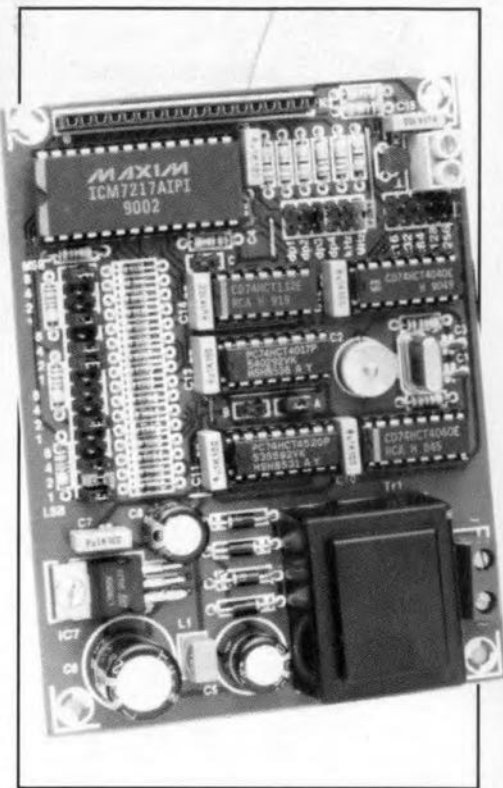


Fig. 6. Completed main board.

few kilohertz only. However, if you have the means to do so, feel free to adjust the trimmer for a clock frequency of 8 MHz exactly. Alternatively, tune the receiver to an accurately known frequency, and adjust C2 until the corresponding readout is obtained.

## Reference:

1. VHF/UHF receiver, *Elektor Electronics* May 1992.

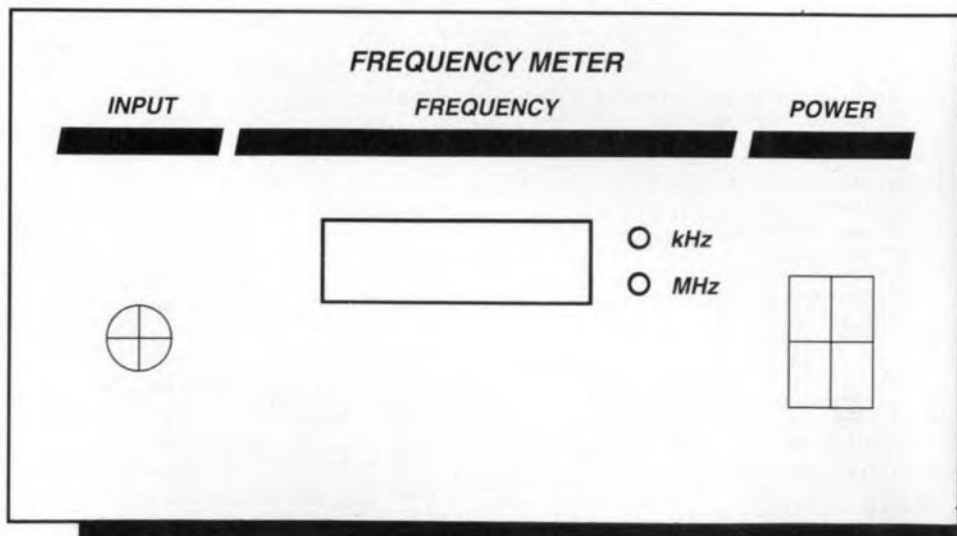


Fig. 7. Suggested front panel layout.

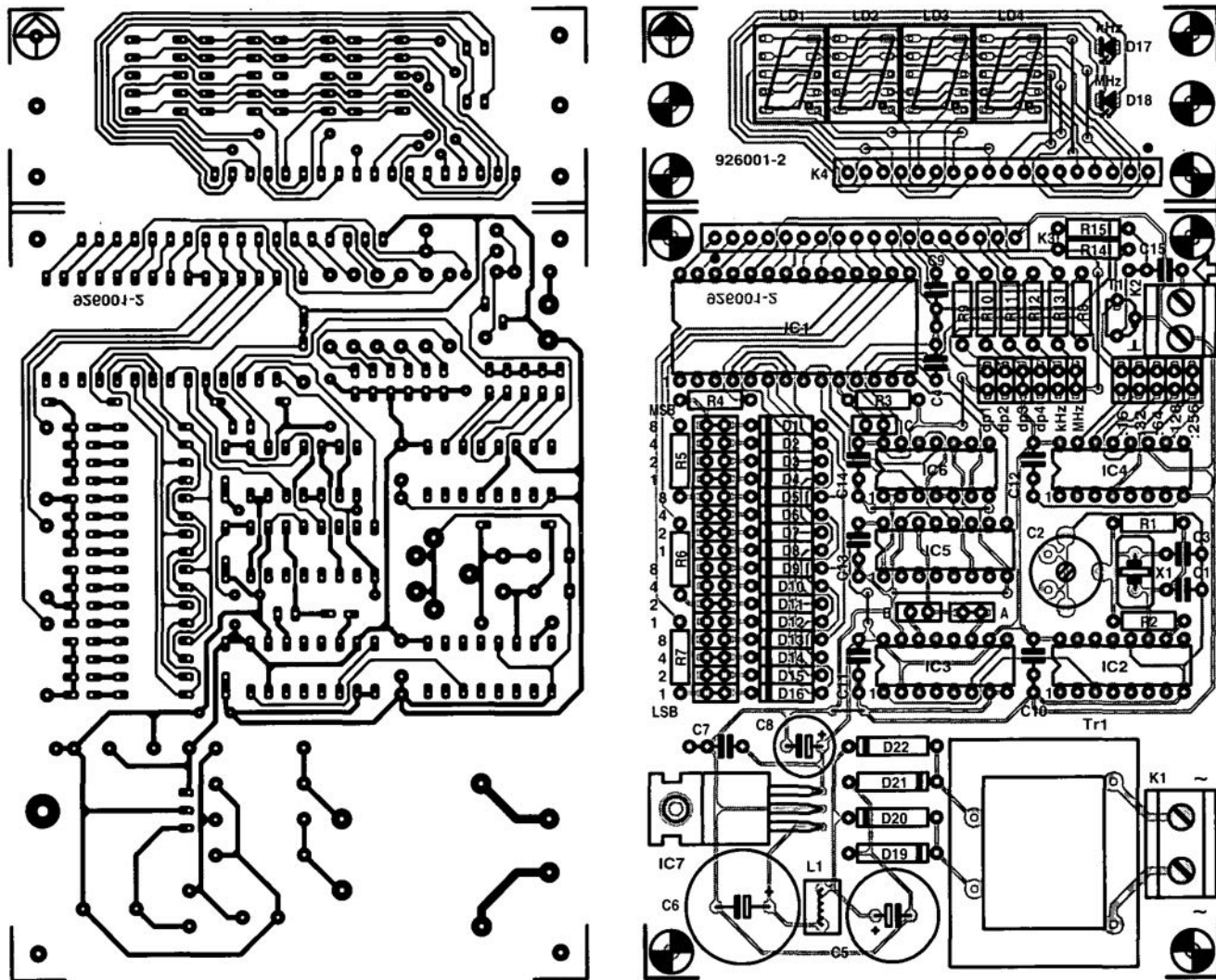


Fig. 4. Track layout (mirror image) and component mounting plan of the printed circuit board designed for the frequency meter.

# MAKING SENSE OF MEASUREMENTS (PART 2)

By Joseph J. Carr

In Part 1 of this two-part article we looked at the subject of measurement variation, and determined that most processes naturally vary according to the **normal distribution curve**, also known as the 'bell shaped' curve. We also discussed the ideas of precision and accuracy, and the different types of measurement (direct, indirect and null). In this final instalment we will discuss measurement errors and some of the arithmetic needed to overcome these difficulties. First, let us look at the various types of measurement error and their sources.

## Theoretical error

All measurements are based on some measurement theory that predicts how a value will behave when a certain measurement procedure is applied. The measurement theory is usually based on some theoretical model of the phenomenon being measured, i.e. an intellectual construct that tells us something of how that phenomenon works. It is often the case that the theoretical model is valid only over a specified range of the phenomenon. For example, nonlinear phenomena that have a quadratic, cubic or exponential function can be treated as a straight line linear function over small, selected, sections of the range. Electronic sensor outputs often fall into this class.

Alternatively, the actual phenomenon may be terribly complex, or even chaotic, under the right conditions, so the model is therefore simplified for many practical measurements. An equation that is used as the basis for a measurement theory may be only a first order approximation of the actual situation. For example, consider the **mean arterial pressure** (MAP) that is often measured in clinical medicine and medical sciences research situations. The MAP approximation equation used by clinicians is:

$$\bar{P} = \text{Diastolic} + \frac{\text{Systolic} - \text{Diastolic}}{3} \quad [3]$$

This equation is really only an approximation (and holds true mostly for well people, not some sick people on whom it is applied) of the equation that expresses the mathematical integral of the blood pressure over a cardiac cycle. That is, the time average of the arterial pressure. The actual expression is written in the

notation of calculus, which is beyond the math abilities of many of the people who use the clinical version above:

$$\bar{P} = \frac{1}{T} \int P dt. \quad [4]$$

The approximation works well, but is subject to greater error owing to the theoretical simplification of the first equation. Incidentally, if you work your way through most of undergraduate and all of graduate school repairing medical and scientific instruments, like I did, then you will understand that it does no good to tell an irate Intensive Care Unit (ICU) nurse that the MAP reading on an instrument is correct when it differs from her calculated value. The actual measured MAP is based on the integral calculus equation (an electronic Miller integrator circuit is used), while her calculated value is based on the simplification. Because some patients lack a considerable part of the time dependent pressure curve (which is sometimes why they are in the hospital), the actual MAP will be lower than the approximation value. Sometimes heat, fire and smoke flow from the tender, loving care hands of ICU nurses!

## Static errors

Static errors include a number of different sub-classes that are all related in that they are always present even in unchanging systems (thus are not dynamic errors). These errors are not functions of the time or frequency variation.

**Reading errors.** These errors result from misreading the display output of the sensor system. An analog meter uses a pointer to indicate the measured value. If the pointer is read at an angle other than straight on, a **parallax reading error** occurs. Another reading error is the **interpolation error**, i.e., an error made in guessing the correct value between two calibrated marks on the meter scale (Fig. 8). Still another reading error occurs if the pointer on a meter scale is too broad, and covers several marks at once.

A related error seen in digital readouts is the **last digit bobble** error. On digital displays, it is often the case that the least significant digit on the display will flip back and forth between two val-

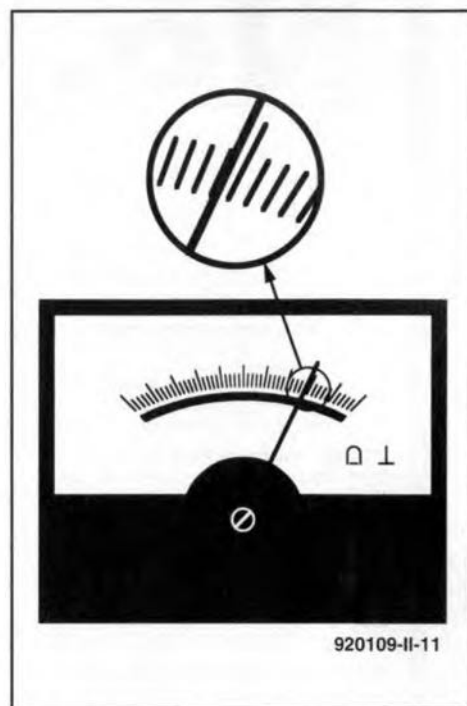


Fig. 8. Analogue meter pointers can suffer both parallax and interpolation of reading errors.

ues. For example, a digital voltmeter might read '12.24' and '12.25' alternately, depending on when you looked at it, despite the fact that absolutely no change occurred in the voltage being measured. This phenomenon occurs when the actual voltage is between the two indicated voltages. Error and uncertainty in the system will make a voltage close to 12.245 V bobble back and forth between the two permissible output states (12.24 and 12.25) on the meter. An example where 'bobble' is of significant concern is the case where some action is taken when a value changes above or below a certain amount — and the digital display bobbles above and below the critical threshold.

**Environmental errors.** All sensors and instruments operate in an environment, which sometimes affect the output states. Factors such as temperature (perhaps the most common error producing agent), pressure, electromagnetic fields, and radiation must be considered in some electronic sensor systems.

**Characteristic errors.** These static errors are still left after reading errors and environmental errors are accounted.



When the environment is well within the allowable limits and is unchanging, when there is no reading error, there will be a residual error remaining that is a function of the measurement instrument or process itself. Errors found under this category include zero offset error, gain error, processing error, linearity error, hysteresis error, repeatability error, resolution error and so forth.

Also included in the characteristic error are any design or manufacturing deficiencies that lead to error. Not all of the 'ticks' on the ruler are truly 1.0000 inch apart at all points along the ruler. While it is hoped that the errors are random, so that the overall error is small, there is always the possibility of a distinct bias or error trend in any measurement device.

For digital systems one must add to the resolution error a **quantization error** that emerges from the fact that the output data can only take on certain discrete values. For example, an 8-bit analogue-to-digital converter allows 256 different states, so a 0 to 10 V range is broken into 256 discrete values in 39.06 mV steps. A potential that is between two of these steps is assigned to one or the other according to the rounding protocol used in the measurement process. An example is the weight sensor that outputs 8.540 V, on a 10-V scale, to represent a certain weight. The actual 8-bit digitized value may represent 8.502, 8.541, or 8.580 V because of the ±0.039 V quantization error.

**Dynamic errors**

Dynamic errors arise when the measurement is changing or in motion during the measurement process. Examples of dynamic errors include the inertia of mechanical indicating devices (such as analog meters) when measuring rapidly changing parameters. There are a number of limitations in electronic instrumentation that fall into this category, as you will find out by consulting any competent book on the subject.

**Instrument insertion error**

A fundamental rule of making engineering and scientific measurements is that **the measurement process should not significantly alter the phenomenon being measured**. Otherwise, the measurement is actually the altered situation, not the original situation that is of true interest. Examples of this error are found in many places. One such is the fact that pressure sensors tend to add volume to the system being measured, so slightly reduce the pressure indicated below the actual pressure. Similarly, a flow meter might add length, a different pipe diameter, or turbulence to a system being measured. A voltmeter with a low

impedance of its own could alter resistance ratios in an electrical circuit and produce a false reading (Fig. 9). This problem is seen when using cheap analogue volt-ohm-milliammeters (VOMs), that have a low sensitivity hence a low impedance ( $R_m$  in Fig. 9), to measure a voltage in a circuit. The meter resistance  $R_m$  is effectively shunted across the circuit resistance across which the voltage appears.

Instrument insertion errors can usually be minimized by good instrument design and good practices. No measurement device has zero effect on the system being measured, but one can reduce the error to a very small value by appropriate selection of methods and devices.

**Dealing with measurement errors**

Measurement error can be minimized through several methods, some of which are lumped together under the rubric 'procedure' and others under the legend 'statistics'.

Under 'procedure' one can find methods that will reduce, or even minimize, error contributions to the final result. For example, in an electrical circuit, use a voltmeter that has an extremely high input impedance compared with circuit resistances. The idea is to use an instrument (whether a voltmeter, a pressure meter or whatever) that least disturbs the thing being measured.

A way to reduce total error is to use several different instruments to measure the same parameter. In Fig. 10 we see an example where the current flow in a circuit is being measured by three different ammeters: M1, M2 and M3. Each of these instruments will produce a result that contains an error term de-correlated

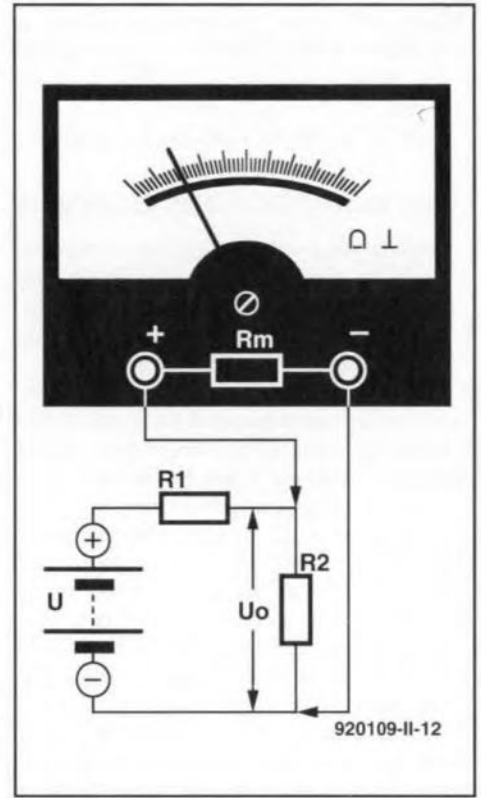


Fig. 9. If a low-impedance VOM is used to measure voltages in a circuit, it can load the circuit and produce an erroneous reading. This is an example of an instrument insertion error.

from the error of the others and not biased (unless, by selecting three identical model meters we inherit the characteristic error of that type of instrument). We can estimate the correct value of the current flow rate by taking the average of the three:

$$M_0 = \frac{M_1 + M_2 + M_3}{3} \tag{5}$$

One must be careful to either randomize

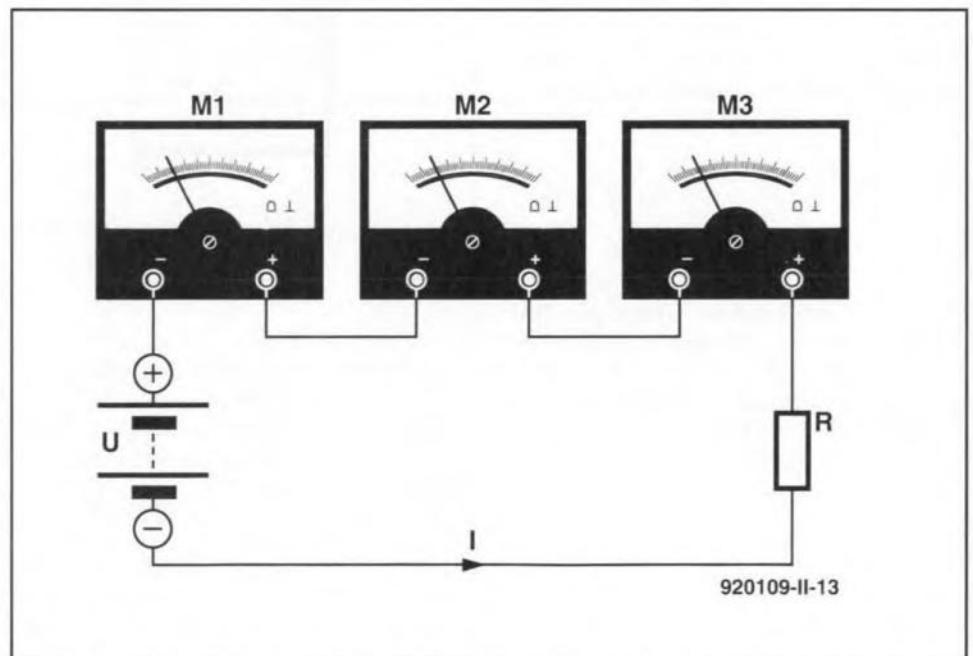


Fig. 10. Use of multiple instruments, and then averaging the results, can reduce error.

the system in cases where the sensor or instruments used tend to have large error terms biased in one direction, or calibrate the average error so that it may be subtracted from of the final result.

## Error contributions analysis

An **error analysis** should be performed in order to identify and quantify all contributing sources of error in the system. A determination is then made regarding the randomness of those errors, and a **worst case analysis** is made. Under the worst case, one assumes that all of the component errors are biased in a single direction and are maximized. We then attempt to determine the consequences (to our purpose for making the measurement) if these errors line up in that manner, even if such an alignment is improbable. The worst case analysis should be done on both the positive and negative side of the nominal value. An **error budget** is then created to allocate an allowable error to each individual component of the measurement system in order to ensure that the overall error is not too high for the intended use of the system.

If errors are independent of each other, and are random rather than biased, and if they are of the same order of magnitude, then one can find the **root of the sum of the squares** (RSS) value of the errors, and use it as a composite error term in planning a measurement system. The RSS error is:

$$\epsilon_{\text{rms}} = \sqrt{\sum \epsilon_i^2} \quad [6]$$

The RSS error term is a reasonable estimate or approximation of the combined effects of the individual error components.

A collection of repetitive measurements of a phenomenon can be considered a sampled population, and treated as such. If we take  $N$  measurements ( $M_1$  through  $M_n$ ) of the same parameter, and then average them we get:

$$\bar{M} = \frac{M_1 + M_2 + M_3 + \dots + M_n}{N} \quad [7]$$

The average value obtained in Eq. [7] is the **mean arithmetic average**. This value is usually reported as the correct value for the measurement, but when taken alone does not address the issue of error. For this purpose we add a fudge factor by quoting the **standard error** of the mean, or

$$\sigma_m = \frac{\sigma_m}{\sqrt{N}} \quad [8]$$

which is reported in the result as:

$$M = \bar{M} \pm \sigma_m \quad [9]$$

Any measurement contains error, and this procedure allows us to estimate that error, and thereby understand the limitations of that particular measurement.

## Operational definitions in measurement

Some measurement procedures suggest themselves immediately from the nature of the phenomenon being measured. In other cases, however, there is a degree of ambiguity in the process, and it must be overcome. Sometimes the ambiguity results from the fact that there are many different ways to define the phenomenon, or perhaps no way is established. In cases such as these, one might wish to resort to an **operational definition**, i.e., a procedure that will produce consistent results from measurement to measurement, or when measurements are taken by different experimenters.

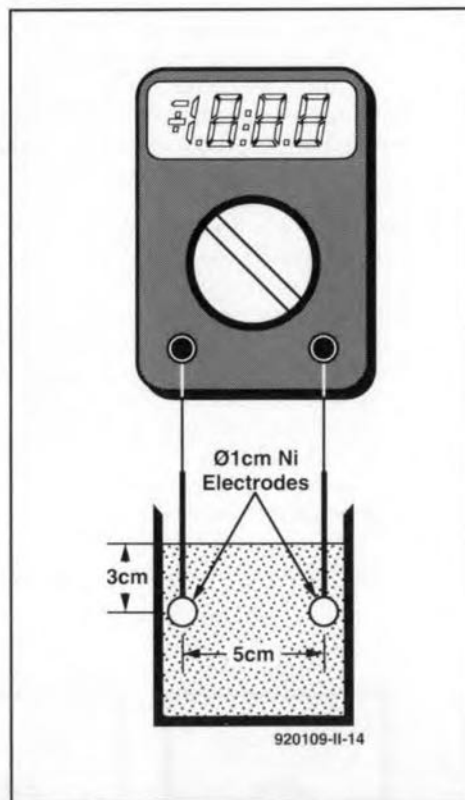


Fig. 11. Example of an 'operational definition'.

An operational definition, therefore, is a procedure that must be followed, and specifies as many factors as are needed to control the measurement so that changes can be properly attributed only to the unknown variable. The need for operational definitions (as opposed to absolute) definitions arises from the fact that things are only rarely so neat and clean as to suggest their own natural definition; ambiguity reigns. By its very definition, the operational definition does

not ask 'true' or 'false' questions, but rather it asks 'what happens under given sets of assumptions or conditions'. What an operational definition can do for you, however, is to standardize a measurement in clear and precise way so that it remains consistent across numerous trials. Operational definitions are used extensively in science and technology. When widely accepted, or promulgated by a recognized authority, they are called **standards**.

An operational definition should embrace what is measurable quantitatively, or at least in non-subjective terms. For example, in measuring the 'saltiness' of saline solution (salt water), one might taste it and render a subjective judgement such as 'weak' or 'strong'. Alternatively, one can establish an operational definition that calls for you to measure the electrical resistance of the saline under certain specified conditions:

1. immerse two 1-cm diameter circular nickel electrodes, spaced 5 cm apart and facing each other, to a depth of 3 cm into a 500-ml beaker of the test solution.
2. Bring the solution to a temperature of 4 °C.
3. Measure the electrical resistance ( $R$ ) between the electrodes using a Snotz Model 1120 digital ohmmeter.
4. Find the conductance ( $G$ ) by taking the reciprocal of resistance ( $G = 1/R$ ).

You can probably come up with a better definition of the conductance of saline solution that works for some peculiar situation. Keep in mind that only rarely does a preferred definition suggest itself naturally.

The use of operational definitions results in both strengths and weaknesses. One weakness is that the definition might not be honed fine enough for the purpose at hand. Sociologists and psychologists often face this problem because of difficulties in dealing with non-linearities such as human emotions. But such problems also point to a strength. We must recognize that scientific truth is always tentative, so we must deal with uncertainties in experimentation. Sometimes, the band of uncertainty around a point of truth can be reduced by using several operational definitions in different tests of the same phenomenon. By taking different looks from different angles, we may get a more refined idea of what is actually happening.

When an operational definition becomes widely accepted, and is used throughout an industry, it may become part of a formal **standard** or test procedure. You may, for example, see a procedure listed as 'performed in accordance with NIST XXXX.XXX<sup>1</sup>' or 'ANSI Standard XXX'.<sup>2</sup> These notations mean that whoever made the measurement fol-

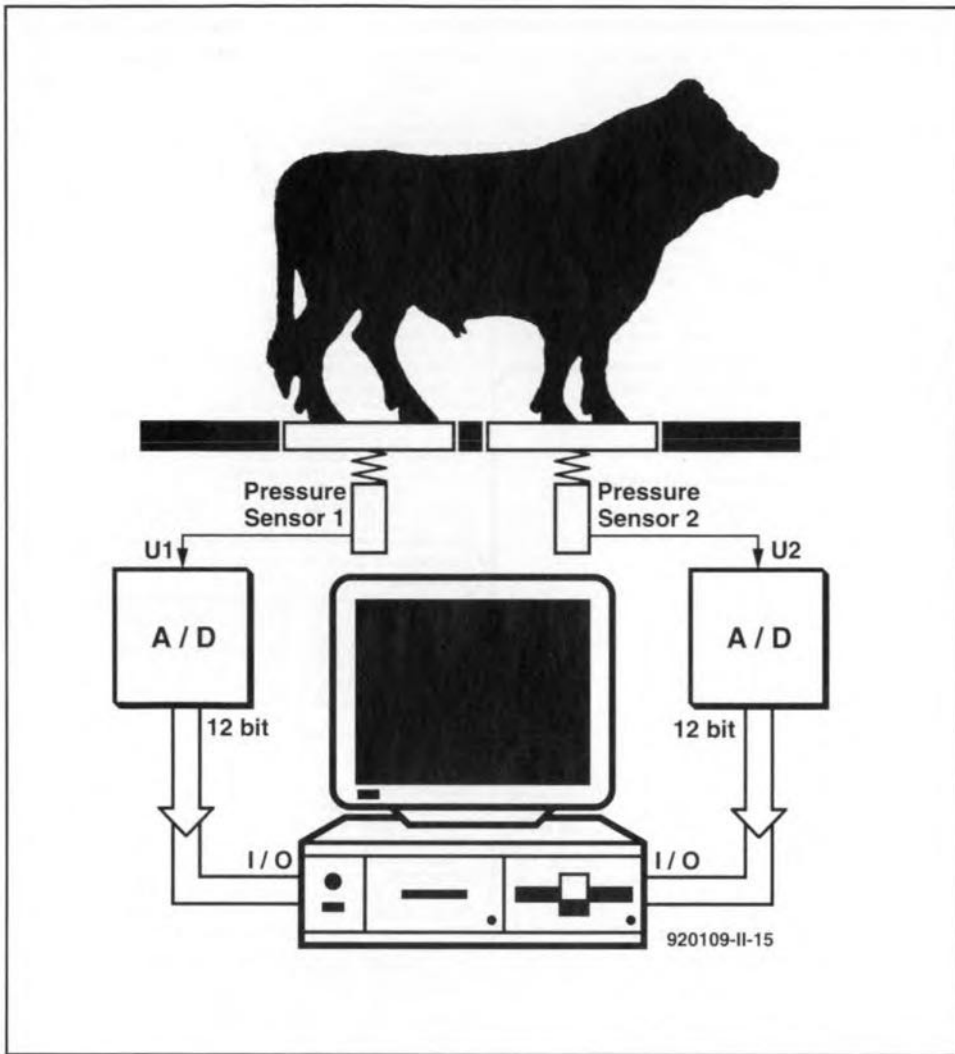


Fig. 12. Instrument for weighing a bull.

lowed one or another of a published standard.

### Weighing a cow

Now let us get back to the issue of weighing a cow on an electronic scale. The main problem is that the cow will not stand still long enough to make a static measurement. As a result, it is necessary to use statistical methods to weigh the animal. Figure 12 shows the cattle scale seen by my electronically literate political aide. The animal stands on two platforms, one for the front legs and another for the rear legs, that are each connected to an electronic pressure sensor. The voltage outputs of each sensor ( $U_1$  and  $U_2$ ) are each approximately equal to half the weight of the animal. Therefore, the sum of  $U_1$  and  $U_2$  is proportional to the total weight of the animal.

These voltages ( $U_1$  and  $U_2$ ) are converted to binary numbers by the analogue-to-digital (A-D) converters, and input to a desktop computer. Because very fast A-D converters are now available, it is possible to take several thousand samples of the two half weights in the ten to twenty seconds the animal is held on the scale. The average of each is taken, along with the error factor, and

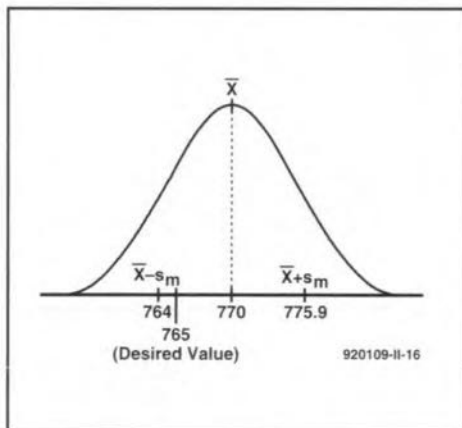


Fig. 13. Plot of oven test data showing error limits.

they are then added together. As long as the error factor is less than the desired resolution, the scale's reading is accepted.

Now let us take a look at another situation that involves ambiguous measurements.

### Did it pass the test?

An adhesives curing oven is supposed to have an equilibrium temperature of

765 °F after 10 minutes. A test technician inserted an electronic thermometer and a timer to take the temperature measurement after exactly ten minutes; the oven was allowed to cool back to room temperature between trials. She took 20 measurements and found the mean to be 770 °F with a standard deviation of 26.2. Did this oven pass the test? The situation is shown in Fig. 13 — the answer seems to be: yes. Why? Because the error term represented by the standard error of the mean (shown as  $\pm s_m$  in Fig. 13) encompasses the desired value of 765 despite the dispersion of the data. We can only claim that the test is failed if the desired value is outside these limits. ■

#### Notes:

1. NIST is the National Institute for Standards and Technology, formerly called National Bureau of Standards.
2. ANSI is the American National Standards Institute.

# 'SMARTWATCH' REAL-TIME CLOCK FOR 80C32 COMPUTER

A 'Smartwatch' real-time clock is described that provides a time/date indication and a stopwatch function on the *Elektor Electronics* 80C32 single-board computer<sup>1,2</sup>.

Design by W. Hackländer

DALLAS Semiconductor's 'Smartwatch' Type DS1216C is a real-time clock IC which is, unusually, housed in a 28-way IC socket. The device is pin compatible with 64-kBit and 256-kBit static CMOS RAMs, and is simply inserted between the RAM on the 80C32 computer and its socket. The 'intelligent socket' between the RAM and the processor contains a clock circuit, a Lithium battery and a power supply controller for the CMOS RAM. The Lithium battery contained in the DS1216C doubles as a RAM backup for the computer, which means that the existing 3.6-V battery and battery holder board may be removed from the board.

## Smartwatch intelligent socket

With the exception of pins 20 and 28, the 'intelligent socket' (Fig. 1) connects all RAM pins directly to the corre-

sponding PCB holes. The DS1216C may be used with all static RAMs organized as  $8\text{ k} \times 8$  or  $32\text{ k} \times 8$ . Its principal feature, the real-time clock, counts hundredths of a second, seconds, minutes, hours, days, months and years, and automatically updates the date information. The clock error is less than  $\pm 1$  minute per month, and the clock takes leap years into account. Both 12-hour (AM/PM) and 24-hour time indications are possible.

Communication with the clock starts with pattern recognition. This is achieved by sending 64 successive write cycles to port DQ0. The 64-bit datastream is compared with a fixed pattern (Fig. 2), which arranges the bits into eight bytes (groups of 8 bits). This results in a byte pattern as shown to the right in Fig. 2. The probability of an identical datastream intended for the RAM is smaller than 1 in 1019 instances. The 64-bit pattern is followed by 64 further read or write cycles to set

or read the clock. RAM access is disabled during these operations. Any write instruction to the RAM that actuates CE\ (chip enable) and OE\ (output enable) starts the pattern recognition operation by setting up a pointer to the first of the 64 bits in the comparison register. Obviously, the next 64 write operations that enable the CPU to access the clock end up in the RAM also. Consequently, one address in the RAM should be reserved for use as a kind of scratch pad, and the clock should be accessed via this address.

The pattern recognition that selects the clock is a sequential (bit-by-bit) operation. The DS1216C compares the first write instruction with bit 0 of the 64-bit pattern register. If the bits match, the pointer is increased to bit 1, and waits for the next instruction. This continues until all 64 bits have been compared, or the first mismatch occurs, when the pointer is 'frozen', and the clock ignores all further write instructions. If a read operation occurs during the pattern recognition, the comparison is terminated, and the pointer reset.

The clock is accessible when a sequence of 64 bits received via DQ0 matches the clock selection pattern, whereupon the next 64 bits can be read from, or written to, DQ0. This is

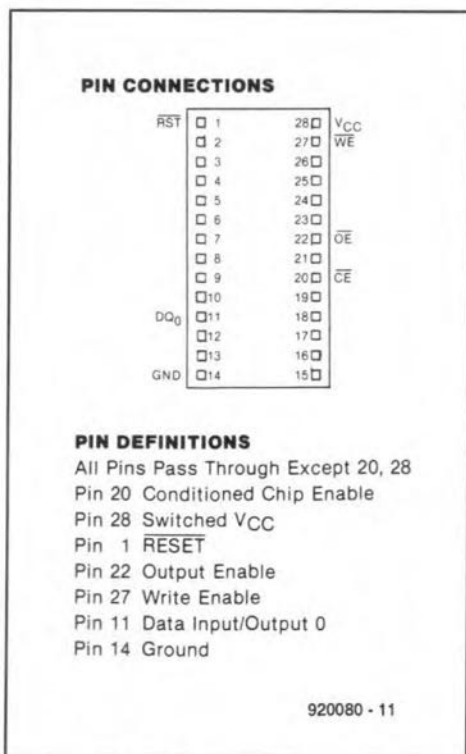


Fig. 1. DS1216C Smartwatch pin-out (courtesy Dallas Semiconductor).

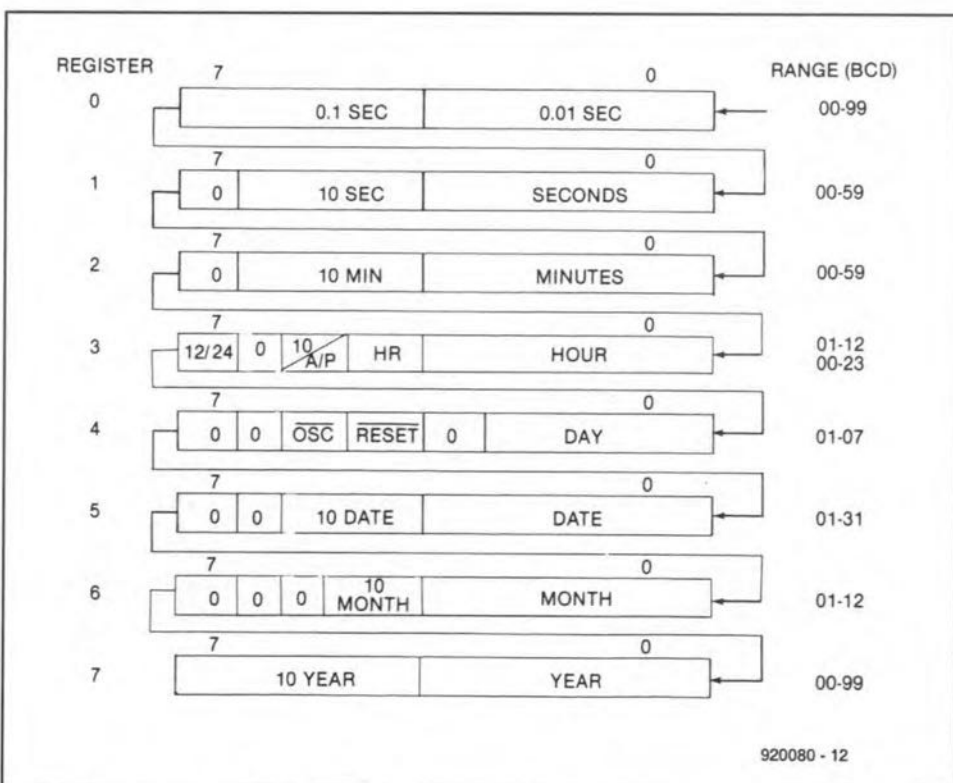


Fig. 2. Smartwatch register definition.

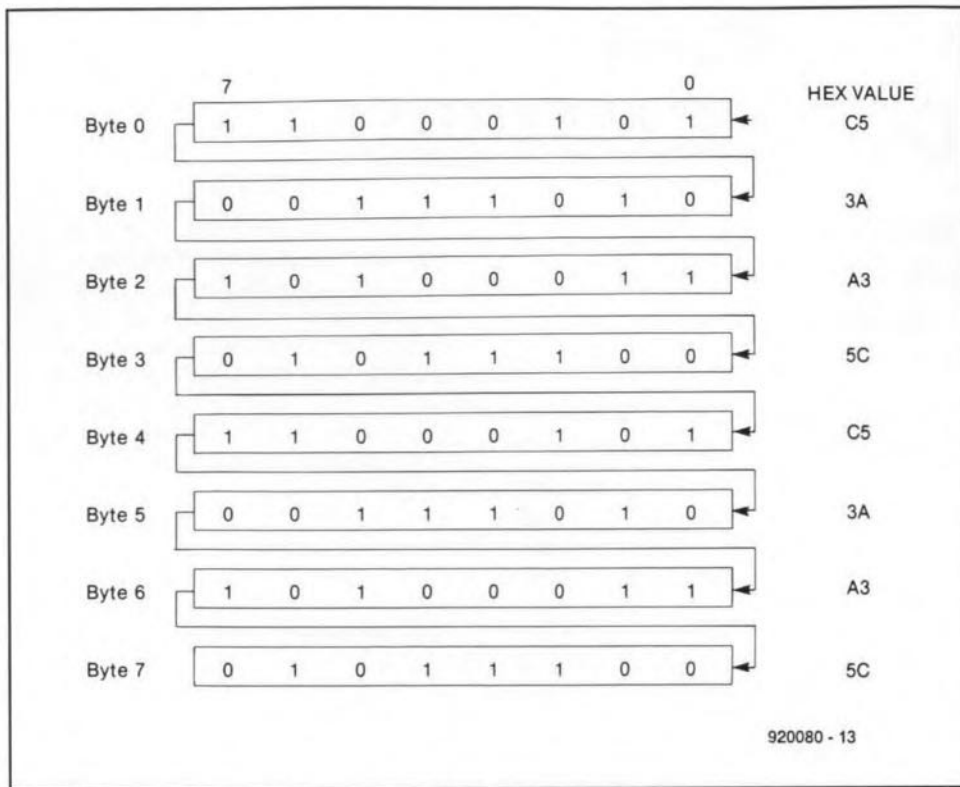


Fig. 3. Smartwatch comparison register definition.

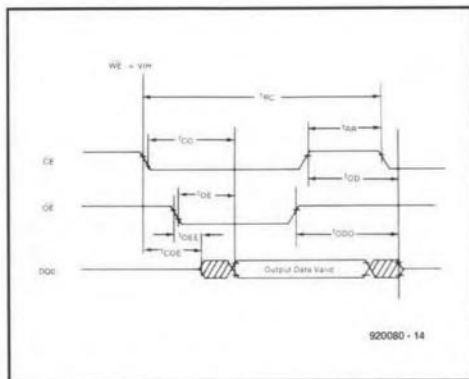


Fig. 4. Timing diagram — read cycle to Smartwatch.

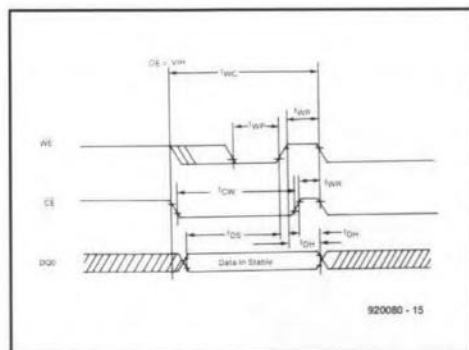


Fig. 5. Timing diagram — write cycle to Smartwatch.

achieved by pulling OE\ (read clock) or WE\ (set clock) low. The timing for read and write cycles is shown in Fig. 3. Instructions to addresses outside the RAM range may occur during the pattern recognition or the data exchange with the clock.

The time information is organized in

eight 8-bit registers (Fig. 4). These bits appear serially on port DQ0. Since it is not possible to write or read individual bits, data exchange between the CPU and the clock should always be organized in groups of eight bits at a time. The register data are BCD coded.

The internal organization of the clock registers is fairly simple: with the exception of register 4, all registers are divided into two 4-bit sections, each of which allows decimal numbers 0 through 9 to be represented. Some bits are fixed as a '0', and can not be changed into '1' by writing to the clock. An example is found in register 6a, which should only contain decimal '0' or '1'.

Registers 4a and 3a are exceptions. Bit 7 of the hours register (3) selects between 12-hour (AM/PM) and 24-hour time indication. A high in this bit location selects the 12-hour clock, when bit 5 is the AM/PM indicator. In 24-hour indication mode, bit 5 represents the second tens-of-hours bit (20-23 hours).

Finally, a word about the RESET and OSC bits, numbers 4 and 5, in the days register. Both control 'active low' functions. If bit 5 is programmed low, the data exchange is interrupted, but the register contents are retained. Bit 4 controls the internal oscillator. The DS1216C is supplied with the OSC bit set, i.e., '1', to save battery power while the device is not in use. The bit must be made low to get the clock to tick.

The operation of the battery backup system is simple. The DS1216C compares the voltage on the Vcc line of the

80C32 board with the voltage supplied by its internal Lithium battery, and switches the RAM from mains supply to battery supply as soon as Vcc drops below the battery voltage. The voltage drop across the electronic switch used to accomplish this is only 0.2 V.

The DS1216C also features a power-fail detection circuit that continuously monitors the supply voltage line for dips. As soon as the supply voltage drops below 4.25 V, the IC switches to 'emergency supply' from the internal battery. While in battery backup mode, the DS1216C keeps the RAM's CE\ line logic high, so that the memory is write-protected. Normally, this control line follows the CE\ signal to the DS1216C within 20 ns.

## DS1216C and 80C32 computer

The DS1216C is simply inserted between the RAM and its IC socket, while D4 is replaced by a wire link. After changing the monitor EPROM, the following example programs may be loaded:

### CLKTST.HEX

start address

```
4100 Interrogate clock status on or off
4200 Switch on clock
4300 Switch off clock
4400 Clock setting demo, change date from 31.12.1991 to 1.1.1992
```

### EBTST5A.HEX

```
4100 Start melody in loudspeaker, stopwatch function
```

These example programs display their results on the LCD. ■

### References:

- 80C32/8052AH-BASIC single board computer. *Elektor Electronics* May 1991.
- 8051/8032 Assembler. A course in 8 instalments. *Elektor Electronics* February through November 1992.

### Note:

Dallas Semiconductor distributors in the UK are

Dialogue Distribution, Top House, 403 London Road, Camberley, Surrey GU15 3HL. Telephone (0276) 682001. Fax (0276) 683722.

Joseph Electronics Ltd., 2 The Square, Broad Street, Birmingham B15 1AP. Telephone (02164) 36999.

DS1216C SMARTWATCH software for Elektor Electronics 80C32 computer

### 1. Smartwatch address assignment

```
CLKADDR EQU 03FFFH ;Smartwatch dummy address
```

### 2. Eight registers assigned in internal RAM.

Registers for intermediate storage of data exchanged between CPU and Smartwatch. 80C32 board RAM definitions including eight RTC registers.

#### ; RAM definitions

```
;
; ORG 030H
COMMAND: DS 1 ;for MON call, MUST be address 030H!
CNT1: DS 1
HEXLEN: DS 1
HEXSUM: DS 2
;
dBYTES EQU 5 ;must be 5, loop unrolling used;
;
dREG1: DS dBYTES
dACCU: DS dBYTES
;
PWSAV: DS 1 ;used for snapshot and MON
ACCSAV: DS 1
DPHSAV: DS 1
DPLSAV: DS 1
;
; arithmetic storage
;
top EQU dREG1 ;overlay 2 bytes
next EQU dREG1+2 ;overlay 2 bytes
;
FAC1 EQU top ;overlay factors for 16*16 bit
FAC2 EQU next ;overlay
DIVI EQU FAC2 ;overlay divisor for 32/16 bit division
QUOT EQU FAC1 ;overlay quotient for 32/16 bit divis.
PROD EQU dACCU ;overlay 5 bytes (4+ ext.) for division
DIVCNT: DS 1
;
; date and clock storage
;
CLOCK: DS 4 ;Smartwatch, Time
DAY_NR: DS 1 ;Smartwatch, Day of Week (+OSC/RES-Bits)
DATE: DS 3 ;Smartwatch, Date
;
Rtop EQU $
;
```

### 3. Command codes assignment

Allow the courseware RAM to access Smartwatch via courseware EPROM. All relevant EMON51 codes are listed; additions are marked.

#### ; function codes for MON calls

```
;
ccCHR EQU 001H
ccSTXT EQU 002H
ccBYTE EQU 003H
ccHEX16 EQU 004H
ccRO16 EQU 005H
ccRO32 EQU 006H
cchRO16 EQU 007H
cchRO32 EQU 008H
;
ccGETC EQU 010H
ccTSTC EQU 011H
ccGET16 EQU 012H
ccGET10 EQU 013H
ccGETU EQU 014H
;
ccSNAP EQU 020H
ccLTIME EQU 021H
ccSTIME EQU 022H
;
ccCLKREQ EQU 030H **** New
ccCLKRUN EQU 031H **** New
ccCLKSTP EQU 032H **** New
ccCLK_WR EQU 033H **** New
ccCLK_RD EQU 034H **** New
;
ccLINK EQU 040H
;
ccADD EQU 050H
ccSUB EQU 051H
ccMUL EQU 052H
ccDIV EQU 053H
ccABS EQU 054H
ccNEG EQU 055H
;
```

4. Embedding the above command codes into the EPROM jump table in EMON51. Refer to the program section 'main monitor service routine'. For clarity lines before and after the insertion are given also.

```
.....
ttGETU: CJNE A,#ccGETU,ttLINK
LJMP GETUPC
ttLINK: CJNE A,#ccLINK,ttCLKEQ
LJMP LINK1
ttCLKEQ: CJNE A,#ccCLKREQ,ttCLKRUN
LJMP CLKREQ
ttCLKRUN: CJNE A,#ccCLKRUN,ttCLKSTOP
LJMP CLK_ON
ttCLKSTP: CJNE A,#ccCLKSTP,ttCLKWR
LJMP CLKOFF
ttCLKWR: CJNE A,#ccCLK_WR,ttCLK_RD
LJMP CLKWR
ttCLKRD: CJNE A,#ccCLK_RD,ttADD
LJMP CLKRD
ttADD: CJNE A,#ccADD,ttSUB
LJMP rADD16
.....
.....
```

### 5. The actual program

This program arranges the data exchange between 8051 and the Smartwatch module. In the EMON51 monitor, it is located between routines "snap" and "Arithmetic routines".

```
;
;***** Routines for Smartwatch DS 1216C *****
;
;----- Clear and switch off clock (OSC bit)
;
CLKOFF: LCALL C_REGO ;Clear storage register
MOV DAY_NR,#00110000B ;Oscillator off, RES passive
SJMP CLK_WR
;
;----- Clear and switch on clock (OSC bit)
;
CLK_ON: LCALL C_REGO ;Clear storage register
MOV DAY_NR,#00010000B ;Oscillator on, RES passive
;
;----- convey data from internal RAM to clock
;
CLK_WR: LCALL C_OPEN ;convey code word
;
MOV DPTR,#CLKADDR ;Smartwatch dummy address
MOV R0,#CLOCK ;Pointer to storage register
MOV R7,#8 ;8 Bytes
MOV R6,#8 ;8 Bits
MOV A,@R0 ;Read byte
WRBYTE: @DPTR,A ;Clock write pulse
RR A ;Bit 1 --> Bit 0
DJNZ R6,WRBIT ;8 Bits written?
INC R0 ;Next register
DJNZ R7,WRBYTE ;8 Bytes written?
NOP
RET
;
;----- Get clock status (OSC bit)
;
CLKREQ: ACALL CLK_RD ;Read hours register
MOV A,DAY_NR ;Fetch control register
JB ACC.5,C_OFF ;Bit 5 set (clock off)?
;
MOV DPTR,#C_TXT1 ;Monitor report, clock active
LCALL STXT
RET
;
C_OFF: MOV DPTR,#C_TXT2 ;Monitor report, clock passive
LCALL STXT
RET
;
C_TXT1: DB 'Smartwatch active',13,10,0
C_TXT2: DB 'Smartwatch passive',13,10,0
;
;----- Transfer clock data to internal RAM
;
UHR_RD: LCALL C_REGO ;Clear storage register
LCALL C_OPEN ;Convey code word
MOV DPTR,#CLKADDR ;Dummy address
MOV R0,#CLOCK ;Pointer to lowest storage reg.
MOV R7,#8 ;8 Bytes
MOV R6,#8 ;8 Bits
RDBYTE: MOV A,@DPTR ;Clock read pulse
RRC A ;Bit 0 --> C bit
MOV A,@R0 ;Read register
RRC A ;C bit --> bit 7
MOV @R0,A ;Write register
DJNZ R6,RDBIT ;8 Bits read?
INC R0 ;Next byte
DJNZ R7,RDBYTE ;8 Bytes read
NOP
RET
;
;----- Enable access to clock (64-bit code word)
;
C_OPEN: MOV DPTR,#CLKADDR ;Dummy address
MOVX A,@DPTR ;Initialize clock
MOV DPTR,#C_CODE
MOV R7,#8 ;8 Bytes
MOV R6,#8 ;8 Bits
CDBYTE: CLR A
MOVC A,@A+DPTR ;Fetch constant
PUSH DPH ;Save string pointer (DPTR)
PUSH DPL
MOV DPTR,#CLKADDR ;Dummy address
CDBIT: MOVX @DPTR,A ;Clock write pulse
RR A ;Bit 1 --> Bit 0
DJNZ R6,CDBIT ;8 Bits written?
POP DPL ;Restore string pointer
POP DPH
INC DPTR ;Next constant
DJNZ R7,CDBYTE ;8 Bytes (64 bits) transf'd?
NOP
RET
;
C_CODE: DB 0C5H,03AH,0A3H,05CH,0C5H,03AH,0A3H,05CH
;
;----- Clear 8 registers in internal RAM
;
C_REGO: CLR A
MOV R7,#8
MOV R0,#CLOCK
ALL_0: MOV @R0,A
INC R0
DJNZ R7,ALL_0
NOP
RET
;
```

## I<sup>2</sup>C interface for PCs

**February 1992**

The PCD8584 used in this project is no longer manufactured by Philips Semiconductors, and replaced by the PCF8584. This is a fully compatible IC and only improved as regards the 4-wire long-distance mode, which did not work correctly on the PCD8584.

## Real-time clock for 80C32 computer

**June 1993**

Contrary to what is implied by the description of the parallel connection of the SmartWatch IC pins with the EPROM pins, pin 1 of the SmartWatch

# CORRECTIONS AND UPDATES

should be connected separately to +5V, for instance, to EPROM pin 28, via a short wire. This is necessary because pin 1 on the SmartWatch is 'reset', while on the EPROM it is address line A14, which may be made high by 'high' addressing or glitches, causing the clock to be reset.

## VHF-low converter

**June 1993**

The parts list should be corrected to

read:

1	2 $\mu$ H2	L3
1	0 $\mu$ H1	L5

The circuit diagram is correct. The sub-1 $\mu$ H chokes used in this project are available from, among others, Cricklewood Electronics.

## 1.2 GHz multifunction frequency meter

**December 1992**

The recommended LCD module Type LTN211-F10 is no longer manufactured by Philips Components, and may be replaced by the compatible types LM016L from Hitachi, or the LM16A21 from Sharp.

# ELECTROMAGNETIC COMPATIBILITY (2)

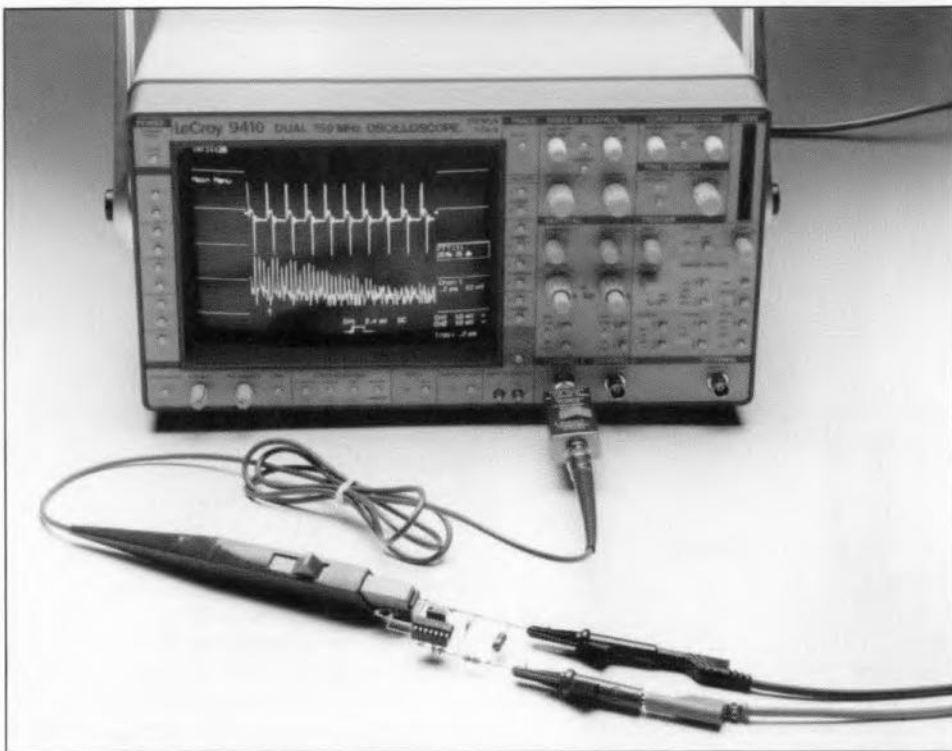
## From theory to practice

By J. Ruiters

As already stated in Part 1 of this two-part article, the EMC Directive must be taken into consideration when the marketing, and thus the design, specification is drawn up. This makes it far cheaper for the final product to meet the EMC guidelines than taking corrective measures in the later stages of the production process.

Although much work has been done by, for instance, the Department of Trade & Industry, The Institution of Electrical Engineers, and organizations like ERA Technology, in informing industry and all who are affected by the Directive, the practical application of EMC is still in its infancy. This is mainly because of the great variety of possible compatibility problems: after all, each design is different from the next, each product may be used in a different environment. On top of that, there are specific requirements for specific systems. Here are a few guide lines for designers.

- **Design on the basis of representative models.** In other words, use models that are characteristic of reality. Too often designers take decisions on the basis of analyses on non-valid models. If, therefore, a design decision does not yield the desired effect or result, the conclusion must be that the model used was not, or only partly, correct.
- **Always consider component properties as a function of frequency.** This rule applies to the range 0 Hz to 12 GHz. For instance, in an optoisolator common-mode signals are converted to differential-mode signals; this process, in EMC terms, is frequency-dependent. Another example is that one metre of yellow/green earth wire (as found in mains cable) represents an inductance of 1  $\mu$ H (this will be reverted to later). At 10 MHz, this gives an impedance of 63  $\Omega$ , which



shows that much equipment cannot be made EMC approved by just 'earthing it properly'.

Figure 7 shows that the behaviour of electrolytic capacitors is strongly frequency-dependent: above about 10 kHz, an electrolytic capacitor is no longer a capacitor, but an inductor. This fact is important in decoupling power supply lines for high frequencies.

- **Think in terms of current.** It is well known that in a closed circuit current can flow even though the circuit is not connected to a voltage source. If such a circuit is placed in a varying magnetic field, a current equal to  $-1/R \cdot d\phi/dt$  flows. This makes it clear that each measured potential difference (pd) is determined partly by the meter leads and the magnetic flux,  $d\phi$ , which (accidentally) is enclosed by these leads. It is, therefore, virtually impossible to conform to the EMC Directive on the basis of voltage considerations.

Even a more fundamental consideration of 'potential difference' leads to a preference of thinking in terms of current. From Maxwell's Second Law, which is applicable to each and every electromagnetic phenomenon, it follows that at frequencies that are not zero the potential difference between two points is dependent on the route along which the

electric field is integrated. Strictly speaking, therefore, potential difference has meaning only in the context of electrostatic fields. Note that Kirchhoff's Second Law ( $\sum U=0$ ) is merely a special case of Maxwell's Second Law ( $\sum U=-d\phi/dt$ ) and is, therefore, often not sufficiently accurate. However, Kirchhoff's First Law ( $\sum I=0$ ) is always valid. In other words, voltage does not always have a rational physical meaning, whereas current does.

### Properties of current

From what has been said, it is important to be well aware of a number of properties of current. In the first place: **currents always flow in closed circuits (loops)**. This is an important fact, because it is these loops that determine the emission and susceptibility to interference of an electronic circuit. It also explains why earthing does not always have the desired effect. After all, a current will flow to earth only if it cannot flow elsewhere. Mother earth is definitely not a bottomless pit into which we can dump all our interfering signals.

**Each and every current sets up an electromagnetic field.** A current-carrying conductor is always surrounded by a magnetic field ( $H$ ), while as a result of the charge on the conductor an electric field ( $B$ ) ensues between the conductor and its

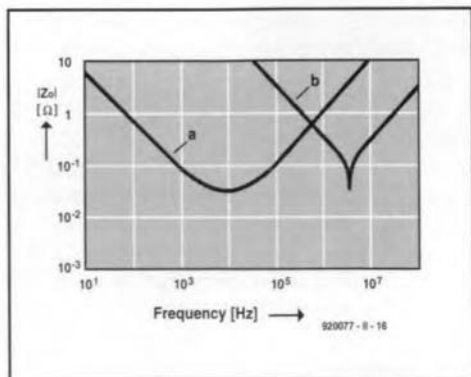


Fig. 7. Impedance as a function of frequency, (a) of a 2200  $\mu$ F capacitor, and (b) of a 470 pF ceramic capacitor.



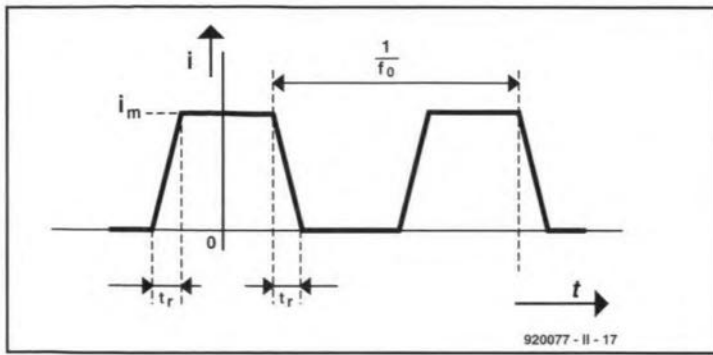


Fig. 8. True rectangular waveforms cannot be attained; the usual shape is trapezoidal as shown (slightly exaggerated).

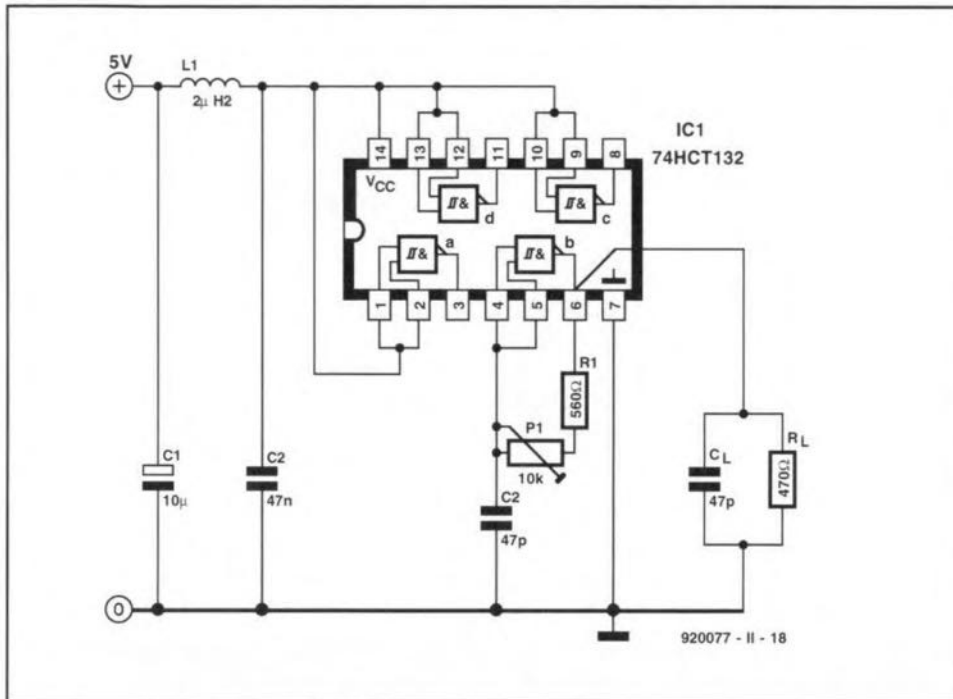


Fig. 9. In this digital oscillator, several currents have been measured. The measurement set-up is as shown in the introductory photograph.

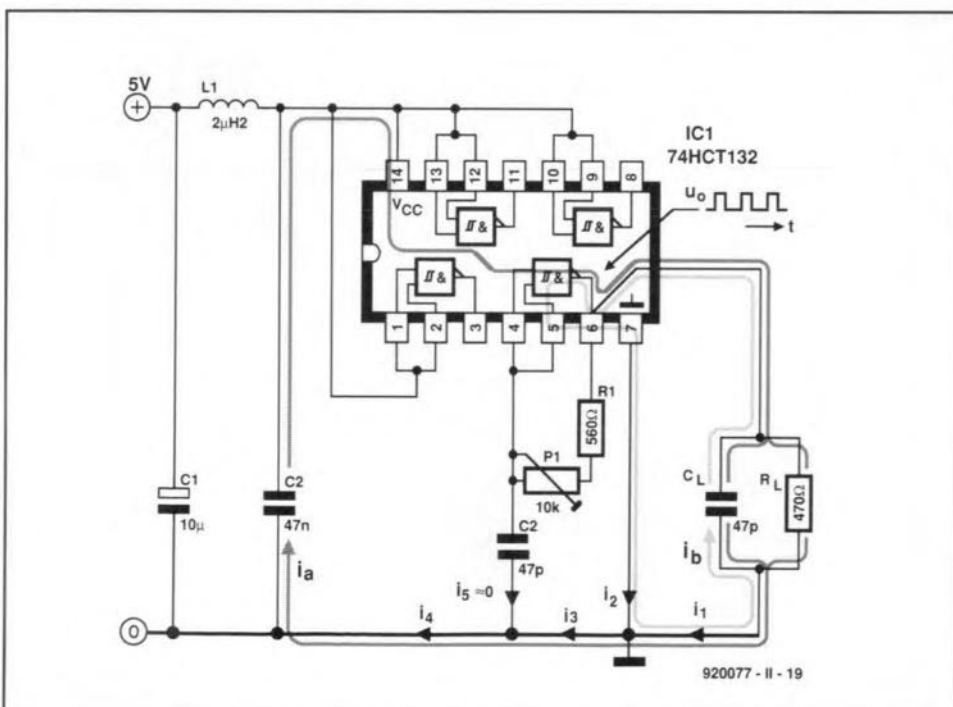


Fig. 10. The radiation of the oscillator is determined by currents  $i_a$  and  $i_b$ .

environment. The electromagnetic field causes the conductor to have not only resistance, but also several parasitic properties, such as inductance ( $1 \text{ nH mm}^{-1}$ ) and capacitance (read: coupling) to its ambience. The electromagnetic fields cause couplings over (electrically) short distances: cross talk.

To be able to predict the electrical behaviour of a design on the basis of a (low-frequency) network model (the CAD drawing, for instance), these field effects must be taken into account by adding to the model the correct parasitic components and sources. *E*-field couplings (interfaces) are indicated by parasitic *C*s (important in, for instance, cross talk in high-impedance clock circuits), and *H*-field couplings by parasitic *M*s (mutual inductance) or *L*s (self inductance).

It is obvious that a knowledge of these matters is of importance in the design of printed-circuit board layouts. Many current CAD programs were written before the EMC Directive was formulated, so that, in order to comply with EMC guide lines, many critical tracks (usually about half of the total) must be laid manually by the designer.

## Low and high frequency

Network theory enables the designer to approximate physical reality with models by replacing the *E*- and *H*-fields by impedances. It must be borne in mind, however, that the familiar low-frequency approximation is permitted only if the length,  $\ell$ , of the current loop is small with respect to the wavelength  $\lambda = 3 \cdot 10^8 f^{-1}$ . In words, the low-frequency approximation is valid for small systems only, that is, systems that satisfy the rule of thumb  $\ell \leq \lambda/10$ . Even then, as has already been hinted at, a low-frequency analysis will already lose much of its value if the effects of the *E*- and *H*-fields are not, or insufficiently, specified in the network elements (for instance, because it was assumed that there are no fields around or between the connecting wires).

In the case of a large electrical system ( $\ell \geq \lambda/10$ ), that is, a high-frequency system, the designer must apply transmission line theory (characteristic impedance, reflections, standing waves, and so on).

## Designing current loops

The electric field strength around a current-carrying circuit (read: small magnetic dipole) is directly proportional to the area of the loop in which the conductive or capacitive displacement currents flow. The maximum radiated field,  $E_m$ , at a distance  $r$  from a small current loop through which a trapezoidal current flows (see Fig. 8), is estimated from:

$$E_m = 2Z_0 S / \pi r c^2 f_0 i_m / t_r \quad [\text{V m}^{-1}]$$

where  $Z_0$  is the radiation resistance in

air ( $377 \Omega$ ),  $S$  is the area of the current loop,  $c$  is the speed of propagation of electromagnetic waves ( $3 \cdot 10^8 \text{ m s}^{-1}$ ),  $f_0$  is the frequency of the trapezoidal current,  $i_m$  is the pulse magnitude, and  $t_r$  is the first transition duration (rise time). The expression applies to a distant-field situation, which assumes that the observer distance,  $r > \lambda / 2\pi$ .

The wavelength  $\lambda = 3 \cdot 10^8 / f$  is thus a yardstick of whether the approximation formula may or may not be used. It is important to note that  $\lambda$  is not the fundamental frequency, but the harmonic nearest to  $1/\pi t$  Hz. This is because the electric field strength reaches its highest value with harmonics around this spectral cut-off point.

That the area,  $S$ , in the above expression must include the entire loop is made clear by considering a Schmitt trigger oscillator (see Fig. 9), which is based on a Type 74HCT132 NAND gate. The oscillator frequency can be varied with  $P_1$  over the range 1–10 MHz.

Capacitor  $C_1$  and low-pass filter  $L_1$ - $C_2$  bound the emission area in the direction of the power supply. Because of  $L_1$ ,  $C_1$ , and  $C_2$ , the spectrum of the supply current (to the left of  $L_1$ ) consists of low-frequency components that do not contribute to the radiation.

Because of the load on the gate,  $R_L$ - $C_L$ , two current loops ensue that determine the radiation. The first, indicated in Fig. 10 by  $i_a$ , carries the sum of the currents through  $R_L$ , the charging current of  $C_L$ , and the switching current of the IC. The second mesh current,  $i_b$ , is characterized by the displacement current that arises as a result of  $C_L$  discharging at the instant the output of IC<sub>1b</sub> goes low.

The current waveforms,  $i_1$ - $i_3$ , mea-

sured with a current probe are shown sequentially in Fig. 11. Note that  $i_5$  is negligibly small, whence  $i_4 \approx i_3$ . Note also that the amplitude of the currents (and thus the strength of the radiated field) is determined by  $C_L$  and not by  $R_L$ . In practice,  $C_L$  consists of the sum of the wiring capacitance, and the input capacitance of the digital circuit.

Characteristic values for the IC are:  $t = 3 \text{ ns}$ ,  $i_m = 40 \text{ mA}$  and  $S = 25 \text{ cm}^2$ . Substituting these values in the radiation formula, it is possible to estimate the maximum field to be expected at a distance of 10 m from the oscillator. From this, it appears that the radiation limit of  $30 \mu\text{V m}^{-1}$  is already reached at an oscillator fre-

quency of 3.3 MHz. The harmonics responsible for the limit to be exceeded lie above  $1/\pi t$ , that is, 106 MHz, or from the 33rd harmonic up ( $1/\pi t f_0$ ).

To keep the radiation from current loops within bounds, a well thought out PCB design is imperative. Particularly effective is a board with a reference plane or reference grid. On such a board, the main part of the return current flows underneath the supply line (in agreement with the minimum-flux principle, this is the route of least impedance). A further benefit is that this also gives the smallest possible area of the current loop. All these measures reduce the radiation. On single-sided boards and double-sided

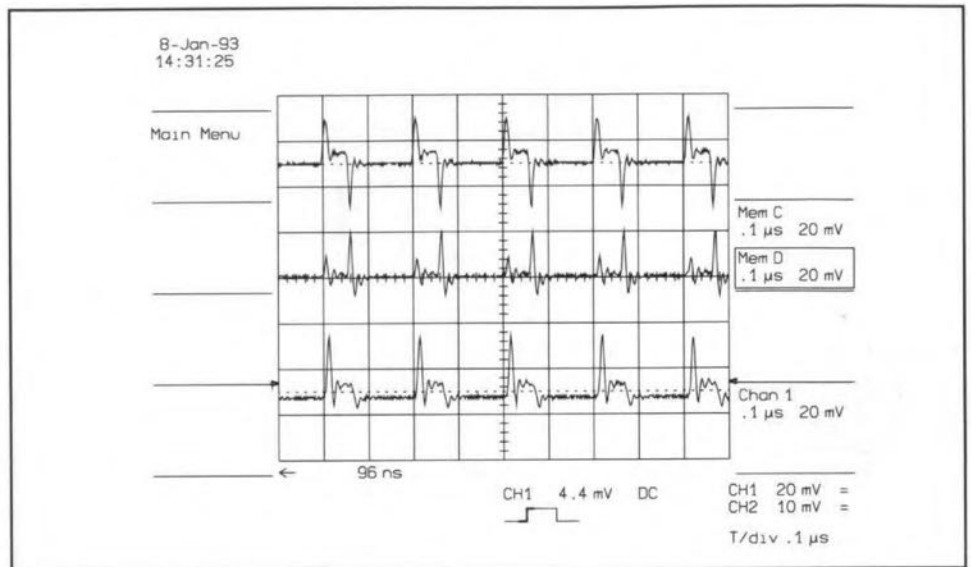


Fig. 11. The output current of the IC, 1, consists of the charging and discharge current of  $C_L$  B and the current through  $R_L$ . The current in the earth conductor, 2, consists of the discharge current of  $C_L$  and the switching current of the IC itself. The current in the large loop is equal to currents 1 and 2.

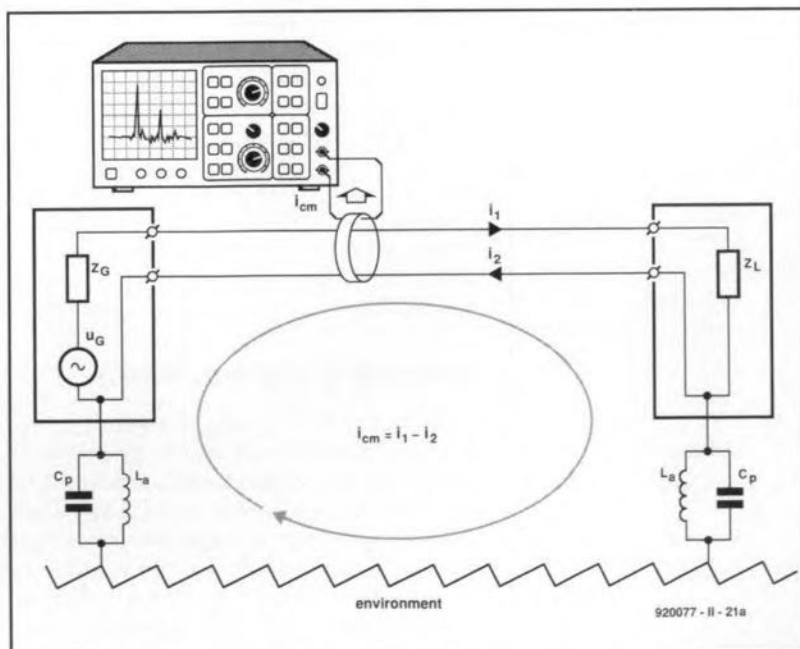


Fig. 12. Common-mode currents occur as the result of a coupling between the circuit and its environment. They may be measured with an HF tong-test ammeter and a spectrum analyser. The coupling is represented here by parasitic capacitances  $C_p$  and earth connections  $L_2$ .

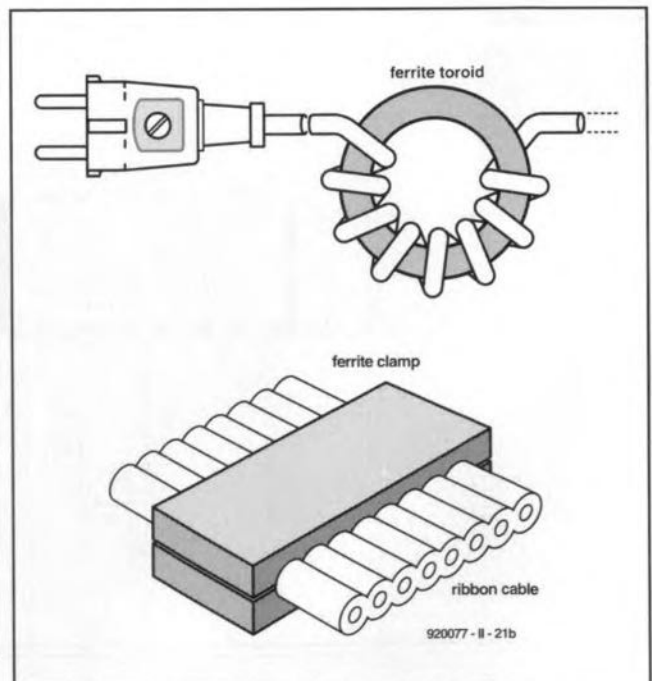


Fig. 13. Radiation may be reduced by ferrite materials like a clamp around a flatcable or the mains cable wound around a ferrite toroid.

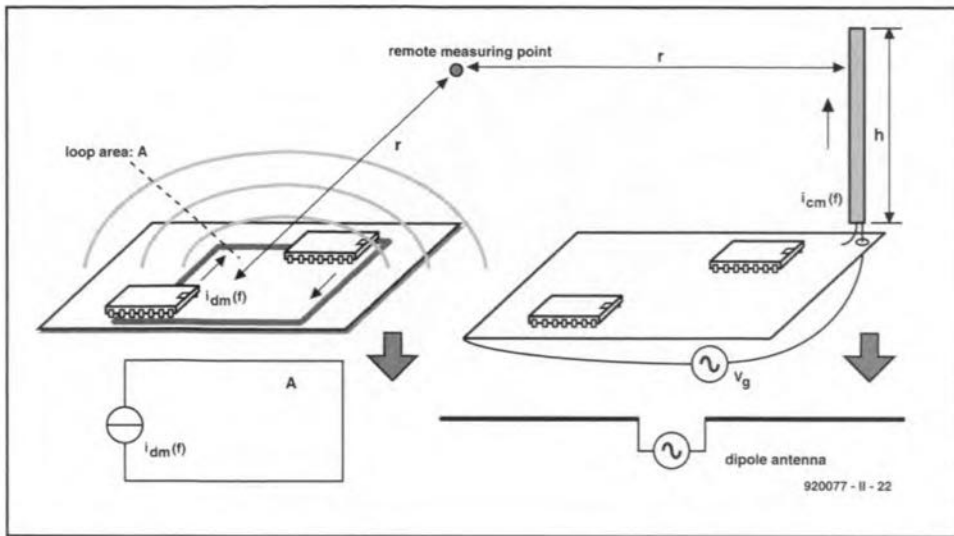


Fig. 14. Energy transfer by radiation. Differential mode radiation (left) is a result of the (wanted) current through an electrically small loop. Common-mode radiation (right) results from an (unwanted) antenna current through the cables.

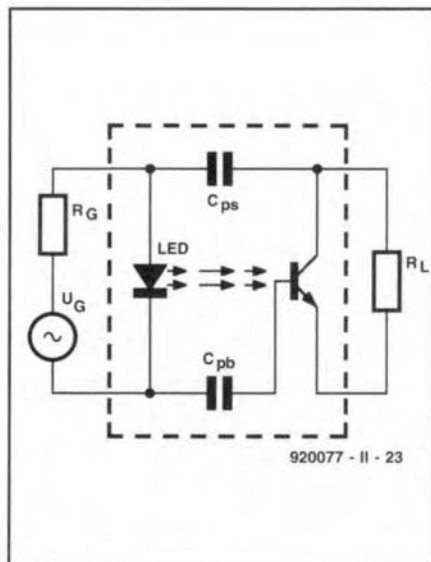


Fig. 15. Parasitic capacitances  $C_{pb}$  and  $C_{ps}$  cause the conversion in the optoisolator of CM signals into DM signals.

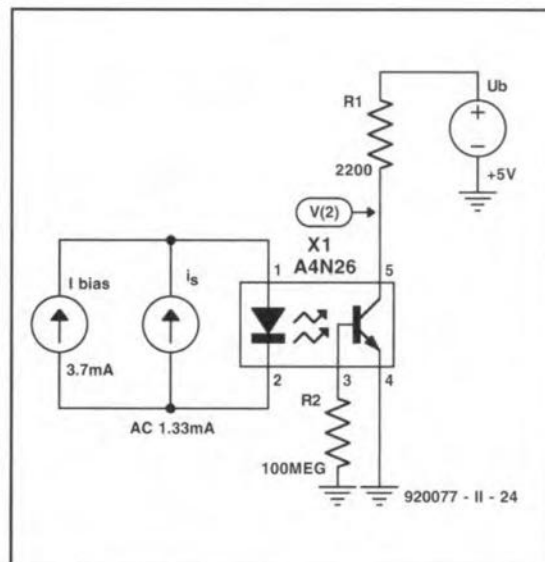


Fig. 16. Pspice model of the electrically isolated data connection in Fig. 15.

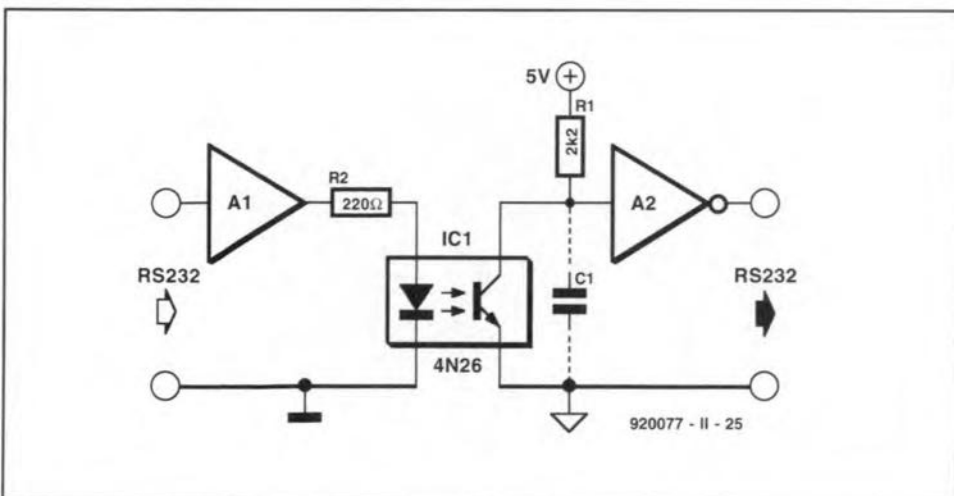


Fig. 17. Basic circuit of an electrically isolated data connection.

ones without a reference grid, the current-loop areas may be kept small by keeping the distance between the supply and return conductors small.

Also, it is advisable never to use faster logic circuits than is necessary: a higher  $t_r$  will after all cause a lower  $E_m$ . Furthermore, it is clear from the radiation formula that the clock frequency should be as low as possible. The phenomenon that  $E_m$  is directly proportional to the clock is a consequence of the fact that the amplitude of the harmonic near to  $1/\pi t$  is directly proportional to  $f_0$ . Since the electric-field strength is directly proportional to the amplitude of the current, it is also directly proportional to  $f_0$ .

## Beware of common-mode currents

A current loop always maintains a coupling with its surroundings, either by conduction or by radiation. 'Surroundings' include objects such as a metal table top, a central heating radiator, an earthing point, and so on. It all depends on which coupling predominates at a given frequency. Owing to the coupling to the surroundings, common-mode currents, also called asymmetrical currents, arise—see Fig. 12. Unfortunately, common-mode currents often flow through conductors (supply cables), whose dimension is of the same order as the wavelength: for instance,  $106 \text{ MHz} = 2.8 \text{ m}$ . This means that in electronic systems whose dimensions are much smaller than the wavelength of the signals, the cables connected to the system radiate more than the tracks on the PCB. Therefore, **the radiation of most products is determined by the magnitude of the high-frequency common-mode currents flowing in the cables.**

The CM currents may be measured with an HF tong-test ammeter and a spectrum analyser. In the design stages this test and the rule of thumb  $I_{CM} < 5 \mu\text{A}$  gives a good idea of whether the radiation will be higher or lower than the legal limit of  $30 \mu\text{V m}^{-1}$ . If, in the prototype, the measured CM current through one of the cables (mains lead, cable to printer, signal cables) is greater than  $5 \mu\text{A}$ , the final product will almost certainly exceed the maximum permissible radiation.

The radiation can be reduced by inserting a high CM impedance in the current path. For example, a ferrite clamp may be placed around a flatcable as shown in Fig. 13. The same drawing shows how the CM currents in a mains lead may be reduced by winding the lead through a ferrite toroid.

Figure 14 shows two other ways via which interference may be transferred through radiation.

## Design example

An optoisolator can often be used to put

some of the rules stated into practice. It is an analogue device that is frequently used with digital hardware. In such cases, the optoisolator is controlled digitally, so that, at least from a functional point of view, its output is also digital.

A suitable optoisolator for use in EMC designs is shown in Fig. 15. As usual in such a device, the signal transfer is effected by light. Capacitors  $C_{pb}$  and  $C_{ps}$  show, however, that there is another, spurious coupling between input and output. The effect of these parasitic capacitances has been investigated with a simulation program, Pspice. A setup with which this program can be used is shown in Fig. 16. This model is derived from the electrically isolated data connection in Fig. 17.

In Fig. 16, the optoisolator has been set to its linear operating range with a direct current of 3.7 mA. This value has been determined empirically and ensures that a direct voltage, whose level is equal to half the supply voltage, is present at the output. To enable the differential mode to differential mode transfer,  $u_{out}/i_s = V(2)/i_s$ , to be computed, an alternating current source, providing 1.33 mA, has been added at the input. With Pspice this source can be frequency-swept and the amplitude characteristic shown in Fig. 18 calculated. The most important datum to be gleaned from the characteristic is that the bandwidth for the wanted signal transfer is about 25 kHz.

In practice, the electrically isolated data connection will be affected by the common mode source of interference across the optoisolator. To study the effect of this, a voltage source,  $u_{CM}$ , and two 50- $\Omega$  impedances have been added to the model in Fig. 19. Since the optoisolator is not ideal ( $C_{ps}$  and  $C_{pb}$ ), part of  $u_{CM}$  will appear at the output. This is awkward, because this interference signal is in series with the output voltage. If the level of the interference is (relatively) high, it is possible that gate A2 (read: wideband amplifier) produces erroneous logic levels during the transition from one to the other. This comes down to insufficient immunity. Note that this transition in EMC literature is called common-mode/dif-

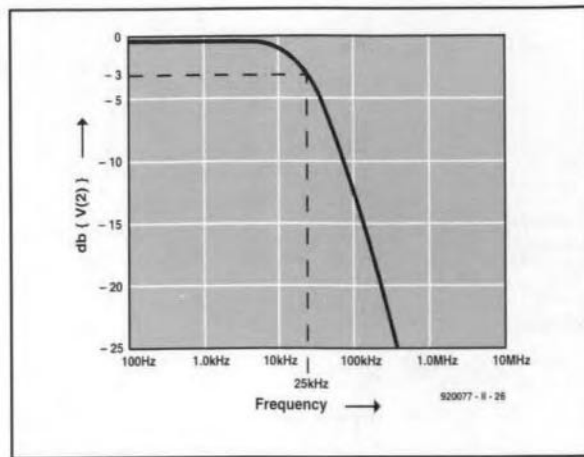


Fig. 18. The simulated DM-DM characteristic according to Fig. 16.

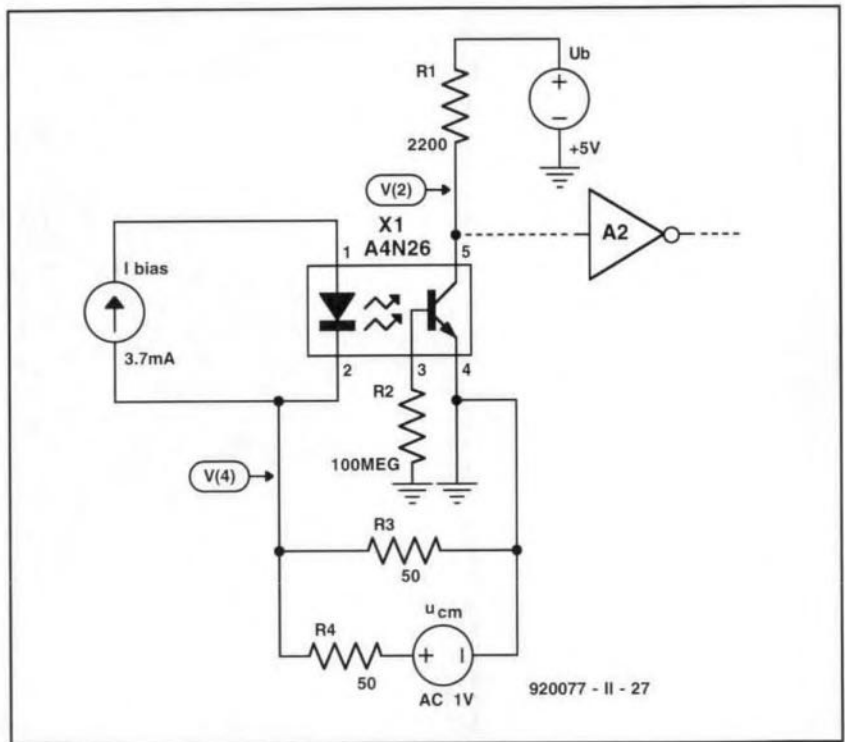


Fig. 19. To compute the CM-DM transfer, voltage source  $u_{CM}$  was added to the model in Fig. 16.

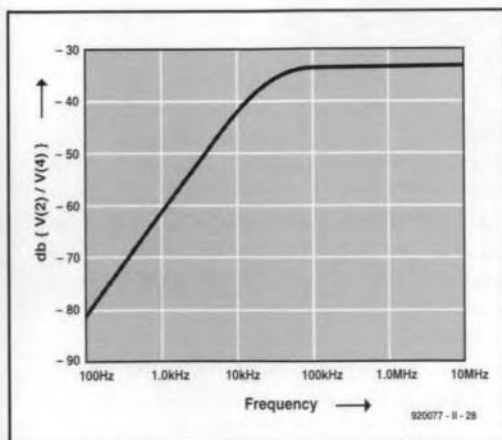


Fig. 20. CM-DM transfer characteristic computed from the setup in Fig. 19.

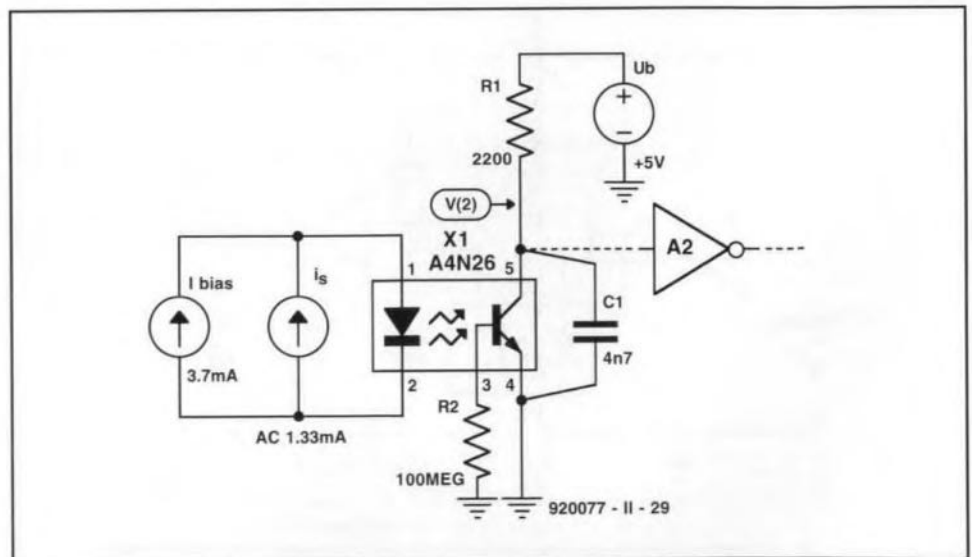


Fig. 21. Capacitor  $C_1$  reduces the DM transfer at high frequencies.

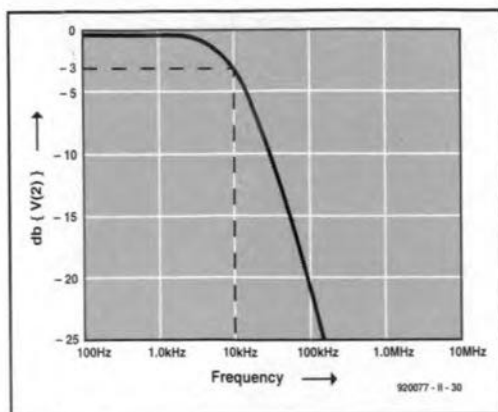


Fig. 22. The DM-DM characteristic for the set-up in Fig. 21.

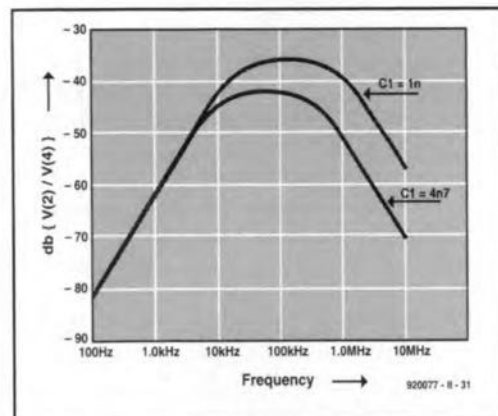
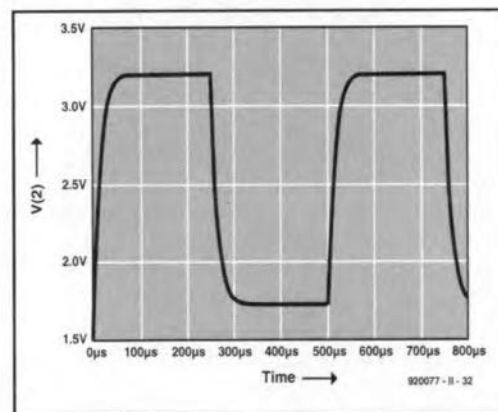


Fig. 23. The CM-DM transfer characteristic for Fig. 21 with different values for  $C_1$ .



ferential mode (CM-DM) transition.

The quality of an optoisolator, as far as immunity is concerned, is a measure of the degree to which CM signals are suppressed. The characteristic calculated on the basis of the model in Fig. 19 is shown in Fig. 20. This indicates that the suppression of CM signals reduces with rising frequency. Again, this is awkward, because, in practice,  $u_{CM}$  contains primarily HF (>1 MHz) components. The characteristic can, however, be improved greatly by reducing the bandwidth of the optoisolator. This is done in Fig. 21 by shunting the switching transistor with a 4.7 nF capacitor. This reduces the bandwidth to about 10 kHz—see Fig. 22; the CM suppression for high frequencies is thereby increased. The CD-DM characteristic for the model in Fig. 21 with shunt capacitors of 1 nF and 4.7 nF is given in Fig. 23. It is clear from the curves that the CM suppression is inversely proportional to the bandwidth.

When the electrically isolated data connection in Fig. 17 operates at a bandwidth (BW) of 10 kHz, the first transition duration (rise time),  $t_s$ , of the pulses at the output of the optoisolator is  $t_s = 0.35/BW = 35 \mu s$ . The maximum input frequency at which a correct digital signal can be measured at the collector of the phototransistor is, by rule of thumb,  $BW/5 = 2$  kHz. The output signal simulated with Pspice is shown in Fig. 24; the model is given in Fig. 25. The circuit is thus suitable for use in an RS232 connection with baud rates up to 4000 Bd (which coincides with the frequency limit of 2 kHz). A complete design was published earlier this year\*.

\*Electrically isolated RS232 interface. *Elektor Electronics*, March 1993.

Fig. 24. Characteristic of the output voltage with a channel bandwidth of 10 kHz and a rectangular (2 kHz) input current.

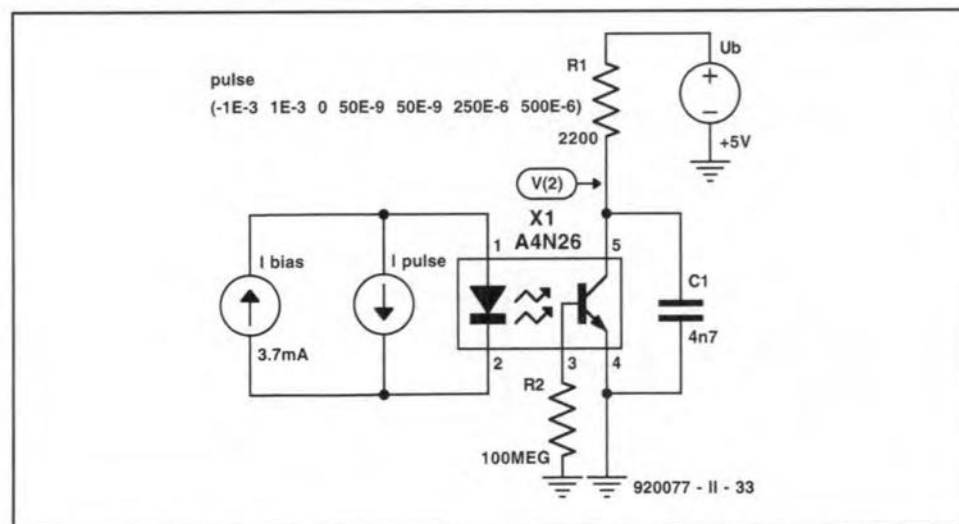


Fig. 25. Model used by Pspice for computing the characteristic in Fig. 24.

#### Further reading:

*Electronic system design: interference and noise control techniques*, ISBN 0-13-252 123-7, by J.R. Barnes, Prentice Hall, 1987.

*Interference-free electronics: design and applications*, ISBN 0-86238-255-6, by S. Benda, Chartwell Bratt, 1991.

*Electromagnetic compatibility: Europe*, ISBN 0-580-20917-2, British Standards Institution, 1992.

*EMC: electromagnetic theory to practical design*, ISBN 0-471-82878-X, by P.A. Chatterton & M.A. Holden, Wiley, 1992.

*ZZAAP! taming ESD, RFI and EMI*, ISBN 0-12-189930-6, by M.B. Corp, Academic, 1990.

*Electromagnetic compatibility: bibliography and information pack (2nd Edition)*, ISBN 0-85296-495-1, by J. Coupland & P. Fountain, IEE Technical Information Unit, 1993.

*Grounding for the control of EMI*, ISBN 0-932 263-17-8, by H.W. Denny, Don White Consultants, 1989.

*Electromagnetic compatibility in radio engineering*, ISBN 0-444-99722-9, by W. Rotkiewicz (ed), Elsevier Scientific, 1982.

*Electromagnetic compatibility: applied principles of cost-effective control of electromagnetic interference and hazards*, ISBN 0-8247-1887-9, by H.M. Schlicke, Marcel Dekker, 1982.

*Electromagnetic compatibility handbook*, ISBN 0-442-28903-0, by J.L.N. Violette, D.R.J. White & M.F. Violette, Van Nostrand, 1987.

Designers may also note that Rohde & Schwarz's Type ESHS 10 and ESVS 10 test receivers are now available from Livingstone Hire. These instruments meet the measurement requirements of European EMC Standards incl. 55 011 to 55 022, ETS, FCC, VCCI and VDE 0871 to 0879. Full information on these versatile instruments from Livingstone Hire, Livingstone House, Queens Road, Teddington TW11 0LB, England. Telephone (0)81 943 5151; Fax (0)81 977 6431.

# CW COMPATIBLE T/R SWITCH

The use of CW (morse) on a high-power transmitter/receiver presents a serious risk of burned antenna (coax) relay contacts or destruction of a GaAs FET preamplifier. Fortunately, that problem can be overcome quite easily at a very small outlay with the circuit described here.

Design by Pedro Wyns, ON4AWQ

ALTHOUGH a number amateur radio magazines have recently carried designs that ensure that antenna relays change before the transmitter is powered, most of these circuits are suitable for 'phone' (voice) transceivers only. Just in case you did not know, early switching of the antenna relay is necessary to protect the expensive and

highly sensitive GaAs FET preamplifier(s) against the huge power produced by the transmitter.

The trouble starts if you want to use a commercial VHF or UHF transceiver for high-power, high-speed CW modes such as Meteor-scatter, Tropo-DX or EME (earth-moon-earth). These modes require high transmitter power levels

and extremely sensitive preamplifiers. Unfortunately, most commercial transceivers have a built-in COR (carrier operated relay), which powers the transmitter the instant the morse key is pressed, not allowing sufficient time for the antenna relay to switch over.

The circuit shown here is connected between the microphone, CW key and the transceiver. The operation of the circuit is quite simple: in 'phone' mode, the antenna relay is energized the instant the PTT switch on the microphone is pressed. The transmitter, however, is switched on a little later by a timer built around Schmitt-trigger NAND gate IC1c. When the PTT switch is released, the reverse takes place: the transmitter is switched off immediately, while the relay is de-energized a little later because of the delaying action of gate IC1d.

When CW is used, the key signals are blocked by wired-AND gate IC1a-T2 until the delay introduced by timer IC1c has elapsed (approx. 200 ms). The circuit around IC1b provides a 'hang' time of about 2 seconds to prevent relay clatter while the transmitter is being keyed. Transistor T4 is a darlington type to enable relays 'outside' the transceiver to be controlled also. If this is not required, the BD675 may be replaced by a BC547. Note that the collector of T5 is supplied via the coil of the Tx/Rx relay in the transceiver. ■

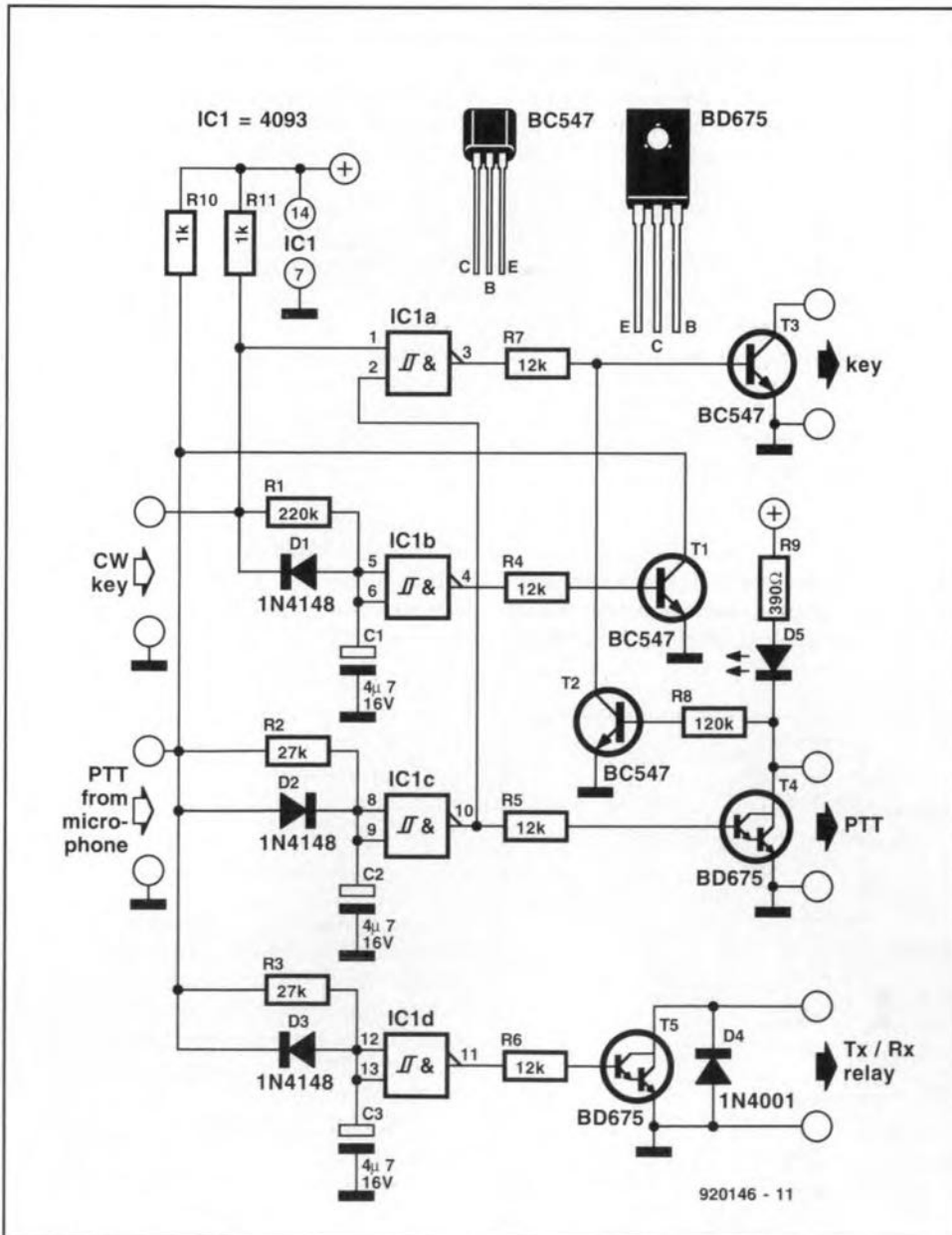


Fig. 1. Circuit diagram of the transmit/receive switch

**A two-monthly column by Keith Hamer and Garry Smith**

SEVERAL intense tropospheric openings punctuated the bleakness of February and March. Signals were plentiful in Band III and at UHF, particularly on February 14th when many French, German and Benelux stations emerged at considerable strength.

By comparison, Band I reception was relatively quiet, apart from several sustained sporadic-E openings in the latter half of February. Other Band-I activity was due to meteor-scatter and auroral activity.

**Reception reports**

Andrew Jackson of Birkenhead has written to say that tropospheric reception conditions were excellent during February. The most productive day was Sunday 14th when most of the 'usual' signals were around plus some new ones. Transmissions received in clear colour included RTBF-1 (Belgium) on channel E57, RTBF-TELE 21 on channel E60, and Canal Plus (France) on channel E63. The 'VOX-Koeln' FuBK test card was received on the 5th and the 13th, and this was also strong. Sporadic-E activity occurred on February 15th at 2037h with prolonged reception from a German ARD-1 transmitter on channel E2.

Andrew has been monitoring the new Irish TV channel allocations from the Kippure transmitter on a daily basis. RTE-1 can be good at times although co-channel interference from the Maghera transmitter does occur. Signals from the Band-I channel B Maghera outlet have also been available during tropospheric activity.

On the 14th, a strange-looking test pattern was present on channel E11 for most of the day and well into the evening. It resembled the FuBK pattern, but had a distinctive central 'window'; there was no identification. This was subsequently identified as 'Canal Plus Belgique' on test from the Leglise transmitter, which once broadcast RTBF-1 programmes.

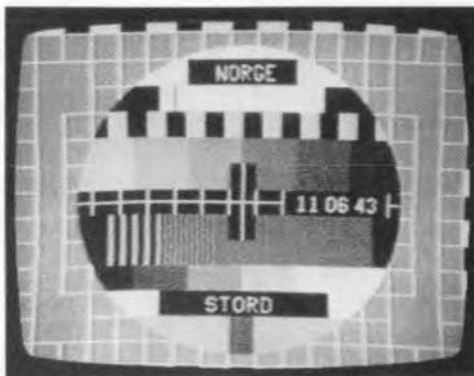
Davis Asher of Wrexham has only DX-ed at UHF so far, but plans are afoot to install VHF equipment in the near future. His successes include several Dutch and German outlets, with the reception of almost perfect Teletext from the Nederland-3 network. Unfortunately, Nederland-2 on channel 27 is now blocked by a local relay station. His equipment consists of a 10-element wide-band aerial, aligned East North-East.

This is fed into a home-brew mast-head amplifier with 15-20 dB gain. A Goodmans 20-inch Teletext receiver and Goodmans 2500 VCR completes the set-up.

Stephen Michie of Bristol found that early February was active with sporadic-E on the 2nd from Hungary. Reception consisted of a tennis match and later the PM5544 test pattern with the identification 'MTV-1' at the top, and 'Budapest' in the lower black rectangle. There was enhanced tropospheric reception on at least seven days, with the weekend of the 13/14th being the most active. One German station was transmitting the FuBK test pattern with the inscription 'ARD 1 PROG' and the date and digital clock below the central block. There was an unidentified German signal on channel E36 which was possibly RTL PLUS from Dusseldorf. Stephen found that March was very quiet with only the daily signals from the Goes transmitter, and the occasional reception from Lopik (both outlets are located in the Netherlands).

Iain Menzies of Aberdeen has been monitoring the HF bands to evaluate the MUF (maximum usable frequency) and the reception conditions in general. On 24th February, a station in Michigan reported a MUF of 46 MHz. Sporadic-E signals were noted two days later at 1900h UTC on channel R1, almost totally masked by baby alarms! On the 27th on 28 MHz between 0830h and 1030h UTC, Australia was heard at S9+ with several FM transmissions at over 30 MHz. Unfortunately, the MUF did not reach TV frequencies.

During the first five days of March, South African stations reported working as far North as Brittany. On March 11th,



The PM5534 test card from the Stord transmitter (30 kW ERP channel E5) in Norway, received in Derby via Sporadic-E.

an aurora produced GI and G stations with excellent results from the Lerwick beacon. The usual beacon received via auroral activity was not heard. During the same opening, weak unidentified signals were present on TV channels E2 and R1. On 12th March at 1930h UTC the Lerwick beacon was received again via Aurora, but this time there were no TV signals. The MUF has since been extremely poor. Even 28 MHz has been a struggle at times!

According to Simon Hamer of New Radnor in Powys, the weather forecast on Scottish TV is sponsored by *Kwik-Fit*, and not *Legal and General*. Grampian ITV's clock resembles the old TVS one, though blue and white. The identification in red and white on the Danish PM5534 test pattern is, according to Simon, to tie in with their national flag.

Simon has confirmed that RTL-2 is now operational on the Astra 1A satellite, replacing Screensport. RTL-2 is a spin-off from RTL Plus, but more family-oriented and without 'adult' films. The RTL-2 news is called *Action News*. This service is also available on Eutelsat II F1.

Simon has also advised that various BBC Radio broadcasts can now be found on the UK Gold transponder of the Astra 1B, using the Wegener Panda-1® system. The satellite subcarriers transmit the BBC World Service on 7.38 MHz, Radio 4 (long wave version) on 7.56 MHz, Radio 1 on 7.74 MHz and Radio 5 on 7.92 MHz.

**Log for February**

**02.02.93:** Norwegian PM 5534 test pattern via meteor scatter propagation on channel E3 at 0815h UTC, plus unidentified signals on channel E2. Sporadic-E signals from Hungary were noted between 1145h and 1330h UTC.

**13.02.93:** Sporadic-E activity at 1235h on channel E3. The unidentified reception consisted of an historical play.

**15.02.93:** Strong sporadic-E signals from Germany on channel E2 at 2037h UTC.

**18.03.93:** A small sporadic-E opening from Denmark on channel E3 at 0730h UTC. Also, meteor scatter activity noted on channel R2 at 0750h.

**26.02.93:** Unidentified sporadic-E signals on R1 at 1900h.

Tropospheric reception from France, Eire, Belgium, Germany and the Netherlands was noted on the following dates during February: 1st, 4th, 5th, 9th, 10th, 13th, 14th and 15th. In addition, Luxembourg and Denmark were logged on the 14th.

**Log for March**

**09.03.93:** SVT-1 (Sweden) on channel E6 and SVT-2 E30 via tropospheric propagation.

**11.03.93:** Unidentified signals on channels E2 and R1 via auroral activity.

**14.03.93:** Serbia on channel E3 plus unidentified signals on R2 (meteor scatter).

**18.03.93:** Sporadic-E reception from Germany on channel E2 and Denmark E3.

**20.03.93:** Unidentified FuBK test pattern on channel E2 via meteor scatter at 0825h.

The DX-TV logs were kindly supplied by the following enthusiasts: Andrew Jackson (Birkenhead), Simon Hamer (New Radnor), Iain Menzies (Aberdeen) and Stephen Michie (Bristol).

### 1993 Sporadic-E Season

This is now underway and should last from May to September. An in-depth look at sporadic-E reception was featured in the February 1993 issue of *Elektor Electronics*. To briefly recap, throughout the summer, signals can be received in Band I from transmitters located at distances in excess of 1,100 km. The basic equipment required for reception consists of a tuner covering Band-I channels (48-70 MHz) plus an aerial, such as a dipole with a total length of approximately 2.8 metres.

The modified MP3 converters mentioned in the previous column have all been sold, but several readers have been in contact who purchased the basic unit. Even in their original form they are suitable for sporadic-E work, provided they have Band-I coverage. With the original 5.5-MHz ceramic sound filters fitted, the TV sound from most countries in Western Europe will be heard.

### Service information

**Portugal:** Since its launch in mid-1992, RAP International (RTPi) has been broadcasting for 42 hours per week, taking the best Portuguese programmes from among the four RAP channels (RAP-1 and RAP-2 in Portugal, RAP-Madeira and RAP-Azores). In addition, there are regular news programmes and live football coverage. RTPi also produces a daily news magazine that serves as an interface among the many Portuguese communities throughout the world.

**France:** Canal Plus is gradually introducing a new scrambling system in an attempt to make pirate decoders unusable. The new scrambling system, called 'Syster', has been developed in Switzerland. It is a technically more sophisticated system than 'Discret 1', which was originally adopted for Canal Plus transmissions. It is hoped that the new system will offer greater security, and will be more difficult to 'hack'.

**Belgium:** The Canal+ programme is now aired from the Leglise transmitter on channels E11 and E63. A colour test card with a small but distinctive 'window' in the centre has been used for recent tests. No identification is shown.

### TV systems

During the recent periods of enhanced tropospheric reception conditions, tuning through the UHF band on a normal TV set may have revealed several foreign stations dotted about the band. Given favourable conditions, some of these would be complete with Teletext information. However, the biggest mystery for the viewer is the absence of sound. This is due to the differences in TV systems adopted by various countries, for example, in the UK and Eire the sound carrier sits at 6 MHz above the vision carrier, whereas in countries such as Belgium and Germany the carrier off-set is only 5.5 MHz. In Eastern Europe and the CIS the spacing is 6.5 MHz.

The FM intercarrier sound system is used by every country throughout the world, apart from France and Monaco where AM sound continues to be used. With the intercarrier system, both the sound and vision IF signals are handled by the vision detector, the resultant beat frequency (the frequency difference) being fed into the sound IF stages which respond to either 5.5, 6.0 or 6.5 MHz signals.

The characteristics that make up a TV system can be divided into five main elements: (1) the number of scan lines; (2) positive or negative vision modulation; (3) FM or AM sound; (4) the sound subcarrier off-set; (5) the colour system. Any combination of these can make up a TV system.

Many different systems were originally adopted in Europe. Even during the early eighties there were at least four different line standards in use: 405 by the UK and Eire; 819 by France and Monaco, 525 by the American forces transmitters, and 625 by other countries. Since the closure of the 405-line system in 1985, only 525-line and 625-line systems exist. Transmissions using 819 lines were phased out a number of years ago.

With the exception of France, Monaco and Luxembourg, negative vision modulation is used worldwide. Positive vision modulation was also used by the UK, Eire and Belgium. If such a transmission is received on a 'normal' set, the pictures tend to resemble a black and white photographic negative, i.e., black areas appear white and vice-versa, when viewed on a UK receiver. The synchronization may also be poor due to the incorrect sense of the video detection.

Amplitude modulation (AM) is used for the sound carrier accompanying positive modulated vision signals. The FM intercarrier system is used elsewhere with four different spacings, depending on the system.

PAL and SECAM colour systems are used throughout Europe. SECAM was adopted by Russia, Eastern-bloc countries and France, while PAL was used elsewhere. Since the recent political changes in Eastern Europe, SECAM is gradually being phased out in favour of the PAL system in some countries. Already the Czech and Slovak republics have initiated this change, and the former East German transmitters have radiated PAL for some time.



The station opening caption of the Dutch third network, photographed by David Glenday in Arbroath.

The 'BRT' header information on the PM5544 test pattern as used by the Flemish-speaking networks now reads 'BRTN'. The lower identification 'TV1' or 'TV2' remains unchanged.

**United Kingdom:** DAB (Digital Audio Broadcasting) test transmissions are due to start in London this summer (they will commence in France during 1994 with ten local programmes in the Paris area). Frequencies around 60 MHz in Band I and 220 MHz in Band III have been chosen, which could present problems for UK DX-ers. The choice of Band I frequencies again demonstrates the irresponsibility shown by the powers-that-be, because it is likely to cause interference to European TV services during periods of Sporadic-E propagation.

**Eire:** The channels used for RTE-1 and Network-2 transmissions from Kippure have changed. RET-1 has moved from channel H to E, and Network-2 from channel J to H. Channel J is no longer used. The E and H pair of channels are also used by other Irish transmitters such as Achill, Castletownbere, Clencolumcille, Kilmacthomas and Suir

Valley.

A new RTE-1 transmitter at Maghera is now operating on channel E with 100 kW ERP, and it seems likely to replace the existing channel B outlet. Network-2 is already broadcast from the Maghera site on channel E. A similar move to channel H for RTE-1 seems a possibility for the low-power Glanmire relay which currently radiates the first programme on channel C and Network-2 on channel E.

**Finland:** MTV, which used to provide programmes for the TV1 and TV2 networks, has transferred its output to the commercial TV3 network, which now covers most of the country. The test card is the FuBK with the 'MTV 3' identification.

The TV1 and TV2 networks have recently undergone a complete face-lift because of this move. TV1 is now described as being modern, international and up-to-date; the TV2 network caters for specialist programmes.

**Germany:** The MDR-3 network is now using the FuBK colour test pattern with the identification 'MDR 3 Dresden'. VOX TV, who were given two terrestrial channels previously occupied by WEST-3, also radiate the FuBK pattern with the identification 'VOX — Koeln'.

This month's service information was kindly supplied by Gösta van der Linden and the Benelux DX club, Netherlands; Bernd Trutenau, Lithuania; Pertti Salonen, Finland; Reflexion Club, Germany; Roger Bunney, UK; Simon Hamer, UK; André Gille, France. Please send any news about DX-TV in your part of the world to: Keith Hamer, 7 Epping Close, Derby DE3 4HR, England.



# 80C32 COMPUTER APPLICATION NOTES - 3

## X2404 EEPROM interfacing to an 8751

Design by Zoran Stojsavljevic

XICOR's X2404 is a 4096-bit serial Electrically Erasable PROM (EEPROM), internally organized as two pages, each containing 256x8 bits. The X2404 features a serial interface and an I2C compatible software protocol that allows it to be operated via a 2-wire bus. The pinning and internal architecture of the IC are given in Fig. 1. The SCL (serial clock) input is used to clock all data into and out of the device. The serial data pin, SDA, is bidirectional, and used to transfer data into and out of the device. SDA is an open-drain output, and may be wire-ORed with any number of open-drain or open-collector outputs to form a bus. Address input A0 is not used by the X2404, although it must be tied to  $V_{SS}$  for proper device operation. Address inputs A1 and A2 are used to set the least-significant two bits of the six-bit slave address assigned to the device. The address inputs are static, and should be tied to logic high or low levels, to give one unique address per device.

The circuit diagram in Fig. 2 shows an example application of the X2404 in a 8751 microcontroller driven racing car computer. The functions of this computer are not our prime concern here, hence the following discussion will concentrate mainly on the way the 8751 and the X2404 are set up to communicate properly. The functions of the four push-buttons are:

- S2: adjust clock;
- S3: display max. rpm during race;
- S4: display max. rpm ever.
- S5: reserved.

The hardware implementation of the X2404 is simplicity itself, being essentially restricted to two lines only. In the application circuit, the X2404 records the highest rpm (revolutions per minute) value of the car engine. This is achieved by reducing the ignition pulses to a suitable level, digitizing (Tx), and feeding them to the P3.2 input of the 8751 microcontroller.

### X2404 device operation

The X2404 supports a bidirectional, bus oriented protocol. This protocol defines any device that sends data on to the bus as a transmitter, and the receiving device as a receiver. The device

Following the eight instalment '8051/8032 assembler course' featured in last year's issues of *Elektor Electronics*, this column presents design ideas, programming examples and hardware experiments based on and around the popular 80C32 single-board computer. All descriptions are kept as brief as possible to ensure that a wide variety of subjects can be presented. Apart from the knowledge you have hopefully gathered from the assembly language course, you will need the following to get going with the application notes: an 80C32 SBC (with extension board) running the EMON51 system monitor from EPROM, and a PC running the EASM51 assembler. Both programs are contained on the assembler course diskette, no. 1661. This month Zoran Stojsavljevic tells us all about 8751-to-EEPROM interfacing.

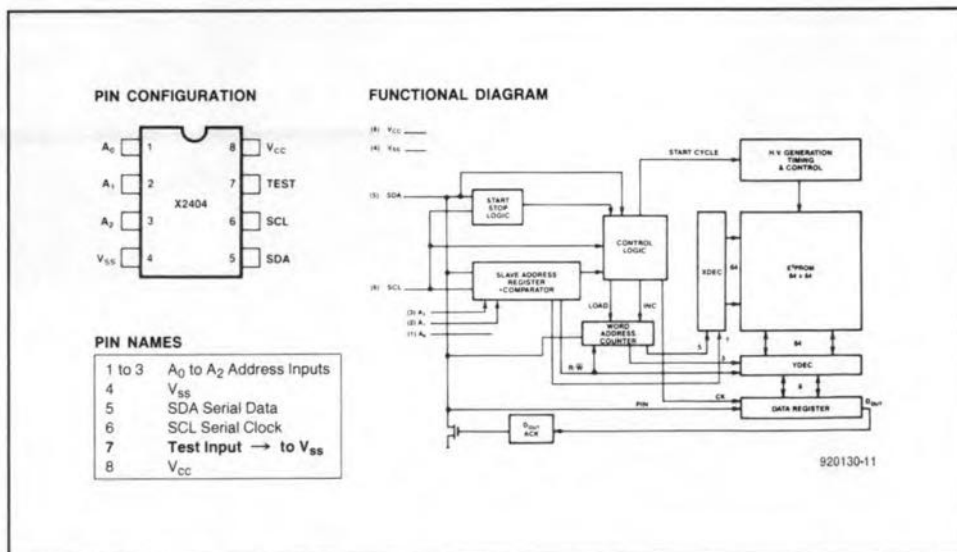


Fig. 1. Pin layout and internal structure of EEPROM X2404.

controlling the data transfer is a master, and the device being controlled is a slave. The master will always initiate data transfers, and provide the clock for both transmit and receive operations. Therefore, the X2404 will be considered a slave in all applications.

Data states on the SDA line can change only when SCL is low. SDA changes during SCL 'high' periods are reserved for indications of start and stop conditions, as illustrated in Fig. 3. All commands are preceded by the start condition, which is a high-to-low transition of SDA when SCL is high. The X2404 continuously monitors the SDA and SCL lines for the start condition, and will not respond to any command until this condition is

satisfied. All communications are terminated by a stop condition, which is a low-to-high transition of SDA when SCL is high. The definitions of the start and stop conditions are illustrated in Fig. 4.

The transmitting device, either a master or a slave, releases the bus after transmitting eight bits. During the ninth clock cycle, the receiver pulls the SDA line low to acknowledge that it received the eight bits of data. The X2404 will always respond with an acknowledge after recognition of a start condition, followed by its slave address. If both the device and a write operation have been selected, the X2404 will respond with an acknowledge on receipt of each subsequent

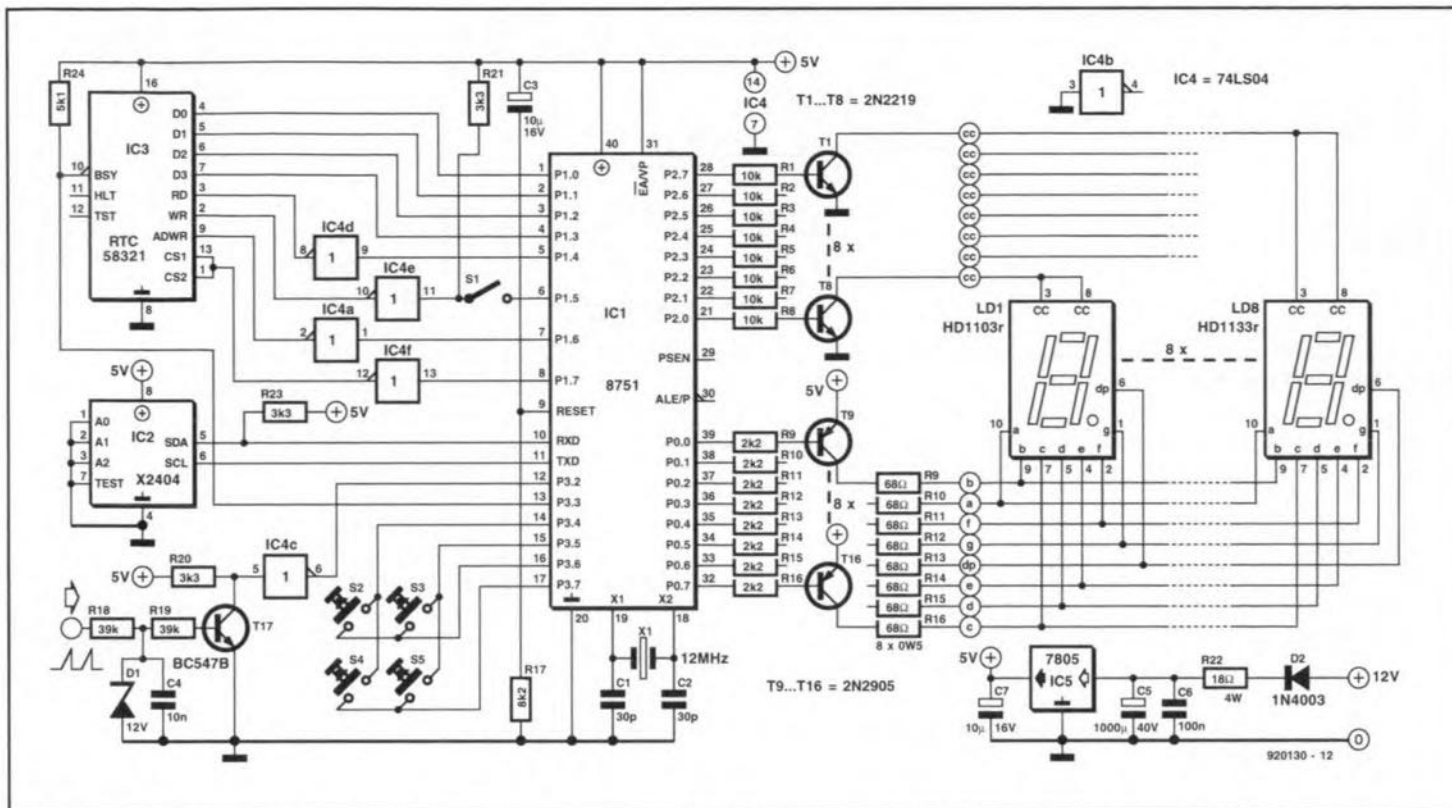


Fig. 2. Application of an X2404 in a car computer based on Intel's 8751 microcontroller. The X2404 serves, among others, to store and retain the highest rpm of the car's engine.

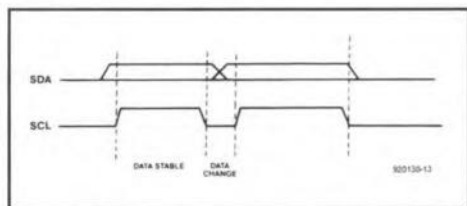


Fig. 3. Clock and data conventions.

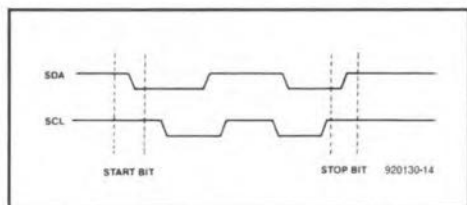


Fig. 4. Definition of start and stop conditions.

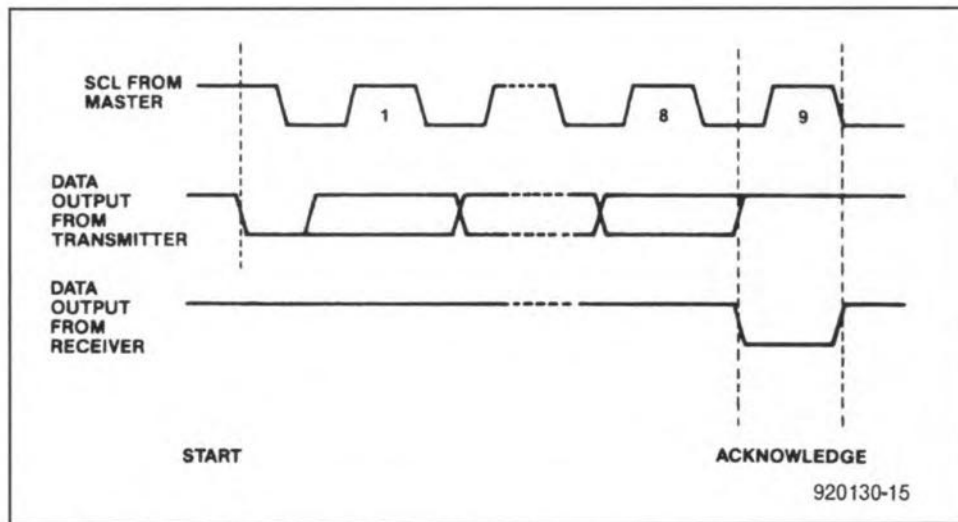


Fig. 5. Response from the receiver.

eight-bit word (Fig. 5). In read mode, the X2404 will transmit eight data bits, release the SDA line, and monitor it for an acknowledge. If an acknowledge is detected and no stop condition is generated by the master, the X2404 will continue to transmit data. If an acknowledge is not detected, the X2404 will terminate further data transmissions, and await the stop condition.

Following a start condition, the bus master must output the address of the slave it is accessing. The most significant four bits of the slave address are the type identifier (see Fig. 6). For the X2404 this is fixed as 1010. The next two bits, A2 and A1, address one of up to four X2404s connected on to the

bus. The next bit, A0, allows the host to toggle between the two 256-word pages contained in the X2404. The last bit in the device address field switches between read (bit=1) and write (bit=0) operations. Following the start condition, the X2404 monitors the SDA bus, comparing the slave address being transmitted with its own address (i.e., four-bit device type and two-bit device number). When the two match, the X2404 generates an acknowledge on the SDA line. Depending on the state of the R/W bit, the device next does a read or a write operation.

Write operations on the X2404 can be divided into two types: byte write and page write. For a byte write opera-

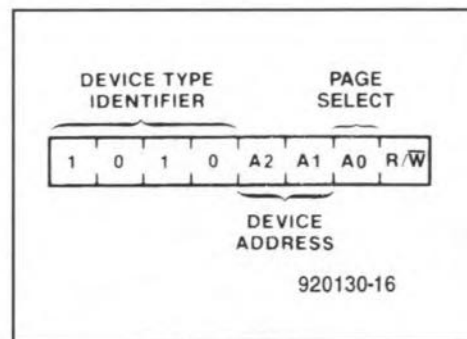


Fig. 6. Address format.

tion (Fig. 7), the X2404 requires a second address field, which forms the word address. This consists of eight

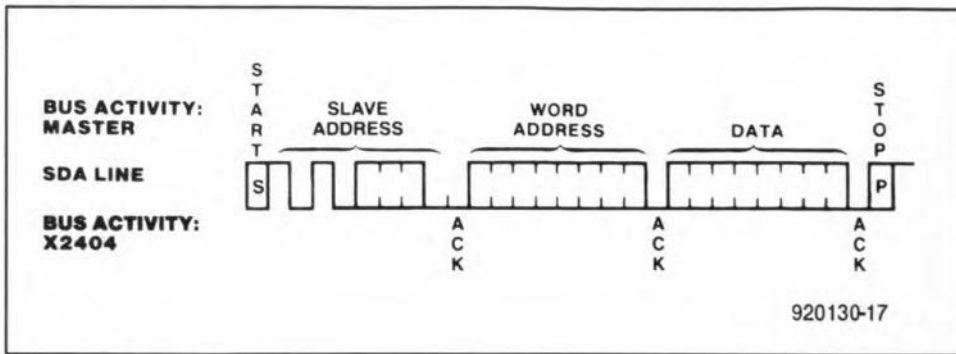


Fig. 7. Byte write operation.

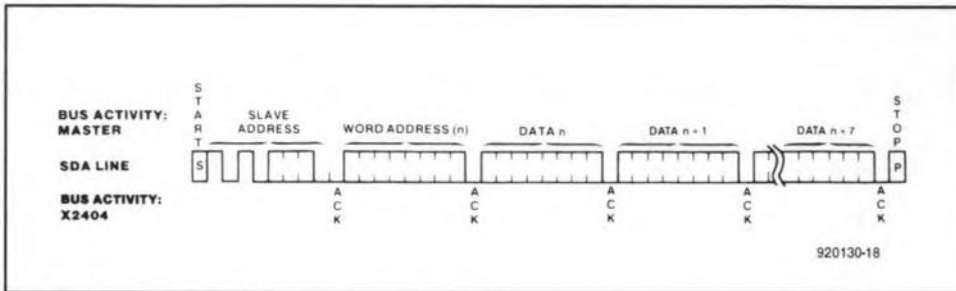


Fig. 8. Page write operation.

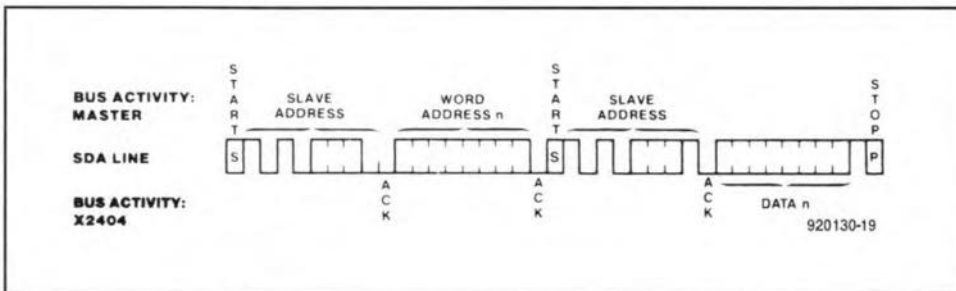


Fig. 9. Random read operation.

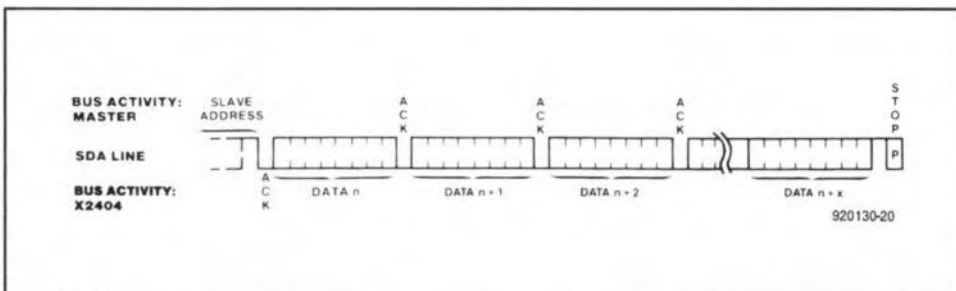


Fig. 10. Sequential read operation.

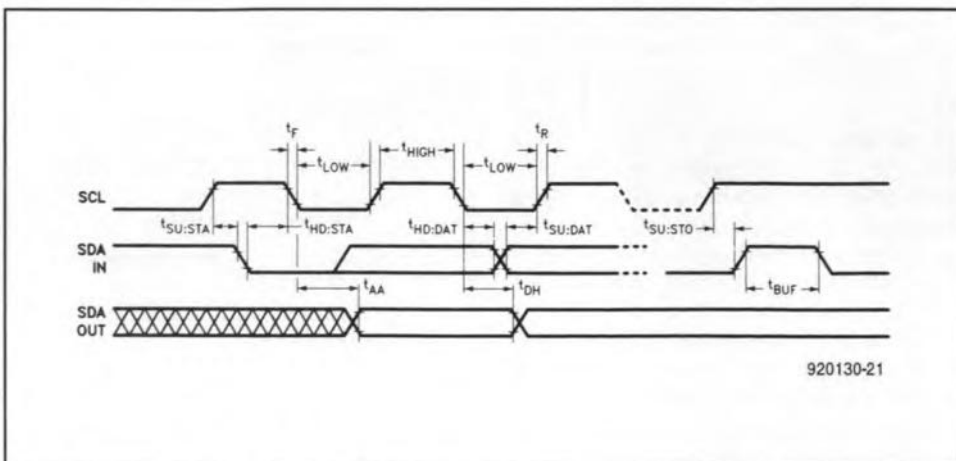


Fig. 11. Control and data line setup times.

bits, and provides access to any one of the 256 words of memory. Upon receipt of the word address, the X2404 responds with an acknowledge, and awaits the next eight bits of data, again responding with an acknowledge. Next, the master terminates the transfer by generating a stop condition, at which time the X2404 starts an internal write cycle to the non-volatile memory. During this write operation, the device disables its inputs, and will not respond to any requests from the master.

Page write operations (Fig. 8) move eight bytes at a time, and are initiated in the same manner as byte write operations. However, instead of terminating the first write cycle after the first data word is transferred, the master can transmit up to seven more words. On receipt of each word, the X2404 will respond with an acknowledge. On receipt of each word, the three low-order address bit are internally increased by one. The high order five bits of the address remain the same. If the master transmits more than eight words before generating the stop condition, the address counter will 'roll over', and the previously stored data will be overwritten. As with the byte write operation, all inputs are disabled until the internal write cycle is completed.

Acknowledge polling can be implemented by making use of the typical 5- $\mu$ s write cycle time. ACK polling involves issuing the start condition followed by the slave address for a write operation. If the relevant X2404 is still busy with the write operation, it will not return an ACK until this operation is finished, after which the host can proceed with the next read or write operation.

Read operations (Fig. 9) are initiated in the same manner as write operations, with the exception that the R/W bit of the slave address is set to a one. There are three basic read operations: current address read, random read and sequential read.

Random read operations allow the master to access any memory location in a random manner. Prior to issuing the slave address with the R/W bit set to one, the master must perform a 'dummy' write operation. The master issues the start condition, and the slave address followed by the word address it is to read. After the word address acknowledge, the master immediately re-issues the start condition and the slave address with the R/W bit set to one. This will be followed by an acknowledge from the X2404, and then by the 8-bit word. The master does not acknowledge the transfer, but generates a stop condition, so that the X2404 stops transmitting.

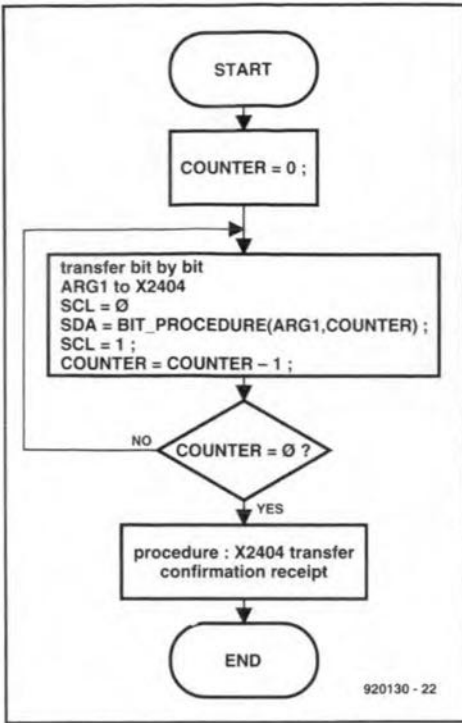


Fig. 12. Flow chart of procedure WRITE\_BYTE.

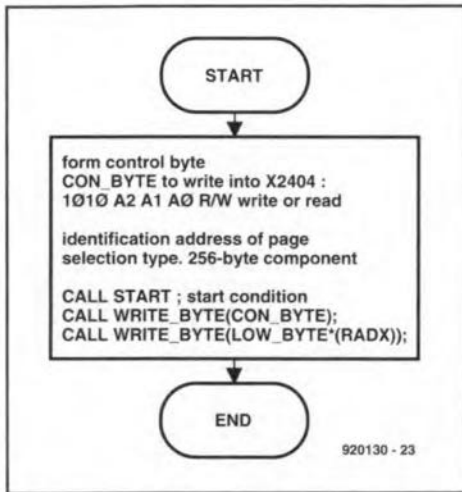


Fig. 13. Flow chart of procedure WRITE\_ADDR.

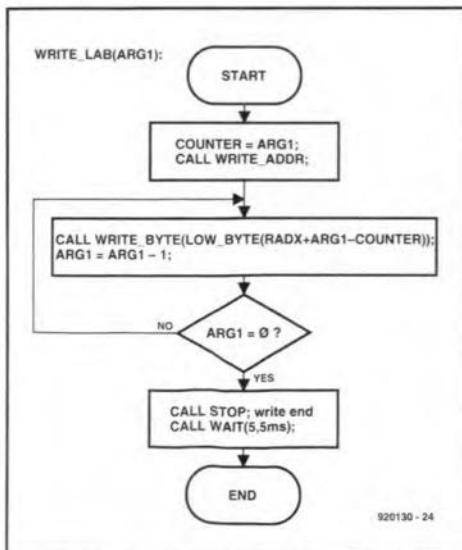


Fig. 14. Flow chart of procedure WRITE\_LAB.

Sequential read operations can be initiated either as a current address read or a random access read. The first word is transmitted as with the other read modes. However, the master now responds with an acknowledge, indicating that it requires additional data. The X2404 continues to output data for each acknowledge received. The read operation is terminated by the master not responding with an acknowledge, and generating a stop condition.

The data output is sequential, with the data from address *N* followed by the data from address *N+1* (Fig. 10). The address counter for read operations increases all eight address bits, allowing the entire memory contents of the current 256-word page to be read serially in one operation. If more than 256 words are read, the counter 'rolls over', and the X2404 continues to output data from the same 256-word page for each acknowledge received.

**X2404 control program**

The control program written to interface the X2404 to an 8751 is based on the previously discussed device operation and the timing specifications given in Fig. 11. Any transmission to the X2404 requires at least three parameters: (1) the number of bytes to be transferred; (2) the initial EEPROM address to or from which the length data, defined by the first parameter, are transferred; (3) the initial address of the 8751 internal RAM to or from which the length data, defined by the first parameter, are transferred. The following program notations apply:  
 RADX: Required initial Address for read/write from/to X2404;  
 RADM: Required initial Address for read/write from/to Microcontroller;  
 RBN: Required Byte Number for read/write program.

The flow charts in Figs. 12 through 16 illustrate the basic operation of the X2404 control program. The flow charts were used as a starting point for the assembler code written to implement the X2404-to-8751 link. Unfortunately, owing to lack of space, it is not possible to print the assembly listing of the interface program. The program is available on an MS-DOS formatted disk, however, and be obtained through the Readers Services — the order code is 1891.

**Conclusion**

The X2404 EEPROM and the software driver developed for it allows an 8051 (or derivate) microcontroller to store a relatively small packet of data that is not lost when the power is switched off. Applications June be found in auto-

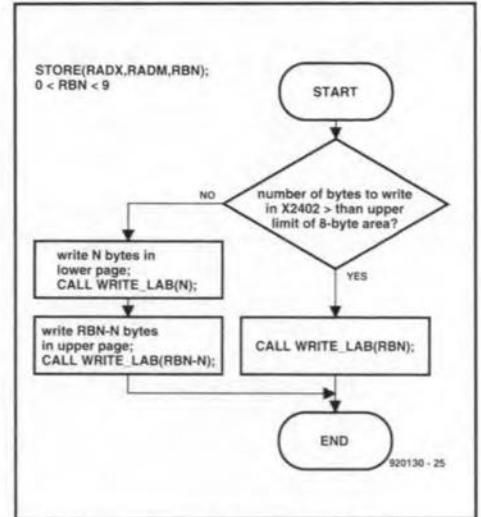


Fig. 15. Flow chart of procedure STORE.

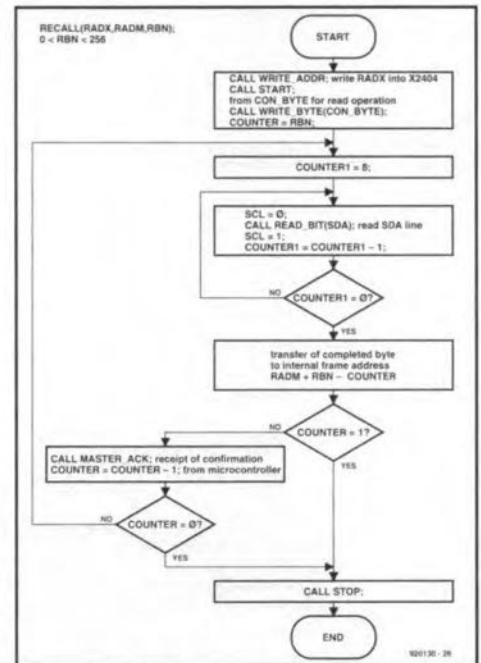


Fig. 17. Flow chart of procedure RECALL.

motive control, test and measurement, and data logging systems. If your application requires more memory space, there are EEPROMs in the X24xx family with a larger capacity, for instance, the X24C16 with a capacity of 2 kBytes, organized as eight pages of 256 bytes each. The software driver described here requires only small changes for use with a variety of serial EEPROMs.

**Literature:**

1. Data Book, Xicor. Xicor Inc., 851 Buckeye Court, Milpitas, California 95035. Telephone (408) 432-8888. Fax: (408) 432-0640.
2. Embedded Controller Handbook, Intel Corp.

**Note:**

Figures 1, and 3 through 11, and extracts from X2404 datasheets reproduced by courtesy of Xicor, Inc.

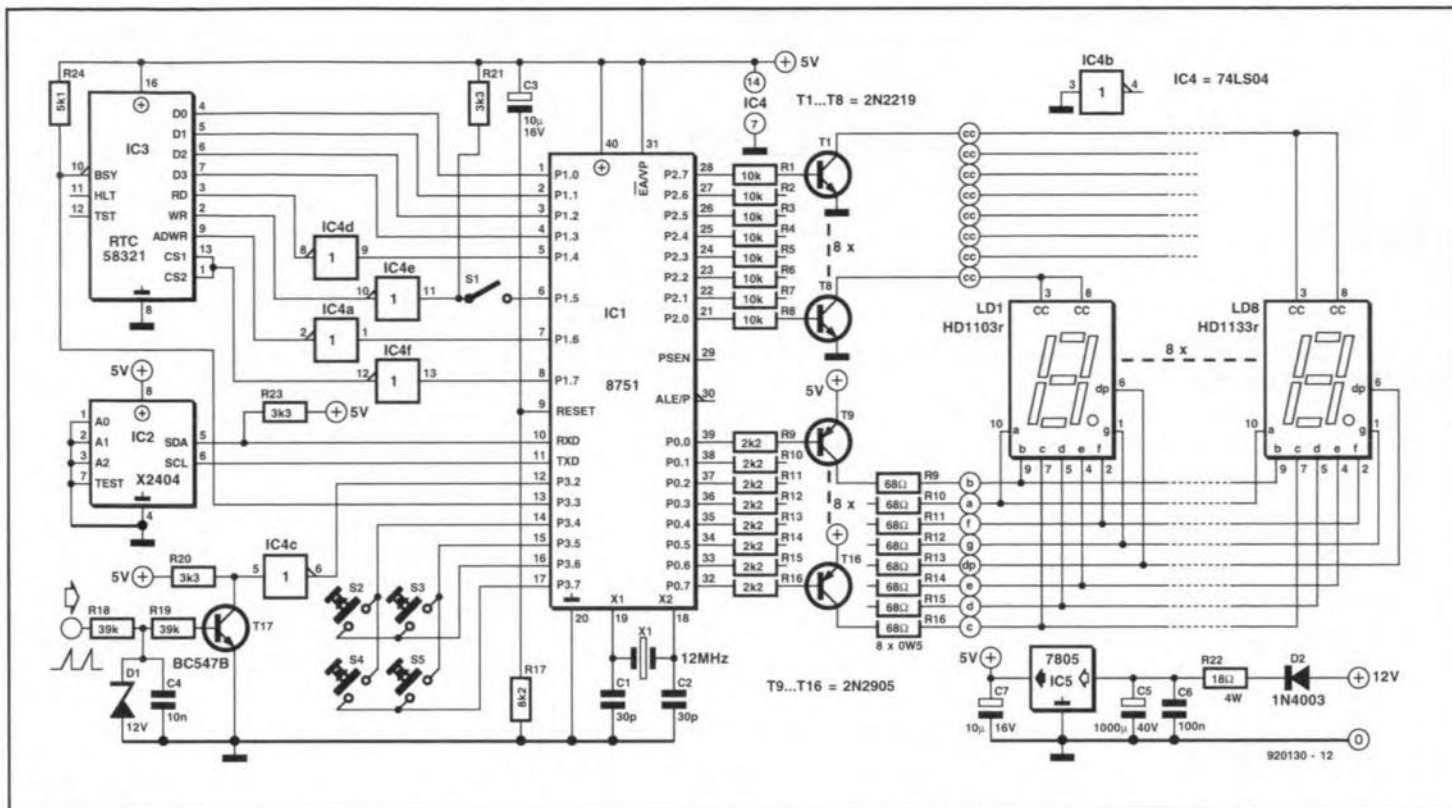


Fig. 2. Application of an X2404 in a car computer based on Intel's 8751 microcontroller. The X2404 serves, among others, to store and retain the highest rpm of the car's engine.

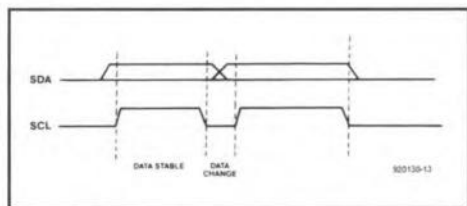


Fig. 3. Clock and data conventions.

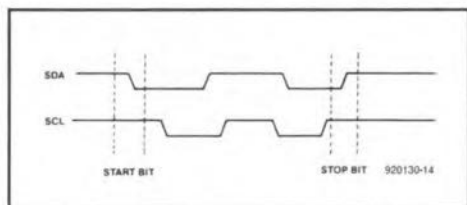


Fig. 4. Definition of start and stop conditions.

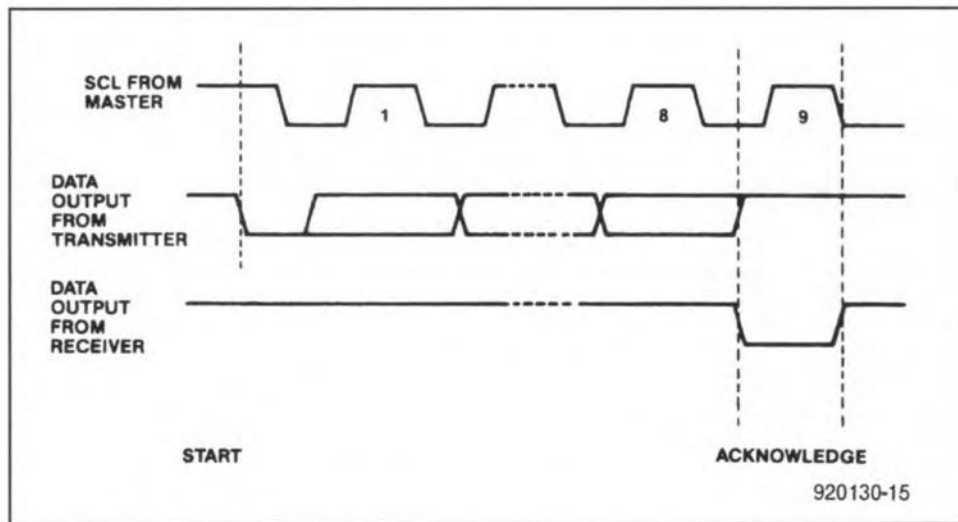


Fig. 5. Response from the receiver.

eight-bit word (Fig. 5). In read mode, the X2404 will transmit eight data bits, release the SDA line, and monitor it for an acknowledge. If an acknowledge is detected and no stop condition is generated by the master, the X2404 will continue to transmit data. If an acknowledge is not detected, the X2404 will terminate further data transmissions, and await the stop condition.

Following a start condition, the bus master must output the address of the slave it is accessing. The most significant four bits of the slave address are the type identifier (see Fig. 6). For the X2404 this is fixed as 1010. The next two bits, A2 and A1, address one of up to four X2404s connected on to the

bus. The next bit, A0, allows the host to toggle between the two 256-word pages contained in the X2404. The last bit in the device address field switches between read (bit=1) and write (bit=0) operations. Following the start condition, the X2404 monitors the SDA bus, comparing the slave address being transmitted with its own address (i.e., four-bit device type and two-bit device number). When the two match, the X2404 generates an acknowledge on the SDA line. Depending on the state of the R/W bit, the device next does a read or a write operation.

Write operations on the X2404 can be divided into two types: byte write and page write. For a byte write opera-

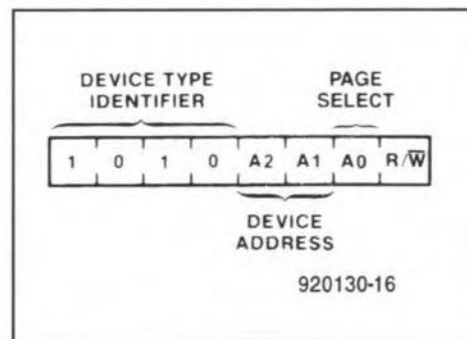


Fig. 6. Address format.

tion (Fig. 7), the X2404 requires a second address field, which forms the word address. This consists of eight

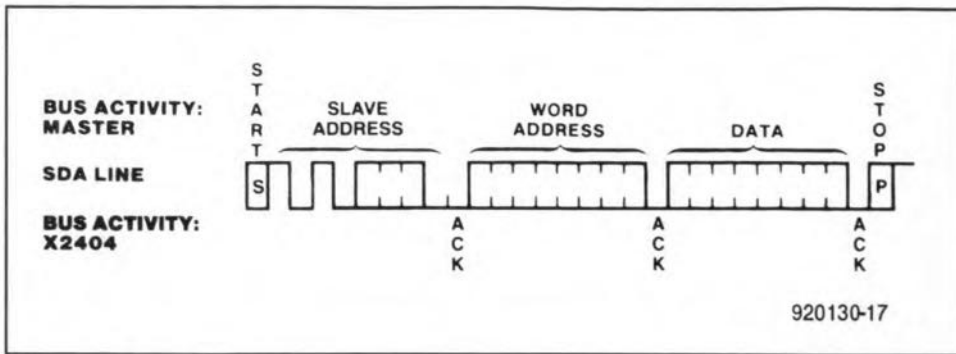


Fig. 7. Byte write operation.

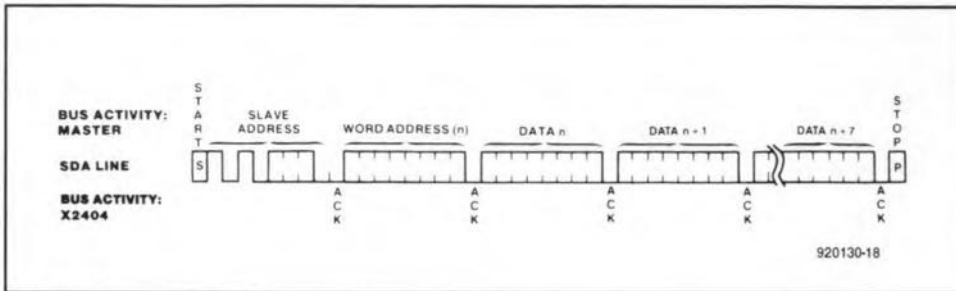


Fig. 8. Page write operation.

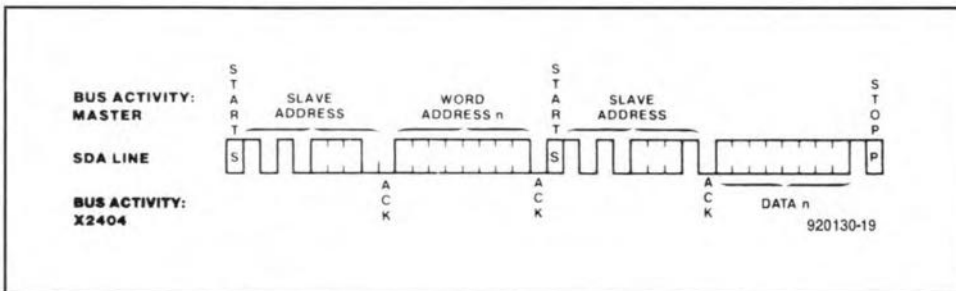


Fig. 9. Random read operation.

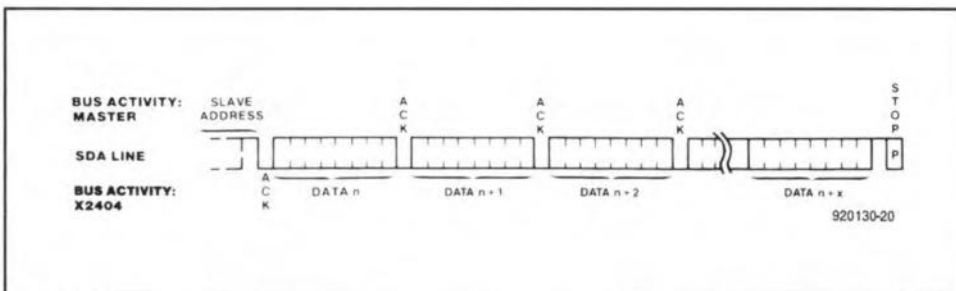


Fig. 10. Sequential read operation.

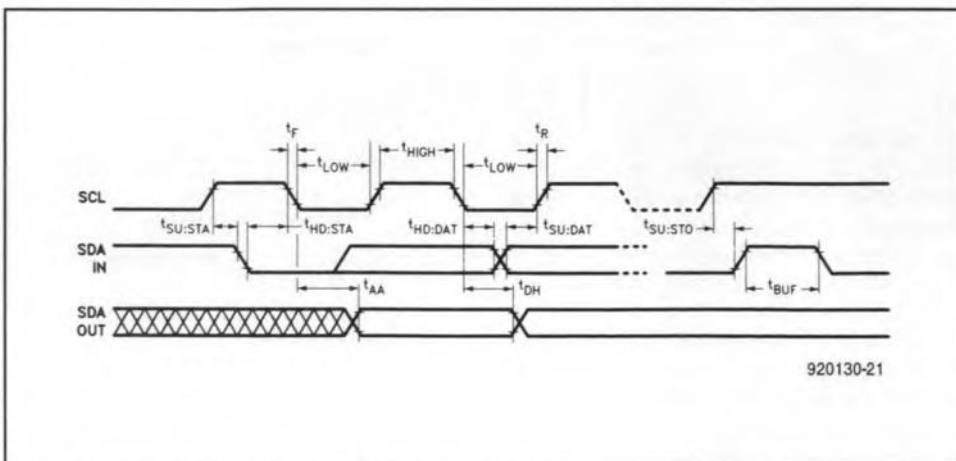


Fig. 11. Control and data line setup times.

bits, and provides access to any one of the 256 words of memory. Upon receipt of the word address, the X2404 responds with an acknowledge, and awaits the next eight bits of data, again responding with an acknowledge. Next, the master terminates the transfer by generating a stop condition, at which time the X2404 starts an internal write cycle to the non-volatile memory. During this write operation, the device disables its inputs, and will not respond to any requests from the master.

Page write operations (Fig. 8) move eight bytes at a time, and are initiated in the same manner as byte write operations. However, instead of terminating the first write cycle after the first data word is transferred, the master can transmit up to seven more words. On receipt of each word, the X2404 will respond with an acknowledge. On receipt of each word, the three low-order address bit are internally increased by one. The high order five bits of the address remain the same. If the master transmits more than eight words before generating the stop condition, the address counter will 'roll over', and the previously stored data will be overwritten. As with the byte write operation, all inputs are disabled until the internal write cycle is completed.

Acknowledge polling can be implemented by making use of the typical 5-ms write cycle time. ACK polling involves issuing the start condition followed by the slave address for a write operation. If the relevant X2404 is still busy with the write operation, it will not return an ACK until this operation is finished, after which the host can proceed with the next read or write operation.

Read operations (Fig. 9) are initiated in the same manner as write operations, with the exception that the R/W bit of the slave address is set to a one. There are three basic read operations: current address read, random read and sequential read.

Random read operations allow the master to access any memory location in a random manner. Prior to issuing the slave address with the R/W bit set to one, the master must perform a 'dummy' write operation. The master issues the start condition, and the slave address followed by the word address it is to read. After the word address acknowledge, the master immediately re-issues the start condition and the slave address with the R/W bit set to one. This will be followed by an acknowledge from the X2404, and then by the 8-bit word. The master does not acknowledge the transfer, but generates a stop condition, so that the X2404 stops transmitting.

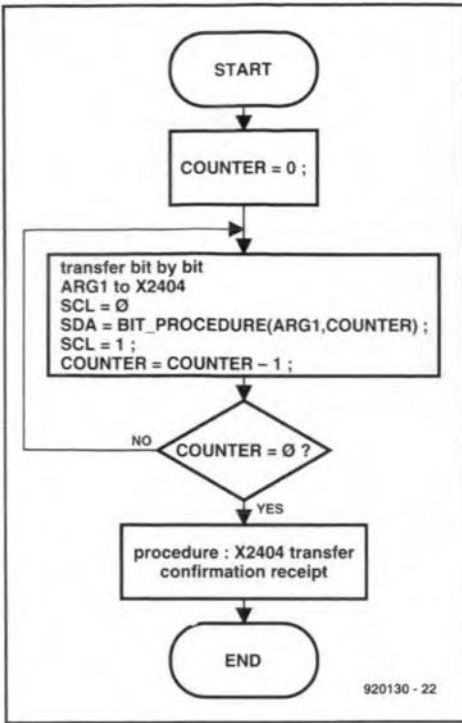


Fig. 12. Flow chart of procedure WRITE\_BYTE.

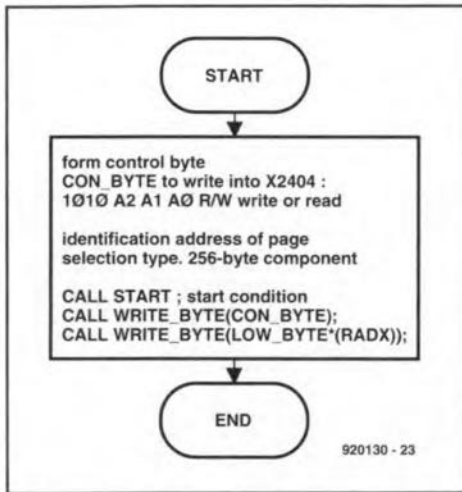


Fig. 13. Flow chart of procedure WRITE\_ADDR.

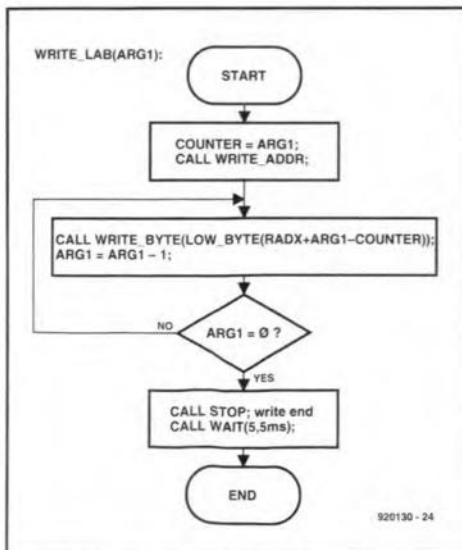


Fig. 14. Flow chart of procedure WRITE\_LAB.

Sequential read operations can be initiated either as a current address read or a random access read. The first word is transmitted as with the other read modes. However, the master now responds with an acknowledge, indicating that it requires additional data. The X2404 continues to output data for each acknowledge received. The read operation is terminated by the master not responding with an acknowledge, and generating a stop condition.

The data output is sequential, with the data from address *N* followed by the data from address *N+1* (Fig. 10). The address counter for read operations increases all eight address bits, allowing the entire memory contents of the current 256-word page to be read serially in one operation. If more than 256 words are read, the counter 'rolls over', and the X2404 continues to output data from the same 256-word page for each acknowledge received.

**X2404 control program**

The control program written to interface the X2404 to an 8751 is based on the previously discussed device operation and the timing specifications given in Fig. 11. Any transmission to the X2404 requires at least three parameters: (1) the number of bytes to be transferred; (2) the initial EEPROM address to or from which the length data, defined by the first parameter, are transferred; (3) the initial address of the 8751 internal RAM to or from which the length data, defined by the first parameter, are transferred. The following program notations apply:  
 RADX: Required initial Address for read/write from/to X2404;  
 RADM: Required initial Address for read/write from/to Microcontroller;  
 RBN: Required Byte Number for read/write program.

The flow charts in Figs. 12 through 16 illustrate the basic operation of the X2404 control program. The flow charts were used as a starting point for the assembler code written to implement the X2404-to-8751 link. Unfortunately, owing to lack of space, it is not possible to print the assembly listing of the interface program. The program is available on an MS-DOS formatted disk, however, and be obtained through the Readers Services — the order code is 1891.

**Conclusion**

The X2404 EEPROM and the software driver developed for it allows an 8051 (or derivate) microcontroller to store a relatively small packet of data that is not lost when the power is switched off. Applications June be found in auto-

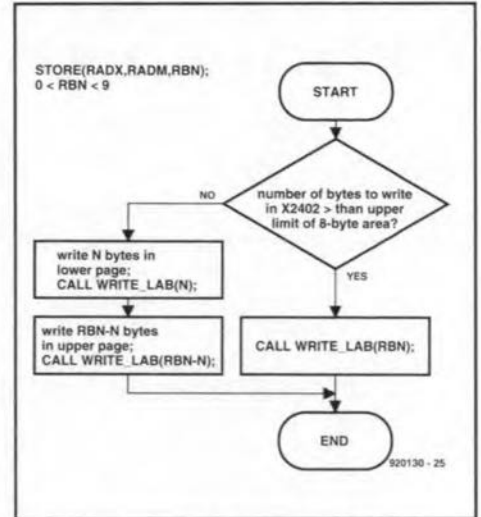


Fig. 15. Flow chart of procedure STORE.

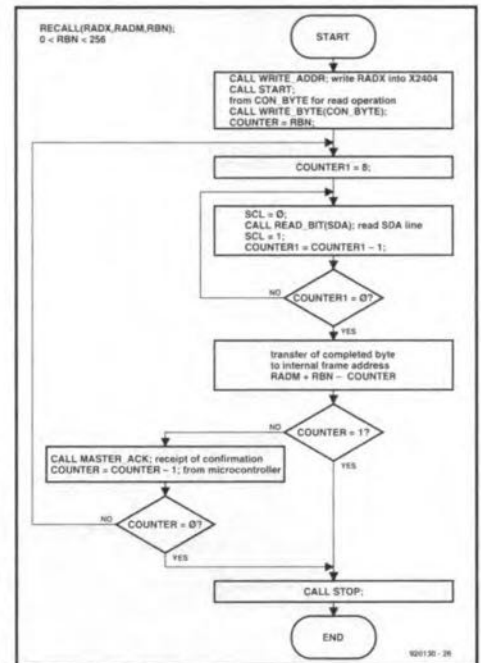


Fig. 17. Flow chart of procedure RECALL.

motive control, test and measurement, and data logging systems. If your application requires more memory space, there are EEPROMs in the X24xx family with a larger capacity, for instance, the X24C16 with a capacity of 2 kBytes, organized as eight pages of 256 bytes each. The software driver described here requires only small changes for use with a variety of serial EEPROMs.

**Literature:**

1. Data Book, Xicor. Xicor Inc., 851 Buckeye Court, Milpitas, California 95035. Telephone (408) 432-8888. Fax: (408) 432-0640.
2. Embedded Controller Handbook, Intel Corp.

**Note:**

Figures 1, and 3 through 11, and extracts from X2404 datasheets reproduced by courtesy of Xicor, Inc.